TESIS DOCTORAL

"TRANSFORMACIÓN DE GLICEROL MEDIANTE CATALIZADORES HETEROGÉNEOS ÁCIDO-BÁSICOS Y METÁLICOS SOPORTADOS EN DIFERENTES AMBIENTES REDOX"

"GLYCEROL TRANSFORMATION ON SEVERAL HETEROGENEOUS ACID-BASE AND SUPPORTED METAL CATALYSTS UNDER DIFFERENT REDOX CONDITIONS"

Manuel Checa Gómez

Directores:

Prof. Dr. Francisco José Urbano Navarro
Prof. Dr. Alberto Marinas Aramendía

Unidad de Química Orgánica Sostenible
Departamento de Química Orgánica
Facultad de Ciencias

Córdoba 2016

TITULO: *TRANSFORMACIÓN DE GLICEROL MEDIANTE CATALIZADORES HETEROGÉNEOS ÁCIDO-BÁSICOS Y METÁLICOS SOPORTADOS EN DIFERENTES AMBIENTES REDOX*

AUTOR: *Manuel Checa Gomez*

Campus de Rabanales
Ctra. Nacional IV, Km. 396 A
14071 Córdoba

www.uco.es/publicaciones
publicaciones@uco.es

TÍTULO DE LA TESIS:

TRANSFORMACIÓN DE GLICEROL MEDIANTE CATALIZADORES HETEROGÉNEOS ÁCIDO-BÁSICOS Y METÁLICOS SOPORTADOS EN DIFERENTES AMBIENTES REDOX

DOCTORANDO: Manuel Checa Gómez

INFORME RAZONADO DEL/DE LOS DIRECTOR/ES DE LA TESIS

(se hará mención a la evolución y desarrollo de la tesis, así como a trabajos y publicaciones derivados de la misma).

Como Directores de esta Tesis Doctoral consideramos que durante el desarrollo de la misma, el doctorando ha adquirido las habilidades y competencias necesarias para obtener el título de Doctor, y que el trabajo desarrollado constituye una aportación relevante en el campo del diseño y aplicación de catalizadores heterogéneos a procesos de valorización de glicerol. Estas afirmaciones se apoyan en los siguientes puntos:

1. El doctorando ha superado con buen aprovechamiento los créditos correspondientes a la formación teórico-práctica de la parte formativa del Programa de Doctorado en Química Fina (Máster en Química Fina Avanzada).

2. El doctorando ha adquirido una sólida formación en la gran variedad de técnicas instrumentales y metodologías que han sido utilizadas durante el desarrollo de la extensa labor experimental asociada a esta Tesis.

3. Los resultados obtenidos han puesto de manifiesto la necesidad de diseñar un catalizador a medida para cada tipo de proceso de interés. Asimismo, el doctorando ha establecido interesantes relaciones estructura-actividad que han arrojado más luz acerca de los procesos estudiados. Así, por ejemplo, mediante la activación de catalizadores basados en nanopartículas metálicas soportadas, se ha logrado una mejor comprensión del efecto de las interacciones fuertes metal-soporte, y su importancia en la actividad de los sólidos en la reacción. Sus resultados en el proceso de hidrogenolisis del glicerol han mostrado aspectos relevantes como la influencia del metal tanto en el proceso de deshidratación del glicerol a acetol como en la posterior hidrogenación de éste a 1,2-PDO.

4. Como resultado de la labor desarrollada directamente relacionada con la presente Tesis, se han presentado 6 comunicaciones a congresos nacionales y 2 a internacionales y publicado dos artículos científicos en la prestigiosas revistas (Catalysis Today y Applied Catalysis A), fruto de la colaboración con los equipos de la Doctora Catherine Pinel (IRCELyon, Francia), en el marco de la Acción COST CM0903:

- M. Checa, F. Auneau, J. Hidalgo-Carrillo, A. Marinas, J.M. Marinas, C. Pinel, F.J. Urbano, Catalytic transformation of glycerol on several metal systems supported on ZnO, Catalysis Today, 196 (2012) 91-100.
- M. Checa, A. Marinas, J. M. Marinas, F. J. Urbano, Deactivation study of supported Pt catalyst on glycerol hydrogenolysis, Applied Catalysis A, General, 507 (2015), pp. 34-43.

5. El doctorando ha participado activamente en el proyecto COST CM0903 sobre "Utilisation of biomass for sustainable fuels and chemicals", en el que han participado científicos de 26 países diferentes. Gracias a dicha Acción europea, pudo realizar una estancia de 3 meses en el IRCELyon de Lyon (Francia) bajo la supervisión de la Dra. Catherine Pinel. Fruto de dicha estancia, se ha familiarizado con la caracterización de materiales y su aplicación en la hidrogenolisis de glicerol. Se trata de dos campos fundamentales para la realización de los trabajos de investigación aquí recogidos y que han permitido presentar la presente Memoria como Doctorado Internacional.

6. El doctorado ha cumplido con las expectativas asociadas con la aceptación y disfrute de la beca FPU-2009 del ministerio de educación. Llevando a cabo con diligencia el trabajo de laboratorio cuyos resultados se recogen en la presente memoria así como las tareas docentes asociadas a este tipo de beca.

Por todo ello, se autoriza la presentación de la Tesis Doctoral.

Córdoba, 18 de Noviembre de 2015

Firma de los directores

Fdo.: Alberto Marinas Aramendía Fdo.: Francisco José Urbano Navarro

D. Antonio Ángel Romero Reyes, Director del Departamento de Química Orgánica de la Universidad de Córdoba

CERTIFICA:

Que el presente Trabajo de Investigación Titulado "**TRANSFORMACIÓN DE GLICEROL MEDIANTE CATALIZADORES HETEROGÉNEOS ÁCIDO-BÁSICOS Y METÁLICOS SOPORTADOS EN DIFERENTES AMBIENTES REDOX**" que constituye la Memoria presentada por Manuel Checa Gómez para optar al Grado de Doctor en Ciencias, ha sido realizado en los laboratorios del Departamento de Química Orgánica, bajo la dirección de D. Alberto Marinas Aramendía y D. Francisco J. Urbano Navarro.

Y para que conste, firmo el presente certificado en Córdoba a 18 de Noviembre de 2015.

Fdo: Antonio Ángel Romero Reyes

Mediante la defensa de esta Memoria de Tesis Doctoral se pretende optar a la obtención del **título de Doctor con Mención Internacional**, habida cuenta de que el doctorando reúne los requisitos para tal mención, según el artículo 35 de la Normativa Reguladora de los Estudios de Doctorado de la Universidad de Córdoba:

1.- El doctorando ha realizado una estancia de tres meses de duración en el grupo de investigación "Chimie durable: du fondamental à l'application (CDFA)" bajo la tutela de la Dra. Catherine Pinel, perteneciente al "Institut de Recherches sur la Catalyse et l'Environnement de Lyon" (IRCELyon), Lyon, Francia.

2.- Parte de la Memoria de la Tesis Doctoral se ha redactado en una lengua distinta de las lenguas oficiales de España.

3.- Cuenta con los informes favorables de dos doctores expertos con experiencia acreditada, pertenecientes a una institución no española de Educación Superior:

Dr. Ali Khalilov (Baku State University, Azerbaijan)

Dr. José Miguel Hidalgo Herrador (Research Institute of Inorganic Chemistry, Litvínov, Czech Republic)

4.- Un miembro del tribunal que ha de evaluar la Tesis es un doctor experto con experiencia acreditada, perteneciente a una institución no española de Educación Superior, y es distinto del responsable de la estancia mencionada en el primer apartado:

Dra. Magali Boutonnet (KTH, Stockholm, Sweden)

5.- La presentación de parte de esta Tesis Doctoral se realizará en una lengua distinta de las lenguas oficiales de España.

Las investigaciones realizadas en la presente Memoria de tesis forman parte de un Plan de Investigación desarrollado por el grupo de investigación FQM-162 del PAIDI, subvencionado con cargo a los Proyectos de excelencia P07-FQM-02695, P08-FQM-03931 y P09-FQM-04781 de la Consejería de Innovación, Ciencia y Empresa de la Junta de Andalucía, cofinanciados con fondos FEDER. Destacar la financiación del Ministerio de Educación mediante la concesión de la beca FPU-2009-1221 que ha permitido llevar a cabo la investigación. Asimismo, a la Acción Cost CM0903 que concedió una beca para la realización de una estancia corta en el "Institut de Recherches sur la Catalyse et l'Environnement de Lyon" (IRCELyon), Lyon, Francia, permitiendo, de esta forma, cumplir con los requisitos para optar a la mención internacional.

Agradecimientos

Este es un momento único en la vida, una transición, y es ahora cuando al observar la meta, te das cuenta con orgullo de todo el valor, la perseverancia y el trabajo que has necesitado para llegar hasta aquí. Sin embargo, es necesario además un poco de humildad para ver que este camino es imposible de recorrer solo. Por eso, siento necesario hacer un pequeño paréntesis y dedicar, con todo el cariño del mundo, unas palabras a todas estas personas que han estado ahí conmigo durante estos años, aportando ese granito de arena.

En primer lugar, me gustaría agradecer a mis directores *D. Francisco José Urbano Navarro* y *D. Alberto Marinas Aramendía* por muchas razones, las cuales no podría enumerar ni aunque dedicara a ello una segunda tesis. Sinceramente, creo que fueron sus consejos, su dedicación, su esfuerzo, sus conocimientos y su forma de trabajar lo que consiguió que se ganaran tanto mi admiración como mi lealtad.

Aún recuerdo mi "verano de los másteres", ese verano con la carrera recién acabada y con la gran pregunta: ¿estudio o trabajo? Esa inquietud me llevó a conocer a *D. José María Marinas Rubio*. Ese encuentro fue el empujón definitivo para comenzar la aventura del doctorado en una universidad que me era extraña y que tenía tanto que ofrecer.

Merci au *Dr Catherine Pinel*, de me donner l'occasion de faire un court séjour dans le groupe de reserche «Chimie durable: du fondamental à l'application (CDFA) » au le Institut de recherche sur la catalyse IRCELYON.

Elle m'a montré une autre façon de travailler dans les problèmes de laboratoire et l'adresse d'un point de vue différent.

Así mismo, no puedo evitar agradecer al profesorado del Departamento de Química Orgánica de la Universidad de Córdoba por todo lo que me han enseñado y el apoyo recibido durante estos años. No podría destacar a nadie en particular porque cada uno ha contribuido en mayor o menor medida, pero de forma indispensable en mi formación tanto académica como personal. *María Ángeles, Antonio Ángel, Campelo, Feli, Rafa Luque, Víctor, Ángel, César, Diego Luna, Marilud, Rafa Arrebola, Paco Romero, Rafa Barbudo, Mercedes, Pablo* y *María*, gracias por toda la amabilidad, la ayuda y vuestra amistad.

También debo recordar con cariño al profesorado de la Universidad de Jaén, en especial a *Joaquín*, *Sofía* y *Pablo*. Ellos fueron no solo mis profesores durante la licenciatura, sino que además sembraron en mí la curiosidad y la inquietud propia de un investigador, y me ayudaron a dar esos difíciles y torpes primeros pasos después de la carrera.

Gracias al personal del SCAI, en especial a *Isabel*, a *Curro* y a *Juan Isidro*, por su paciencia a la hora obtener y tratar datos, sus consejos y su predisposición para ayudarme con cualquier problema o duda.

Agradecer al Ministerio de Educación por la beca FPU-2009, financiación sin la cual no podría defender esta tesis. Así mismo, también debo agradecer a la acción COST-CM0903 por brindarme el apoyo económico para poder realizar una estancia en Lyon, Francia.

Uno de los motivos por los que volvería a recorrer esta aventura es la oportunidad de volver a estar codo con codo con mis compañeros y amigos. No podría agradecer más a *Lucrecia*, *Pineda* y *Diego*, quienes no solo

rompieron el hielo cuando llegue a Córdoba, sino que hoy puedo contarlos entre mis mejores amigos. A *Fran*, *Vicente*, *Lorena*, *Paquito, Kaquisco*, *Elena* y *Yimo* por enseñarme que la tesis no solo es estar en el laboratorio sino una época para disfrutar en buena compañía. A *Esquivel* y *Mari Carmen*, cuyas sonrisas y sus buenos días por la mañana te alegraban el día entero. Como no recordar a mi amigo y vecino *Ojeda*, con quien el desánimo y la frustración del día desaparecían a base de cerveza, una partida en la play con la "gilete" o "manchitas" y por supuesto muchas risas. *Fátima* y *Marisa*, ejemplos de constancia y motivación para todo el que tienen el placer de conocerlas. *Ana*, *Carmen (Illa)* y *Loles*, fundemos de una vez la asociación del perro con monóculo y chistera. Gracias a *Susana*, por ser como es, alguien que solo puede definirse como *Susana*.

Me alegro de haber coincidido con personas tan admirables como *Rafa, Alfonso, Juan, Carlos, Dani, Manolo Mora, Rafa Navarro, Eli, M. José* o *Cristóbal* y extranjeros en Córdoba como *Jalila, Ali* y las "*polacas*". Aunque hemos coincidido poco tiempo en el departamento, sé que de una forma u otra habéis dejado vuestra marca en esta tesis.

Fue durante la estancia en el IRCELyon, donde descubrí no solo una forma de trabajar diferente sino una cultura y una forma de vida que todavía me fascinan. *Florian, Benoit, Antonio, Stefano, Lis, Adriana, Dani, Elodie* y *Alper*, todos buenos compañeros que vienen a mi memoria cada vez que recuerdo esa época.

Debo reconocer el papel de mis familiares y amigos cuyo apoyo, muchas veces en la sombra, siempre incondicional permite a cualquiera superar todos los retos y obstáculos que la vida nos pone, independientemente de lo complejos o difíciles que sean. Gracias a mis hermanos, *Laura*, *Alberto*

y *Loli*, por estar siempre con su “hermanu” listos para una escapada a la sierra, cine, piscina o cualquier otro bombardeo. A mis abuelos, tíos y primos, mi familia, que me han apoyado en esta difícil empresa y cuyos consejos ha permitido que este proyecto llegase a buen puerto. A mi colega *Jesús Daniel*, a quien considero más un hermano que un amigo y demás compañeros de la UJA, *Carmen, José Alberto, Ana María, los gemelos, Rocío, Julia, Araceli, Escudero, Maricarmen*, etc. por animarme a seguir con mis estudios. No puedo olvidar a los miembros de la asociación “AMECO”, *Emilio, Maricruz, David, Javi, Ana, María Elena, Franki, Pedro*, etc., con quienes comparto ese sentimiento de camaradería fundido con un amor profundo por el medio ambiente. Gracias en especial a *Antonio de Haro*, por su amistad, su apoyo y el gran trabajo que ha hecho con la portada de esta tesis. A *Faloya, Adolfo, David, Beni, Polo, Jaime, Capitán, Luis* y, en general, a esos colegas que siempre han estado ahí, que nos hemos visto crecer y que son esos amigos para toda la vida.

Finalmente, quiero agradecer y dedicar esta tesis, o mejor, este fruto del esfuerzo y la constancia a mis padres. Ellos fueron quienes, a base de entrega y sacrificio, han hecho de mi la persona que soy hoy en día. Han estado ahí en lo mejor y lo peor de mi vida, guiándome de la mano hacia el camino correcto en cada punto y decisión que me han conducido hasta aquí. Papá, Mamá, esta tesis es más vuestra que mía.

Muchas gracias a todos sin excepción, al fin hemos llegado al final de este tramo y ahora, con todo el orgullo del mundo, ya podemos decir:

“*Lo hemos conseguido*”.

“Jamás desesperes en medio de las más sombrías aflicciones de tu vida,
pues de las nubes más negras cae agua limpia y fecundante.”
Proverbio japonés.

Índice General

Índice general:

Capítulo I

Introducción

I. Introducción

Conceptos previos

Durante los últimos años, los investigadores han dirigido sus esfuerzos hacia la protección del medio ambiente y al desarrollo de procesos sostenibles con el entorno [1,2]. Esta orientación ha conducido a avances importantes como son los biocombustibles (biogás, biodiésel,…). El uso de la biomasa como materia prima no solo hace posible la producción de energía sino que también proporciona una serie de compuestos funcionalizados que pueden ser empleados como punto de partida en diferentes tipos de procesos [1,3-6]. Con esta premisa, investigadores del *Pacific Northwest National Laboratory* (USA) y del *National Renewable Energy Laboratory* (USA) publicaron un informe en el que se analizaban los posibles compuestos de partida (*building blocks* o *platform molecules*) para el desarrollo de una química basada en la biomasa como fuente de estos compuestos fácilmente transformables en otros productos de alto valor añadido [5,6]. El glicerol ha sido identificado como una de esas 12 moléculas de partida [1,4-7].

El glicerol se encuentra en la biomasa utilizada como materia prima para la obtención de biodiésel en forma de ésteres con ácidos grasos o triglicéridos provenientes principalmente de aceites vegetales [9]. Su obtención se realiza vía hidrólisis o metanólisis de los triglicéridos [10], en un proceso donde los ácidos grasos se transforman en ésteres metílicos y se genera glicerol como principal subproducto, alcanzando un 10% en peso con respecto al biodiesel. El glicerol obtenido viene acompañado de diversas moléculas disueltas e impurezas y, tras su purificación, se ha venido utilizando en multitud de aplicaciones [11,12]. En este sentido, los principales procesos químicos que se han empleado en la valorización del glicerol pasan por su reformado en fase acuosa, polimerización, fermentación, deshidratación, eterificación, esterificación, oxidación selectiva e hidrogenolisis [5].

La aplicación de la catálisis en estos procesos de valorización supone una ventaja importante, ya que no solo reduce los costes de la producción de biodiesel sino que, además, ayuda a reducir la huella ecológica de esta industria al permitir la comercialización de los derivados de este subproducto de biorefinería.

I.1. El Glicerol

El glicerol (1,2,3-propanotriol) es una molécula altamente funcionalizada que puede ser empleada para sintetizar una amplia gama de productos químicos. Señalar que, en el sentido más estricto, el término "glicerol" solo es aplicable a la molécula pura mientras que el término "glicerina" es válido para productos comerciales purificados hasta del 95 % [13]. Pese a que existen unas ligeras diferencias entre ambos términos a parte del contenido en glicerol, tales como el olor, el color o las impurezas, en la práctica se suelen emplear ambos términos de forma indistinta, aunque parece haber cierta tendencia por la comunidad científica a emplear el primer término mientras el segundo suele encontrarse más a nivel de planta industrial. Por ello, en la presente tesis doctoral, se tomará como criterio utilizar el término "glicerol".

I.1.1. Producción y mercado del glicerol

El glicerol es uno de los primeros compuestos aislados por el hombre como resultado de la reacción de saponificación de triglicéridos, la cual se conoce desde el año 2800 a.C., donde se calentaban cenizas y grasas para obtener el jabón natural [12].

En cuanto a los procesos industriales tradicionales de producción, estos emplean derivados del petróleo como, por ejemplo, la síntesis a partir de propileno por medio de la diclorohidrina correspondiente o por tratamiento de acroleína con agua oxigenada [14]. Dicho mercado se consideraba estable a principios de la década del 2000, caracterizándose por una producción baja del compuesto y unos precios elevados que hacían que el glicerol fuera usado

únicamente en aplicaciones directas como la síntesis de triacetina (triacetato de glicerol) [15]. Sin embargo, la aparición y el auge de las industrias relacionadas con biocombustibles como la del biodiesel o la del bioetanol, afectaron directamente al glicerol, pues la primera se basa en el proceso de transesterificación de aceites vegetales para obtener los esteres metílicos o etílicos correspondientes y glicerol como subproducto del proceso [16,17]. Paralelamente, la obtención de bioetanol por fermentación de azúcares se trata de otro proceso industrial en auge que aumentaría aún más la producción de glicerol como subproducto [18]. El aumento del número de biorefinerías con estos fines supuso un incremento considerable en la cantidad de glicerol disponible imposible de asimilar por el limitado mercado del mismo [11], provocando, además, el cambio de consideración del glicerol de producto de alto valor añadido a subproducto, disminuyendo su valor de mercado como se aprecia en la Figura 1 [19-22].

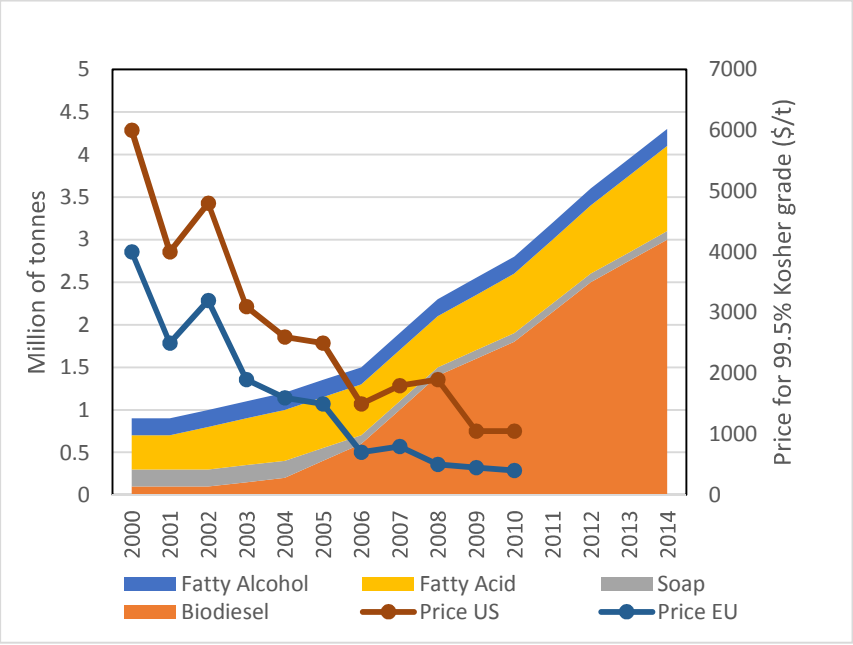

Figura 1. Evolución de la producción anual de glicerol por sectores y del precio en USA y Europa. Adaptado de [20].

El glicerol obtenido como subproducto en la refinería se conoce como "glicerol crudo", el cual es una solución compuesta por glicerol (min. 80%), agua (máx. 10%), NaCl (máx. 10%) y metanol (máx 1%), y no es apto para su uso directo. Para poder ser comercializado debe de someterse a un refinado que, en función del tipo de proceso, del origen del glicerol y de la pureza obtenida, hace que existan diferentes grados de calidad (Tabla 1).

Tabla 1. Grados de pureza del glicerol refinado.

Glicerol refinado	Pureza
Grado técnico	95.5%
USP	96%, Origen vegetal
USP	99.5%, Origen animal
USP/FCC-Kosher	99.5%
USP/FCC-Kosher	99.7%

De esta forma, durante los últimos años, diferentes grupos de investigación se están centrando en el desarrollo de nuevas rutas y procesos cuyo producto de partida sea el glicerol, con el fin de obtener compuestos de alto valor añadido. Aunque, pese a que se están desarrollando estas nuevas tecnologías que pretenden reintroducir este compuesto en el mercado, la asimilación total del glicerol producido está lejos de conseguirse [20].

I.1.2. Propiedades del glicerol

El glicerol anhidro es un líquido viscoso, incoloro, inodoro, no tóxico y de sabor dulce [12]. Algunas de sus propiedades fisicoquímicas se recogen en la Tabla 2.

Tabla 2. Algunas propiedades físico-químicas del glicerol a 20ºC.

Fórmula Química	**$C_3H_5(OH)_3$**
Peso Molecular	92.09 g·mol^{-1}
Densidad	1.261 g·cm^{-3}
Viscosidad	1.5 Pa·s
Punto de Fusión	18.2ºC
Punto de Ebullición	290ºC

Estas propiedades hacen único al glicerol, y son responsables de su empleo en más de 2000 aplicaciones diferentes [19]. Entre ellas lo encontramos como ingrediente en cosmética, productos de higiene personal, formulaciones farmacéuticas y aditivo alimentario [12,13,23].

En este sentido, los procesos que emplean glicerol en mayores cantidades pueden clasificarse en dos grandes grupos: los que lo emplean para preparar productos intermedios en la producción de epiclorhidrinas y la producción de aditivos oxigenados para combustibles [23]. La Figura 2 recoge los principales usos finales del glicerol recogidos en bibliografía, independientemente de su procedencia.

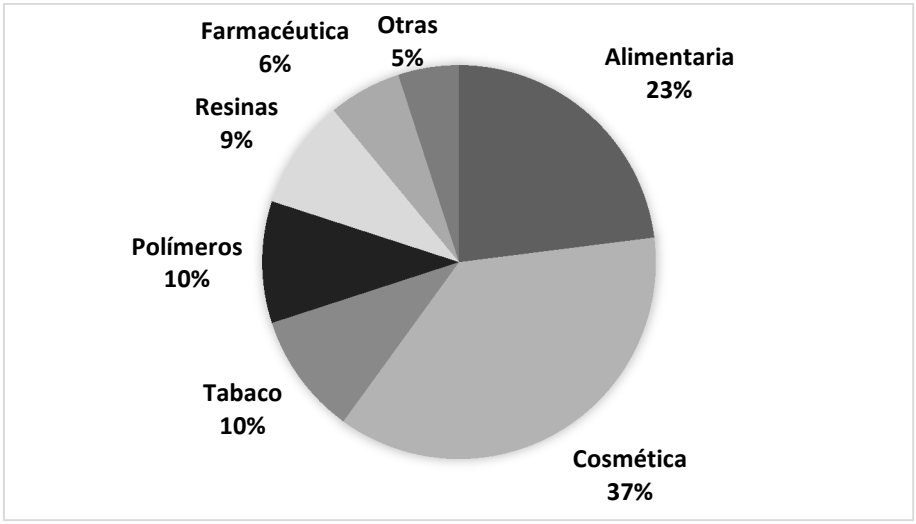

Figura 2. Usos tradicionales en la industria del Glicerol refinado. Adaptado de [13,23].

A parte de estos usos, la caída del precio ha provocado la aparición de nuevos mercados como son el de combustible para caldera o, más llamativo aún, como aditivo alimentario en granjas, mezclado con el maíz, aunque estos están condicionados por el precio del barril de petróleo [24].

I.2. Procesos de valorización del glicerol

Como se ha comentado anteriormente, los usos tradicionales actuales no son capaces de asimilar el exceso de glicerol que hay actualmente en el mercado (véase apartado I.1.1). Esto ha dado lugar al desarrollo de diferentes metodologías que buscan obtener productos de alto valor añadido aplicando los conceptos de química verde, sostenible o sustentable [8,9,11,12,25-27].

En cuanto al glicerol como producto de partida, decir que al tratarse de una molécula altamente funcionalizada, puede ser incorporado en procesos para la obtención de moléculas complejas, de interés industrial o, simplemente, convertirse en ellas mediante rutas alternativas sostenibles que no estarían ligadas al petróleo [5,6,28,29]. Actualmente, el número de publicaciones y grupos que trabajan con glicerol se encuentra en aumento, como se muestra en la Figura 3.

Los productos que suelen obtenerse mediante estos procesos son de diferente naturaleza según la reacción empleada, entre los que destacan oxidaciones para la producción de ácidos carboxílicos (ácidos pirúvico, glicérico o mesoxálico), reducciones selectivas que conducen a los propanodioles, deshidrataciones para obtener acroleína y polimerizaciones, entre otras (Figura 4).

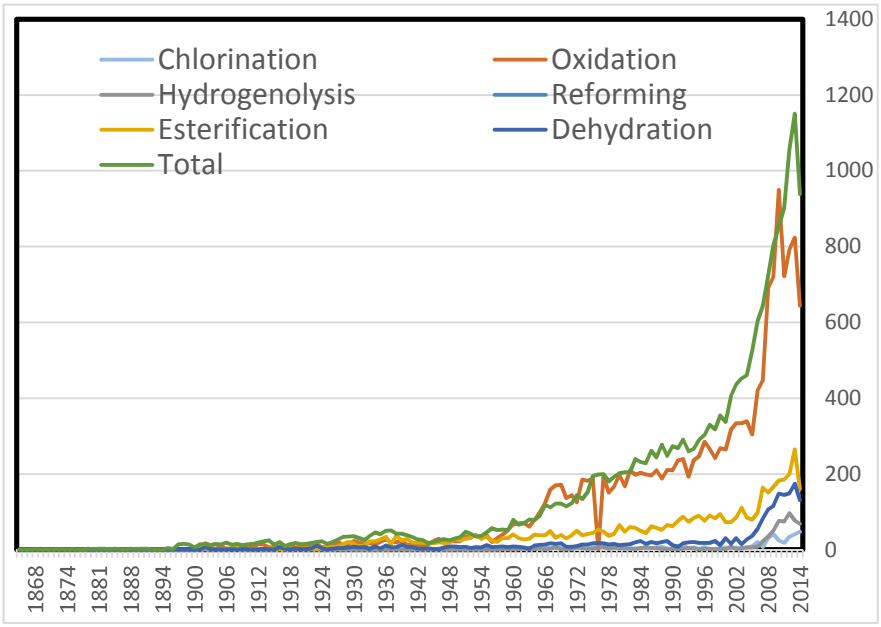

Figura 3. Evolución del número de publicaciones anuales sobre glicerol. Elaborado a partir de los datos de SciFinder® database en Noviembre de 2014, empleando "Glycerol" y cada proceso como criterio de búsqueda.

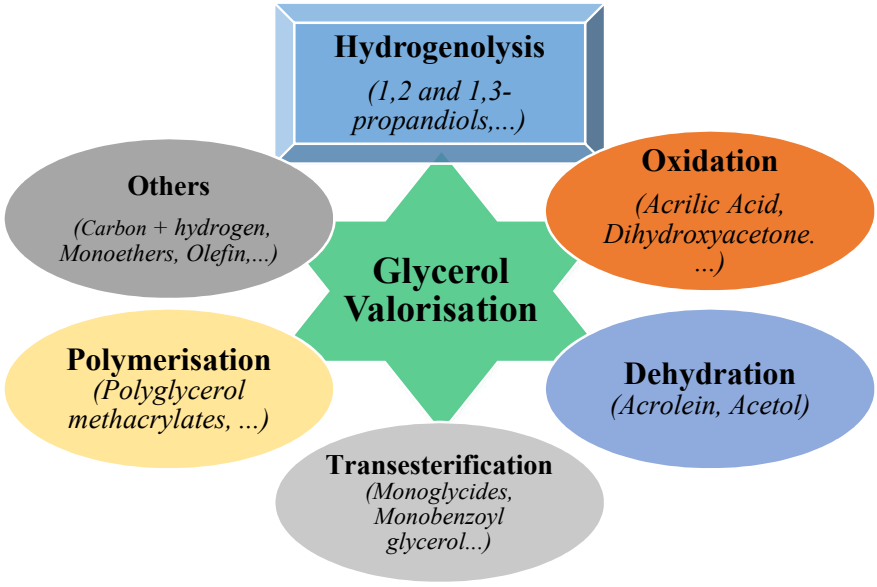

Figura 4. Algunos de los principales procesos en desarrollo para la valorización del glicerol (adaptación de referencia [10]).

I.2.1. Procesos de reducción selectiva de glicerol

La reducción selectiva es uno de los procesos más importantes para la valorización de glicerol. La reacción en sí, puede definirse como un proceso en varias etapas que tiene como resultado el producto de hidrogenolisis directa de la molécula. Así pues, la entrada de una molécula de H_2 podría suponer la aparición de tres productos diferentes según qué enlace sea atacado (ver Esquema 1).

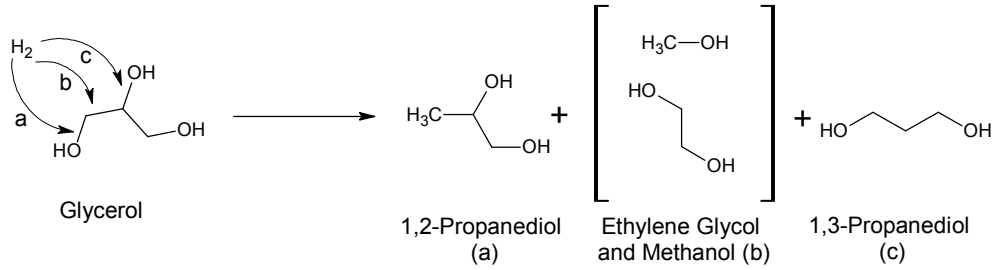

Esquema 1. Productos de reducción selectiva del glicerol [8].

Existen diferentes mecanismos propuestos para la reacción, que dependerá de las condiciones de reacción. Así por ejemplo, mediante el empleo de un catalizador metálico en medio ácido el mecanismo de reacción más aceptado transcurrirá a través del proceso deshidratación-hidrogenación (DH) [30,31], mientras que en medio básico lo hará a través de un proceso de deshidrogenación-deshidratación-hidrogenación (DDH) [30-34]. De esta forma se entreteje una red de compuestos intermedios y/o secundarios conectados mediante una serie de rutas colaterales a la reacción que, en nuestro caso, permite explicar la aparición de la mayoría de los principales subproductos del proceso (ver Esquema 2).

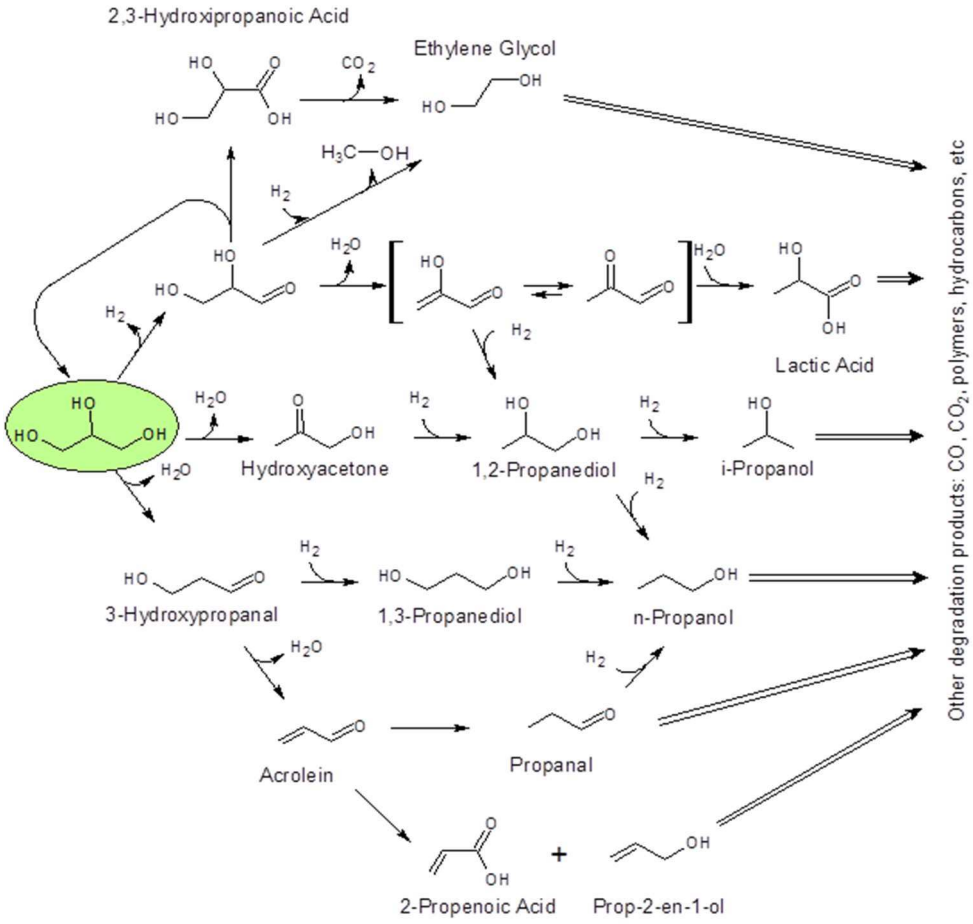

Esquema 2. Mapa de los principales productos y subproductos de reacción en la valorización de glicerol (verde).

Desde nuestro punto de vista, el mayor interés de este proceso es dirigir la reacción hacia los propanodioles. Este proceso asume la deshidroxilación selectiva del triol que implica la ruptura del enlace C-O y la adición de hidrógeno (Esquema 1, ataque a y c). Este tipo de hidrogenación se conoce como hidrogenolisis [2].

En cuanto al 1,2-propanodiol (1,2-PDO), decir que se trata de un compuesto de muy baja toxicidad y bastante práctico [35]. Sus aplicaciones van desde la industria alimentaria hasta la farmacéutica, pasando por industrias tan variopintas como puede ser la serigrafía (Figura 5).

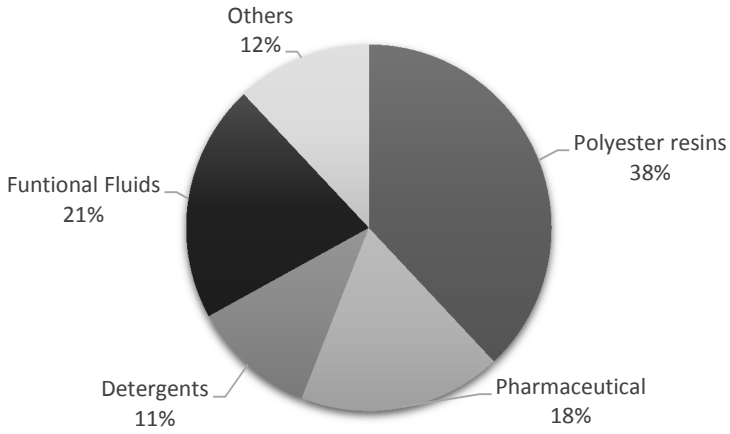

Figura 5. Principales usos industriales del 1,2-propanodiol [35].

La producción anual aproximada de 1,2-PDO se sitúa entre los 1.18 y 1.58 millones de toneladas y un precio que ronda los 1450 euro/t [35], que provienen tanto de industrias petroquímicas como de las nuevas industrias que parten de bioglicerol, siendo Dow, Ashland, Huntsman, Zhenhai Chemical, Ashland/Cargill, Archer-Daniels-Midland y LyonellBasell los principales productores [36].

Por otro lado, el 1,3-propanodiol (1,3-PDO) tiene una mercado muy limitado con respecto a su isómero (alrededor de los 60kt en 2012, se prevé una demanda de 150kt para 2019) aunque es más valioso [2,37]. En cuanto a sus usos finales, decir que la caída en el precio de glicerol ha sido responsable,

junto con el desarrollo de procesos de obtención más económicos, de que diferentes industrias químicas se hayan fijado en él para el desarrollo de nuevos materiales textiles y plásticos biodegradables [36]. El polímero más importante obtenido es el polimetilen 'Corterra™ PTT', resultado de su polimerización con ácido tereftálico comercializado por la compañía Shell [36,37].

I.2.2. Propiedades y métodos de obtención del 1,2-Propanodiol

Como se ha comentado en el apartado anterior, uno de los principales productos de interés al que conduce la hidrogenolisis de glicerol es el 1,2-PDO. Este compuesto se encuentra en diferentes grados de pureza pero, de forma general, se puede definir como un líquido incoloro, inodoro y sin sabor, además de ser bastante viscoso e higroscópico. En cuanto a la solubilidad, decir que es soluble en agua, alcoholes y algunos disolventes orgánicos [38]. La Tabla 3 incluye algunas de sus principales propiedades.

Hoy en día, el principal método de obtención a escala industrial es vía hidratación del óxido de propileno proveniente del petróleo (esquema 3), seguido de una purificación por destilación [35,38,39]. Desde el punto de vista medioambiental, se trata de un proceso que genera multitud de residuos y que, además, supone trabajar con sustancias tan peligrosas como los epóxidos. Si atendemos a la necesidad de reducir los costes ambientales del proceso, el uso de bioglicerol como producto de partida no solo reduciría nuestra dependencia del petróleo, sino que también solucionaría el problema del exceso de stock proveniente de la industria del biodiesel.

Tabla 3. Propiedades físicas del 1,2-propanodiol.

Fórmula Química	**$C_3H_6(OH)_2$**
Peso Molecular	76.08 $g \cdot mol^{-1}$
Densidad	1.0381 $g \cdot cm^{-3}$
Viscosidad	0.581 Pa·s
Punto de Fusión	-60 ºC
Punto de Ebullición	187.3 ºC

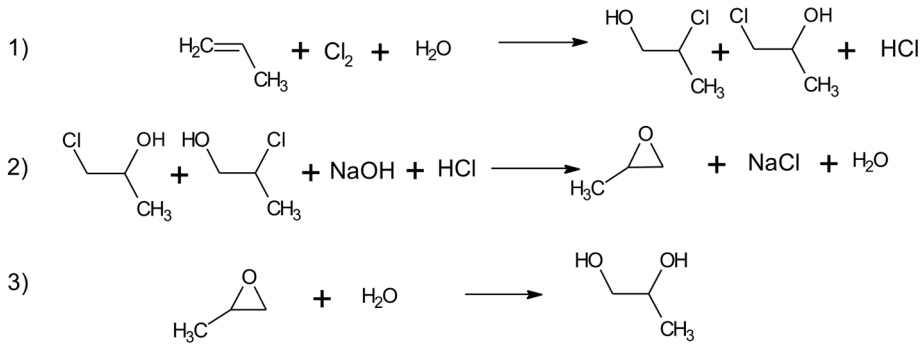

Esquema 3. Ejemplo de producción de 1,2-propanodiol partiendo de propileno [35].

Otro punto a tener en cuenta es la economía del proceso. La producción a nivel industrial de 1,2-PDO partiendo de glicerol debe ser una opción económicamente viable frente al proceso actual, haciendo necesario realizar un estudio comparativo de ambos procesos. En este sentido, destacan los esfuerzos realizados en el marco de la Acción COST CM0903 "Utilisation of biomass for sustainable fuels and chemicals" (UBIOCHEM), donde este problema se ha tenido en cuenta en todos los nuevos procesos que impliquen el empleo de moléculas plataforma y que pretendan sustituir a los ya existentes. El grupo de investigadores que formaron parte de esta Acción COST, desarrolló una serie de criterios con el fin de comparar la sostenibilidad de la producción de un mismo compuesto químico vía petroquímica o vía biomasa. Los resultados más relevantes aparecen publicados en el volumen 239 de la revista Catalysis Today. Los criterios seleccionados fueron la eficiencia material (básicamente el factor E que introdujese el Profesor Roger Sheldon), la eficiencia energética, el uso del suelo y el coste. Los investigadores estudiaron como moléculas objetivo el ácido láctico, el succínico, la metionina, el acrilonitrilo, el isopreno, el 1-butanol y el 1,2-propanodiol. En el análisis de esta última molécula objetivo estuvo involucrado nuestro grupo de investigación [35]. La ruta petroquímica transcurre a través del óxido de propileno cuya epoxidación y posterior hidrólisis conduce a la molécula objetivo. La ruta alternativa vía biomasa, tiene lugar por hidrogenolisis del glicerol. De las diferentes rutas petroquímicas, los autores seleccionaron el proceso vía clorhidrina que, como se ha comentado anteriormente, continúa siendo el más empleado (ver Esquema 3). El estudio concluye que ambos procesos son competitivos. La ruta del glicerol da lugar a una mejor eficiencia material y atómica si bien necesita una mayor cantidad de suelo. En cuanto a los costes económicos,

depende del precio del material de partida que puede fluctuar considerablemente, así como del valor de los posibles subproductos obtenidos. Los autores ponen como ejemplo un estudio de Ghanta y col. [40], en el que describen la rentabilidad del proceso de obtención de óxido de propileno a partir de oxidación del isobutano. Según los autores, el precio estimado en el mercado del óxido de propileno es de unos 2000 euros/tonelada mientras que los costes de producción son de unos 2484 euros/tonelada. El proceso resulta rentable debido a la obtención como subproducto de alcohol tercbutílico (aproximadamente 2,4 toneladas por tonelada de óxido de propileno), que puede ser vendido a unos 680 euros/tonelada. La principal conclusión del estudio sobre el 1,2-PDO fue la mayor eficiencia atómica del proceso alternativo, aunque los costes finales dependerían de factores como el mercado de la materia prima y de la producción de subproductos de interés [35].

La mayoría de la bibliografía referente a la conversión selectiva de glicerol en 1,2-PDO se puede clasificar en tres grandes bloques:

Biocatálisis. En 1881 se describió el microorganismo "*Clostridium"* como el menos peligroso para la reacción y más abundante en la naturaleza. Desde entonces se han descrito multitud de microorganismos que pueden ser empleados en la reacción [37]. La reacción transcurre en dos etapas tanto para producir el 1,2-PDO como para el 1,3-PDO [41]. Aunque, hasta donde hemos sabido buscar, esta opción suele ser más descrita para la producción del 1,3-PDO, siendo una cepa de "*Clostridium*" modificado la que presenta mejores resultados [37,42]. Además, el proceso presenta la ventaja de poder emplear glicerol crudo como sustrato [12,42-44]. Hoy en día, si aplicamos un estudio de viabilidad económica similar a los realizados en la acción COST previamente mencionada, llegaríamos a la conclusión de que esta ruta

biocatalítica se encuentra lo suficientemente optimizada para la producción de 1,3-PDO para ser más rentable que su producción vía petroquímica.

Catálisis homogénea. La aplicación de catalizadores homogéneos basados en metales nobles como el Ru con polialcoholes como el sorbitol es conocida desde los años 80 del pasado siglo [45]. En el caso del glicerol, presentan el inconveniente de ser demasiado activos, siendo difícil detener la reacción en el producto deseado (1,2-PDO ó 1,3-PDO) obteniendo por lo general mezclas más o menos complejas de mono y dialcoholes C1, C2 y C3. Sin embargo, existen diferentes patentes como la de Celanese corp. de 1985 que empleaba gas de síntesis, complejos de Rh como catalizadores y aditivos basados en derivados de W y elementos del grupo VIII [46]. Más tarde Shell patentó un nuevo proceso que empleaba condiciones más suaves y catalizadores basados en complejos de Pt [47].

Catálisis heterogénea. Presenta como principal ventaja la recuperación del catalizador mediante técnicas sencillas. Los estudios más antiguos datan de 1931, cuando se registró una patente en la que se usaron catalizadores de óxido de cromo con cobre o cobalto como metal activo [48]. Los datos mostraban una conversión de glicerol incompleta con rendimientos del 70 al 50% (para Cu y Co respectivamente) a 210ºC. Actualmente, la mayoría de patentes en curso emplean este tipo de catálisis, siendo los catalizadores basados en metales nobles soportados y compuestos de cobre los más registrados.

I.3. Hidrogenolisis del glicerol y catálisis heterogénea

A pesar de los recientes esfuerzos realizados por la comunidad científica, la aplicación de esta reacción potencialmente importante se ha limitado a escala de laboratorio, debido a las diversas limitaciones que presenta en la actualidad. Las presiones de hidrógeno típicas para estos experimentos se sitúan entre 1 y 10 MPa (aunque se puede llegar hasta 35 MPa) y las temperaturas en el intervalo 120-250ºC (o incluso superiores) [49-51]. Una desventaja adicional es la necesidad de utilizar disoluciones diluidas de glicerol, del orden del 1-30% en peso, lo que aumenta el consumo energético del proceso disminuyendo la rentabilidad del mismo. Finalmente, un problema adicional del proceso es la baja selectividad hacia el 1,2-PDO, debido a un elevado rendimiento a otros productos como etilenglicol, acetol, acroleína, y la competencia con los procesos de reformado en fase acuosa [52]. Los esfuerzos investigadores se centran, por tanto, en desarrollar tecnologías que permitan llevar a cabo el proceso a menores temperaturas y presiones, empleando glicerol más concentrado y con selectividades mejoradas a 1,2-PDO y/o 1,3-PDO.

I.3.1. Propiedades de los catalizadores empleados

Los tipos de catalizadores empleados en la reacción de hidrogenolisis del glicerol por lo general consisten en una fase metálica depositada sobre un soporte que puede ser de diferente naturaleza (zeolitas, óxidos de metales de transición, sales inorgánicas insolubles, etc.) [53-56]. Cada metal tiene unas propiedades electrónicas y geométricas características, que influirán en la conversión y la selectividad de la reacción y en la forma de adsorber el sustrato [57,58] mientras que, por otro lado, el soporte afectará tanto a la actividad

como a la selectividad del propio metal, proporcionándole diferentes propiedades [31,58,59]. Si nos paramos a recapacitar sobre esto último, el proceso de reducción de dobles enlaces mediante catálisis heterogénea se puede representar de forma esquemática según la Figura 6.

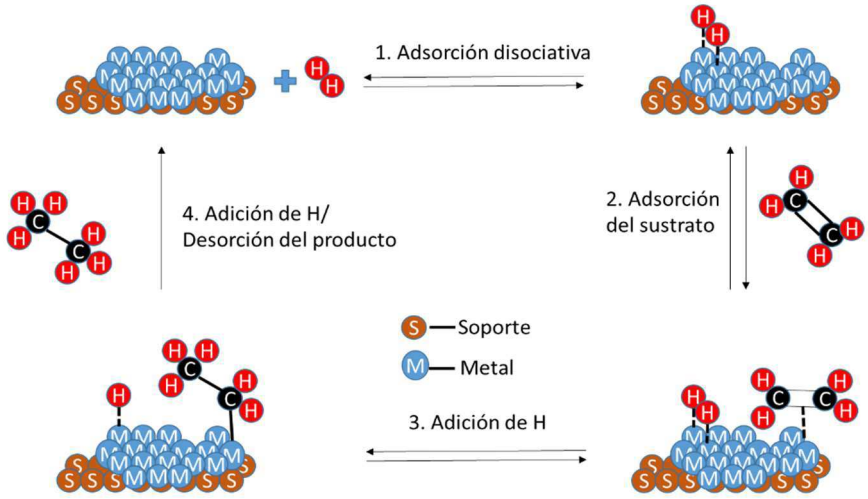

Figura 6. Diagrama del proceso de reducción de un doble enlace sobre catalizadores heterogéneos.

Por otro lado, el glicerol no posee ninguna insaturación que le permita ser adsorbido fuertemente sobre la superficie metálica del catalizador sino que se adsorbería débilmente mediante los grupos hidroxilo. Supongamos como ejemplo que las propiedades del soporte pueden ayudar favoreciendo la adsorción o, como se observa en algunos casos, producir la deshidratación de la molécula hacia productos intermedios como el acetol que sí posee el doble enlace necesario para el proceso (mecanismo DH) [31]. Cuando nos guiamos por este mecanismo en dos etapas los catalizadores que emplearemos serán ácidos pues de esta forma facilitamos la primera etapa de deshidratación.

Así, podemos encontrar una gran variedad de catalizadores empleados industrialmente en hidrogenolisis, como la cromita de Cu [12], aleaciones como la patente en curso de Dalai y colaboradores [60] o con metales nobles soportados como las patentes de Kaneda [61] o de Wei y colaboradores [62].

I.3.1.A. Efecto del metal activo

De forma general, podemos dividir los metales empleados en dos grupos: metales nobles y metales de transición. Los primeros presentan la ventaja de llevar a cabo la reacción en condiciones suaves e incluyen Pd [63,64], Pt [50,65], Ru [66-70], Ir [71,72] y Rh [71,73]. En cuanto a los metales de transición, estos se refieren principalmente a elementos como el Cu [74-77], Co [78,79] y Ni [50,80,81] que son mucho más económicos que los anteriores.

Metales de transición: sobre estos decir que los más comunes están basados en Cu, y que pueden clasificarse según estén soportados en pequeña cantidad sobre otro sólido o que la composición del catalizador sean óxidos, aleaciones o compuestos insolubles de metales de transición. Estos catalizadores se caracterizan por ser menos activos hacia la ruptura del enlace C-C, con lo que la cantidad de productos de degradación es menor. Sin embargo, para obtener buenos resultados, por lo general requieren condiciones de reacción más drásticas.

Metales nobles: el primer trabajo data de 1991, en el que Montassier *et al*., desarrollaron catalizadores de Ru soportado sobre carbón activo y estudiaron el efecto del azufre como veneno en la reacción de hidrogenolisis de diferentes polioles, entre ellos el glicerol [33].

Tabla 4. Algunos catalizadores que se suelen emplear en la hidrogenolisis de glicerol. Datos adaptados de las referencias [12,82,83] y referencias allí citadas.

Catalizador	Condiciones de reacción	Conv. %	% Sel. 1,2-PDO	Ref.
5% Ru/Alúmina	200°C, 1.38 MPa	22-24	60	[12]
5% Ru/C	200°C, 1.38 MPa	42-45	40	[12]
Ru/C+ Amberlita 15	120°C, 8 MPa, 10h	79.3	74.9	[82]
Ru/C+Nb_2O_5	180°C, 6 MPa, 8h	44.6	60.9	[82]
Ru/CsPW	180°C, 0.5 MPa, 10h	21	96	[82]
Ru/bentonita-TiO_2	150°C, 0.2 MPa [(c)], 7h	69.8	80.6	[82]
Ru-Re/ZrO_2	160°C, 8 MPa, 8h	38.9	56.2	[82]
5% Pt/C	200°C, 1.38 MPa	34-35	82-85	[12]
Pt/Hidrotalcita	220°C, 3 MPa, 20h	92.1	93	[82]
Pt/NaY	230°C, 15h	20 (%wt)	64 [(a)]	[83]
Rh/C	180°C, 3 MPa He	5 (%wt)	4[(a)]	[83]
Rh/SiO_2	120°C, 8 MPa [(c)], 10h	19.6	34.6	[82]
5% Pd/C	200°C, 1.38 MPa	4-7	71-73	[12]
10% Pd/C	200°C, 1.38 MPa	8-10	46-48	[12]
20% Pd/C	200°C, 1.38 MPa	10-12	55-58	[12]
Pd/CoO	180°C, 4 MPa [(c)], 24h	70.7	9.2	[82]
Ni Raney	180°C, N_2 (0.1MPa), 1h	100	43	[82]
Ni Raney	200°C, 1.38 MPa	49	52-54	[12]
Cu Raney	200°C, 1.38 MPa	48	69-70	[12]
Ni-Ce/AC	200°C, 5 MPa, 6h	90.4	65.7	[82]
Ni/NaX	200°C, 6 MPa, 10h	94.5	72.1	[82]
Ni/C	200°C, 1.38 MPa	40	68-69	[12]
Ni/Silica-Alúmina	200°C, 1.38 MPa	45	65	[12]
Cromita de cobre	200°C, 200 Pa, 24h	54.8	85	[82]
Cromita de cobre	200°C, 1.38 MPa	55	94-95	[12]
Cu/SiO_2	200°C, 9 MPa, 12h	73.4	94.3	[82]
Cu/Alúmina	200°C, 1.38 MPa	51-53	40	[12]
CuO-ZnO	180°C, 8 MPa, 90h	19	100	[82]
Cu-ZnO	200°C, 4.2 MPa, 12h	22.5	83.6	[82]
Ag/Al_2O_3	220°C, 1.5 MPa, 10h	46	96	[82]
Ir/C	180°C	76[(b)]	7[(a)]	[83]

(a) Rendimiento a 1,2-PDO. (b) Conversión en función del carbono. (c) Medida a temperatura ambiente.

Este envenenamiento reducía la ruptura del enlace C-C, con lo que mejoraba la selectividad hacia los dioles. Más tarde, Dasari *et al*, llevarían a cabo el estudio con Pd, Pt y Ru soportados sobre carbón activo, y unas condiciones de 473 K, 1,4 MPa y disoluciones concentradas (80%) de glicerol. Observaron que el Ru era el más activo, mientras que el Pt era el más selectivo [50]. Grupos como el de Chaminand *et al*. demostraron que además del metal activo, había que tener en cuenta tanto el soporte como el disolvente empleado como se verá más adelante [84].

Por otro lado, se han llevado a cabo diferentes estudios basados en sistemas bimetálicos soportados. Con estos catalizadores se busca combinar las ventajas de los dos elementos en la reacción. Algunos ejemplos serían sistemas bimetálicos como Ir-Re [85], Pt-Ni [86,87], Pt-Ru [88], Au-Ru [88] o Rh-Re [89].

En cuanto a su aplicación en la reacción, los mejores resultados se suelen obtener con metales nobles aunque en algunos casos los metales de transición pueden ser competitivos como se puede observar en la Tabla 4. De todos ellos, el Pt se caracteriza por una alta actividad, ser más respetuoso con el enlace C-C y por su estabilidad frente a la desactivación por depósitos carbonosos [90].

I.3.1.B. Efecto del tamaño de partícula

Cuando trabajamos con metales soportados, el tamaño de la partícula metálica resulta ser un parámetro decisivo [91]. Las reacciones se producen, por norma general, sobre la superficie de la partícula metálica (ejemplo Figura 6), pero la forma y el tamaño de ésta pueden influir en la actividad debido a la coordinación de los átomos metálicos que forman la estructura de la partícula [92]. Cuando las partículas son muy pequeñas tenemos números de coordinación muy bajos (ver Figura 7), como resultado la partícula será inestable y muy reactiva presentando como principal problema su desactivación por formación de depósitos carbonosos, procesos de sinterización, etc [93].

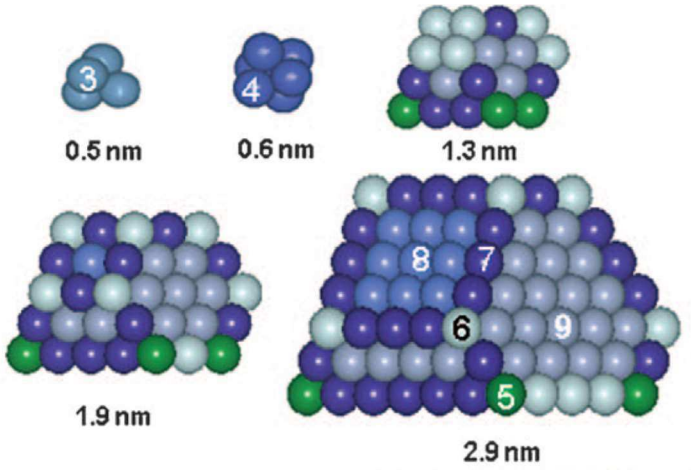

Figura 7. Modelos de nanopartículas de Au indicando el número de coordinación de los átomos. Extraído del trabajo de López-Haro y colaboradores [94].

En ciertos casos, cuanto menor sea el tamaño de la partícula metálica menos acusada será la función metálica de la misma, haciéndose notar en mayor medida el efecto del soporte. Por otro lado, un tamaño de partícula demasiado grande no es deseable debido a que la mayor parte del metal se

encuentra en el interior de la partícula y es por tanto inaccesible para los reactivos. Es necesario indicar que en algunas reacciones un tamaño grande puede ser una ventaja, ya que existen moléculas que se adsorben preferentemente sobre las caras de la partícula metálica y reaccionan o inducen la reacción de otras moléculas (p. e. modificadores quirales).

Por tanto, en función de la reacción en estudio, la forma y el tamaño de la partícula influirán de forma crítica en la actividad y selectividad del catalizador [94]. En lo que respecta a la hidrogenolisis de glicerol, los estudios sobre la influencia de la partícula son muy variados. Veamos algunos ejemplos.

En 2014, Deng y colaboradores publicaron un estudio basado en las nanopartículas de Pt-Re soportadas sobre nanotubos de carbono [95]. Observaron cómo a menores tamaños de partícula (~1.9nm) se obtenían mejores conversiones. Además, las selectividades estaban asociadas al tamaño de partícula de forma que, para las de menor tamaño, se atacaban principalmente los enlaces C-C y C-O primarios del glicerol mientras que, para mayores tamaños de partícula, se producía mayoritariamente el ataque al enlace C-O secundario del glicerol y del 1,2-PDO. En estos casos la estructura de la partícula resulta otra variable que puede afectar a la actividad, pues podemos obtener un producto u otro dependiendo de si los átomos de los dos elementos implicados se encuentran formando partículas independientes o en forma de aleación [96,97].

Las partículas demasiado pequeñas son muy activas en la hidrogenolisis de glicerol, tanto que pueden favorecer la competencia del proceso con el reformado en fase acuosa [98].

I.3.1.C. Efecto del soporte

Cuando empleamos catalizadores metálicos soportados, las propiedades del soporte deben elegirse con sumo cuidado. Los sólidos que suelen emplearse como soportes tienen una serie de propiedades ácido-base superficiales que pueden intervenir de diferentes formas [68], influyendo en nuestro caso en el mecanismo de reacción. Como se comentó en el apartado I.2.1, la hidrogenolisis de glicerol a 1,2-PDO puede transcurrir por dos mecanismos diferentes en función del pH (Figura 8).

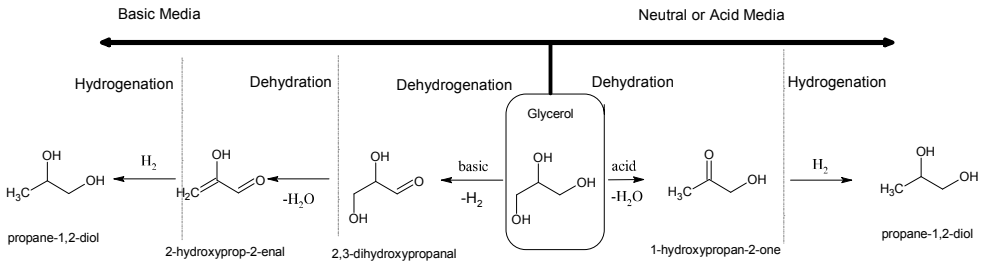

Figura 8. Mecanismos de reacción en función del pH.

En este sentido, Vasiliadou *et al.*, analizaron el efecto del soporte de catalizadores de Ru en la hidrogenolisis de glicerol observando una clara relación entre la acidez total del soporte y la conversión a productos de hidrogenolisis: a mayor acidez mayor actividad [68]. Un estudio más reciente sería del de Gallegos-Suárez *et al.,* que empleó catalizadores de Ru sobre diferentes tipos de soporte (grafito, nanotubos, carbón activado y zeolitas) observando como las propiedades de los mismos afectaban directamente a la actividad del metal, concluyendo que el carácter electrodonador de los soportes induce carga negativa en las partículas metálicas, favoreciendo la producción de 1,2-PDO y la ruptura del enlace C-C que conduce a productos indeseados [70].

Por otro lado, existen trabajos donde los centros básicos del soporte juegan un papel fundamental, favoreciendo el mecanismo DDH [83], conduciendo tanto a 1,2-PDO como a ácido láctico y etilenglicol.

Otra forma de influencia del soporte es mediante su interacción con el disolvente, como ocurre en el caso de la alúmina [99]. Su hidratación parcial puede favorecer la adsorción del glicerol sobre la superficie y facilitar la reacción. Aunque un exceso de agua en la superficie podría desactivar el catalizador con el paso del tiempo. La desactivación puede ocurrir bien por cambios estructurales, bloqueo de poros, lixiviación o sinterización de las partículas de metal activo. El hecho de realizar las reacciones en medio hidrotermal, hace que el empleo de soportes que puedan ser hidrolizados en estas condiciones conduzca a la coalescencia y sinterización de la fase metálica. En condiciones de pH extremas el efecto es más grave, llegando incluso a disolver por completo soportes como la sílice. Muchos grupos de investigación han tratado de sortear este problema empleando metales Raney o usando diferentes tipos de materiales carbonosos como soporte [82,83].

El empleo de determinados compuestos como soporte puede inducir un efecto sinérgico con la fase metálica. Por ejemplo, el empleo de óxidos o complejos metálicos de tungsteno, molibdeno o renio pueden facilitar la reacción orientando de una forma específica la molécula objetivo [100,101]. En estos casos se plantea un mecanismo para la reacción diferente a los anteriores y que puede ser considerado como una "hidrogenolisis directa" [31]. El mecanismo es bastante controvertido, pues pese a que consigue explicar la aparición del producto cinético de la reacción 1,3-PDO, no consigue explicar en algunos casos por qué aparece en tan poca cantidad, lo cual podría ser explicado si consideramos que se da junto con otros mecanismos, como el DH, de forma simultánea [31].

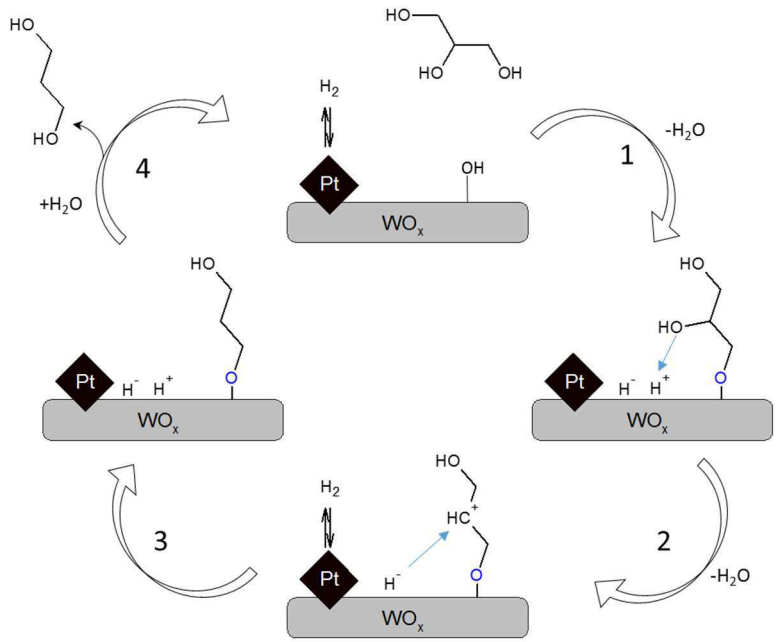

Figura 9. Mecanismo de hidrogenolisis directa. Adaptación de [31,102]

La hidrogenolisis directa se ha descrito con nanopartículas de metales nobles como el Pt, Ir o Rh en presencia de W, bien soportados sobre el óxido metálico o, en algunos casos, cuando se emplean derivados de W como aditivos promotores de la orientación hacia 1,3-PDO [18,37,103,104].

Finalmente, efectos similares a los presentados anteriormente podrían producirse si se emplean soportes parcialmente reducibles como TiO_2, ZnO o SnO_2, lo que podría conducir tras la activación (reducción) del catalizador a una interacción fuerte entre el metal soportado y el soporte, descrito en bibliografía como SMSI (del inglés "*Strong Metal-Support Interaction*"), o incluso, dependiendo de la temperatura de reducción, a la formación de aleaciones entre el metal activo y los soportes parcialmente reducidos [105,106].

I.3.2. Influencia de las condiciones de reacción

De forma complementaria al apartado I.3.1, las condiciones en las que tenga lugar la reacción van a ser decisivas a la hora de definir la selectividad de un proceso y la probabilidad de que el mismo tenga lugar. Los catalizadores son una mera herramienta que disminuye la energía de activación de la reacción, lo cual no significa para nada que no sea necesario un aporte energético.

La optimización de las condiciones de reacción son clave para que un determinado proceso industrial sea viable o no. A ello se suma la limitación de los recursos naturales disponibles y la necesidad de obtener el producto puro para evitar procesos de purificación o la generación de residuos. Así pues, los investigadores centran sus esfuerzos en el desarrollo de catalizadores que permitan trabajar en condiciones más suaves y sostenibles, que permitan obtener los compuestos que deseamos sin comprometer las necesidades de las futuras generaciones. Este concepto fue acuñado por P. T. Anastasy J. C. Warner [107], se conoce como "*Química Verde*" y ha sido identificado como uno de los retos de nuestra época [108].

En este apartado veremos algunos de los efectos que tienen sobre la reacción diferentes parámetros como la presión, temperatura o el disolvente.

I.3.2.A. Efecto del disolvente

Por lo que respecta al disolvente, en la mayoría de los trabajos publicados, se emplea agua. No obstante, existen asimismo algunos intentos de realizar el proceso de conversión de glicerol a 1,2-PDO o 1,3-PDO empleando disolventes orgánicos polares y apróticos como el sulfolano [109]

o la 1,3-dimetil- 2-imidazolidinona [103]. Se han descrito trabajos como el de Wang y colaboradores, que aplicaron disolventes polares prótidos para la hidrogenolisis de glicerol [110]. En dicho estudio, emplearon un catalizador de Cu-ZnO y agua, metanol y etanol como disolventes, observando que en agua se producía la mayor selectividad y la peor conversión (~4,25% de rendimiento), mientras que en metanol se ganaba conversión a costa de la selectividad (~30% de rendimiento) y el etanol presentaba un comportamiento intermedio (~12% de rendimiento). Este hecho fue justificado por las diferentes tensiones superficiales de los disolventes empleados, unido al hecho de que tanto metanol como etanol son capaces de generar hidrógeno "*in situ"* aumentando la conversión.

A parte del metanol y el etanol, existen otros disolventes capaces de intervenir en la reacción actuando como donadores de hidrógeno. Estas sustancias presentan la ventaja de generar H_2 directamente en el medio de reacción, permitiendo disminuir las presiones del sistema al aumentar la disponibilidad de H_2 en la superficie del catalizador. Los más interesantes son alcoholes secundarios como el isopropanol [111-113].

I.3.2.B. Efecto de la concentración

Una desventaja del proceso actual en reactores tipo batch es la necesidad de utilizar disoluciones diluidas de glicerol, del orden del 1-30% en peso, lo que aumenta el consumo energético del proceso disminuyendo la rentabilidad del mismo. El estudio del proceso de hidrogenolisis a mayores concentraciones de glicerol es, por tanto, necesario con el fin de obviar este problema. Así, Mane *et al.*, describen para catalizadores basados en Cu:Al que un incremento de la concentración de glicerol hasta un 60% conduce a un

aumento de la conversión para, a mayores concentraciones producirse un descenso en la misma. La explicación dada por los autores se basa en i) una disponibilidad limitada de los centros activos al mantenerse constante la concentración de catalizador o ii) a un efecto inhibitorio de la cinética por el propio sustrato a elevadas concentraciones del mismo [114]. Por otro lado, Dasari *et al.*, indican, asimismo con catalizadores de Cu, que un aumento de la concentración de glicerol conlleva un aumento en la conversión, manteniéndose la selectividad a 1,2- PDO en niveles del 60-85%. No obstante, para concentraciones superiores al 80% en peso de glicerol, se produce un descenso en la selectividad debido a procesos de polimerización y degradación del sustrato [50].

Una posible alternativa sería el empleo de reactores en flujo continuo, los cuales no sólo permiten la activación del catalizador *in situ*, sino que también pueden llegar a trabajar a mayores concentraciones y presiones, con resultados prometedores [115]. Sin embargo, presentan la desventaja de necesitar un flujo continuo estable de reactivos, sistemas de control del proceso avanzados y son muy específicos para un producto concreto.

I.3.2.C. Efecto de la presión y la atmósfera

La reacción de hidrogenolisis se basa en la incorporación de hidrógeno a la molécula objetivo con la consecuente ruptura de un enlace. Este hidrógeno puede encontrarse como H_2 en la fase gaseosa o puede ser proporcionado por un compuesto donador de hidrógeno [113]. Las presiones de hidrógeno típicas para estos experimentos se sitúan entre 1 y 10 MPa, aunque se puede llegar hasta 35 MPa. No obstante, trabajar con elevadas presiones implica un alto coste en equipamiento, lo que unido a la peligrosidad relacionada con el

hidrógeno a presión hace que se haya investigado el efecto de la presión inicial de hidrógeno en el proceso de hidrogenolisis del glicerol.

En este sentido, Dasari *et al.*, estudiaron el efecto de la presión de hidrógeno cuando se trabaja en el intervalo 0.3-2.1 MPa sobre catalizadores basados en cromita de Cu, encontrando que a medida que aumenta la presión aumentan la actividad y la selectividad del proceso [50]. Otros autores se centraron en un rango algo mayor (3-7 MPa), obteniendo resultados similares que justifican argumentando que a mayor presión de hidrógeno, aumenta su disponibilidad para la reacción [114,116]. Sin embargo, esto ocurre hasta un determinado valor a partir del cual la saturación de los centros activos evitaría la aproximación del glicerol, provocando una caída de la conversión [67,117]. En cuanto a la selectividad a 1,2-PDO, por norma general, aumentará con la presión hasta un valor máximo tras el cual, se mantendría o aumentaría ligeramente [67,81,118].

Diversos investigadores han desarrollado procesos en ausencia de hidrógeno para evitar los riesgos que conlleva su empleo en las condiciones de reacción. Para lograrlo han llevado a cabo procesos de transferencia de hidrógeno en los que, el disolvente u otro reactivo, se emplea para proporcionar una fuente de hidrógeno localizado sobre el catalizador. Como se comentó en el apartado I.3.2.A, los disolventes más comunes serían alcoholes como el metanol o el isopropanol. El uso de otros reactivos como el ácido fórmico como donador permitiría el empleo de agua como disolvente y proporcionaría las mismas ventajas [83,119,120]. En estos casos, la reacción se llevaría a cabo en atmósfera inerte, generalmente de N_2 [18]. Otra forma de solventar el problema es el empleo del propio glicerol como fuente de hidrógeno. Roy *et al*., han centrado sus trabajos en el empleo de la reacción de reformado del glicerol para evitar el aporte externo de hidrógeno. En este

caso el empleo de mezclas físicas de Pt/Al_2O_3 y Ru/Al_2O_3 produce un efecto sinérgico que mejora la conversión de glicerol y la selectividad hacia 1,2-PDO en este tipo de reacciones [121].

Finalmente, destacar el trabajo de Delgado *et al*., quienes emplearon catalizadores de Pt soportado sobre diferentes sólidos con carácter ácido como el TiO_2. Observaron que en igualdad de condiciones, la conversión de glicerol era mayor en atmósfera de N_2 que en H_2, aunque las mejores selectividades se dieron en atmósfera reductora [122].

I.3.2.D. Efecto de la temperatura

La necesidad de reducir en lo posible la temperatura de reacción para reducir el consumo energético del proceso, manteniendo un nivel de conversión y selectividad aceptable también ha sido objeto de estudio. Los autores coinciden en que a mayor temperatura se alcanzan mejores conversiones mientras que la selectividad decae a partir de ciertos valores [67,119].

De igual forma, se deben evitar temperaturas demasiado altas que conducirían a la degradación del glicerol, debido a la formación de polímeros o a procesos de reformado [50,121]. En este sentido, Gong *et al*., observaron para catalizadores de Pt soportado sobre óxidos mixtos de W y Ti depositados sobre SiO_2, cómo la selectividad hacia 1,2-PDO era estable hasta los 170-180ºC, y a partir de este punto decaía en favor de productos C2 y C1 [109]. Algunos autores sugieren que la obtención de estos productos se debe a que a elevadas temperaturas se produce el reformado de glicerol a través de un mecanismo radicalario que predomina sobre la hidrogenolisis, afectando

también intermedios de reacción como la acroleína o el acetol y conduciendo a sustancias gaseosas por la ruptura de los enlaces C-C [123].

Por otro lado, se han descrito trabajos para desarrollar co-catalizadores que puedan facilitar la reacción, de forma que esta se produzca a menor temperatura. Existe una amplia gama de compuestos como son las resinas ácidas tipo Amberlita [124], sólidos ácidos como el Nb_2O_5 [125], óxidos de metales de transición soportados [125,126] o incluso la propia estructura cristalina del soporte [127]. Estos compuestos pueden añadirse mezclados con el catalizador físicamente aunque se pueden encontrar como nanopartículas soportadas sobre el mismo catalizador, lo que se conoce como catalizador bifuncional [126].

I.3.2.E. Efecto de aditivos

De forma general, podemos decir que el aditivo es una sustancia que se incorpora al medio de reacción y que va a modificar las características del catalizador. De esta forma, podemos decir que tenemos tres tipos de aditivos: los que se añaden directamente a la reacción, los que se añaden al soporte del catalizador y los que se añaden a la fase metálica.

En cuanto al primer tipo, decir que se han desarrollado trabajos en los que los catalizadores son modificados por medio de ácidos [128] o bases [129] que son añadidas directamente a la reacción. La adición de una base puede tener un efecto sobre el mecanismo de reacción, catalizando procesos como la retroaldolización de los aldoles formados y favoreciendo la obtención de productos mediante el mecanismo DDH [88]. Por otro lado, la adición de ácidos al medio de reacción debería favorecer la deshidratación del glicerol a acetol. En este sentido, Miyazawa *et al*., han observado que la combinación

de Ru/C y Amberlita potencia la deshidratación del glicerol a acetol que posteriormente es hidrogenado a 1,2- PDO sobre la fase metálica, mejorando globalmente la hidrogenolisis del glicerol a temperaturas de reacción moderadas (140ºC) [130].

Otra forma de emplearlos sería incorporándolos a la estructura del catalizador. En este sentido los óxidos de circonio son de los más estudiados [131,132]. Por último, es posible dopar al metal activo soportado con otro metal, con el fin de reducir su actividad o incrementarla, obteniendo sistemas bimetálicos [133].

I.4. Bibliografia

1. J.H. Clark, F.E.I. Deswarte, T.J. Farmer, Biofuels, Bioproducts and Biorefining, 3 (2009) 72-90.
2. G. Centi, R.A. van Santen, Catalysis for Renewables: From Feedstock to Energy Production, John Wiley and Sons, 2007, Messina, Italy.
3. T.E. Amidon, S. Liu, Biotechnology Advances, 27 (2009) 542-550.
4. P. Gallezot, Catal Today, 121 (2007) 76-91.
5. T. Werpy, G. Petersen, Top Value Added Chemicals from Biomass: Volume I -- Results of Screening for Potential Candidates from Sugars and Synthesis Gas, National Renewable Energy Lab., Golden, CO (US), 1 (2004) 1-76.
6. N. Dimitratos, J.A. Lopez-Sanchez, G.J. Hutchings, Topics in Catalysis, 52 (2009) 258-268.
7. K. Pathak, K.M. Reddy, N.N. Bakhshi, A.K. Dalai, Applied Catalysis A: General, 372 (2009) 224-238.

8. M. Pagliaro, R. Ciriminna, H. Kimura, M. Rossi, C.D. Pina, Eur. J. Lipid Science Technology, 111 (2009) 788-799.
9. A. Brandner, K. Lehnert, A. Bienholz, M. Lucas, P. Claus, Topics in Catalysis, 52 (2009) 278-287.
10. C.H. Zhou, J.N. Beltramini, Y.X. Fan, G.Q. Lu, Chemical Society Reviews, 37 (2007) 527-549.
11. D.T. Johnson, K.A. Taconi, Environmental Progress, 26 (2007) 338-348.
12. Mario Pagliaro, Michele Rossi, The Future of Glycerol : 2nd Edition, RSC, Cambridge, UK, 2010.
13. C.A.G. Quispe, C.J.R. Coronado, J. Carvalho, Renewable Sustainable Energy Reviews, 27 (2013) 475-493.
14. T.S. Viinikainen, R.S. Karinen, A.O.I. Krause, Conversion of Glycerol into Traffic Fuels, John Wiley and Son, Helsinki, 2007, p. 45.
15. M. Pagliaro, R. Ciriminna, H. Kimura, M. Rossi, C. Della-Pina, Angewandte Chemie International Edition, 46 (2007) 4434-4440.
16. P.P. Oh, H.L.N. Lau, J. Chen, M.F. Chong, Y.M. Choo, Renewable Sustainable Energy Reviews, 16 (2012) 5131-5145.
17. R.A. Sheldon, Green Chemistry, 16 (2014) 950-963.
18. M. Besson, P. Gallezot, C. Pinel, Chemical Reviews, 114 (2014) 1827-1870.
19. J.C.J. Bart, N. Palmeri, S. Cavallaro, Biodiesel Science and Technology: From Soil to Oil, Elsevier Ltd., Messina, 2010.
20. R. Ciriminna, C.D. Pina, M. Rossi, M. Pagliaro, European Journal of Lipid Science Technology, 116 (2014) 1432-1439.
21. Z. Gholami, A.Z. Abdullah, K.T. Lee, Renewable Sustainable Energy Reviews, 39 (2014) 327-341.

22. M. Stelmachowski, M. Marchwicka, E. Grabowska, M. Diak, A. Zaleska, J. Adv. Oxid. Technol., 17 (2014) 167-178, 12.
23. A. Talebian-Kiakalaieh, N.A.S. Amin, H. Hezaveh, Renewable Sustainable Energy Reviews, 40 (2014) 28-59.
24. Galen J.Suppes, The Biodiesel Handbook: Glycerol Technology Options for Biodiesel Industry, AOCS Publishing, 2010, US.
25. J. Clark, D. Macquarrie, M. Gronnow, V. Budarin, Green Chemistry Principles, John Wiley & Sons, Ltd, 2013, p. 33.
26. L. Prati, P. Spontoni, A. Gaiassi, Topics in Catalysis, 52 (2009) 288-296.
27. J.E. Holladay, J.F. White, J.J. Bozell, D. Johnson, Top Value-Added Chemicals from Biomass - Volume II—Results of Screening for Potential Candidates from Biorefinery Lignin, Pacific Northwest National Laboratory (PNNL), Richland, WA (US) (2007) 1-87.
28. Z. Herseczki, T. Varga, G. Marton, International Journal of Chemical Reactor Engineering, 7 (2009)
29. S. Datta, Y.J. Lin, S.W. Snyder, Advances in Biorefineries: Current and emerging separations technologies in biorefining, Woodhead Publishing, 2014, Cambridge (UK).
30. Y. Nakagawa, K. Tomishige, Catalysis Science and Technology, 1 (2011) 179-190.
31. J. Feng, B. Xu, Progress in Reaction Kinetics and Mechanism, 39 (2014) 1-15.
32. F. Auneau, L.S. Arani, M. Besson, L. Djakovitch, C. Michel, F. Delbecq, P. Sautet, C. Pinel, Topics in Catalysis, 55 (2012) 474-479.
33. C. Montassier, J.C. Ménézo, L.C. Hoang, C. Renaud, J. Barbier, Journal of Molecular Catalysis, 70 (1991) 99-110.

34. J. Ge, Z. Zeng, F. Liao, W. Zheng, X. Hong, S.C.E. Tsang, Green Chemistry, 15 (2013) 2064-2069.
35. A. Marinas, P. Bruijnincx, J. Ftouni, F.J. Urbano, C. Pinel, Catalysis Today, 239 (2015) 31-37.
36. A.V. Bridgwater, R. Chinthapalli, P.W. Smith, Final Report: Identification and market analysis of most promising added-value products to be co-produced with the fuel, Aston University (2010). http://www.bioref-integ.eu/publications/
37. C.S. Lee, M.K. Aroua, W.M.A.W. Daud, P. Cognet, Y. Pérès-Lucchese, P.L. Fabre, O. Reynes, L. Latapie, Renewable Sustainable Energy Reviews, 42 (2015) 963-972.
38. Richard J., S. Lewis, Condensed Chemical Dictionary 15th edition, Wiley-Interscience a John Wiley & Sons, Inc., Publication, Hoboken, New Jersey, 2007
39. T.A. Nijhuis, M. Makkee, J.A. Moulijn, B.M. Weckhuysen, Industrial & Engineering Chemistry Research, 45 (2006) 3447-3459.
40. M. Ghanta, D.R. Fahey, D.H. Busch, B. Subramaniam, ACS Sustainable Chemistry & Engineering, 1 (2013) 268-277.
41. R. Lin, H. Liu, J. Hao, K. Cheng, D. Liu, Biotechnology Letters, 27 (2005) 1755-1759.
42. D. Dietz, A.P. Zeng, Bioprocess and Biosystems Engineering, 37 (2014) 225-233.
43. J.R. Almeida, L.C. Favaro, B. Quirino, Biotechnology for Biofuels, 5 (2012) 48-64
44. S.H. Lee, D.J. Moon, Catalysis Today, 174 (2011) 10-16.
45. D.K. Sohounloue, C. Montassier, J. Barbier, Reaction Kinetics and Catalysis Letters, 22 (1983) 391-397.

46. T.M. Che, Celanese Corp., US4642394A, USA . (1987) 1-4
47. E. Drent, W.W. Jager, United States Patent, US006080898A (2000)
48. O. Schmidt, I. G. Farbenindustrie AG, DE 524101, (1931)
49. A. Martin, U. Armbruster, I. Gandarias, P.L. Arias, European Journal of Lipid Science and Technology, 115 (2013) 9-27.
50. M.A. Dasari, P.P. Kiatsimkul, W.R. Sutterlin, G.J. Suppes, Applied Catalysis A: General, 281 (2005) 225-231.
51. C.H. Zhou, H. Zhao, D.S. Tong, L.M. Wu, W.H. Yu, Catalysis Reviews - Science and Engineering, 55 (2013) 369-453.
52. C. Len, R. Luque, Sustainable Chemical Processes, 2 (2014) 1-10
53. J. ten Dam, K. Djanashvili, F. Kapteijn, U. Hanefeld, ChemCatChem, 5 (2013) 497-505.
54. O.M. Daniel, A. DeLaRiva, E.L. Kunkes, A.K. Datye, J.A. Dumesic, R.J. Davis, ChemCatChem, 2 (2010) 1107-1114.
55. Z. Yuan, P. Wu, J. Gao, X. Lu, Z. Hou, X. Zheng, Catalysis Letters, 130 (2009) 261-265.
56. D. Stosic, S. Bennici, S. Sirotin, C. Calais, J.L. Couturier, J.L. Dubois, A. Travert, A. Auroux, Applied Catalysis A: General, 447–448 (2012) 124-134.
57. K.J.J. Mayrhofer, B.B. Blizanac, M. Arenz, V.R. Stamenkovic, P.N. Ross, N.M. Markovic, J. Phys. Chem. B, 109 (2005) 14433-14440.
58. K. Lehnert, P. Claus, Catalysis Communications, 9 (2008) 2543-2546.
59. G. Larsen, G. Haller, Catalysis Letters, 3 (1989) 103-110.
60. A.K. Dalai, R.V. Sharma, P. Kumar, Catalysis Letters, WO2014134733A1, (2014)
61. K. Kaneda, H. Matsuda, Osaka University, Japan-Daicel Corp. , JP2013166096A, (2013)

62. R. Wei, G. Xiao, L. Niu, X. Li, Southeast University, Peop. Rep. China, CN102344341A (2012).
63. F. Mauriello, H. Ariga, M.G. Musolino, R. Pietropaolo, S. Takakusagi, K. Asakura, Applied Catalysis B: Environmental, 166-167 (2015) 121-131.
64. S. Xia, Z. Yuan, L. Wang, P. Chen, Z. Hou, Applied Catalysis A: General, 403 (2011) 173-182.
65. E.S. Vasiliadou, V.L. Yfanti, A.A. Lemonidou, Applied Catalysis B: Environmental, 163 (2015) 258-266.
66. E.P. Maris, R.J. Davis, Journal of Catalysis, 249 (2007) 328-337.
67. A. Alhanash, E.F. Kozhevnikova, I.V. Kozhevnikov, Catalysis Letters, 120 (2008) 307-311.
68. E.S. Vasiliadou, E. Heracleous, I.A. Vasalos, A.A. Lemonidou, Applied Catalysis B: Environmental, 92 (2009) 90-99.
69. J. Feng, W. Xiong, B. Xu, W. Jiang, J. Wang, H. Chen, Catalysis Communications, 46 (2014) 98-102.
70. E. Gallegos-Suarez, A. Guerrero-Ruiz, I. Rodriguez-Ramos, A. Arcoya, Chemical Engineering Journal, 262 (2015) 326-333.
71. F. Auneau, L.S. Arani, M. Besson, L. Djakovitch, C. Michel, F. Delbecq, P. Sautet, C. Pinel, Topics in Catalysis, 55 (2012) 474-479.
72. F. Auneau, S. Noel, G. Aubert, M. Besson, L. Djakovitch, C. Pinel, Catalysis Communications, 16 (2011) 144-149.
73. Y. Nakagawa, K. Tomishige, Catalysis Surveys From Asia, 15 (2011) 111-116.
74. D. Sun, Y. Yamada, S. Sato, Applied Catalysis A: General, 475 (2014) 63-68.

75. E.S. Vasiliadou, T.M. Eggenhuisen, P. Munnik, P.E. de Jongh, K.P. de Jong, A.A. Lemonidou, Applied Catalysis B: Environmental, 145 (2014) 108-119.
76. D. Sun, Y. Yamada, S. Sato, Applied Catalysis A: General, 475 (2014) 63-68.
77. E.S. Vasiliadou, T.M. Eggenhuisen, P. Munnik, P.E. de Jongh, K.P. de Jong, A.A. Lemonidou, Applied Catalysis B: Environmental, 145 (2014) 108-119.
78. X. Guo, Y. Li, W. Song, W. Shen, Catalysis letters, 141 (2011) 1458-1463.
79. V. Montes, M. Boutonnet, S. Järås, M. Lualdi, A. Marinas, J.M. Marinas, F.J. Urbano, M. Mora, Catalysis Today, 223 (2014) 66-75.
80. B.C. Miranda, R.J. Chimentão, J.B.O. Santos, F. Gispert-Guirado, J. Llorca, F. Medina, F.L. Bonillo, J.E. Sueiras, Applied Catalysis B: Environmental, 147 (2014) 464-480.
81. J. Zhao, W. Yu, C. Chen, H. Miao, H. Ma, J. Xu, Catalysis Letters, 134 (2010) 184-189.
82. J. Ma, W. Yu, M. Wang, X. Jia, F. Lu, J. Xu, Chinese Journal of Catalysis, 34 (2013) 492-507.
83. A. Martin, U. Armbruster, I. Gandarias, P.L. Arias, European Journal of Lipid Science and Technology, 115 (2013) 9-27.
84. J. Chaminand, L.A. Djakovitch, P. Gallezot, P. Marion, C. Pinel, C. Rosier, Green Chemistry, 6 (2004) 359-361.
85. Y. Nakagawa, Y. Shinmi, S. Koso, K. Tomishige, Journal of Catalysis, 272 (2010) 191-194.
86. N. Ueda, Y. Nakagawa, K. Tomishige, Chemistry Letters, 39 (2010) 506-507.

87. M.L. Barbelli, M.D. Mizrahi, F. Pompeo, G.F. Santori, N.N. Nichio, J.M. Ramallo-Lopez, Journal of Physical Chemistry C, 118 (2014) 23645-23653.
88. E.P. Maris, W.C. Ketchie, M. Murayama, R.J. Davis, Journal of Catalysis, 251 (2007) 281-294.
89. Y. Shinmi, S. Koso, T. Kubota, Y. Nakagawa, K. Tomishige, Applied Catalysis B: Environmental, 94 (2010) 318-326.
90. N.H. Tran, G.S.K. Kannangara, Chem. Soc. Rev., 42 (2013) 9454-9479.
91. M.A. Aramendía, V. Boráu, I.M. García, C. Jiménez, F. Lafont, A. Marinas, J.M. Marinas, F.J. Urbano, Journal of Catalysis, 187 (1999) 392-399.
92. A.Y. Stakheev, L.M. Kustov, Applied Catalysis A: General, 188 (1999) 3-35.
93. A.L.M. da Silva, J.P. den Breejen, L.V. Mattos, J.H. Bitter, K.P. de Jong, F.B. Noronha, Journal of Catalysis, 318 (2014) 67-74.
94. M. López-Haro, J.J. Delgado, J.M. Cies, E. Del Rio, S. Bernal, R. Burch, M.A. Cauqui, S. Trasobares, J.A. Pérez-Omil, P. Bayle-Guillemaud, J.J. Calvino, Angewandte Chemie - International Edition, 49 (2010) 1981-1985.
95. C. Deng, X. Duan, J. Zhou, D. Chen, X. Zhou, W. Yuan, Catalysis Today, (2014)
96. V. Montes, M. Boutonnet, S. Järås, M. Lualdi, A. Marinas, J.M. Marinas, F.J. Urbano, M. Mora, Catalysis Today, 223 (2014) 66-75.
97. S. Alayoglu, G.A. Somorjai, Catalysis Letters, 145 (2014) 249-271.
98. A. Wawrzetz, B. Peng, A. Hrabar, A. Jentys, A.A. Lemonidou, J.A. Lercher, Journal of Catalysis, 269 (2010) 411-420.

99. P. Hirunsit, C. Luadthong, K. Faungnawakij, RSC Advances, 5 (2015) 11188-11197.
100. T. Mizugaki, T. Yamakawa, R. Arundhathi, T. Mitsudome, K. Jitsukawa, K. Kaneda, Chemistry Letters, 41 (2012) 1720-1722.
101. Y. Nakagawa, M. Tamura, K. Tomishige, Journal of Materials Chemistry A, 2 (2014) 6688-6702.
102. S. García-Fernández, I. Gandarias, J. Requies, M.B. Güemez, S. Bennici, A. Auroux, P.L. Arias, Journal of Catalysis, 323 (2015) 65-75.
103. T. Kurosaka, H. Maruyama, I. Naribayashi, Y. Sasaki, Catalysis Communications, 9 (2008) 1360-1363.
104. S. Zhu, Y. Qiu, Y. Zhu, S. Hao, H. Zheng, Y. Li, Catalysis Today, 212 (2013) 120-126.
105. R. Rodrigues, N. Isoda, M. Goncalves, F.C.A. Figueiredo, D. Mandelli, W.A. Carvalho, Chemical Engineering Journal (Amsterdam, Neth.), 198-199 (2012) 457-467.
106. J. Feng, H. Fu, J. Wang, R. Li, H. Chen, X. Li, Catalysis Communications, 9 (2008) 1458-1464.
107. P.T. Anastas, J.C. Warner, Green Chemistry: Theory and Practice, Oxford University Press, Oxford (UK), 1998.
108. R.A. Sheldon, Journal of Environmental Monitoring, 10 (2008) 406-407.
109. L. Gong, Y. Lu, Y. Ding, R. Lin, J. Li, W. Dong, T. Wang, W. Chen, Applied Catalysis A: General, 390 (2010) 119-126.
110. C. Wang, H. Jiang, C. Chen, R. Chen, W. Xing, Chemical Engineering Journal, 264 (2015) 344-350.
111. I. Gandarias, P.L. Arias, J. Requies, M. El Doukkali, M.B. Güemez, Journal of Catalysis, 282 (2011) 237-247.

112. M.A. Aramendía, V. Boráu, C. Jiménez, J.M. Marinas, A. Porras, F.J. Urbano, Journal of Materials Chemistry, 9 (1999) 819-825.
113. M.A. Aramendía, V. Boráu, C. Jiménez, J.M. Marinas, A. Porras, F.J. Urbano, Journal of the Chemical Society - Faraday Transactions, 93 (1997) 1431-1438.
114. R.B. Mane, A.M. Hengne, A.A. Ghalwadkar, S. Vijayanand, P.H. Mohite, H.S. Potdar, C.V. Rode, Catalysis Letters, 135 (2010) 141-147.
115. D. Sun, Y. Yamada, S. Sato, Applied Catalysis A: General, 475 (2014) 63-68.
116. S. Zhu, Y. Zhu, S. Hao, L. Chen, B. Zhang, Y. Li, Catalysis Letters, 142 (2012) 267-274.
117. J. Tao, M. Ren, S. Chen, H. Qiang, W. Ying, F. Cao, Advanced Materials Research, 906 (2014) 103-111, 10.
118. A. Wolosiak-Hnat, E. Milchert, B. Grzmil, Chemical Engineering and Technology, 36 (2013) 411-418.
119. I. Gandarias, J. Requies, P.L. Arias, U. Armbruster, A. Martin, Journal of Catalysis, 290 (2012) 79-89.
120. E.S. Vasiliadou, V.L. Yfanti, A.A. Lemonidou, Applied Catalysis B: Environmental, 163 (2015) 258-266.
121. D. Roy, B. Subramaniam, R.V. Chaudhari, Catal Today, 156 (2010) 31-37.
122. S.N. Delgado, D. Yap, L. Vivier, C. Especel, Journal of Molecular Catalysis A: Chemical, 367 (2013) 89-98.
123. Ž. Knez, E. Markocic, M.K. Hrncic, M. Ravber, M. Skerget, The Journal of Supercritical Fluids, 96 (2015) 46-52.

124. C.I.C.B. Zanin, E. Jordao, D. Mandelli, F.C.A. Figueiredo, W.A. Carvalho, E.V. Oliveira, Reaction Kinetics, Mechanisms and Catalysis, 115 (2015) 293-310.
125. M. Balaraju, V. Rekha, P.S.S. Prasad, B.L.A.P. Devi, R.B.N. Prasad, N. Lingaiah, Applied Catalysis A: General, 354 (2009) 82-87.
126. S. Zhu, X. Gao, Y. Zhu, Y. Li, Journal of Molecular Catalysis A: Chemical, 398 (2015) 391-398.
127. J. Hu, Y. Fan, Y. Pei, M. Qiao, K. Fan, X. Zhang, B. Zong, ACS Catalysis, 3 (2013) 2280-2287.
128. J. ten Dam, K. Djanashvili, F. Kapteijn, U. Hanefeld, ChemCatChem, 5 (2013) 497-505.
129. F. Auneau, C. Michel, F. Delbecq, C. Pinel, P. Sautet, Chemical Eurpean Journal, 17 (2011) 14288-14299.
130. T. Miyazawa, Y. Kusunoki, K. Kunimori, K. Tomishige, Journal of Catalysis, 240 (2006) 213-221.
131. B.M. Reddy, M.K. Patil, Chemical Reviews, 109 (2009) 2185-2208.
132. C. García-Sancho, R. Moreno-Tost, J. Mérida-Robles, J. Santamaría-González, A. Jiménez-López, P. Maireles-Torres, Applied Catalysis A: General, 433–434 (2012) 179-187.
133. X. Li, C. Zhang, H. Cheng, L. He, W. Lin, Y. Yu, F. Zhao, Journal of Molecular Catalysis A: Chemical, 395 (2014) 1-6.

Capítulo II

Hipótesis y objetivos

II. Hipótesis y Objetivos

II.1. Motivación de la tesis

Uno de los grandes retos actuales de la comunidad científica en relación con la denominada Química Sostenible, es la búsqueda de alternativas a los modelos energéticos actuales basados en la industria petroquímica. Los nuevos sistemas han de ser benévolos con el medio ambiente y utilizar, preferentemente, recursos renovables. En este sentido, se han propuesto diferentes alternativas a los combustibles fósiles tales como las energías eólica, solar o la biomasa, entre otras. De entre las alternativas propuestas, sólo la biomasa es, además de fuente energética, una fuente renovable de productos químicos lo que resulta especialmente interesante desde el punto de vista socioeconómico, ya que permite obtener energía y productos químicos a partir de una única fuente.

Entre los diferentes productos químicos procedentes de la biomasa cuya valorización es interesante desde el punto de vista económico, destaca el glicerol (o glicerina), obtenido como subproducto en la producción de biodiesel. El interés en este compuesto se debe a la elevada cantidad que se obtiene de este subproducto y que se ha introducido en el mercado produciendo una caída importante en el precio del mismo al no existir tecnologías capaces de consumir el "stock" generado en biorefinería. En cuanto a las diferentes posibilidades para la valorización del glicerol, una de las reacciones que más interés suscita es la hidrogenolisis, para la que se utilizan catalizadores metálicos soportados, entre los que se encuentran aquéllos que incorporan metales nobles como fase activa (ej. Pt, Rh, Pd, Au).

Respecto al catalizador empleado en este proceso, otro de los aspectos a tener en cuenta en el comportamiento catalítico del mismo es el soporte empleado, cuyo papel puede no limitarse a la mera dispersión de la fase

metálica, sino que por sus características ácido-base y/o redox pueden influir en el proceso químico. De particular interés son los óxidos metálicos parcialmente reducibles (como ZrO_2, TiO_2, SnO_2, CeO_2 y ZnO), susceptibles de inducir, en mayor o menor medida, interacciones fuerte metal-soporte, o SMSI de sus siglas en inglés. En particular, nuestro grupo de investigación tiene experiencia previa en el empleo del ZnO como soporte de Pt, describiendo la aparición de esta interacción a temperaturas de reducción del orden de 200-400ºC y habiendo estudiado su influencia en algunos procesos catalizados como la reducción quimioselectiva del C=O frente al C=C.

II.2. Planteamiento de objetivos

El objetivo principal de esta Tesis Doctoral consistió en evaluar las diferentes posibilidades de transformación, mediante procesos catalizados, del glicerol en productos de alto valor añadido, a partir de fuentes alternativas y procesos sostenibles.

Para la consecución de este objetivo general se establecieron una serie de objetivos transversales que sirvieron de base para definir el trabajo a realizar y que se detallan a continuación:

- Estudiar la conversión de glicerol, en fase líquida, catalizada por sólidos con características ácido-básicas superficiales, en diferentes ambientes redox. Establecer un abanico de posibilidades tan amplio como sea posible para la conversión de glicerol en productos de alto valor añadido.

- Estudiar la conversión de glicerol, en fase líquida, sobre catalizadores metálicos soportados en atmósfera reductora. Optimizar la actividad y selectividad en función de las variables de reacción.
- Establecer, en la medida de lo posible, una relación entre la actividad observada y el metal o soporte empleados. Determinar el origen de la desactivación que afecta a los catalizadores durante la reacción.

En base a estas consideraciones previas, se definió un plan de trabajo con una serie de objetivos específicos.

II.3. Síntesis de catalizadores

Se abordará una síntesis dirigida de catalizadores metálicos soportados que permita estudiar la influencia del metal soportado y de las propiedades acido-básicas y redox de los soportes en la hidrogenolisis en fase liquida de glicerol.

II.3.1. Influencia del metal noble y de las propiedades redox del soporte

En un primer estudio, se realizará una comparativa del comportamiento de diferentes metales nobles en la reacción. La incorporación del metal se realizará mediante deposición-precipitación, teniendo como objetivo establecer la influencia del metal y del soporte empleado en la reacción, en particular en lo que respecta al papel que juegan las interacciones fuertes metal-soporte. Para ello, se sintetizarán los catalizadores metálicos de Pt soportado sobre soportes parcialmente reducibles como ZnO, ZrO_2, TiO_2 y SnO_2. Una vez determinado el soporte más activo, se procederá a sintetizar una nueva batería de catalizadores incorporando distintos metales nobles como Rh, Pd, Pt y Au sobre dicho soporte.

II.3.2. Influencia de las propiedades ácido-básicas de los soportes

Se prepararán, mediante el procedimiento de impregnación hasta humedad incipiente, una segunda serie de catalizadores de Pt soportado sobre diferentes soportes comerciales con distintas propiedades ácidas (Al_2O_3 ácida), básicas (Al_2O_3 básica, CeO_2 y La_2O_3) y anfóteras (ZnO), con la finalidad de analizar la influencia de estas propiedades en la reacción.

II.3.3. Potenciación de las propiedades ácidas de los soportes

Se sintetizará una tercera serie de catalizadores de Pt soportado sobre un óxido de zirconio (ZrO_2) preparado mediante el método sol-gel y convenientemente modificado mediante la incorporación, por impregnación, de aditivos que potencien sus propiedades ácidas, tales como B_2O_3 y H_2SO_4 o polioxometalatos del tipo $H_3SiW_{12}O_{40}$ o $H_3PMo_{12}O_{40}$.

II.4. Caracterización de los catalizadores sintetizados

Los catalizadores sintetizados serán exhaustivamente caracterizados tanto desde el punto de vista textural, estructural como químico-superficial. Dicha caracterización se llevará a cabo mediante diferentes técnicas como la obtención de isotermas de adsorción/desorción de N_2 a su temperatura de ebullición, microscopia electrónica de transmisión (TEM) y barrido (SEM), difracción de rayos-X (DRX), espectroscopias de infrarrojo (FTIR) y Raman (FT-Raman), plasma inductivamente acoplado (ICP-MS) y espectroscopia fotoelectrónica de rayos-X (XPS).

Por otro lado, las propiedades químico-superficiales de los catalizadores, de especial interés desde el punto de la actividad catalítica, serán determinadas mediante quimisorción de moléculas sonda como piridina, para determinar la acidez superficial, y dióxido de carbono, para la basicidad

superficial. El análisis de dicha interacción podrá llevarse a cabo mediante desorción térmica programada (TPD) o espectroscopia infrarroja.

Finalmente, las propiedades de la fase metálica de los catalizadores de Rh, Pd, Pt y Au soportados se determinarán mediante quimisorción selectiva de hidrógeno sobre la fase metálica, así como a través del estudio por microscopia electrónica de transmisión (TEM) de las partículas metálicas soportadas.

Todas las técnicas instrumentales enumeradas anteriormente se encuentran disponibles en el Departamento de Química Orgánica, el Instituto Universitario de Investigación en Química Fina y Nanoquímica (IUIQFN) o en los Servicios Centrales de Apoyo a la Investigación (SCAI) de la Universidad de Córdoba.

II.5. Conversión de glicerol en fase líquida

Los catalizadores sintetizados se ensayarán en diferentes tipos de procesos de reacción, en fase líquida, conducentes a la conversión del glicerol en disoluciones acuosas en productos de alto valor añadido.

El dispositivo experimental se basa en una autoclave tipo "Berghoff" de media presión y 150 mL de volumen del vaso de reacción. El equipo está dotado de un sistema de válvulas que permite la extracción de muestras (líquidas y gaseosas) así como controlar la calefacción del vaso de reacción hasta una temperatura máxima de 250ºC. El análisis de los productos de reacción se realizará en un cromatógrafo de gases Agilent® 7890, equipado con una columna Nukol® de 30 m y 0.53 mm ID.

II.5.1. Efecto del metal noble y del soporte del catalizador

La primera serie de catalizadores sintetizados permitirá estudiar la eficacia de los distintos metales nobles seleccionados (Rh, Pd, Pt, Au) en el proceso de hidrogenolisis de glicerol, así como analizar la influencia de las posibles interacciones fuertes metal soporte (SMSI) en la actividad catalítica y selectividad a los distintos productos de reacción. Se analizará la influencia de la atmósfera, inerte o reductora, en la conversión de glicerol.

II.5.2. Estudio del proceso de desactivación del catalizador

La segunda serie de catalizadores a base de Pt soportado sobre soportes comerciales con diferentes propiedades ácido-básicas permitirá estudiar la influencia de dichas propiedades en la distribución de productos de reacción así como un análisis de las posibles causas de desactivación de los catalizadores utilizados en el proceso. En este sentido, los artículos publicados sobre la desactivación de catalizadores sólidos en el proceso de transformación de glicerol en medio reductor son escasos. Se abordará dicho estudio en base al papel que juegan las propiedades ácidas o básicas del catalizador y los diferentes intermedios de reacción formados en el proceso sobre la desactivación de los sólidos.

II.5.3. Influencia de las propiedades ácidas superficiales del catalizador

De acuerdo con la bibliografía, la reacción de hidrogenolisis de glicerol presenta como etapa limitante la deshidratación de glicerol hasta acetol, el cual se reduce con rapidez a propilenglicol en las condiciones de reacción. El desarrollo de catalizadores con propiedades ácidas mejoradas puede suponer una ventaja para el proceso, al facilitar la deshidratación a acetol. Los catalizadores de Pt soportado sobre ZrO_2 modificado con aditivos

que potencien la acidez se ensayarán en la hidrogenolisis de glicerol en atmósfera reductora con el fin de evaluar el impacto de los diferentes modificadores sobre la actividad catalítica y la distribución de productos de reacción. Se estudiará, asimismo, el efecto de la temperatura y del tiempo de reacción, así como la estabilidad de los posibles intermedios de reacción formados. También se llevarán estudios de desactivación y reutilización para el mejor catalizador (durabilidad).

Capítulo III

Transformación catalítica de glicerol sobre diferentes sistemas metálicos soportados sobre ZnO

Chapter III

Catalytic transformation of glycerol on several metal systems supported on ZnO

III. Catalytic transformation of glycerol on several metal systems supported on ZnO

Catalysis Today 196 (2012) 91–100

Contents lists available at SciVerse ScienceDirect

Catalysis Today

journal homepage: www.elsevier.com/locate/cattod

Catalytic transformation of glycerol on several metal systems supported on ZnO

Manuel Checa [a], Florian Auneau [b], Jesús Hidalgo-Carrillo [a], Alberto Marinas [a], José M. Marinas [a], Catherine Pinel [b], Francisco J. Urbano [a] *

[a] Faculty of Sciences, University of Córdoba, Campus de Rabanales, Marie Curie Building, E-14014 Córdoba, Spain
[b] IRCELYON, UMR 5256 CNRS/UCBL, 2 avenue Albert Einstein, 69626 Villeurbanne Cedex, France

ARTICLE INFO

Article history:
Received 14 November 2011
Received in revised form 8 February 2012
Accepted 8 February 2012
Available online 15 March 2012

Keywords:
Glycerol hydrogenolysis
Strong metal–support interaction (SMSI)
Platinum
Rhodium
Palladium
Gold
1,2-Propanediol (1,2-PDO)
Lactic acid
Acetol

ABSTRACT

Different metal systems consisting in platinum supported on several reducible supports (5% by weight) were synthesized through the deposition–precipitation technique and tested for glycerol hydrogenolysis. Interestingly, supports exhibiting the highest conversions were those with the greatest strong metal–support interaction (SMSI) effect, ZnO and SnO_2, eventually forming alloys (Pt–Zn and Pt–Sn, respectively). ZnO was subsequently selected for further studies as support for Rh, Pt, Pd and Au and the resulting solids were tested again for glycerol catalytic transformation under reductive or inert atmosphere at 453 K. Under similar reaction conditions, glycerol conversion order followed the sequence Pt > Rh ≫ Pd ≫ Au. Moreover, the solids reduced at 473 K were more active than those activated at 673 K, which evidences the detrimental effect of the increase in metal particle size and/or alloy formation on the catalytic performance. Quite high yields to lactic acid were achieved in a basic medium (e.g. 68% for Rh/ZnO–473 under H_2) whereas yield to 1,2-PDO was more modest (26% for Rh/ZnO-673 under similar reaction conditions).

1. Introduction

Glycerol, obtained as a by-product in biodiesel manufacture, is a versatile feedstock for the production of a full range of chemicals, polymers and fuels. Some of the processes described in the literature for glycerol valorization include polymerization [1], etherification to produce fuel additives as octane boosters [2], dehydration to acrolein, an important intermediate in the manufacture of polymers [3], or selective oxidation to dihydroxyacetone [4] a versatile compound extensively used as a cosmetic ingredient, among others. Moreover, glycerol catalytic transformation on different metals under hydrogen or inert atmosphere can lead to a wide range of chemicals [5–9], some of the routes being indicated in Fig. 1. Hydrogen generated through aqueous phase reforming allows the formation of reduction products under inert atmosphere. Two of the most interesting chemicals produced through glycerol catalytic transformation are 1,2-propanediol (1,2-PDO) and lactic acid (LA). The former can be used in the food industry, as a less toxic alternative to 1,2-ethanediol in antifreeze and as a deicer or as a feedstock in the preparation of polyester resins for film and fiber manufacture [9]. As for the latter, it is well-known as a moisturizer (cosmetics) and a mordant (i.e. a chemical that help fabrics accept dyes in textiles). Moreover, it is used in the dairy industry as pH regulator or preservative. Ethyl lactate is also a common solvent. Finally, poly-lactic acid is a well-known biodegradable polymer (for food packaging, surgical implants, etc.) [10].

Ruthenium is probably the most-widely used noble catalysts in glycerol hydrogenolysis [8,11] though some others such as Pt [6], Rh [12,13] Pd [12,13], Ir [14] or even first row transition metals (Cu [13], Ni [15], Co [16]), just to cite some examples, have also been reported. As can be inferred from Fig. 1, not only activity but also selectivity to the target molecule should be considered when choosing a metal. In this sense, Ru is probably the most active metal though it normally leads to large amounts of liquid (ethylene glycol and 1-propanol) and gaseous (methane, ethane and propane) by-products. There also have been several attempts at tuning the selectivity of metals through the addition of acid or bases [6,12] or the modification of the noble-metal with low-valent metal oxides (e.g. ReO_x) [17]. Finally, some other factors affecting the process are metal particle size or support [18–20].

In several previous papers we showed that reducible supports can lead to interesting catalytic performance in several oxidations and reductions [21,22] through the promotion of strong metal–support interactions (SMSI), eventually resulting, in some cases, in the formation of alloys.

* Corresponding author. Fax: +34 957212066.
E-mail address: FJ.urbano@uco.es (F.J. Urbano).

0920-5861/$ – see front matter © 2012 Elsevier B.V. All rights reserved.
doi:10.1016/j.cattod.2012.02.036

In this chapter, different metal systems consisting in platinum supported on several reducible supports (5% by weight) were synthesized through the deposition-precipitation technique and tested for glycerol hydrogenolysis. Interestingly, supports exhibiting the highest conversions were those with the greatest strong metal-support interaction (SMSI) effect, ZnO and SnO_2, eventually forming alloys (Pt-Zn and Pt-Sn, respectively). ZnO was subsequently selected for further studies as support for Rh, Pt, Pd and Au and the resulting solids were tested again for glycerol catalytic transformation under reductive or inert atmosphere at 453K. Under similar reaction conditions, glycerol conversion order followed the sequence Pt>Rh>>Pd>>Au. Moreover, the solids reduced at 473K were more active than those activated at 673K, which evidences the detrimental effect of the increase in metal particle size and/or alloy formation on the catalytic performance. Quite high yields to lactic acid were achieved in a basic medium (e.g. 68% for Rh/ZnO-473 under H_2) whereas yield to 1,2-PDO was more modest (26% for Rh/ZnO-673 under similar reaction conditions).

III.1. Introduction

Glycerol, obtained as a by-product in biodiesel manufacture, is a versatile feedstock for the production of a full range of chemicals, polymers and fuels. Some of the processes described in the literature for glycerol valorization include polymerization [1], etherification to produce fuel additives as octane boosters [2], dehydration to acrolein, an important intermediate in the manufacture of polymers [3], or selective oxidation to dihydroxyacetone [4] a versatile compound extensively used as a cosmetic

ingredient, among others. Moreover, glycerol catalytic transformation on different metals under hydrogen or inert atmosphere can lead to a wide range of chemicals [5-9], some of the routes being indicated in Figure 1. Hydrogen generated through aqueous phase reforming allows the formation of reduction products under inert atmosphere. Two of the most interesting chemicals produced through glycerol catalytic transformation are 1,2-propanediol (1,2-PDO) and Lactic acid (LA). The former can be used in the food industry, as a less toxic alternative to 1,2-ethanediol in antifreeze and as a de-icer or as a feedstock in the preparation of polyester resins for film and fiber manufacture [9]. As for the latter, it is well-known as a moisturizer (cosmetics) and a mordant (i.e. a chemical that help fabrics accept dyes in textiles). Moreover, it is used in the dairy industry as pH regulator or preservative. Ethyl lactate is also a common solvent. Finally, poly-lactic acid is a well-known biodegradable polymer (for food packaging, surgical implants, etc) [10].

Ruthenium is probably the most-widely used noble catalysts in glycerol hydrogenolysis [8,11] though some others such as Pt [6], Rh [12, 13] Pd [12, 13], Ir [14] or even first row transition metals (Cu [13], Ni [15], Co [16]), just to cite some examples, have also been reported. As can be inferred from Figure 1, not only activity but also selectivity to the target molecule should be considered when choosing a metal. In this sense, Ru is probably the most active metal though it normally leads to large amounts of liquid (ethylene glycol and 1-propanol) and gaseous (methane, ethane and propane) by-products. There also have been several attempts at tuning the selectivity of metals through the addition of acid or bases [6,12] or the modification of the noble-metal with low-valent metal oxides (e.g. ReO_x) [17]. Finally, some other factors affecting the process are metal particle size or support [18-20].

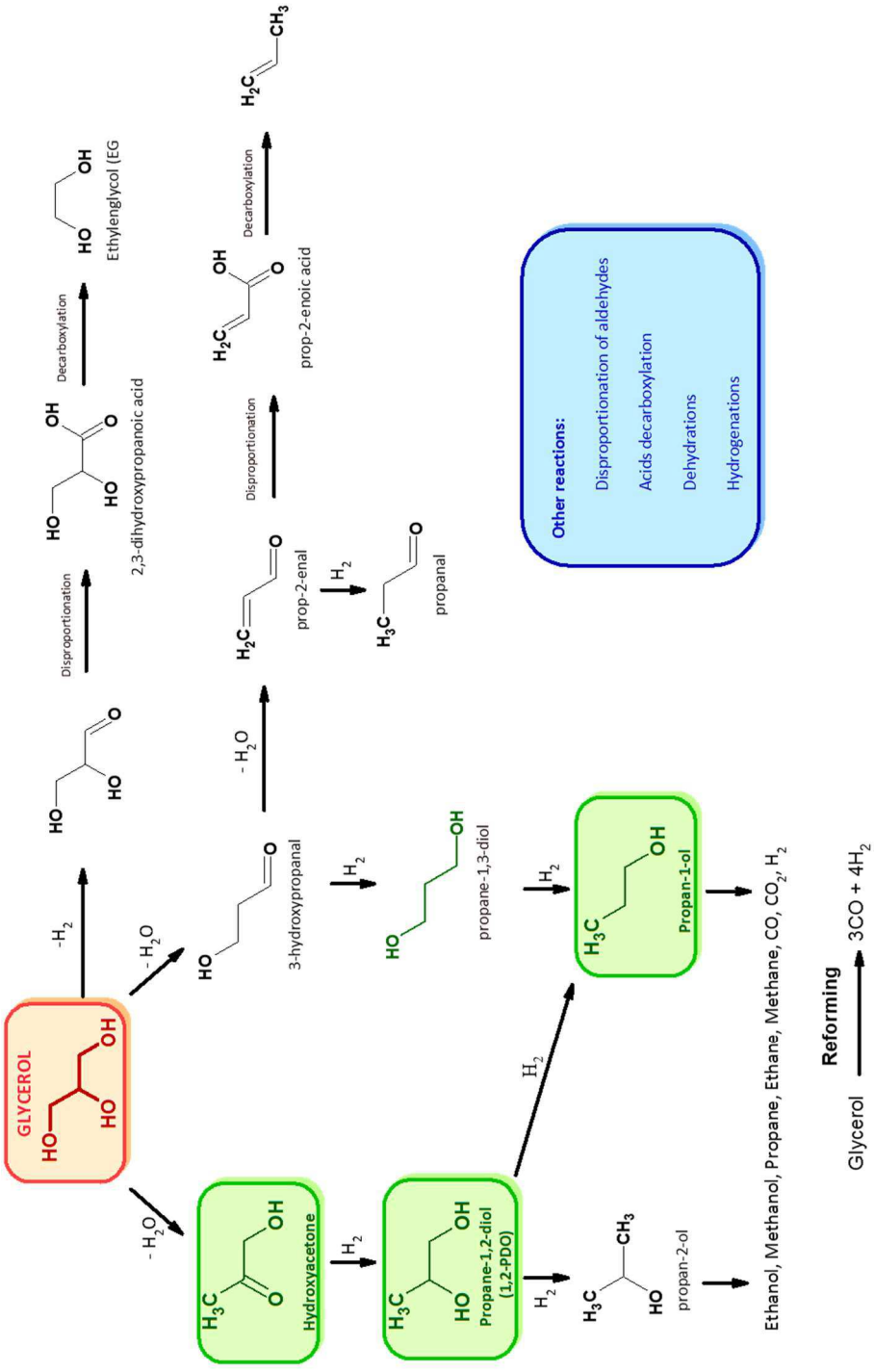

Figure 1: Some catalytic transformation routes from glycerol described in the literature under hydrogen or inert atmosphere.

In several previous papers we showed that reducible supports can lead to interesting catalytic performance in several oxidations and reductions [21, 22] through the promotion of strong metal-support interactions (SMSI), eventually resulting, in some cases, in the formation of alloys.

The present piece of research is aimed at exploring the effect of several reducible supports on the catalytic performance of diverse metal systems in glycerol transformation, paying special attention to the selectivity to 1,2-PDO or lactic acid.

III.2. Experimental

III.2.1. Synthesis of different platinum-supported systems

A first screening was carried out using different platinum-containing systems synthesized through the deposition-precipitation method. The synthesis and characterization of the solids are described elsewhere [22]. Therefore, an aqueous solution containing 8% (w/w) chloroplatinic acid (Sigma–Aldrich Ref. 262587) was used as the metal precursor and the following metal oxides as supports: tin (IV) oxide (Sigma–Aldrich Ref. 549657), zirconium (IV) oxide (Sigma–Aldrich Ref. 544760), zinc (II) oxide (Sigma–Aldrich Ref. 544906), and titanium (IV) oxide (Degussa, P-25).

The synthetic procedure was as follows: a volume of 6.57 mL of chloroplatinic acid solution was diluted to 200 mL with Milli-Q water and adjusted to pH 7 by adding 0.1M NaOH (FLUKA Ref. 43617). Then, an amount of 4.75 g of support was added and the mixture readjusted to pH 7 with NaOH for acid supports or HCl for basic supports. The solution containing the support was refluxed at 353K under vigorous stirring for 2 h.

Then, a volume of 10mL of isopropanol was added, the temperature raised to 383K and refluxing continued for 30 min, after which the mixture was vacuum filtered and the filtrate washed with three portions of 25mL of water each.

The resulting solid was dried in a muffle furnace at 383K for 12 h, ground and calcined at 673K for 4 h. After calcination, the solid was ground again, sieved through a mesh of 0.149 mm pore size and stored in a topaz flask. The nominal proportion of Pt in the catalyst thus obtained was 5 wt%. Finally, the catalyst was reduced under a hydrogen stream flowing at 30 $mL \cdot min^{-1}$ at selected temperatures for 2 h. Reduction temperature was chosen according to significant features observed in the temperature-programmed reduction profiles. The solid names include the metal, its support and the reduction temperature used, in Kelvin (e.g. Pt/ZnO-473).

III.2.2. Synthesis of ZnO-supported metal systems

The first screening of supports resulted in the choice of ZnO for subsequent incorporation of metals (Pt, Rh, Au or Pd) in a 5 wt% nominal content. The synthetic procedure (see supplementary information Figure S1) was the same as described for Pt-containing solids but using the following precursors: H_2PtCl_6, $RhCl_3$, $HAuCl_4$ and $Pd(NO_3)_2$.

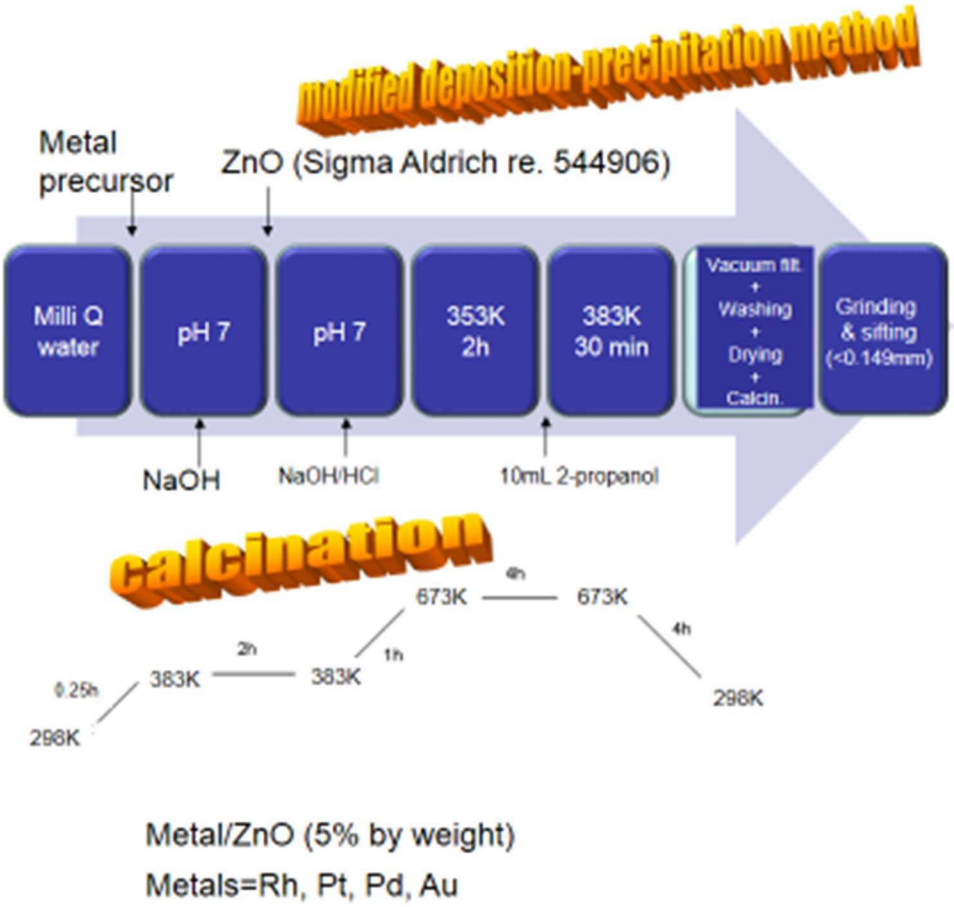

Figure S1. Schematic representation of the synthetic procedure used to obtain the different ZnO-supported metal systems used in the present work.

In the case of palladium no chloride precursor was used since its solubility in water is very low, requiring the use of HCl to dissolve it which results in a pH 3 which could attack the support. Catalyst nomenclature follows the same criteria as described in section 2.1. Therefore, for instance, Rh/ZnO or Pd/ZnO-673 describes the as-synthesized Rh-system or the palladium solid reduced at 673K, respectively.

III.2.3. Characterization

Elemental analysis of metal containing samples was performed using inductively coupled plasma mass spectrometry (ICP-MS). Measurements were made on a Perkin–Elmer ELAN DRC-e instrument following dissolution of the sample in a 1:1:1 H_2SO_4/HF/H_2O mixture. Calibration was done by using PE Pure Plus atomic spectroscopy standards, also from Perkin–Elmer.

Surface areas of the solids were determined from nitrogen adsorption–desorption isotherms obtained at liquid nitrogen temperature on a Micromeritics ASAP-2010 instrument, using the Brunnauer–Emmett–Teller (BET) method. All samples were degassed to 0.1 Pa at 383K prior to measurement.

Transmission electron microscopy (TEM) images were obtained using a Philips CM-10 microscope. All samples were mounted on 3mm holey carbon copper grids.

X-ray patterns for the samples of the first screening for supports were obtained with a Siemens D-5000 diffractometer equipped with a DACO-MP automatic control and data acquisition system. The instrument was used with CoK_α radiation and a graphite monochromator. In the case of the ZnO-supported metal systems, the X-Ray diffractograms were performed with a Bruker D8A25 Advance diffractometer (λ = 1.54184 Å) using a one dimensional multistrip fast detector (LynxEye) with 191 channels on 2.94° at 50 kV and 35 mA.

Temperature-programmed reduction (TPR) measurements were made with a Micromeritics TPD-TPR 2900 analyser. An amount of 200mg of catalyst was placed in the sample holder and reduced in a 5:95 H_2/Ar stream

flowing at 40 $mL \cdot min^{-1}$. The temperature was ramped from 313 to 758K at $10K \cdot min^{-1}$ (213K and 673K in the case of Pd/ZnO solid).

X-ray photoelectron spectroscopy (XPS) data were recorded on 4mm ×4mm pellets 0.5mm thick that were obtained by gently pressing the powdered materials following outgassing to a pressure below about 2×10^{-8} Torr at 423K in the instrument pre-chamber to remove chemisorbed volatile species. The main chamber of the Leibold-Heraeus LHS10 spectrometer used, capable of operating down to less than 2×10^{-9} Torr, was equipped with an EA-200MCD hemispherical electron analyser with a dual X-ray source using AlKα (hv = 1486.6 eV) at 120 W, at 30 mA, with C(1s) as energy reference (284.6 eV).

III.2.4. Catalytic reaction and analytical method

Initial screening of the supports was conducted in a Berghof HR-100 stainless steel high-pressure autoclave equipped with a 75 mL PTFE vessel and a magnetic stirrer. Under standard conditions, 20 mL of a 1.36M solution of glycerol in water and 200mg catalysts were introduced in the vessel. Reactor was then purged with hydrogen and temperature (448K) and hydrogen pressure (6 bar) adjusted. The stirring rate was 1000rpm. After 6h or 15h of reaction, stirring was stopped and the vessel cooled with an ice bath. Reaction mixture was homogenized and analyzed by GC-FID (Agilent Technologies 7890, with a Supelco 25357 Nukol™ capillary column). Quantification was carried out through the corresponding calibration curves for glycerol, acetol, 1,2-PDO and n-propanol.

In the case of reactions on diverse ZnO-supported metal systems, two different reactors were used, utilising the same temperature (453K), pressure (20 bar of He or H_2) glycerol concentration (0.68 M, i.e. 5% glycerol in water), stirring rate (1000 rpm) and glycerol/catalyst ratio. The first reactor was a stainless still autoclave with a 200 mL Teflon vessel which allowed sampling at different time intervals. Reaction volume was 100mL and catalyst weight 500 mg. The second reactor was a Slurry Phase Reactor 16 (AMTEC), using 6mL of the 0.68M glycerol aqueous solution and 30 mg of catalyst. Reaction time was 12h. For reactions at pH 13, pH value was adjusted with NaOH 1M. In both cases, quantification was carried out by HPLC on a CarboSep 107H column (0.5 mL·min^{-1} 0.005 N H_2SO_4, 313K). 1,3-PDO, 1,2-PDO, ethylene glycol, 1-propanol, 2-propanol, ethanol, methanol, acetol, lactic acid, formic acid and acetic acid were analyzed. GC-MS analysis confirmed the identification of lactic acid and 1,2-propanediol.

Conversion (Conv(%)) of glycerol was defined as the number of mol of glycerol consumed reported to the initial number of mol of glycerol. Selectivity to a given product *i* was calculated according to the following equation:

$$Sel_i^t(\%) = \frac{X_i^t \times nC_i}{X_{gly}^t \times 3} \times 100$$

Yields were similarly expressed as:

$$Y_i^t(\%) = \frac{X_i^t \times nC_i}{X_{gly}^0 \times 3} \times 100$$

.

$$\text{Or, } Y_i^t(\%) = Conv(\%) \times \frac{Sel_i^t(\%)}{100}$$

with X_i^t and X^t_{gly}: mol of product *i* and mol of reacted glycerol at reaction time *t*, respectively; X^0_{gly} initial amount of glycerol; nC_i standing for the number of carbon atoms of the product *i*.

III.3. Results and discussion

III.3.1. First screening of supports

Initially, different systems based on platinum supported on SnO_2, ZrO_2, ZnO and TiO_2 were synthesized through the deposition-precipitation method as described in section 2.2. Platinum nominal content was 5% by weight. The systems were then tested for glycerol hydrogenolysis. Two different temperatures were used for reduction of the solids: 473K and 673K. In the case of using SnO_2 as the support, the higher temperature was 573K in order to avoid tin sublimation. Results found in terms of conversion for t=6h and 15h are represented in Figure 2A. As can be seen, the most active systems were those supported on SnO_2 and ZnO. Results found for characterization of the above-mentioned systems (see supplementary information, Figures S2 and S3) showed that the most active systems Pt/SnO_2 and Pt/ZnO were those exhibiting a strongest metal-support interaction, eventually resulting, at the highest reduction temperature (573K or 673K), in the formation of an alloy.

Considering both Pt/ZnO and Pt/SnO_2 solids, Pt/ZnO is the most selective solid to 1,2-PDO after 15h of reaction (Figure 2B) which prompted us to select Pt/ZnO for further studies.

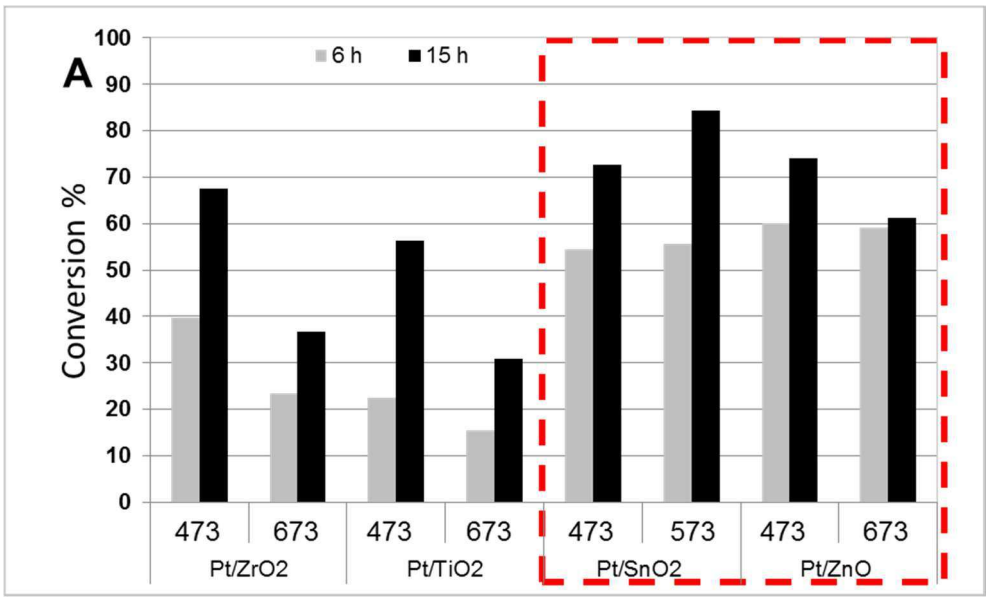

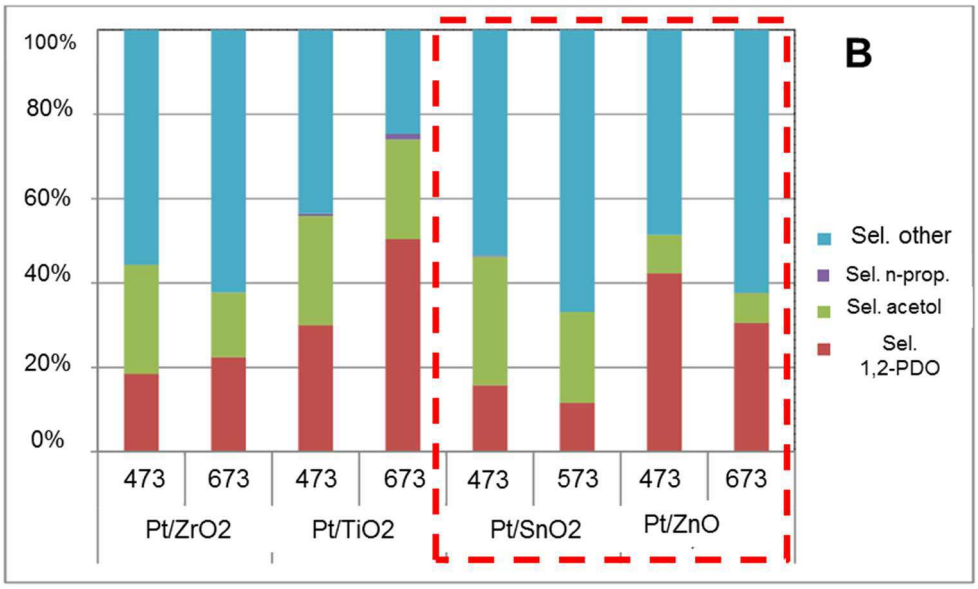

Figure 2: Results obtained for hydrogenolysis of glycerol expressed in terms of conversion for t=6h or 15h (A) or selectivity for t=15h (B). Reaction conditions: 20 mL of 1.36 M glycerol in water, 200 mg catalyst, 448K, 6 bar H_2.

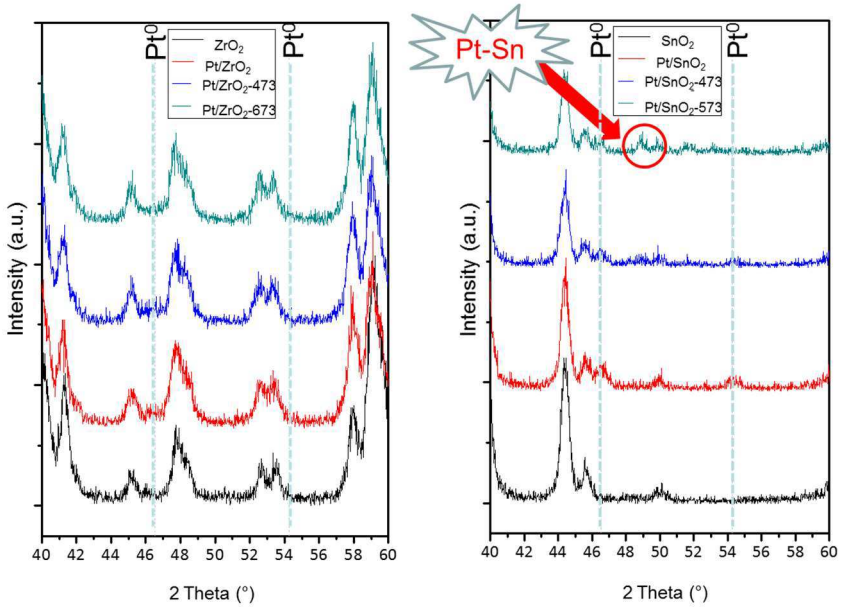

Figure S2: X-Ray diffractograms of platinum-systems on different supports.

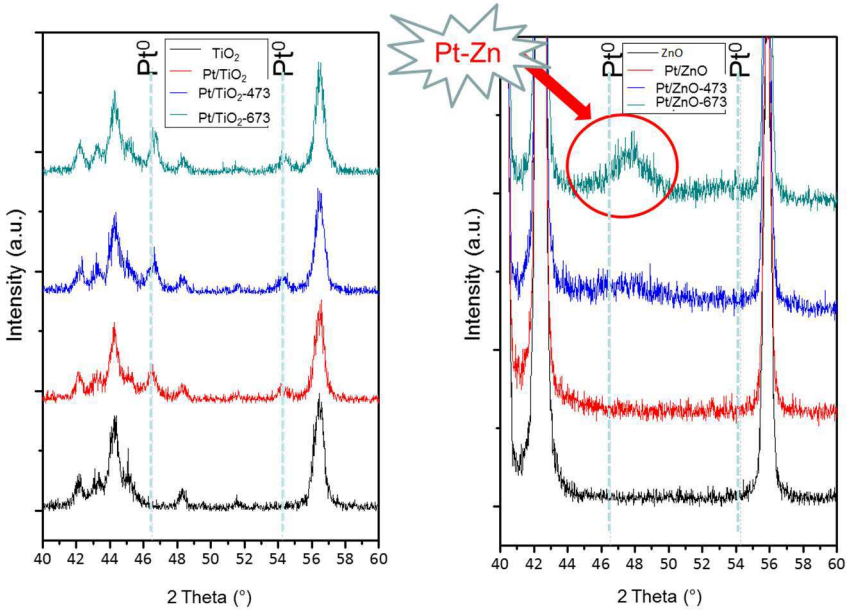

Figure S3: X-Ray diffractograms of platinum-systems on different supports.

III.3.2. Study of different metals supported on ZnO

Given the above reported results, ZnO was selected as a support for other metals. The synthesis was again carried out through the deposition-precipitation technique, in order to obtain a metal nominal content of 5% by weight. Some features concerning the characterization of the as-synthesized solids as well as those resulting from the reduction at 473K and 673K are given in Table 1 and Figures 3-6.

A first conclusion from Table 1 is that BET surface areas of all as synthesized solids are in the 14-25$m^2 \cdot g^{-1}$ range. Moreover, reduction at 673K results in a decrease in surface area which suggests that metal particle size could have increased, thus leading to a partial blocking of pores. If metal content is considered, there has been a good incorporation of the metal, the exception being Rh/ZnO for which ca. only 50% of the metal was incorporated as evidenced by ICP-MS (Rh content of 2.37% instead of 5.0%, nominal value). Furthermore, XPS data reveal that in all cases the metal/Zn ratio decreases with the reduction temperature, thus suggesting the progressive decoration of metal particles by the support, a typical phenomenon in reducible supports such as TiO_2 or ZnO [21-23].

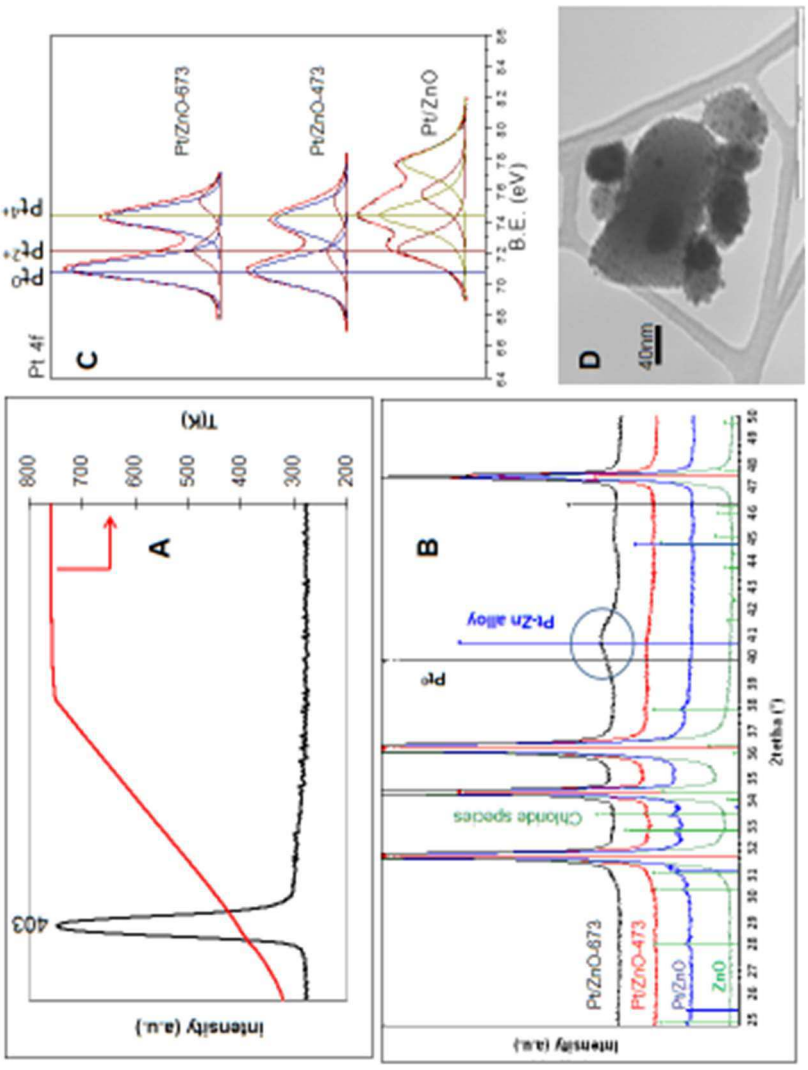

Figure 3. Characterization of Pt/ZnO systems: TPR (A), XRD (B), XPS (C) and TEM micrograph of Pt/ZnO-673 (D)

CATALYST	BET ($m^2 \cdot g^{-1}$)*	Metal atomic %					BET ($m^2 \cdot g^{-1}$) of M/ZnO-673
		Nominal	ICP-MS	XPS			
				M/ZnO	M/ZnO-473	M/ZnO-673	
Pt/ZnO	19	5.00	5.17	5.26	5.26	4.42	17
Pd/ZnO	17	5.00	4.10	1.16	0.89	0.39	12
Rh/ZnO	25	5.00	2.37	3.21	2.90	2.76	20
Au/ZnO	14	5.00	5.05	2.13	1.87	1.39	11

Surface composition from XPS data**							
	$\%Pt^0$	$\%Pt^{+2}$	$\%Pt^{+4}$		$\%Rh^0$	$\%Rh^{+1}$	$\%Rh^{+3}$
Pt/ZnO	0.0	43.9	56.1	Rh/ZnO	0	0	100
Pt/ZnO-473	82.2	17.8	0.0	Rh/ZnO-473	0.0	76.3	23.7
Pt/ZnO-673	90.4	9.6	0.0	Rh/ZnO-673	68.9	19.7	11.3
	$\%Pd^0$	$\%Pd^{+2}$			$\%Au^0$		
Pd/ZnO	0	100		Au/ZnO	100		
Pd/ZnO-473	73.6	26.3		Au/ZnO-473	100		
Pd/ZnO-673	75.6	24.3		Au/ZnO-673	100		

Table 1. Some features concerning characterization of the different ZnO-supported metal systems.

*The support (ZnO) has a BET area of $15 m^2 \cdot g^{-1}$

**The possibility of certain re-oxidation of the samples during preparation for XPS analyses (especially in the case of Pd) cannot be ruled out.

We are going to study now each metal system individually, having a look at Figures 3 to 6. The TPR profile of Pt/ZnO (Figure 3A) exhibited a strong reduction peak at 403K in addition to another much weaker tail. The synthetic procedure could account for the appearance of our TPR peak ca. 423K below the value described in the literature [24, 25]. Therefore, the addition of 2-propanol to the reaction mixture may have caused the partial reduction of chloroplatinic acid. In fact, XPS spectrum of Pt/ZnO (Figure 3C) exhibits not only Pt 4f 7/2 peaks of Pt^{4+} species but also of Pt^{2+} at binding energies of 74.4 and 72.3 eV, respectively [26]. Moreover, XRD of Pt/ZnO system (Figure 3B) shows some peaks at 2θ values of 32.8º, 33.6º and 37.8º which can be ascribed to oxychloride species of the type $Zn_5(OH)_8Cl_2 \cdot H_2O$ which suggests that during calcination of the system at 673K, chloride species passed to the support. In line with TPR profile, reduction at 473K (Pt/ZnO-473 solid) results in the appearance of Pt^0, as evidenced by the XPS peak at 70.9eV [27]. Finally, Pt/ZnO-673 solid exhibits Pt^{2+} and Pt^0 peaks at 72.2 eV and 71.0 eV, respectively. XRD evidences the formation of a Pt-Zn alloy with a peak at 2θ=40.6 eV. Interestingly, no Pt^0 peaks are observed in XRD of Pt/ZnO-473 or Pt/ZnO-673 solids which given the high metal content (ca. 5% by weight, as confirmed by ICP-MS) indicates that platinum particle size is low. In fact, TEM micrographs showed mean particle diameters of 3.1 nm and 5.2 nm (Figure 3D), respectively.

As regards Rh/ZnO solid, TPR profile (Figure 4A) shows two peaks, the major one exhibiting a maximum at ca. 467K. This peak, which corresponds to a reduction between 373K and 513K could be ascribed to the reduction of Rh^{3+} to Rh^0, whereas the peak at higher temperatures could indicate the reduction of some rhodium species interacting with the support, since TPR profile of ZnO does not exhibit any peak. Hwang et al [28] found

that the reduction of RhO_x to Rh(0) occurs at 373K whereas higher temperatures values (ca. 443K) are required when a chloride precursor (as it is our case) have been used. XPS spectrum of Rh/ZnO (Figure 4C) shows the presence of Rh^{3+} with Rh 3d 5/2 values of 308.8 eV. Reduction at 473K results in the formation of Rh^{+} (307.2 eV) whereas all three oxidation states (Rh^0, Rh^{+} and Rh^{3+}), coexist at 673K, with binding energies of 306.2, 307.6 and 306.8 eV r respectively [29]. In a similar way as for Pt/ZnO, no rhodium peaks are observed in X-ray diffractograms (Figure 4B) but only Rh-Zn alloy, at 2θ=42.6º in Rh/ZnO-673 system. Again, this suggest a small rhodium particle size, TEM micrographs showing average particle sizes of 3.7 nm and 6.2 nm for Rh/ZnO-473 and Rh/ZnO-673, respectively (see TEM micrograph of Rh/ZnO-673 in Figure 4D).

In the case of palladium, TPR profile (Figure 5A) evidences that Pd^0 is easily reduced, the reduction peak appearing at 313K. XPS spectra of Pd/ZnO solid (Figure 5C) has Pd 3d5/2 peaks at 336.2eV which can be ascribed to PdO species which exhibit XRD peaks at 2θ=33.9º (101 reflection) [30] (Figure 5B). Subsequent reduction at 473K results in the formation of Pd^0 (XPS peak at 335.0 eV and XRD peak of 111 reflection at 2θ=40.4º) [30, 31]. Finally, at 673K a Pd-Zn alloy is observed by XRD, with peaks at 2θ=41.2º and 44.2º. These results suggest that palladium particle size is bigger as compared to Pt and Rh (15nm for Pd/ZnO-473 as estimated from XRD using Scherrer equation). Unfortunately, TEM micrographs are not clear enough as to estimate Pd particle size (see micrograph for Pd/ZnO-673, Figure 5D as an example).

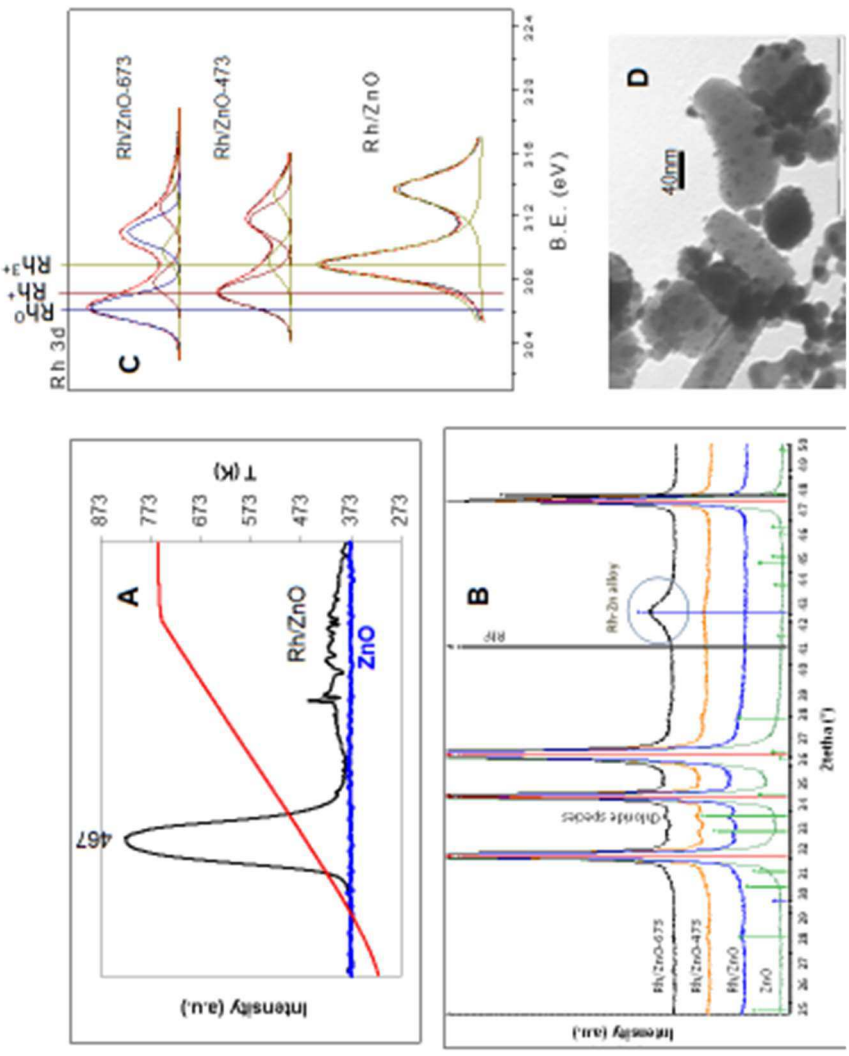

Figure 4: Characterization of Rh/ZnO systems: TPR (A), XRD (B), XPS (C) and TEM micrograph of Rh/ZnO-673 (D).

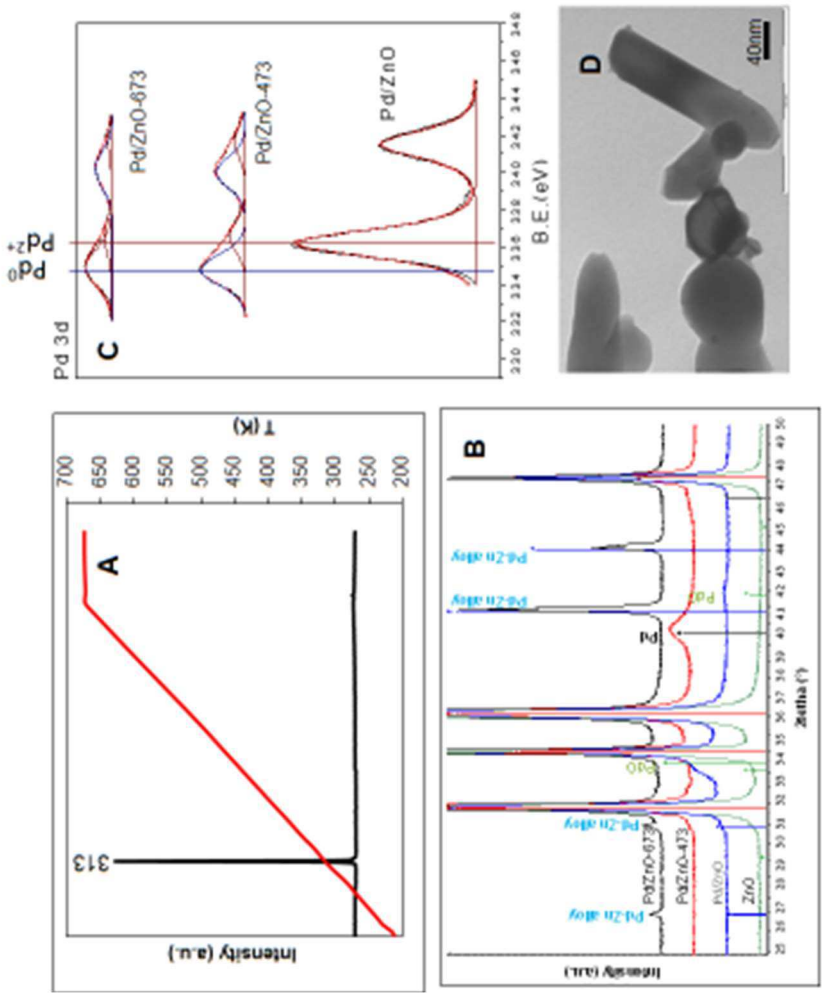

Figure 5: Characterization of Pd/ZnO systems: TPR (A), XRD (B), XPS (C) and TEM micrograph of Pd/ZnO-673 (D).

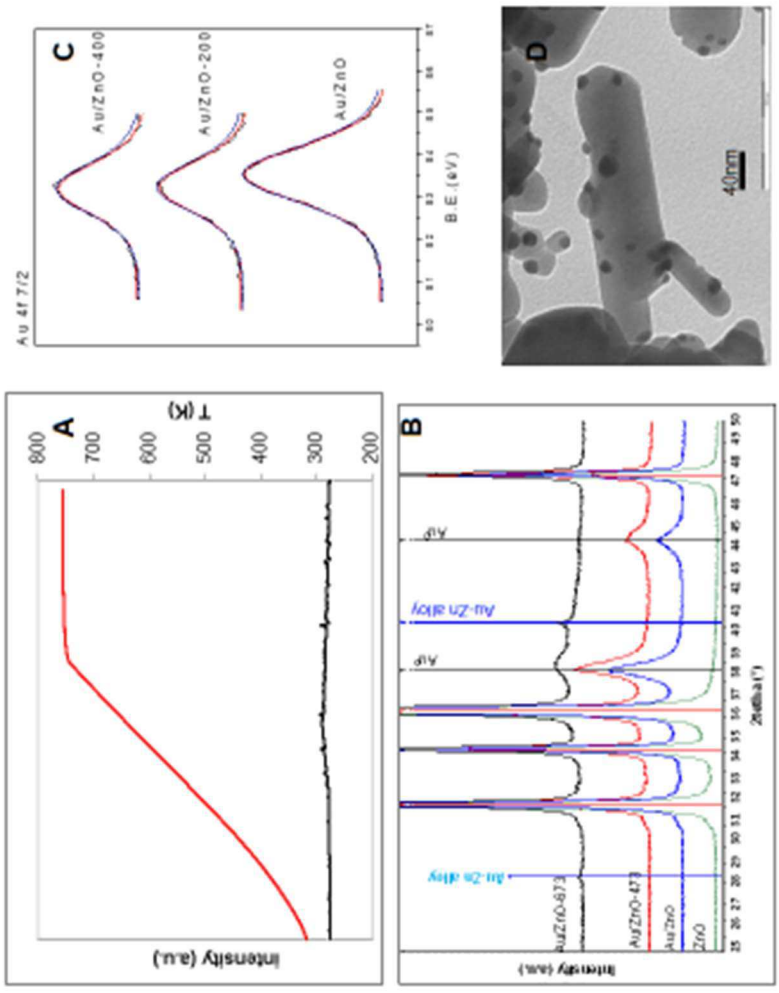

Figure 6: Characterization of Au/ZnO systems: TPR (A), XRD (B), XPS (C) and TEM micrograph of Au/ZnO (D).

Finally, regarding gold systems, Au^0 is already formed during the synthetic procedure thus not exhibiting peaks in the TPR profile (Figure 6A). This is also clear from XPS spectra (Figure 6C) which show for all gold-containing solids a typical Au^0 4f7/2 signal at ca. 83.5 eV [32]. Moreover, X-Ray diffractograms present a peak of Au^0 at $2\theta=38.2^\circ$ (111 reflection) [33] in Au/ZnO, the signal shifting to higher values with reduction temperature (just as the Au^0 XPS signal shifts to lower binding energies) which together with the appearance of a new peak at $2\theta=40.5^\circ$ in Au/ZnO-673 system suggests the formation of a Au-Zn alloy. Finally, TEM micrographs show that gold particle size is 12 nm and 14 nm for Au/ZnO-473 and Au/ZnO-673, respectively.

All in all, these results evidence that, as desired, in all cases there is a SMSI effect, a metal-Zn alloy is formed at 673K and that particle size increases from M/ZnO-473 to M/ZnO-673 solids. Moreover, the smallest particle sizes correspond to Rh and Pt solids whereas the biggest ones are those of palladium and gold-containing systems.

III.3.3. Catalytic performance of M/ZnO-200 and M/ZnO-400 solids

Results found for liquid-phase catalytic transformation of glycerol on the different ZnO-supported systems are represented in Figures 7 and 8. Analyses were performed in the "Parallel Slurry Phase Reactor" (SPR16) for t=12 h, under two different atmospheres (H_2 or He) and using neutral or basic (pH 13) medium. A first conclusion from Figure 7 is that in terms of conversion, the reaction is faster in the basic medium as compared to the neutral one and in helium as compared to hydrogen, which is consistent with results reported in the literature for other metals, such as iridium [14].

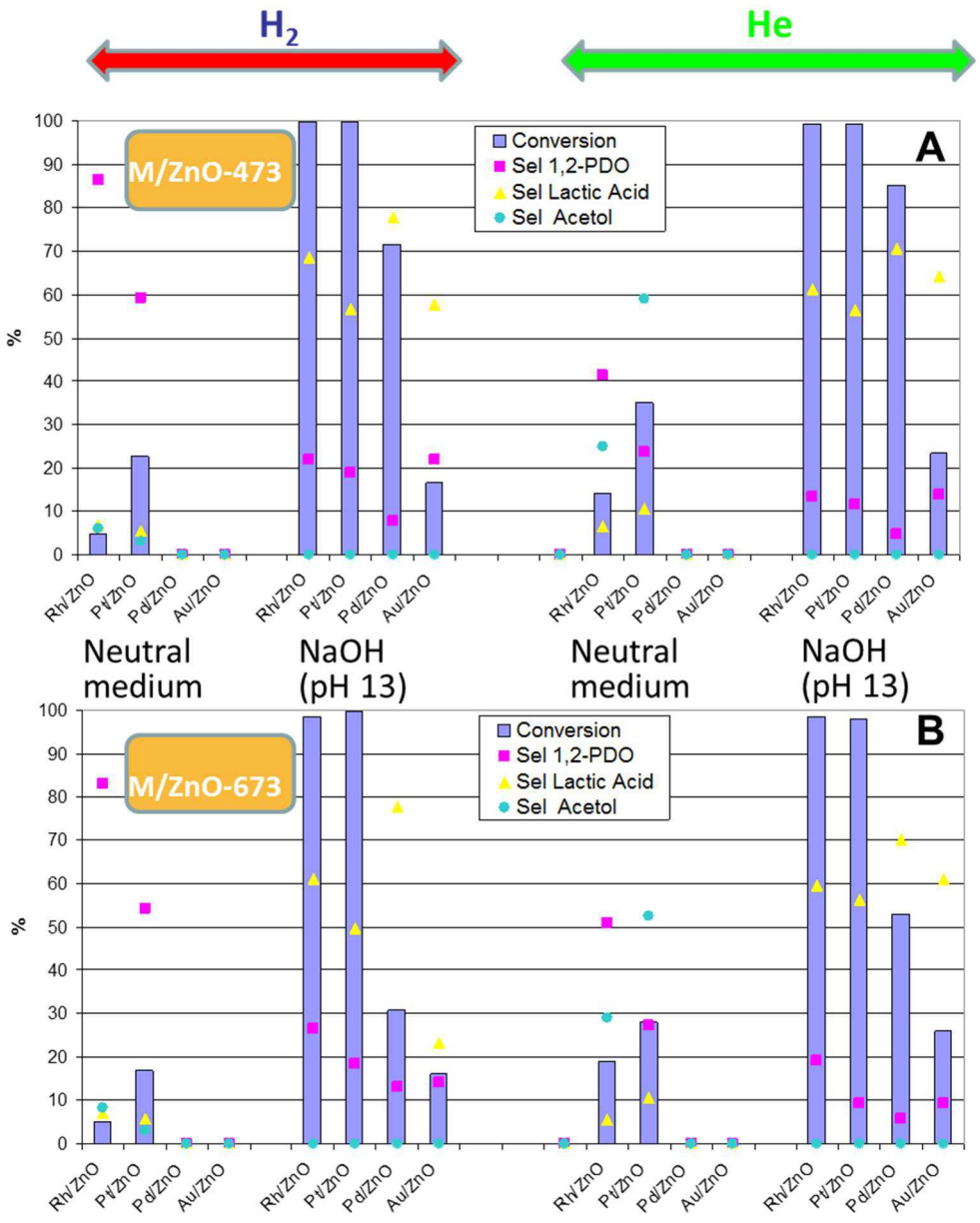

Figure 7: Results found for glycerol catalytic transformation on the different ZnO-supported metal systems reduced at 473K (A) or 673K (B) expressed as conversion and selectivity for t=12h. Reaction conditions: 100mL of a 0.68M glycerol aqueous solution, 30mg catalyst, 453K, 20 bar of He or H_2

Moreover, under similar reaction conditions conversion order follows the sequence Pt>Rh>>Pd>>Au. If selectivity is considered, 1,2-PDO is preferentially obtained in neutral medium whereas, in general, the main product in basic medium is lactic acid. Auneau [34] studied the reaction mechanism of glycerol hydrogenolysis on several supported Rh systems. Experimental results together with the theoretical studies (DFT) on a model Rh surface (111) prompted him to suggest the reaction mechanism presented in Figure 9, where glycerol is firstly dehydrogenated. As shown in such a figure, there are different equilibria from pyruvaldehyde (PAL) to 1,2-PDO whereas formation of lactic acid from that chemical through intramolecular Cannizaro reaction is favoured in basic media and there is no equilibrium. In fact, if we start from lactic acid, it is not converted to any other product whereas 1,2-PDO results in certain production of lactic acid under basic conditions. This mechanism also accounts for the production of acetol in helium whereas in the presence of a high hydrogen concentration equilibrium shifts up to 1,2-PDO.

When both M/ZnO-473 and M/ZnO-673 solids are compared (Figure 7), the former is more active than the latter, which suggests that the strong metal-support interaction favors the reaction but the eventual formation of an alloy at 673K and/or the increase in particle size (as evidenced by TEM) are detrimental to the activity. Finally, in terms of yield to 1,2-PDO or lactic acid (Figure 8), Pt, Pd and Rh reduced at 473K affords lactic acid in a 55-68% yield (basic medium), the highest value corresponding to Rh/ZnO-473, whereas production of 1,2-PDO is more modest (26% for Rh/ZnO-673).

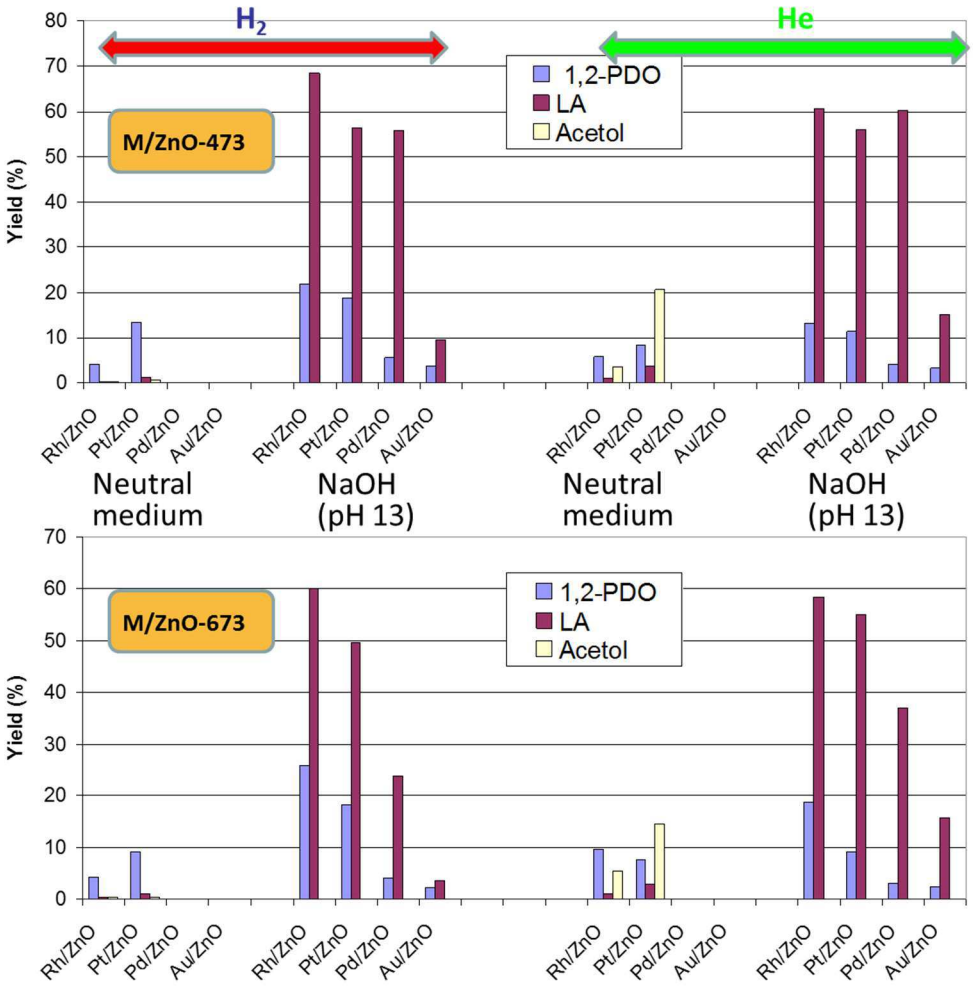

Figure 8: Results found for glycerol catalytic transformation on the different ZnO-supported metal systems reduced at 473K (A) or 673K (B) expressed as yields for t=12h. Reaction conditions: 100mL of a 0.68M glycerol aqueous solution, 30mg catalyst, 453K, 20 bar of He or H_2.

All in all, Pt and Rh systems are the most active solids among the synthesized solids. One could think that, given the fact that both Pt/ZnO and Rh/ZnO solids exhibit quite similar metal particle sizes (3.3 nm and 3.7 nm for Pt/ZnO-473 and Rh/ZnO-473, respectively) the highest activity of the former is just a result of the highest metal content (ca. the double than for Rh/ZnO as evidenced by ICP-MS, see Table 1).

However, conversion values achieved in neutral medium for Pt/ZnO are 22.6% and 35.0% under H_2 and He, respectively (Figure 8), whereas under similar conditions, Rh/ZnO afforded 4.9% and 6.6%, respectively. This represents conversion values of ca. 4-5 times higher for Pt, which suggests that under our experimental conditions platinum systems are intrinsically more active than rhodium solid. Additional experiments in the 200mL-stainless steel autoclave, in neutral medium, showed that, for the same conversion value, selectivity to lactic acid or 1,2-PDO obtained with Pt/ZnO and Rh/ZnO solids are quite similar. Therefore, for instance, at 5% and 10% conversion, selectivity to 1,2-PDO is ca. 80-85% for both solids whereas the main product is acetol under helium (ca. 80%).

In contrast, selectivity to acetol achieved with Pd-containing solids is higher at the expense of 1,2-PDO (18% acetol and 70% 1,2-PDO at 5% conversion, under H_2). Finally, this study was not possible with gold systems given their low activity.

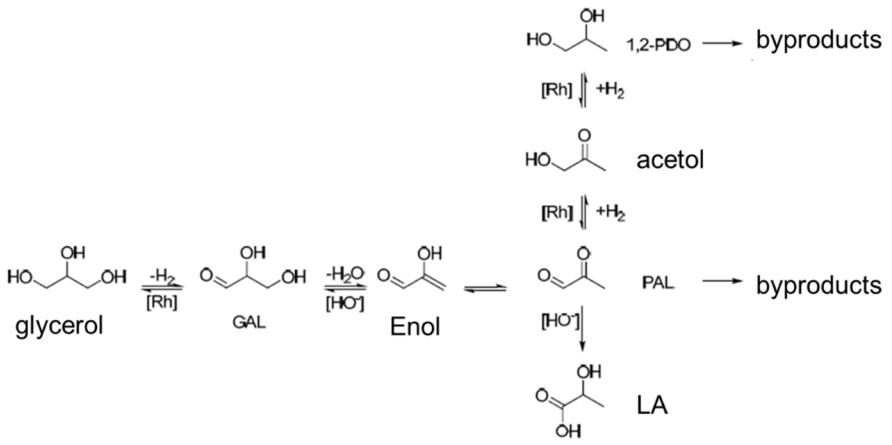

Figure 9: Mechanism proposed by Auneau [34] for conversion of glycerol in lactic acid (LA) or 1,2-propanediol (1,2-PDO) considering dehydrogenation of glycerol as the initial step. GAL and PAL denote glyceraldehyde and pyruvaldehyde, respectively.

Some new synthetic procedures are currently being optimized in order to achieve a better control of the metal particle size with a view to perform a comparative study of metals with a range of particle sizes in glycerol hydrogenolysis.

III.4. Conclusions

Different reducible oxides (TiO_2, ZnO, SnO_2 and ZrO_2) were screened as support for platinum and tested for glycerol hydrogenolysis. The solids exhibiting the greatest metal-support interaction, eventually forming an alloy (ZnO and SnO_2) were the most active solids. Moreover, selectivity to 1,2-PDO was higher for ZnO what prompted us to select this solid as support for further studies.

Diverse ZnO-supported metals (Pt, Rh, Pd and Au) were then synthesized through the deposition-precipitation technique (5% by weight)

and tested for catalytic transformation of glycerol under hydrogen and helium atmosphere. Under similar reaction conditions, glycerol conversion followed the sequence Pt>Rh>>Pd>>Au. Furthermore, the solids reduced at 473K were more active than those activated at 673K. The increase in metal particle size and/or the formation of an alloy (as evidenced by TEM and XRD, respectively) could account for that. Results suggest that the strong metal-support interaction achieved at 473K could be beneficial to the process though the eventual formation of the alloy at higher temperatures (673K) should be avoided. The most active systems were Pt/ZnO-473 and Rh/ZnO-473 which exhibited a similar particle size (ca. 3-4 nm). Studies at iso-conversion conditions in neutral medium evidenced similar selectivities for Pt and Rh-containing solids whereas Pd systems yielded more acetol at the expense of 1,2-PDO. All in all, quite high yields to lactic acid were achieved in basic medium (68% for Rh/ZnO-473 under H_2 in basic medium) whereas yield to 1,2-PDO was more modest (26% for Rh/ZnO-673 under similar reaction conditions).

III.5. Acknowledgements

The authors are thankful to Spanish MICINN, MEC, Junta de Andalucia and FEDER funds (CTQ2008-01330, CTQ2010-18126, P08-FQM-3931 and P09-FQM-4781 projects) for financial support. F. Auneau is grateful to the French Government for a Doctorate grant. SCAI at the University of Cordoba is also acknowledged for ICP-MS measurements and the use of TEM and XPS. Finally, the authors are grateful to COST Action CM0903 for financial support, including a short-term scientific mission (STSM) of M. Checa. M. Checa also acknowledge the Spanish Ministery of Education for a FPU grant.

III.6. References

1. Parvulescu, M. Rossi, C. Della Pina, R. Ciriminna, M. Pagliaro, Green Chem. 13 (2011) 143-148. J. Janaun, N. Ellis, J. Appl. Sci. 10 (2010) 2633-2637.
2. M. H. Haider, N. F. Dummer, D. Zhang, P. Miedziak, T. E. Davies, S. H. Taylor, D. J. Willock, D.W. Knight, D. Chadwick, G. J. Hutchings, J. Catal. 286 (2012) 206-213.
3. E. G. Rodrigues, M.F.R. Pereira, J. J. Delgado, X.Chen, J. J.M. Órfão, Catal. Commun. 16 (2011) 64-69.
4. M. Balaraju, V. Rekha, P.S. Sai Prasad, B.L.A. Prabhavathi Devi, R.B.N. Prasad, N. Lingaiah, Appl. Catal. A 15 (2009) 82-87.
5. J. Ten Dam, F. Kapteijn, K.Djanashvili, U.Hanefeld, Catal. Commun. 13 (2011) 1-5.
6. Y. Nakagawa, Y. Shinmi, S. Koso, K. Tomishige, J. Catal. 272 (2010) 191-194.
7. Montassier, J.C. Ménézo, L.C. Hoang, C. Renaud, J. Barbier, J. Mol. Catal. 70 (1991) 99-110.
8. Z. Yuan, P. Wu, J. Gao, X. Lu, Z. Hou, X. Xheng, Catal. Lett. 130 (2009) 261-265.
9. M. A. Abdel-Rahman, Y. Tashiro, K. Sonomoto, J. Biotechnol. 156 (2011) 286-301.
10. K.Tomishige, Catal. Sci. Technol. 1 (2011) 179–190.
11. T. Miyazawa, Y. Kusunoki, K. Kunimori, K. Tomishige, J. Catal. 240 (2006) 213-221.
12. J. Chaminand, L. Djakovitch, P. Gallezot, P. Marion, C. Pinel, C. Rosier, Green Chem. 6 (2004) 359-361.

13. F. Auneau, S. Noël, G. Aubert, M. Besson, L. Djakovitch, C. Pinel, Catal. Commun. 16 (2011) 144-149.
14. M.C. Sanchez-Sanchez, R.M. Navarro, J.L.G. Fierro, Appl. Catal. B 106 (2011) 83-93.
15. Q. Liu, X. Guo, Y. Li , W. Shen, Langmuir 25 (2009) 6425–6430.
16. Y. Shinmi, S. Koso, T. Kubota, Y. Nakagawa, K. Tomishige, Appl. Catal. B 94 (2010) 318–326.
17. Wawrzetz, B. Peng, A. Hrabar, A. Jentys, A.A. Lemonidou, J.A. Lercher, J. Catal. 269 (2010) 411-420.
18. Y. Nakagawa, K.Tomishige, Catal. Sci. Technol. 1 (2011) 179–190.
19. Iriondo, J.F. Cambra, V.L. Barrio, M.B. Guernez, P.L. Arias, M.C. Sanchez-Sanchez, R.M. Navarro, J.L.G. Fierro, Appl. Catal. B 106 (2011) 83-93.
20. M.A. Aramendía, J.C. Colmenares, A. Marinas, J.M. Marinas, J.M. Moreno, J.A. Navío, F.J. Urbano, Catal.Today 128 (2007) 235–244.
21. J. Hidalgo-Carrillo, M.A. Aramendía, A.Marinas, J.M. Marinas, F.J. Urbano, Appl. Catal. A 385 (2010) 190–200.
22. S. Bernal, J.J. Calvino, M.A. Cauqui, J.M. Gatica, C. Lopez Cartes, J.A. Perez Omil, J.M. Pintado, Catal. Today 77 (2003) 385–406.
23. M. Consonni, D. Jokic, D. Yu Murzin, R. Touroude, J. Catal. 188 (1999) 165–175.
24. F. Ammari, J. Lamotte, R. Touroude, J. Catal. 221 (2004) 32–42.
25. Katrib, C. Petit, P. Légaré, L. Hilaire, G. Maire, Surf. Sci. 189/190 (1987) 886-893.
26. A.K Shukla, A.S Aricò, K.M El-Khatib, H Kim, P.L Antonucci, V Antonucci, Appl. Surf. Sci. 137 (1999) 20-29.
27. C.-P. Hwang, C.-T. Yeh, Q. Zhu, Catal. Today 51 (1999) 93-101.

28. G.Munuera, A.R.González-Elipe, J.P. Espinos, A. Muñoz, J.C. Conesa, J. Soria, J. Sanz, Catal. Today 2 (1988) 663-673.
29. G. Ketteler, D.F. Ogletree, H. Bluhm, H. Liu, E.L.D. Hebenstreit, M. Salmeron, J. Am. Chem. Soc. 127 (2005) 18269.
30. O. Demoulin, M. Navez, P. Ruiz, Catal. Lett. 103 (2005) 149.
31. K. Zakrzewska, Thin Solid Films 451-452 (2004) 93-97.
32. J. Strunk, K. Kähler, X. Xia, M. Comotti, F. Schüth, T. Reinecke, M. Muhler, Appl.Catal. A 359 (2009) 121–128.
33. F. Auneau, PhD, Université Claude Bernard Lyon I (France), 2011, page 134.

Capítulo IV

Estudio de la desactivación de catalizadores de Pt soportado en la hidrogenolisis de glicerol

Chapter IV

Deactivation study of supported Pt catalyst on glycerol hydrogenolysis

IV. Deactivation study of supported Pt catalyst on glycerol hydrogenolysis

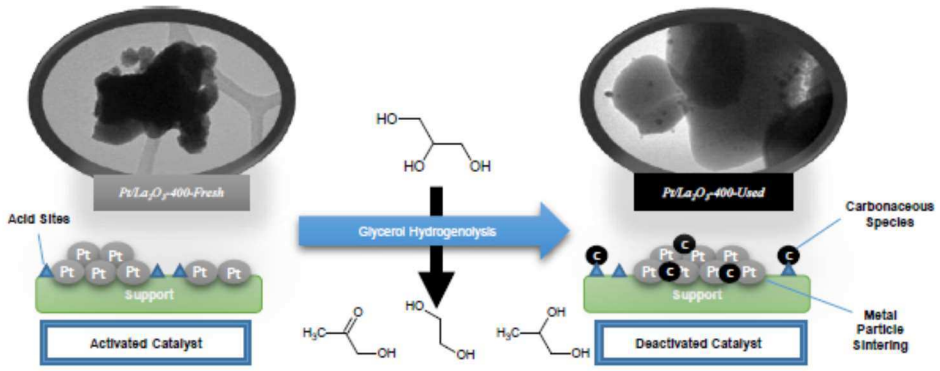

Graphical Abstract

Applied Catalysis A: General 507 (2015) 34–43

Contents lists available at ScienceDirect

Applied Catalysis A: General

journal homepage: www.elsevier.com/locate/apcata

Deactivation study of supported Pt catalyst on glycerol hydrogenolysis

Manuel Checa, Alberto Marinas, José M. Marinas, Francisco J. Urbano*

Department of Organic Chemistry, Campus de Excelencia Internacional CeiA3, University of Córdoba, Campus de Rabanales, Marie Curie Building (Annex), E-14014 Córdoba, Spain

ARTICLE INFO

Article history:
Received 4 June 2015
Received in revised form 7 September 2015
Accepted 21 September 2015
Available online 25 September 2015

Keywords:
Glycerol hydrogenolysis
Supported Pt catalysts
Support effect
1,2-Propanediol
Catalyst Deactivation
Catalysts fouling

ABSTRACT

Different Pt-based systems (5% by weight) were obtained through impregnation of chloroplatinic acid on Al_2O_3, CeO_2, La_2O_3 and ZnO. The solids were tested for glycerol hydrogenolysis. Results showed that metal sites are needed both for dehydration of glycerol and subsequent reduction to 1,2-propanediol (1,2-PDO). Moreover, as the reaction proceeds there is a progressive decrease in 1,2-PDO yield as a consequence of acetol oligomerization which already takes place at temperatures as low as 150 °C. Among all tested supports, ZnO was the one exhibiting better characteristics for glycerol selective transformation into 1,2-PDO as a result of the combination of the appropriate surface acidity, limited deactivation and stability under hydrothermal working conditions.

1. Introduction

Transportation fuels and chemicals have traditionally been produced from fossil sources. The increasing demand for these products together with the depletion of petroleum resources and environmental concern has led to the search for environmentally acceptable alternatives. Among them, only biomass can produce both energy and chemicals [1] and, therefore, the research on this field is continuously growing [2]. Some examples of the most relevant biomass-derived platform chemicals studied are furfural and its derivatives, succinic acid, sorbitol, lactic acid or glycerol [3–7]. The latter chemical has received much attention in recent years both from academia and industry due to its high functionalization, high reactivity, availability and low price [8]. In fact, glycerol is obtained as a by-product in biodiesel production by transesterification in large amount (10 kg of impure glycerol per 100 kg of produced biodiesel) [9,10]. Because of its high functionalization, glycerol can be transformed into a number of value-added products such as 1,2-propanediol (1,2-PDO), 1,3-propanediol (1,3-PDO), acrolein, olefins, etc., by a range of heterogeneously-catalyzed chemical processes that can compete with the classical petrochemical—route [11].

Regarding glycerol valorization, a great deal of reactions can be found in the literature, each one leading to different products as a function of the type of process or the proper reaction conditions [12]. One of the most interesting options is glycerol transformation under hydrogen pressure [2,7,13], consisting in glycerol reduction in such way that there is a dissociation of a C—OH chemical bond, the OH group being replaced by a H atom. The main products obtained in glycerol hydrogenolysis are 1-hydroxy-propan-2-one (ACETOL) [14], 1,2-PDO [15], 1,3-PDO [16] and ethylene glycol (EG), the latter involving a C–C cleavage [17]. However, depending on the used catalyst and reaction conditions, other products such as propan-1-ol and propan-2-ol can be obtained in high yields [18]. Selectivity of products can be tuned by using different metals [14], supports [19] or additives [16]. In particular, 1,2-PDO is the target of various investigations due to its interesting applications in pharmaceutical industry, costumer care products, antifreeze and tobacco industry, where it is used as humectant [13]. In the case of ACETOL, it is easy to find it as starting point in routes to produce polyols or acrolein [14]. Several transition metals have been described as catalysts in glycerol hydrogenolysis, the most common being Cu [20], Co [21] and Ni [22] and some noble metals such as Ru [23], Ir [24], Pd [14], Rh [25] or Pt [16,23]. Among them, Pt has been found to produce propylene glycol through glycerol hydrogenolysis, avoiding the C–C cleavage [26].

Platinum-catalyzed glycerol conversion into 1,2 or 1,3-propanediol on acid-base catalysts has been described to occur via glycerol dehydration followed by its hydrogenation to propanediols (Scheme 1). Depending on the hydroxyl group involved in glycerol dehydration (either primary or secondary), 1,2-PDO or 1,3-PDO can be obtained, respectively [14]. Platinum has been supported on a great variety of solids including both acid and basic ones and thus glycerol hydrogenolysis has been studied over Pt sup-

* Corresponding author. Fax: +34 957212066.
E-mail address: fj.urbano@uco.es (sc1 F.J. Urbano).

http://dx.doi.org/10.1016/j.apcata.2015.09.028
0926-860X/

In this chapter, different Pt-based systems (5% by weight) were obtained through impregnation of chloroplatinic acid on Al_2O_3, CeO_2, La_2O_3 and ZnO. The solids were tested for glycerol hydrogenolysis. Results showed that metal sites are needed both for dehydration of glycerol and subsequent reduction to 1,2-PDO. Moreover, as the reaction proceeds there is a progressive decrease in 1,2-PDO yield as a consequence of acetol oligomerization which already takes place at temperatures as low as 150ºC. Among all tested supports, ZnO was the one exhibiting better characteristics for glycerol selective transformation into 1,2-PDO as a result of the combination of the appropriate surface acidity, limited deactivation and stability under hydrothermal working conditions.

IV.1. Introduction

Transportation fuels and chemicals have traditionally been produced from fossil sources. The increasing demand for these products together with the depletion of petroleum resources and environmental concern has led to the search for environmentally acceptable alternatives. Among them, only biomass can produce both energy and chemicals [1] and, therefore, the research on this field is continuously growing [2]. Some examples of the most relevant biomass-derived platform chemicals studied are furfural and its derivatives, succinic acid, sorbitol, lactic acid or glycerol [3-7]. The latter chemical has received much attention in recent years both from academia and industry due to its high functionalization, high reactivity, availability and low price [8]. In fact, glycerol is obtained as a by-product in biodiesel production by transesterification in large amount (10 kg of impure glycerol per 100 kg of produced biodiesel) [9,10]. Because of its high functionalization, glycerol can be transformed into a number of value-added products such as 1,2-propanediol

(1,2-PDO), 1,3-propanediol (1,3-PDO), acrolein, olefins, etc., by a range of heterogeneously-catalyzed chemical processes that can compete with the classical petrochemical – route [11].

Regarding glycerol valorization, a great deal of reactions can be found in the literature, each one leading to different products as a function of the type of process or the proper reaction conditions [12]. One of the most interesting options is glycerol transformation under hydrogen pressure [2,7,13], consisting in glycerol reduction in such way that there is a dissociation of a C—OH chemical bond, the OH group being replaced by a H atom. The main products obtained in glycerol hydrogenolysis are 1-hydroxy-propan-2-one (ACETOL) [14], 1,2-PDO [15], 1,3-PDO [16] and ethylene glycol (EG), the latter involving a C-C cleavage [17]. However, depending on the used catalyst and reaction conditions, other products such as propan-1-ol and propan-2-ol can be obtained in high yields [18] .Selectivity of products can be tuned by using different metals [14], supports [19] or additives [16]. In particular, 1,2-PDO is the target of various investigations due to its interesting applications in pharmaceutical industry, costumer care products, antifreeze and tobacco industry, where it is used as humectant [13]. In the case of ACETOL, it is easy to find it as starting point in routes to produce polyols or acrolein [14]. Several transition metals have been described as catalysts in glycerol hydrogenolysis, the most common being Cu [20], Co [21] and Ni [22] and some noble metals such as Ru [23], Ir [24], Pd [14], Rh [25] or Pt [16,23]. Among them, Pt has been found to produce propylene glycol through glycerol hydrogenolysis, avoiding the C-C cleavage [26].

Platinum-catalyzed glycerol conversion into 1,2 or 1,3-propanediol on acid-base catalysts has been described to occur via glycerol dehydration followed by its hydrogenation to propanediols (Scheme 1). Depending on the

hydroxyl group involved in glycerol dehydration (either primary or secondary), 1,2-PDO or 1,3-PDO can be obtained, respectively [14]. Platinum has been supported on a great variety of solids including both acid and basic ones and thus glycerol hydrogenolysis has been studied over Pt supported on alumina [16], carbon [27], other transition metal oxides [15,28], zeolites [29], etc. In these studies, the role of both metal and surface acid sites in product selectivity has been pointed out as crucial for glycerol transformation into 1,2-PDO [30]. In a recent work, we reported that metal sites could participate not only in hydrogenation of ACETOL to 1,2-PDO but also in the previous dehydration step of glycerol to ACETOL [14]. Additional work on this subject is needed to clarify the synergies between metal and acid sites.

An additional point to take into account is catalyst deactivation which has been reported in both gas- and liquid-phase catalyzed glycerol transformation processes. There are some studies dealing with catalysts deactivation in the gas-phase glycerol dehydration to acrolein [31-33] or in the gas-phase glycerol reforming process [33,34]. Regarding the liquid-phase glycerol hydrogenolysis, there are some reports on the deactivation of supported copper or ruthenium [35-41]. In these cases, deactivation is associated to carbon deposition and metal particle aggregation. However, to the best of our knowledge, there are no in depth studies dealing with catalysts deactivation in the liquid-phase glycerol hydrogenolysis over supported Pt catalysts.

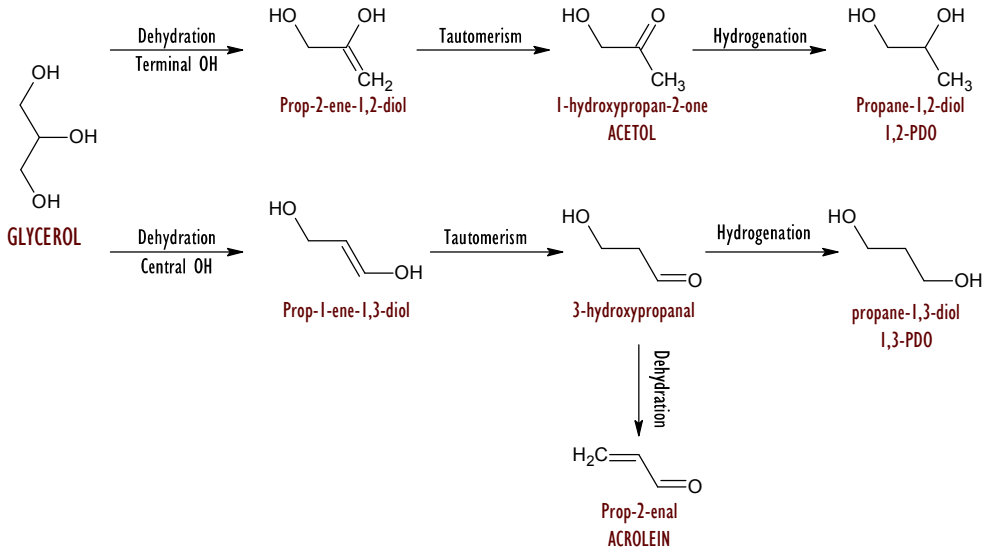

Scheme 1.- Reaction network for the hydrogenolysis of glycerol aqueous solutions over supported metal catalysts.

This work is aimed at studying the support effects in Pt-based catalysts used in the liquid-phase glycerol hydrogenolysis, looking for synergies between metal and acid sites. Moreover, a detailed study of the spent catalysts could give some valuable information on the role of such acid sites in the catalytic process and in deactivation of supported Pt catalysts.

IV.2. Experimental

IV.2.1. Synthesis of the catalysts

Aluminium oxide activated acid (Al_2O_3-AC Sigma-Aldrich ref. 199966), aluminium oxide activated basic (Al_2O_3-BA Sigma-Aldrich ref. 199443), cerium oxide (CeO_2, Sigma-Aldrich ref. 544841), lanthanum oxide (La_2O_3, Sigma-Aldrich ref. 634271) and zinc oxide (ZnO, Sigma-Aldrich ref. 544906) were selected as supports for the synthesis of supported Pt catalysts.

All supports were calcined at 400°C for 6h in air flow (30 mL min^{-1}) before use.

Platinum was incorporated onto the support by incipient wetness impregnation with chloroplatinic acid (8% w/w, Sigma-Aldrich ref. 262587). The synthesis was designed to achieve a Pt loading of 5% (w/w). The procedure consisted in introducing 4.75 g of support in a 50 mL round bottom flask and 6.4 mL of chloroplatinic acid were subsequently added. In some cases, 2 - 3 mL of water were added in order to completely fill the porous system of the support. Then the mixture was rotated (150 rpm) at room temperature for 1h and then evacuated under controlled temperature until dryness (1h at 30°C, 1h at 50 °C and 80°C until dryness). The flask was removed and placed in an oven at 110°C overnight. After that, the catalyst was calcined at 400°C for 6h, in synthetic air flow (30 mL min^{-1}). Finally, the calcined material was crushed and sieved (0.149 mm) in order to prevent diffusional problems. The catalysts were reduced in H_2 flow (30 mL min^{-1}) at 200 or 400°C for 2h (heating rate 10 °C min^{-1}) in order to activate them for the reaction. Once reduced, the solid was cooled down in H_2 to room temperature and then purged for 15 min with N_2 (30 mL min^{-1}).

Solid nomenclature includes a suffix indicating the reduction temperature. Therefore, for instance, CeO_2 denotes the ceria support whereas Pt/CeO_2-400 refers to the ceria supported platinum system reduced at 400ºC.

IV.2.2. Characterization of the catalysts

IV.2.2.1. ICP-MS analysis

Elemental analysis of Pt-containing samples was carried out by the staff at the Central Service for Research Support (SCAI) of the University of Córdoba. It was performed by inductively coupled plasma mass spectrometry (ICP-MS). Measurements were made on a Perkin-Elmer ELAN DRC-e instrument following dissolution of the sample. Due to the different chemical properties of the supports, different recipes were needed.

Alumina-based catalysts were dissolved in a two-step process: 100 mg were treated with 25 mL of HF for 10 min at mild temperature and then 15 mL of HCl were added in order to complete the digestion of Pt particles. In the case of ZnO and La_2O_3 based catalyst, the treatment with 20 mL of the HCl:HNO_3 (3:1) mixture was enough to obtain a homogeneous solution. In order to dissolve CeO_2 supported Pt catalysts, *i)* 25 mL of the H_2O_2:HNO_3 (4:1) oxidant mixture were carefully added and then *ii)* 15 mL of HCl were incorporated at 50°C and the mixture stirred until complete dissolution of the sample.

All solutions were diluted to 100 mL with 3% HNO_3 before analysis. Calibration plots were performed using Perkin Elmer Pure Plus atomic spectroscopy standards.

IV.2.2.2. XRD analysis

XRD of all catalyst were performed on a Siemens D-5000 X-Ray diffractometer, using a cobalt source, CoKα, and a graphite monochromator. The voltage and current intensity used were 20 kV and 25 mA, respectively. Scans were performed at 0.05° 2θ intervals over the 2θ range from 5 to 75°.

IV.2.2.3. TEM and SEM-EDX analysis

Transmission electron microscopy (TEM) images were obtained using a JEOL JEM 1400 microscope at the Central Service for Research Support (SCAI) of the University of Córdoba. All samples were mounted on 3 mm holey carbon copper grids.

SEM-EDX measurements were performed on a JEOL JSM-6300 scanning electron microscope (SEM) equipped with an energy-dispersive X-ray (EDX) detector. It was operated at an acceleration voltage of 20 keV with a resolution of 65 eV.

IV.2.2.4. XPS analysis

X-ray photoelectron spectroscopy (XPS) analysis was carried out at the Central Service for Research Support (SCAI) of the University of Córdoba. XPS data were recorded on 4 mm × 4 mm pellets 0.5 mm thick that were obtained by gently pressing the powdered materials following outgassing to a pressure below about 2×10^{-8} Torr at 150°C in the instrument prechamber to remove chemisorbed volatile species. The main chamber of the Leibold–Heraeus LHS10 spectrometer used, capable of operating down to less than 2×10^{-9} Torr, was equipped with an EA-200MCD hemispherical electron analyser with a dual X-ray source using AlKα (hv = 1486.6 eV) at 120 W, at 30 mA, with C(1s) as reference energy (284.6 eV).

IV.2.2.5. BET surface area

Surface areas of the solids were determined from nitrogen adsorption–desorption isotherms obtained at liquid nitrogen temperature on a Micromeritics ASAP-2010 instrument, using the Brunnauer–Emmett–Teller

(BET) method. All samples were degassed to 0.1 Pa at 120°C prior to measurement.

IV.2.2.6. Temperature-programmed reduction (TPR)

Temperature-programmed reduction (TPR) measurements were performed on a Micromeritics Autochem II chemisorption analyser. An amount of 200 mg of catalyst was placed in the sample holder and reduced in a 10% H_2/Ar stream flowing at 40 mL min^{-1}. The temperature was ramped from 50 to 600ºC at 10°C min^{-1} (50 to 450ºC in the case of Pt/ZnO).

IV.2.2.7. Surface acid properties of the catalysts

Surface acidity of the catalysts were determined by temperature-programmed desorption of pyridine in a PID Eng&Tech instrument furnished with a TCD detector. The sample (50 mg) was placed in a quartz U tube, connected to a He flow (10 mL min^{-1}), introduced in an oven, and ramped up to its calcination temperature (at a rate of 10ºC min^{-1}) in order to remove chemisorbed species. After a cooling down process, the clean sample was treated with a pyridine saturated helium stream at room temperature for 30 min. Physisorbed pyridine was removed by flowing the sample with pure helium at 50ºC for additional 30 min. The pyridine desorption step starts heating the sample, in He flow, from 50°C up to 400°C at 10ºC min^{-1}.

IV.2.2.8. TG-DTA of spent catalysts

The catalysts were subjected to thermogravimetric and differential thermal analysis on a Setaram SetSys 12 instrument. An amount of 20 mg of sample was placed in an alumina crucible for TGA–DTA analysis and heated at temperatures from 30 to 600ºC at a rate of 10ºC/min under a stream of

synthetic air at 40 mL/min in order to measure weight loss, heat flow and derivative weight loss.

IV.2.3. Reactivity tests

Supported Pt catalysts were tested in the liquid-phase glycerol hydrogenolysis in a Berghof HR-100 high pressure reactor. The 75 mL PTFE lined reaction vessel was loaded with 20 mL of an aqueous solution 1.36M in glycerol (99%, Sigma-Aldrich, ref. G7757) or Acetol (90%, Sigma-Aldrich, ref. 13185) and 200 mg of freshly activated catalyst. Then, the reactor was closed and purged with H_2 for 1 min and then pressurized with hydrogen to 6 or 10 bar. At this moment, the temperature was set at 180ºC and waited for 1h for stabilization. The reaction started by switching on the stirring at 1000 rpm for 15h. Blank experiments were carried out without Pt catalyst and with bare supports. The reaction was stopped by cooling down the reactor in an ice bath. Then, the reactor was depressurized, the reaction mixture homogenized by adding water (1:1 ratio), centrifuged and filtered through a PTFE syringe filter (0.45µm). Finally, the liquid phase was analyzed by GC-TCD (Agilent 7890) equipped with a 30 m Nukol capillary column (Supelco, ref.25357). Quantification was based on the corresponding calibration plots obtained for reagents and products.

IV.3. Results and Discussion

IV.3.1. Characterization of the solids

Supports and supported Pt catalysts were thoroughly characterized by a number of techniques, Table 1 presenting the main features.

Catalyst	S_{BET} m^2/g	Pore diameter (A)	Acidity µmol PY/g	Acidity µmol PY/m^2	%Pt (w/w)			Pt particle size TEM (nm)
					ICP-MS	SEM	XPS	
Al_2O_3-AC	174	4.1	110	0.6	—	—	—	—
Pt/Al_2O_3AC-200	158	5.1	120	0.8	3.9	6.8	4.7	2.3
Pt/Al_2O_3AC-400	163	5.0	136	0.8	3.9	6.5	5.2	2.6
Al_2O_3BA	163	4.5	87	0.5	—	—	—	—
Pt/Al_2O_3BA-200	151	5.2	128	0.8	4.6	5.7	5.4	1.7
Pt/Al_2O_3BA-400	153	5.6	91	0.6	4.6	6.9	5.0	1.9
CeO_2	60	7.9	59	1	—	—	—	—
Pt/CeO_2-200	46	9.0	43	0.9	4.2	4.3	4.7	2.7
Pt/CeO_2-400	49	8.1	42	0.9	4.2	4.1	6.4	2.8
La_2O_3	14	21.0	10	0.7	—	—	—	—
Pt/La_2O_3-200	12	45.6	70	5.8	3.9	2.5	2.6	n.d.
Pt/La_2O_3-400	12	30.8	10	0.9	3.9	2.4	2.4	2.3
ZnO	18	28.2	3	0.1	—	—	—	—
Pt/ZnO-200	10	41.3	32	3.2	6.1	3.4	5.7	2.1
Pt/ZnO-400	10	41.7	20	2	6.1	3.6	6.6	4.5

Table 1. Some features concerning characterization of the different supported Pt systems. BET surface area, surface acidity, Pt metal loading and Pt particle size of the catalysts used in this work.

Solids used as supports in this work present different surface areas ranging from 174 and 163 m^2/g for alumina based supports (activated acid and basic, respectively) to 18 and 14 m^2/g for ZnO and La_2O_3, CeO_2 presenting an intermediate surface area (60 m^2/g).

Platinum was incorporated to the supports in a nominal loading of 5%. Chemical analysis of Pt catalysts by ICP-MS, SEM and XPS is given in Table 1. According to ICP-MS, Pt incorporation to the support was close to nominal value, ranging from 3.9 % for Pt/ La_2O_3 and Pt/Al_2O_3-AC to 6.1 % for Pt/ZnO. SEM-EDX and XPS normally give higher values probably due to a surface concentration of Pt species and/or to heterogeneous distribution of Pt particles. Regarding Pt particle size, it has been determined by TEM microscopy, the

exception being the Pt/La_2O_3-200 catalyst for which TEM images gave too low contrast to reliable measuring Pt particle size.

IV.3.1.1. Surface acid properties of the catalysts

The surface acid properties of supports and Pt catalysts were determined by temperature-programmed desorption of pyridine and the results are collected in Table 1.

Results indicate that the most acidic support used is Al_2O_3-AC followed by Al_2O_3-BA, CeO_2 and finally La_2O_3 and ZnO which are the least acidic supports. Incorporation of Pt to the supports has a diverging effect on the final catalysts acidity, also depending on the reduction temperature. Thus the incorporation of Pt on both acidic and basic Al_2O_3 increased moderately the acidity of the final catalyst, especially for the acidic one. On the other hand, incorporation of Pt to the ZnO support (which is the least acidic one) induced in the final catalyst an increase in acidity by a factor of 10. There was also an increase in acidity for the La_2O_3 support upon incorporation of Pt but only after reduction at 200°C. Finally, ceria-based catalysts did not increase their acidity on Pt incorporation. The increase in the acidity observed for the catalysts after the incorporation of Pt from H_2PtCl_6 precursor could be related to the presence of chlorine atoms at the surroundings of the Pt particles [14-15].

IV.3.1.2. X-ray diffraction analysis

XRD patterns corresponding to supports and catalysts used in this work are given as supplementary material (Figure S1). As for the supports, both basic and acidic alumina were amorphous as evidenced by the absence of diffraction peaks in their patterns, while cerium and zinc oxides show

diffraction profiles corresponding to cerianite (PDF 34-0394) and zincite (PDF 36-1451) structures, respectively.

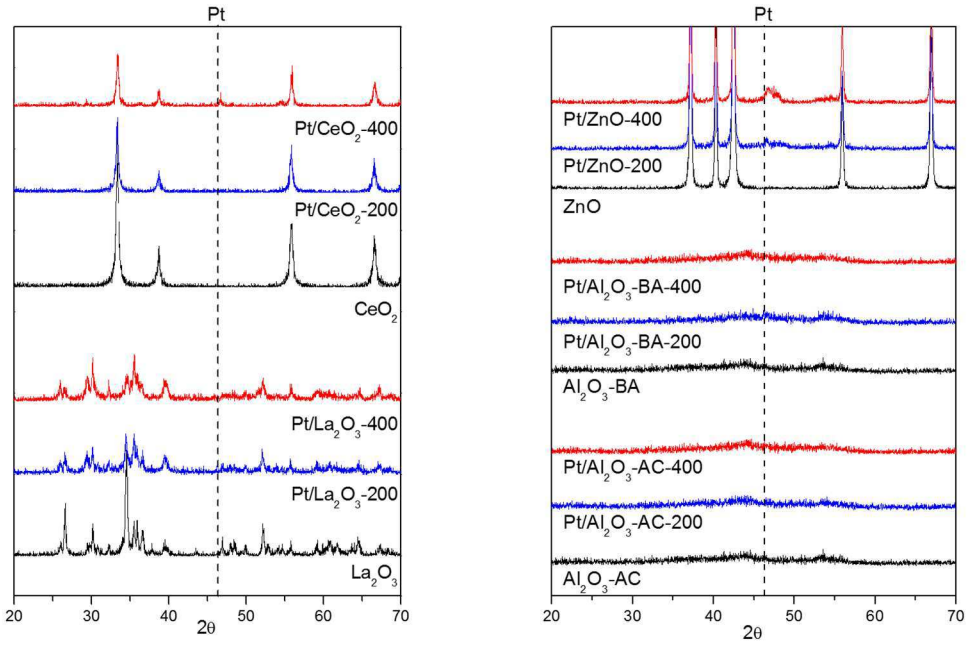

Figure S1.- XRD patterns corresponding to supports and Pt catalysts used in this work.

As far as lanthanum oxide is concerned, the support calcined at 400°C presented a diffraction profile corresponding mainly to both monoclinic and hexagonal lanthanum oxide carbonate (PDF 23-0320 and 37-0804) [40]. After the incorporation of Pt from H_2PtCl_6, in addition to lanthanum oxide carbonate, lanthanum oxychloride was formed and detected in the Pt/La_2O_3 XRD pattern (LaOCl, PDF 08-0477). Since thermal treatment can affect the carbonated phases [41], a sample of the Pt/La_2O_3 catalyst was calcined in air at 600°C for 12h and, as result, part of the carbonated phases decomposed into La_2O_3 although most of the $La_2O_2CO_3$ remained in the calcined solid. Therefore it is expected that Pt/La_2O_3 catalysts is stable under thermal treatment at reaction temperatures.

Furthermore, Pt is observed in the diffractograms as a wide and low intensity diffraction peak indicating high dispersion of small Pt metal particles [42]. Moreover, in the case of Pt/ZnO catalyst, the shape and position of the Pt diffraction peaks change depending on the reduction temperature as a consequence of sintering and alloying of Pt with Zn [43,44]. Thus, the Pt/ZnO-400 catalyst clearly presents a PtZn alloy band displaced to higher 2θ values as compared to Pt metal signal.

IV.3.1.3. Temperature-programmed reduction (TPR)

The as-synthesized (calcined) supported Pt catalysts were analyzed by temperature-programmed reduction in order to collect some information on the reducibility of the catalytic systems. The obtained TPR profiles, presented in Figure 1, indicate that all catalysts only show low temperature reduction peaks (below 225°C), the exception being Pt/La_2O_3 that, in addition to a small reduction peak centered at 160°C, exhibits a high-temperature peak (325-600°C). However, the integrated area of this peak is too large to be associated to reduction of Pt species. As commented above, XRD profiles for the Pt/La_2O_3 indicate the presence of lanthanum oxycarbonate that partially decomposes at temperatures around 600°C and therefore such a peak in the TPR profile of Pt/La_2O_3 could be assigned to the partial decomposition of lanthanum oxycarbonate (the TPR detection is based on TCD and thus it is not very selective).

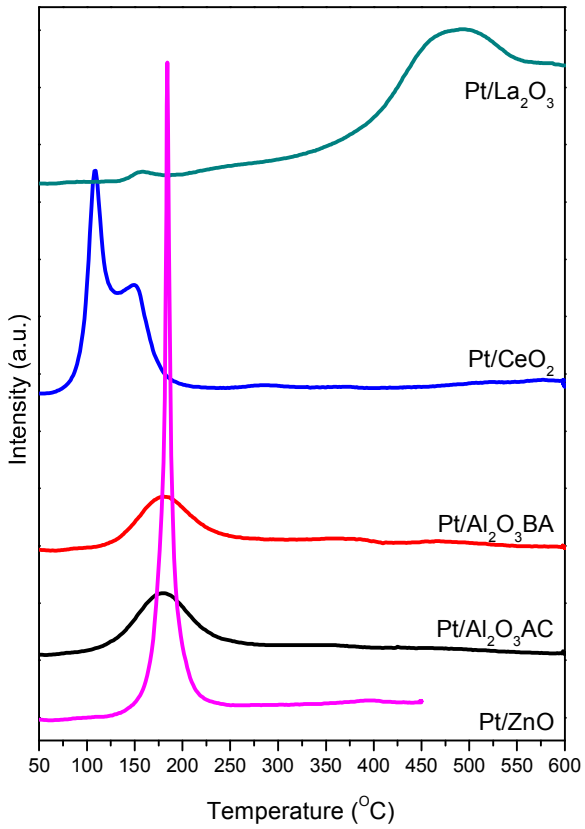

Figure 1. Temperature-programmed reduction (TPR) profiles obtained for the supported Pt catalysts synthesized in this work.

The low temperature reduction peaks are usually associated to Pt^{2+} or Pt^{4+} reduction to metallic Pt [43,45]. Thus, in Pt/CeO_2, there are two different reduction peaks possibly indicating two Pt species interactions with the support. Pt/ZnO shows a narrow and intense reduction peak centered at 185°C probably indicating a monomodal particle size distribution of Pt metal particles. Finally, both alumina supported Pt catalysts present a wide reduction peak centered at 180°C.

Considering TPR profiles, the chosen catalyst reduction temperatures were 200 (low-temperature reduction, LTR) or 400°C (high-temperature

reduction, HTR), both ensuring the complete reduction of the Pt species on the catalysts.

IV.3.2. Glycerol hydrogenolysis

IV.3.2.1. First screening of catalysts

In order to evaluate the influence of the support on the catalytic activity, a first screening of the supported Pt catalysts was carried out. As stated above, catalysts were previously reduced at 200°C (LTR) or 400°C (HTR), and the reaction conditions used were an initial hydrogen pressure of either 6 or 10 bars, an initial glycerol concentration of 1.36M and a reaction temperature of 180°C. The main reaction products detected were 1,2-propanediol (1,2-PDO), 1-hydroxyacetone (ACETOL) and ethylene glycol (EG) in addition to some traces of n-propanol and ethanol. According to the literature, acetol is obtained by dehydration of the primary hydroxyl group of glycerol whereas its subsequent hydrogenation leads to 1,2-PDO [14]. Blank reactions corresponding to glycerol hydrogenolysis without catalyst and with bare supports were carried out and, in all cases, no reaction products were detected after 15h of reaction. Therefore, this seems to suggest that both acid and metal sites are needed to promote glycerol dehydration to acetol [14,29].

The results obtained for the supported Pt catalysts, in terms of glycerol conversion, products selectivity and yield to 1,2-PDO for t=15h, are presented in Table 2.

Table 2.- Glycerol conversion, selectivity to products and 1,2-PDO yield obtained in glycerol hydrogenolysis over supported Pt catalysts. Reaction conditions: 1.36M glycerol in water at a reaction temperature of 180°C, an initial hydrogen pressure of 6 or 10 bars and 15h of reaction time.

Catalyst	Pressure (bar)	Conversion (mole, %)	Product selectivity (%)				Yield (1,2-PDO, %)
			1,2-PDO	ACETOL	EG	Others	
Pt/Al_2O_3-AC-200	6 bar	14	36	26	17	21	5
Pt/Al_2O_3-AC-400	6 bar	23	26	10	29	35	6
Pt/Al_2O_3-BA-200	6 bar	16	44	21	13	22	7
Pt/Al_2O_3-BA-400	6 bar	11	36	21	22	21	4
Pt/CeO_2-200	6 bar	33	35	25	15	25	12
Pt/CeO_2-400	6 bar	37	17	27	29	27	6
Pt/La_2O_3-200	6 bar	18	44	18	29	9	8
Pt/La_2O_3-400	6 bar	33	38	32	30	15	13
Pt/ZnO-200	6 bar	28	32	31	7	30	9
Pt/ZnO-400	6 bar	25	26	47	4	23	7
Pt/Al_2O_3-AC-200	10 bar	5	41	17	6	36	2
Pt/Al_2O_3-AC-400	10 bar	9	35	7	9	49	3
Pt/Al_2O_3-BA-200	10 bar	3	72	5	23	0	2
Pt/Al_2O_3-BA-400	10 bar	4	60	3	11	26	2
Pt/CeO_2-200	10 bar	12	47	31	9	13	6
Pt/CeO_2-400	10 bar	2	4	78	8	10	0
Pt/La_2O_3-200	10 bar	4	54	11	2	33	2
Pt/La_2O_3-400	10 bar	9	4	77	0	19	0
Pt/ZnO-200	10 bar	3	98	2	0	0	3
Pt/ZnO-400	10 bar	2	98	2	0	0	2

As can be observed in this Table, high hydrogen pressure (10 bars) led to lower glycerol conversions but higher 1,2-PDO selectivities, the exception being Pt/CeO_2-400 and Pt/La_2O_3-400 that exhibited high selectivities to acetol to the detriment of 1,2-PDO. Briefly, at 6 bar the selectivity to 1,2-PDO is in the 17-44% range (11-37% conv.) in contrast to the reactions at 10 bar for which the 1,2-PDO selectivity is the 35-98% range (2-12% conv.). Overall, 1,2-PDO yield is better for the experiments carried out at 6 bars (Table 2).

Moreover, no clear pattern or trend is observed when analyzing the effect of the catalyst reduction temperature on catalytic activity. This effect, if any, could be due to many different factors such as a possible increase in metal particle size at HRT, the appearance of strong metal-support interactions or some kind of alloying between Pt and the reduced supports.

However, when 1,2-PDO yield is plotted against conversion (Figure 2) it is observed that as the reaction proceeds there is a progressive loss in 1,2-PDO yield probably due to the formation of polymeric species that could not be detected by GC. Gas phase was analyzed by GC-FID, accounting for 1-2% of the reaction products. CO_2 was identified as the main gaseous product in all cases but for CeO_2 catalyst, in which case C_2 hydrocarbons were the main gaseous compounds. Therefore, the mass balance (considering liquid and gas phase) is not closed and the gap is increasing as the glycerol conversion does. For the reactions at 6 bar (Table 2), the best performing catalysts in terms of 1,2-PDO yield are Pt/La_2O_3-400 and Pt/CeO_2-200 (13 and 12% yield, respectively). Moreover, Pt/CeO_2-400 presents the highest glycerol conversion (37%) but associated to a rather low selectivity to 1,2-PDO (17%), thus leading to a 1,2-PDO yield of 6%. On the other hand, Pt/ZnO catalyst presents an intermediate yield to 1,2-PDO (9% and 7% yield for the catalyst reduced at 200 and 400ºC, respectively).

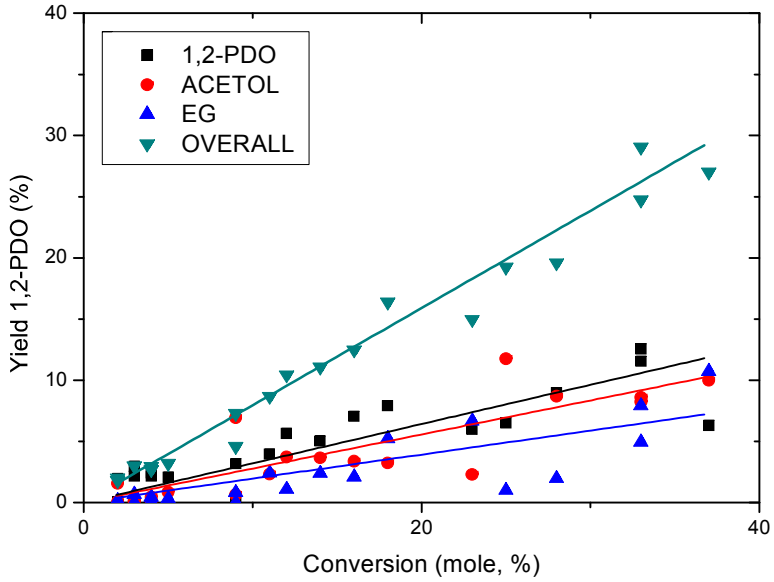

Figure 2.- Yield-conversion relationship obtained for the supported catalysts tested in glycerol hydrogenolysis. Reaction conditions: 1.36M glycerol in water at a reaction temperature of 180°C, an initial hydrogen pressure of 6 or 10 bars and 15h of reaction. "Overall" refers the sum of the yield to 1,2-PDO, acetol and ethyleneglycol.

Finally, in general, Al_2O_3 based catalysts are the solids yielding less 1,2-propanediol (1,2-PDO yield in the 4-7% range). According to the above presented yields to 1,2-PDO, a general sequence of catalytic activity can be stated:

Pt/La_2O_3 > Pt/CeO_2 > Pt/ZnO > Pt/Al_2O_3-BA ≈ Pt/Al_2O_3-AC

Therefore, Pt/La_2O_3-400, Pt/CeO_2-400 and Pt/ZnO-400 were selected in order to perform new experiments to gain some additional information on the reaction mechanism.

IV.3.2.2. Acetol hydrogenation

As commented above, production of 1,2-PDO is known to occur through hydrogenation of acetol which, in turn, is obtained via dehydration of a primary hydroxyl group of glycerol (Scheme 1) [14]. Our results indicate that calcined supports showed no activity in glycerol dehydration in spite of their acidic properties (Table 1) and, therefore, both acid and metal functions are needed to accomplish the dehydration of glycerol to acetol. Moreover, it has been reported that dehydration of glycerol to acetol is slower than hydrogenation of acetol to 1,2-PDO [46]. Therefore, in order to get some additional information on the role of both support and Pt metal particles, acetol hydrogenation experiments were carried out, the results being presented in Table 3.

Calcined supports easily transform acetol, at a reaction temperature of 180°C, with conversion in the 67-80% range after 5h of reaction and 83-95% for 15h reactions. As for the reactions products, glycerol is obtained with a ca. 10% selectivity, indicating that bare supports are capable of partly perform acetol re-hydration to glycerol.

This is hardly surprising considering that both species are in equilibrium and in a water medium. On the other hand, 1,2-PDO and EG selectivities are normally under 2% and 1%, respectively. Therefore, acetol is converted into other products that were not identified in this work but that could be observed as many, small chromatographic peaks or as water insoluble polymeric species appearing deposited on the catalysts surface and reaction vessel. These sub-products account for 79-88% of converted acetol (Table 3).

Support Catalyst	Reaction Time (h)	Reaction Temperature (°C)	Acetol Conversion (%)	S_{GLY}	$S_{1,2\text{-PDO}}$	S_{EG}	Mass Balance (%)
CeO_2-400	5	180	67	15	1	0	16
La_2O_3-400	5	180	68	12	1	1	14
ZnO-400	5	180	80	11	1	0	13
CeO_2-400	15	180	95	10	2	0	12
La_2O_3-400	15	180	90	10	10	1	21
ZnO-400	15	180	83	11	2	0	13
Pt/CeO_2-400	5	180	58	16	84	0	100
Pt/La_2O_3-400	5	180	62	17	71	0	88
Pt/ZnO-400	5	180	75	8	64	0	72
Pt/CeO_2-400	15	180	96	11	4	0	15
Pt/La_2O_3-400	15	180	98	12	8	3	23
Pt/ZnO-400	15	180	92	18	59	2	79
Pt/CeO_2-400	15	150	87	8	13	1	22
Pt/La_2O_3-400	15	150	81	7	10	1	18
Pt/ZnO-400	15	150	70	9	66	0	75

Table 3.- Acetol conversion and selectivity to products in the liquid-phase acetol transformation on bare supports and supported Pt catalysts. Reaction conditions: 1.36M acetol in water, reaction temperature of 150 or 180°C, an initial hydrogen pressure of 6 bar and 5 or 15h of reaction time.

This is consistent with results found in the literature, where it is described that acidic solids deactivated in the gas-phase acetol transformation as a consequence of oligomerization processes leading to furan derivatives or even to phenolic compounds [30].In our case, GC-MS studies evidenced the formation of several water insoluble C4-C9 liquid oxygenates, as ethers or esters, that could account for the low mass balance observed in these reactions. As far as the Pt supported catalysts are concerned, acetol conversion at 5h of reaction are in the 58-75% range, increasing up to 92-98% for t=15h. Among reaction products, glycerol is also obtained at similar levels than those obtained for bare supports. Thus glycerol selectivity obtained for supported Pt catalysts is in the 8-17% range at 5h of reaction and maintaining this selectivity level after 15h in the 11-18% range. However, the most interesting distinctive behavior between bare supports and supported Pt catalysts is in the 1,2-PDO selectivity.

Thus, Pt catalysts exhibited 64-84% selectivity to 1,2-PDO for t=5h, in contrast to the ca. 1% selectivity obtained for calcined supports. It is reasonable to conclude that acetol hydrogenation needs a metal function to proceed [8]. After 15h of reaction, Pt/ZnO-400 affords a 1,2-PDO selectivity level of about 59% while Pt/La_2O_3-400 and Pt/CeO_2-400 exhibit 1,2-PDO selectivities of 8 and 4%, respectively. Probably, the C4-C9 oligomeric compounds formed at longer reaction time from acetol condensations on the support acid sites finally deposited on the metallic active sites deactivating them for acetol hydrogenation to 1,2-PDO. Alternatively, it could be argued that, when close to 100% acetol conversion (92-98%), catalysts convert the formed 1,2-propanediol into additional reaction products, thus lowering the 1,2-PDO yield. However, experiments carried out with 1,2-propanediol as

starting substrate revealed that neither bare supports nor supported Pt catalysts were able to convert it under the reaction conditions (180°C, 6 bar, 15h).

The role of the support on the oligomerization processes is also confirmed by the low mass balance obtained for the bare supports (13-16%, 5h) in contrast to the mass balance for the supported Pt catalysts for the same reaction time: 100, 88 and 72% for Pt/CeO_2-400, Pt/La_2O_3-400 and Pt/ZnO-400 respectively. For longer reaction time, the mass balance significantly decreases for Pt/La_2O_3-400 (23%, 15h) and Pt/CeO_2-400 (15%, 15h) catalysts whereas Pt/ZnO-400 maintains a higher mass balance level (79%, 15h). These results point out that ZnO behaves better than La_2O_3 or CeO_2 as supports for supported Pt catalysts since it is able to keep the acetol oligomerization under control. It is interesting to note here that bare ZnO presented very low surface acidity and that Pt incorporation generated new acid sites probably located around Pt metallic particles. Therefore, this metal-acid bifunctional sites are responsible for glycerol dehydration to acetol and its subsequent hydrogenation to 1,2-PDO, thus enhancing 1,2-PDO selectivity versus other by products.

Finally, in an attempt to reduce the extent of acetol oligomerization reactions, some experiments consisting in acetol hydrogenation were carried out at 150°C and 15h of reaction for supported Pt catalysts (Table 3). As expected, lower conversion levels were obtained at 150ºC as compared to 180ºC. Moreover, a slight increment in selectivity to 1,2-PDO was observed for Pt/ZnO-400 (66%) a system which also kept low oligomerization activity (mass balance, 75%) while both Pt/La_2O_3-400 and Pt/CeO_2-400 solids presented low 1,2-PDO selectivities (10-13%) and poor mass balances (18-22%). Therefore, it has to be concluded that oligomerization also takes place

significantly at low temperature and that the reaction time is essential to determine the extent of this process.

Taking the above presented discussion into account, it seems to be clear that, both metal and acidic functions are needed to dehydrate glycerol to acetol and further hydrogenate acetol to 1,2-propanediol, that behaves as stable secondary product in our reaction conditions (no further transformation was observed). Moreover, the support acidity that is not associated to Pt metal sites is detrimental to this process since acetol oligomerization takes place on these acid sites leading to catalysts deactivation. Some additional information could be obtained from characterization of the catalysts used in glycerol hydrogenolysis.

IV.3.2.3. Characterization of spent catalysts

In order to collect some additional information on the reaction mechanism and to justify changes in 1,2-PDO selectivity with reaction time, Pt catalysts were recovered from the reaction mixture after 15h of reaction by filtration, washed with 3 portions of water (25mL each) and dried overnight at 110ºC in an oven, before characterization. Used Pt catalysts were analyzed by determining their BET surface area and performing XPS, TGA, TEM and XRD analysis. The results obtained are presented in Table 4, Figures 3 and 4 and in Supplementary Figures S2 and S3.

From Table 4, it is clear that Pt/CeO_2-400 and Pt/La_2O_3-400 used catalysts exhibit a small loss of surface area (around 25% loss) after 15h of reaction, suggesting that there is some degradation of the porous structure of CeO_2 and La_2O_3 supports due to the hydrothermal reaction conditions.

		S_{BET} (m^2/g)	Pore diameter D_P (A)	Pt particle size TEM (nm)	Pt content (weight %) (XPS)	Pt content (weight %) (ICP-MS)
Pt/CeO_2-400	Fresh	49	8.1	2.8	6.4	4.2
	Used	40	7.2	3.6	8.2	6.0
Pt/La_2O_3-400	Fresh	12	30.8	2.3	2.4	3.9
	Used	9	20.8	9.7	2.5	4.4
Pt/ZnO-400	Fresh	10	41.7	4.5	6.6	6.1
	Used	10	42.7	11.0	7.4	2.5

Table 4. Comparison of textural and metallic properties corresponding to fresh and used Pt catalysts.

Alternatively, there could have been some pore blocking by adsorbed species. On the contrary, Pt/ZnO-400 used catalyst does not lose any surface area suggesting that ZnO support is rather stable at such reaction conditions. Additionally, ICP-MS analyses were carried out for the liquid-phase resulting after 15h of reaction. The results obtained indicate that the amount of Pt in the liquid phase is below 0.01% pointing to a good stability of Pt metal particles in the reaction conditions. On the contrary, as far as the supports are concerned, the percentages of lixiviated support are 7.8% (ZnO), 28.4% (La_2O_3) and 29.5% (CeO_2).

Pt particle size of the spent catalysts as determined by TEM (Supplementary material, Figure S2) showed an increase as compared to fresh catalysts. This increase is larger for Pt/La_2O_3-400 (from 2.3 to 9.7 nm for fresh and used catalyst, respectively) and Pt/ZnO-400 (from 4.5 to 11.0 nm). For Pt/CeO_2-400, the change is somehow smaller, just increasing Pt particle size from 2.8 to 3.6 nm for fresh and used catalysts, respectively..

XRD pattern for the used Pt/CeO_2-400 catalyst presented in Figure 3 shows, in addition to cerium oxide (ICDD PDF 34-0394), new diffraction peaks corresponding to cerium carbonate hydroxide (ICDD PDF 32-0189) as a consequence of the partial degradation of CeO_2 under hydrothermal reaction conditions. Moreover, in agreement with TEM results, an increase in the intensity of the Pt^0 diffraction peak is observed associated to an increase in Pt

particle size. Similarly, the XRD pattern for the spent Pt/La_2O_3-400 catalyst also presents new diffraction peaks associated to lanthanum carbonate hydroxide (ICDD PDF 26-0815) and, with lower intensity, lanthanum hydroxide (ICDD PDF 36-1481) formed under hydrothermal reaction conditions (Figure 3). As far as Pt diffraction signals are concerned, small diffraction peaks appear below $2\theta = 46°$ that could be associated to LaPt alloy (ICDD PDF 17-0364 or 19-0657) formed under reductive and hydrothermal reaction conditions. Finally, for the Pt/ZnO-400 used catalyst, no change in the ZnO support is observed by XRD under reaction conditions, indicating a stable support. However, as far as platinum is concerned, Pt_0 signal almost disappears and a very intense signal associated to PtZn alloy is clearly observed (ICDD PDF 04-0802) in the XRD profile.

Recently, Oberhauser *et al.* described the effect of carbonaceous supports on Pt sintering on the structure-sensitive glycerol hydrogenolysis, so we assume that the structural changes observed, both in support as in Pt particle size, have an important role in catalyst deactivation [49]. To sum up, CeO_2 and specially La_2O_3 are unstable at the reaction conditions, while ZnO is quite stable and, in addition, metallic function also changes during reaction, since an increase in Pt metal particle and/or alloying is observed in the spent catalysts.

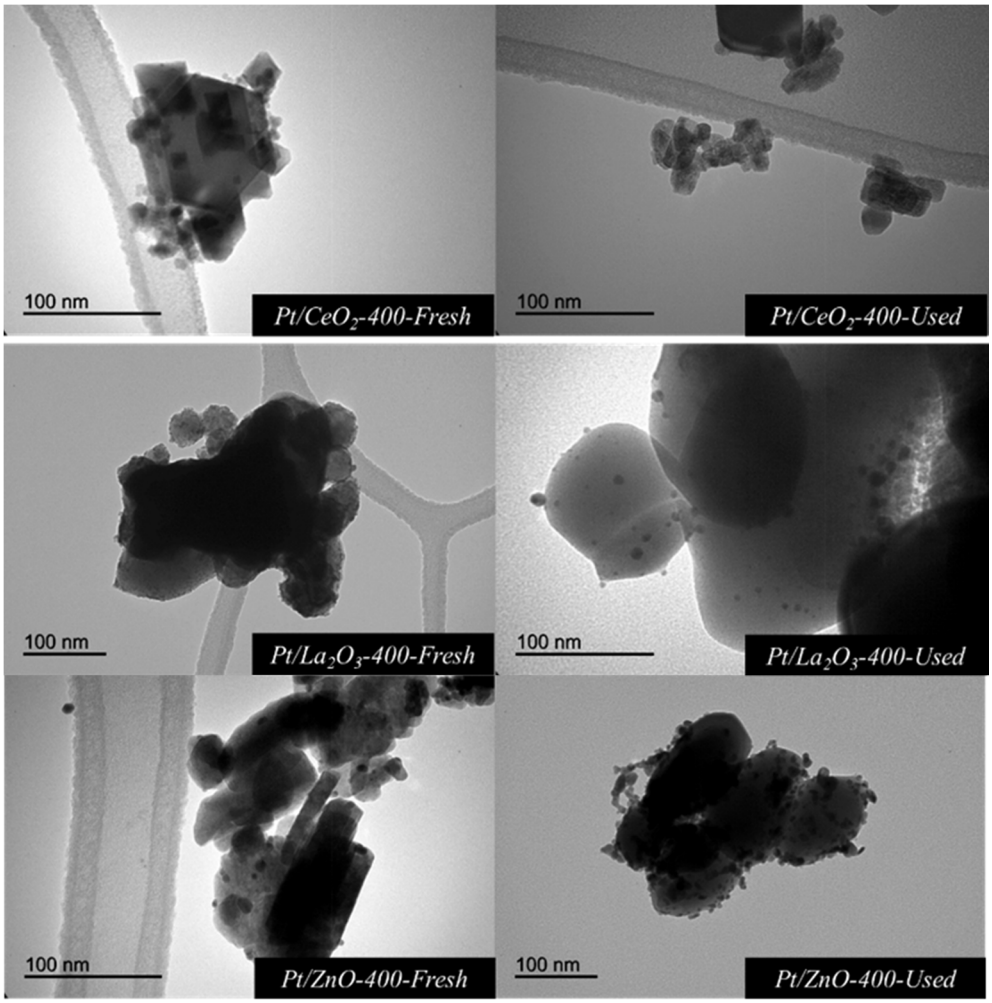

Figure S2.- TEM images corresponding to Pt catalysts fresh and used in glycerol hydrogenolysis (6 bar, 180ºC, 15h).

This Pt:Zn alloy provide a new catalyst surface with different properties and, according to Penner *et al.*, the formation of an intermetallic compound can stabilise the metal particle in terms of morphology and crystallography [50].

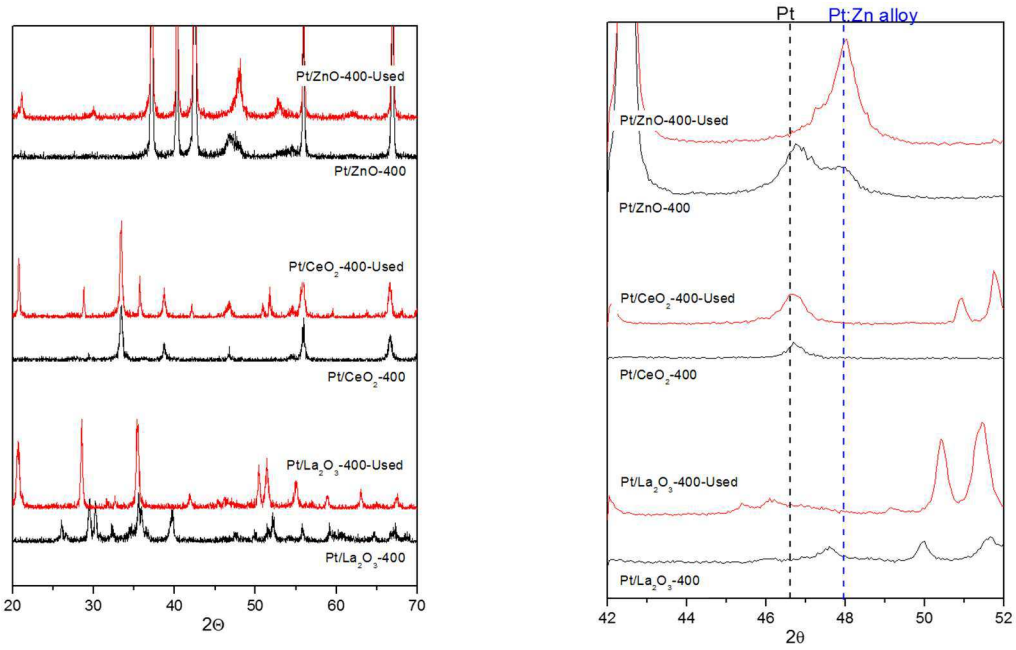

Figure 3.- XRD patterns corresponding to fresh (black line) and used (red line) Pt catalysts in glycerol hydrogenolysis (180°C, 6 bar, 15h).

TGA-DTA experiments performed for the used Pt catalysts revealed different behaviors for the three systems (Figure 4). Overall mass losses obtained for the spent catalysts were 12%, 22% and 30% for Pt/CeO_2-400, Pt/La_2O_3-400 and Pt/ZnO-400, respectively. However, most of the mass lost by Pt/ZnO-400 catalyst (Figure 4c) takes place at temperatures below 110ºC indicating that it corresponds to water or volatile species weakly adsorbed on the catalyst surface (endothermic process). For this catalyst there is only a very

small exothermic combustion peak centered at around 525ºC associated to some graphitized carbonaceous residues. On the contrary, used Pt/CeO_2-400 (Figure 4a) presents three exothermic processes associated to combustion of poorly graphitized organic deposits (main mass loss, centered at 275ºC) and two additional small exothermic peaks appearing at 450-475ºC and associated to the combustion of more graphitized carbonaceous deposits. Finally, spent Pt/La_2O_3-400 (overall mass lost ca. 22%) exhibits a continuous mass loss in the 400-525ºC range that could be associated to combustion of carbonaceous deposits (exothermic signal) and probably to the partial decomposition of lanthanum oxide carbonate formed under reaction conditions (endothermic signal observed at temperatures above 500ºC).

These results clearly correlates with the reactivity results for the catalysts tested in glycerol and acetol transformations. Catalysts exhibiting a poor mass balance due to condensations and/or polymerization reactions leading to carbonaceous residues (Pt/CeO_2-400 and Pt/La_2O_3-400, Table 3, 15h), present high-temperature combustion peaks in TGA-DTA experiments, associated to the accumulation of deposits on the catalysts surface. Interestingly, Pt/ZnO-400 catalyst, that exhibited a 30% selectivity to 1,2-PDO in acetol hydrogenation at long reaction time, only presents very small high-temperature combustion peaks, in agreement with its low polymerization capability and, also, in concordance with its better mass balance (Table 3, mass balance >79% at 15h).

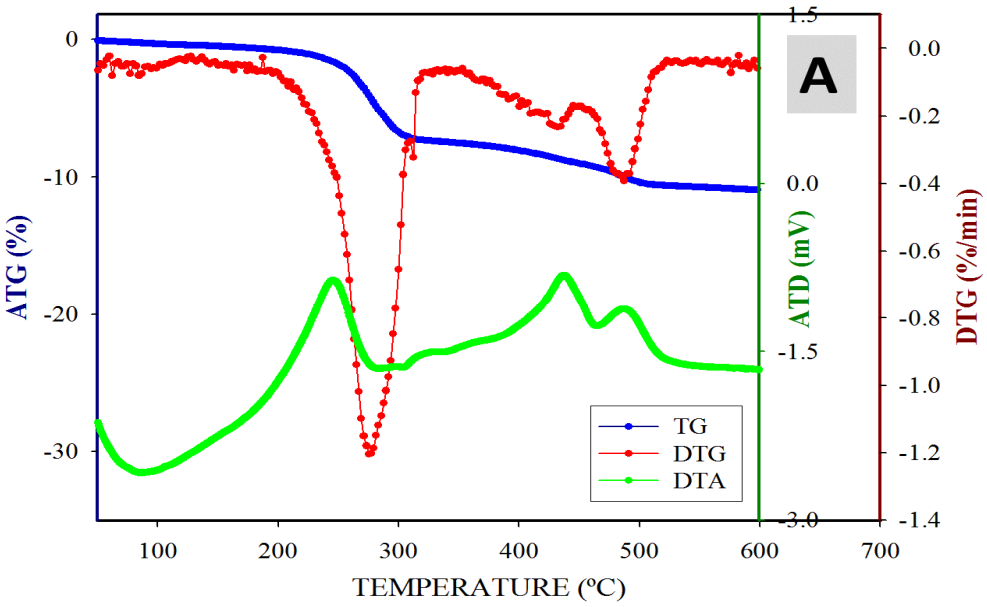

Figure 4.A.- TGA-DTG-DTA analysis of Pt/CeO_2-400 catalysts used in glycerol hydrogenolysis (180°C, 6 bar, 15h).

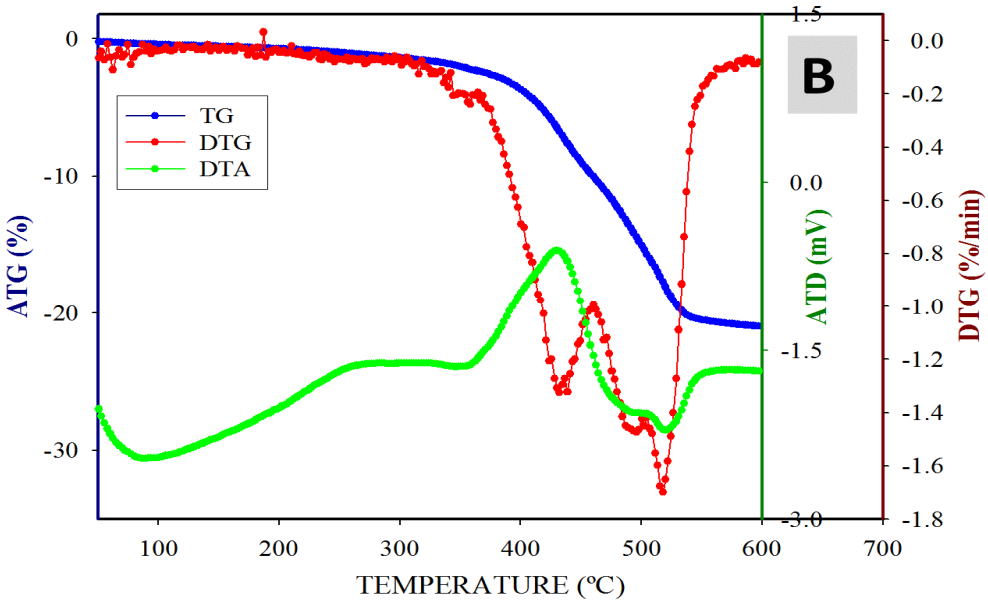

Figure 4.B- TGA-DTG-DTA analysis of Pt/La_2O_3-400 catalysts used in glycerol hydrogenolysis (180°C, 6 bar, 15h).

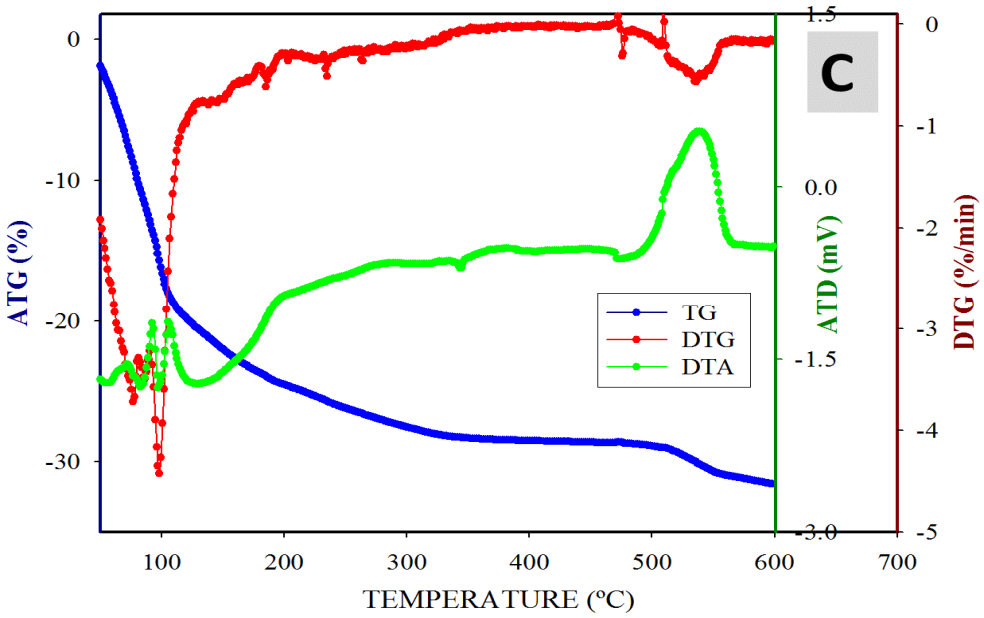

Figure 4.C- TGA-DTG-DTA analysis of Pt/ZnO-400 catalysts used in glycerol hydrogenolysis (180°C, 6 bar, 15h).

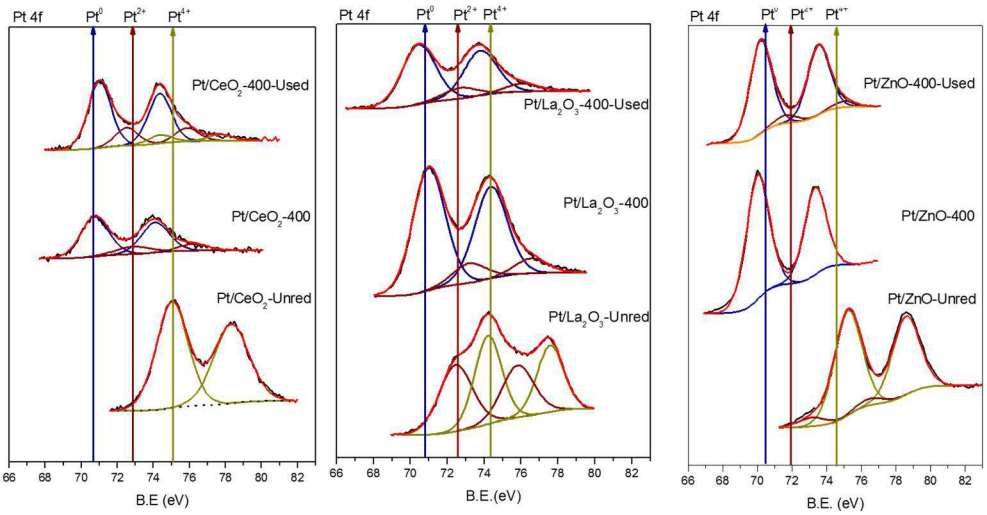

Figure S3.- XPS spectra corresponding to Pt catalysts fresh and used in glycerol hydrogenolysis (6 bar, 180ºC, 15h).

XPS profiles obtained for all three used Pt supported catalysts (Supplementary material Figure S3) do not give any valuable additional information. Only a slight re-oxidation of Pt is observed which, however, could be due to manipulation of the catalysts after reaction (filtration, washing and drying processes).

IV.4. Conclusions

Several supported Pt catalysts were prepared by wet impregnation over different oxide supports such as Al_2O_3, CeO_2, La_2O_3 and ZnO. All those catalysts were characterized and tested in the liquid-phase glycerol hydrogenolysis. From the obtained results, the following conclusions can be extracted.

The bare supports exhibited a wide range of acidity, ZnO presenting the lower acidity among all supports tested. Moreover, acidity was in general enhanced upon Pt incorporation, especially for the Pt/ZnO catalyst for which new acid sites associated to Pt metal particles were created.

Pt/La_2O_3, Pt/CeO_2 and Pt/ZnO behaved better than Pt/Al_2O_3 in terms of 1,2-PDO yield. Moreover, as glycerol conversion increases there is a progressive loss in 1,2-PDO yield due to the formation of some polymeric species, responsible for the poor mass balance observed for some catalysts.

Experiments carried out with acetol as starting substrate indicated that support acidity not associated to the Pt metal sites is detrimental to this process due to the oligomerization of acetol, being this the main cause of the loss of 1,2-PDO yield at long reaction times.

The characterization of used catalysts revealed that under hydrothermal reaction conditions CeO_2 and La_2O_3 supported Pt catalysts

suffer from leaching, lost some of their surface area and presented intense combustion signals associated to organic deposits in agreement with the poor mass balance observed for these solids.

All in all, among all studied catalysts, Pt/ZnO presented the best behavior in the liquid-phase hydrogenolysis in terms of yield to 1,2-PDO both from glycerol and acetol. These good results are based on several factor such as the appropriate surface acidity associated to Pt particles, a low oligomerization capability as consequence of the low acidity of the ZnO support and a reasonable high stability of the catalyst under hydrothermal reaction conditions.

IV.5. Acknowledgments

The authors are thankful to Junta de Andalucía and FEDER funds for financial support (P07-FQM-02695, P08-FQM-3931 and P09-FQM-4781 projects). M. Checa acknowledges the Spanish Ministry of Education for a FPU grant (Ref AP2009-1221). Central Service for Research Support (SCAI) of the University of Córdoba is also acknowledged for the ICP-MS, TEM and XPS measurements.

IV.6. References

1. M. Besson, P. Gallezot, C. Pinel, Chemical Reviews, 114 (2014) 1827-1870.

2. C.H. Zhou, H. Zhao, D.S. Tong, L.M. Wu, W.H. Yu, Catalysis Reviews - Science and Engineering, 55 (2013) 369-453.

3. J.J. Bozell, G.R. Petersen, Green Chemistry, 12 (2010) 539-554.

4. L. Chen, S. Ren, X.P. Ye, Fuel Processing Technology, 120 (2014) 40-47.

5. S. Dutta, S. De, B. Saha, M. Alam, Catalysis Science and Technology, 2 (2012) 2025-2036.

6. T. Werpy, G. Petersen, Top Value Added Chemicals from Biomass VolumeI—Results of Screening for Potential Candidates from Sugars and SynthesisGas, US Department of Energy, Oak Ridge, 1 (2004) 1-76.

7. Y. Nakagawa, K. Tomishige, Catalysis Surveys From Asia, 15 (2011) 111-116.

8. Y. Nakagawa, K. Tomishige, Catalysis Science and Technology, 1 (2011) 179-190.

9. B.M.E. Russbueldt, W.F. Hoelderich, Journal of Catalysis, 271 (2010) 290-304.

10. H.W. Tan, A.R. Abdul Aziz, M.K. Aroua, Renewable and Sustainable Energy Reviews, 27 (2013) 118-127.

11. A. Marinas, P. Bruijnincx, J. Ftouni, F.J. Urbano, C. Pinel, Catalysis Today, 239 (2015) 31-37.

12. D.T. Johnson, K.A. Taconi, Environmental Progress, 26 (2007) 338-348.

13. A. Martin, U. Armbruster, I. Gandarias, P.L. Arias, European Journal of Lipid Science and Technology, 115 (2013) 9-27.

14. V. Montes, M. Checa, A. Marinas, M. Boutonnet, J.M. Marinas, F.J. Urbano, S. Järas, C. Pinel, Catal Today, 223 (2014) 129-137.

15. M. Checa, F. Auneau, J. Hidalgo-Carrillo, A. Marinas, J.M. Marinas, C. Pinel, F.J. Urbano, Catalysis Today, 196 (2012) 91-100.

16. J. Ten Dam, K. Djanashvili, F. Kapteijn, U. Hanefeld, ChemCatChem, 5 (2013) 497-505.

17. M. Pagliaro, R. Ciriminna, H. Kimura, M. Rossi, C.D. Pina, European Journal of Lipid Science and Technology, 111 (2009) 788-799.

18. S. Zhu, Y. Zhu, S. Hao, H. Zheng, T. Mo, Y. Li, Green Chemistry, 14 (2012) 2607-2616.

19. E.S. Vasiliadou, E. Heracleous, I.A. Vasalos, A.A. Lemonidou, Applied Catalysis B: Environmental, 92 (2009) 90-99.

20. D. Sun, Y. Yamada, S. Sato, Applied Catalysis A: General, 475 (2014) 63-68.

21. X. Guo, Y. Li, W. Song, W. Shen, Catal Lett, 141 (2011) 1458-1463.

22. W. Yu, J. Zhao, H. Ma, H. Miao, Q. Song, J. Xu, Applied Catalysis A: General, 383 (2010) 73-78.

23. J. Feng, W. Xiong, B. Xu, W. Jiang, J. Wang, H. Chen, Catalysis Communications, 46 (2014) 98-102.

24. F. Auneau, C. Michel, F. Delbecq, C. Pinel, P. Sautet, Chemical Eurpean Journal, 17 (2011) 14288-14299.

25. Y. Shinmi, S. Koso, T. Kubota, Y. Nakagawa, K. Tomishige, Applied Catalysis B: Environmental, 94 (2010) 318-326.

26. E.P. Maris, R.J. Davis, Journal of Catalysis, 249 (2007) 328-337.

27. O.M. Daniel, A. DeLaRiva, E.L. Kunkes, A.K. Datye, J.A. Dumesic, R.J. Davis, ChemCatChem, 2 (2010) 1107-1114.

28. Z. Yuan, P. Wu, J. Gao, X. Lu, Z. Hou, X. Zheng, Catalysis Letters, 130 (2009) 261-265.

29. J. Zhao, W. Yu, C. Chen, H. Miao, H. Ma, J. Xu, Catalysis Letters, 134 (2010) 184-189.

30. I. Gandarias, P.L. Arias, J. Requies, M.B. Güemez, J.L.G. Fierro, Applied Catalysis B: Environmental, 97 (2010) 248-256.

31. W. Suprun, M. Lutecki, T. Haber, H. Papp, Journal of Molecular Catalysis A: Chemical, 309 (2009) 71-78.

32. W. Suprun, M. Lutecki, R. Gläser, H. Papp, Journal of Molecular Catalysis A: Chemical, 342-343 (2011) 91-100.

33. M. Massa, A. Andersson, E. Finocchio, G. Busca, Journal of Catalysis, 307 (2013) 170-184.

34. V. Nichele, M. Signoretto, F. Menegazzo, A. Gallo, V. Dal Santo, G. Cruciani, G. Cerrato, Applied Catalysis B: Environmental, 111-112 (2012) 225-232.

35. S. Zhu, X. Gao, Y. Zhu, W. Fan, J. Wang, Y. Li, Catalysis Science and Technology, 5 (2015) 1169-1180.

36. E.S. Vasiliadou, A.A. Lemonidou, Applied Catalysis A: general, 396 (2011) 177-185.

37. E.S. Vasiliadou, T.M. Eggenhuisen, P. Munnik, P.E. de Jongh, K.P. de Jong, A.A. Lemonidou, Applied Catalysis B: Environmental, 145 (2014) 108-119.

38. D. Durán-Martín, M. Ojeda, M.L. Granados, J.L.G. Fierro, R. Mariscal, Catalysis Today, 210 (2013) 98-105.

39. S. Zhu, X. Gao, Y. Zhu, Y. Zhu, H. Zheng, Y. Li, Journal of Catalysis, 303 (2013) 70-79.

40. S. Wang, Y. Li, H. Liu, Acta Chimica Sinica, 70 (2012) 1897-193.

41. J. Feng, B. Xu, D.R. Liu, W. Xiong, J.B. Wang, Advanced Materials Research, 791 (2013) 12-15.

42. M.H. Lee, W.S. Jung, Bulletin of the Korean Chemical Society, 34 (2013) 3609-3614.

43. B. Faroldi, M.L. Bosko, J. Múnera, E. Lombardo, L. Cornaglia, Catalysis Today, 213 (2013) 135-144.

44. M.S. Avila, C.I. Vignatti, C.R. Apesteguía, T.F. Garetto, Chemical Engineering Journal, 241 (2014) 52-59.

45. M. Consonni, D. Jokic, D.Y. Murzin, R. Touroude, J. Catal., 188 (1999) 165-175.

46. N. Iwasa, T. Mayanagi, N. Ogawa, K. Sakata, N. Takezawa, Catalysis Letters, 54 (1998) 119-123.

47. F. Ammari, J. Lamotte, R. Touroude, Journal of Catalysis, 221 (2004) 32-42.

48. J. Tendam, U. Hanefeld, ChemSusChem, 4 (2011) 1017-1034.

49. W. Oberhauser, C. Evangelisti, R.P. Jumde, R. Psaro, F. Vizza, M. Bevilacqua, J. Filippi, B.F. Machado, P. Serp, Journal of Catalysis, 325 (2015) 111-117.

50. S. Penner, M. Armbrüster, ChemCatChem, 7 (2015) 374-392.

Capítulo V

Influencia de dopantes en catalizadores de Pt soportado sobre óxido de zirconio para la valorización de glicerol

Chapter V

Dopants influence on zirconia based Pt catalyst for glycerol valorisation

V.Dopants influence on zirconia based Pt catalyst for glycerol valorisation

In this chapter, a zirconia support was synthesized via sol-gel method and subsequently impregnated with different dopant agents in a dopant:Zr atomic ratio of 1:10. Then, Pt-based systems were obtained through impregnation of modified zirconia supports with chloroplatinic acid (5% by weight of Pt). The solids were tested for glycerol hydrogenolysis and the results showed a correlation between surface acidity and the catalytic conversion. The catalyst doped with silicotungstic acid was the most active in the reaction, exhibiting high yields to diols and being active at lower temperatures (160ºC) than the other solids. Moreover, as the reaction proceeds there is a deeper hydrogenolysis process of diols into propanols and C-3 and C-2 hydrocarbons. Metal sites are essential for acetol selective transformation into 1,2-PDO as a result of the combination of the appropriate surface acidity, limited deactivation and stability under hydrothermal working conditions.

V.1. Introduction

Nowadays, society demands to industry the development of new environmentally friendly processes and chemicals [1]. Academy and industry, have focused their attention to biomass based chemistry because it is the only energetic source able to produce both energy and chemicals [1,2]. One example is biodiesel production as an alternative for fossil fuels [3]. The substitution of petrol based fuel by renewable raw materials as vegetable oil can considerably reduce the environmental impact [3]. During the last years, biorefineries introduced large amounts of glycerol in the markets causing a price drop of that by-product [4-7]. In this line, many countries have built facilities in order to increase their biodiesel production [3] as, for example, European countries whose production represents up to 30% of the global

production [8]. Such increment affects glycerol markets directly, because biodiesel industries generate 1 kg of bioglycerol (as by-product) per 10 kg of biofuel [8-10]. The low cost of glycerol caused by the saturation of the markets [6], together with the high functionality of the molecule, make glycerol an ideal starting material for several chemical routes [11].

From the glycerol valorization point of view, one of the most important processes is hydrogenolysis to diols [12]. The reaction can lead to different products such as 1,2-Propanediol (1,2-PDO), 1,3-Propanediol (1,3-PDO) or Ethylene glycol (EG) that, despite of being interesting for polymer industries, present the problem of being produced simultaneously, thus requiring further separation steps and leading to an increase in the production costs [12-14]. 1,2-PDO and Acetol production from glycerol can be an economically important alternative for these compounds, which have several applications for industry as solvent or intermediate for other valuable products or polymers [15-17]. 1,3-PDO, a valuable monomer for the synthesis of different polymers, is traditionally obtained via selective hydration of acrolein but its production from glycerol in biorefineries is a promising alternative [18,19]. By using different tools like heterogeneous catalysis the reaction can be tuned to yield the desirable product, thus avoiding the mentioned separation problems [7,20,21]. In this line, a wise combination of active metal and acid-base properties of the support can influence the reaction in order to maximize the production of one of the desired products, such as 1,2-Propanediol (1,2-PDO), acetol [22,23] or 1,3-Propanediol (1,3-PDO) [18,24-26]. The most described metals in the literature for glycerol hydrogenolysis are transition metals such as Cu, Ni or Co [4,27], but also some noble metals such as Pd [4,23,28], Rh [17,23] or Pt [17,23,29-31] can be used. Among them, Pt is one of the metals able to avoid C2 and C1 products, that is to avoid C-C breakage [26,32].

As regards the support, metals are supported on different solids such as metal oxides [17,23,33,34], zeolites [35], carbonates [36] or charcoal [32,37], just to cite some of them. Among metal oxides, ZrO_2 is an interesting support because its acid-base properties can be easily tuned by employing different dopants or modifiers [38,39]. Sulphated zirconia is well described as a super-acid catalyst, especially useful for dehydration of polyalcohols [40]. On the other hand, borated zirconia exhibits both acid and basic centers [41]. Moreover, zirconia can provide stability as support to polyoxomethalates (POMs), becoming an interesting option for preparing acidic catalysts [42]. In this line, W-based catalysts are described as selective to 1,3-PDO or C-3 mono-alcohols depending on reaction conditions [43,44]. Moreover, both W or Mo based POM are widely described as acid catalysts in different reactions, among them glycerol dehydration or esterification [45-48].

The purpose of this research is to study the effect of the modifier in doped zirconia as Pt support for glycerol hydrogenolysis. Sulphuric acid (H_2SO_4), boric acid (H_3BO_3), silicotungstic acid ($H_4SiW_{12}O_{40}$) and phosphomolibdic acid ($H_3PMo_{12}O_{40}$) were used as dopant agents and their influence on activity and selectivity of glycerol hydrogenolysis studied.

V.2. EXPERIMENTAL

V.2.1. Synthesis of the catalysts

The catalysts were synthesized in three subsequent steps which involves the precipitation of the zirconia as the base of the support, the modification of the support with different dopants agents such as sulphuric acid (FLUKA ref. 93124), boric acid (Sigma-Aldrich ref. B-7660), phosphomolibdic acid hydrate (Sigma-Aldrich ref. 431400) or tungstosilicic

acid hydrate (Sigma-Aldrich ref. T2780) and, finally, the incorporation of Pt following the incipient wetness impregnation method.

With the aim to obtain 50 g of bulk zirconia, 250 mL of zirconyl chloride solution (30% in HCl, Sigma-Aldrich ref.464198) were dissolved in 1 L of distillate water. Then, under mechanical stirring, the pH was increased by adding NH_4OH with a Syrris® Atlas system model "Syringe Pump", in two steps: from 1 to 5.7 by adding NH_4OH 5N and then from 5.7 to 7.6 by using NH_4OH 0.1 N. The zirconia gel was stirred overnight and the filtered and washed repeatedly with water until the $AgNO_3$ chloride test was negative. The gel was then dried overnight at 110ºC and finally milled, sieved and calcined at 300ºC under air flow (30 $mL \cdot min^{-1}$; heating rate: 2 $°C \cdot min^{-1}$). The calcined material was divided in 5 portions (ca. 10 g each). Among them, 4 portions were modified with the corresponding dopant, whereas the fifth unmodified zirconia was used as the reference bare support.

Dopants were incorporated by impregnation in a M/Zr atomic ratio of 1:10, where M stands for B, S, W or Mo. The appropriate amount of a 1 M solution of the dopant was placed in a 50 mL round bottom flask together with 10 g of ZrO_2. The mixture was rotated (150 rpm) at room temperature for 5h and then the solvent was evaporated under controlled temperature (1h at 30°C, 1h at 50 °C and 80°C until dryness). The flask was removed from the rotary evaporator and placed in an oven at 110 °C overnight. The solid was then milled, sieved and calcined at 300°C for 6h, in air flow (30 $mL.min^{-1}$). Finally, the calcined material was milled and sieved again (0.149 mm). The calcined supports were labeled as Dopant/ZrO_2, were "Dopant" makes reference to sulphuric acid (S), boric acid (B), phosphomolibdic acid (PMo) or tungstosilicic acid (SiW).

Finally, the incorporation of Pt catalysts was carried out via impregnation with chloroplatinic acid (8% wt, Sigma-Aldrich ref. 262587) over the previously synthesized supports. The appropriate amount of chloroplatinic acid to obtain a Pt loading of 5% wt was introduced in a 50 mL round bottom flask containing 9.5 g of support. The mixture was the rotated for 5h, the solvent evaporated, dried, milled, sieved and calcined in a similar way to the above presented procedure for dopant incorporation.

Before the reactivity test, each catalyst was purged with N_2 and reduced in H_2 flow (30 mL.min^{-1}) at 200°C for 2h (heating rate 10 °C.min^{-1}). Once reduced, the solid was cooled down in H_2 to room temperature and then purged for 15 min with N_2 (30 mL.min^{-1}). The reduced catalysts were labeled including the metal, dopant, support and reduction temperature: Pt//Dopant/ZrO_2-200.

V.2.2. Characterization of the catalysts

V.2.2.A. ICP-MS analysis

Elemental analysis of Pt-containing samples was carried out by the staff at the Central Service for Research Support (SCAI) of the University of Córdoba, by inductively coupled plasma mass spectrometry (ICP-MS). Measurements were made on a Perkin-Elmer ELAN DRC-e instrument following dissolution of the sample.

The catalysts were dissolved in a two-step process: 100 mg were treated with 20 mL of the HCl:HNO_3 (3:1 v/v) and stirred under mild temperature for 5 min. Then, 5 mL of HF were added to the mixture at 50°C and stirred until complete dissolution of the solid sample. All solutions were

diluted to 100 mL with 3% HNO_3 before analysis. Calibration plots were performed using Perkin Elmer Pure Plus atomic spectroscopy standards.

V.2.2.B. XRD analysis

X-ray patterns of the samples were obtained with a Bruker D8 Discover A25 diffractometer equipped with a VÅNTEC-500 bidimensional detector automatic control and data acquisition system. The instrument was used with CuKα radiation and a graphite monochromator.

V.2.2.C. XPS analysis

X-ray photoelectron spectroscopy (XPS) data were recorded on 4 mm × 4 mm pellets (0.5 mm thick) that were obtained by gently pressing the powdered materials following outgassing to a pressure below about 2×10^{-8} Torr at 423 K in the instrument prechamber to remove chemisorbed volatile species. The main chamber of the Leibold–Heraeus LHS10 spectrometer used, capable of operating down to less than 2×10^{-9} Torr, was equipped with an EA-200MCD hemispherical electron analyzer with a dual X-ray source using AlKα (hν = 1486.6 eV) at 120 W, at 30 mA, with C (1s) as energy reference (284.6 eV).

V.2.2.D. B.E.T. surface area

Surface areas of the solids were determined from nitrogen adsorption–desorption isotherms obtained at liquid nitrogen temperature on a Micromeritics ASAP-2010 instrument, using the Brunnauer–Emmett–Teller

(BET) method. All samples were degassed to 0.1 Pa at 120 °C prior to measurement.

V.2.2.E. Temperature-programmed reduction (TPR)

Temperature-programmed reduction (TPR) measurements were made with a Micromeritics Autochem II chemisorption analyser. An amount of 200 mg of catalyst was placed in the sample holder and reduced in a 10:90 H_2/Ar stream flowing at 40 ml min^{-1}. The temperature was ramped from 50 to 600 ºC at 10 ºC min^{-1} (50 to 450 ºC in the case of Pt/ZnO solid).

V.2.2.F. Surface acid–base properties of the catalysts

Surface acid-base properties of the catalysts were determined by the propan-2-ol transformation test reaction. This reaction, widely described as a model process, can provide valuable information on surface acid-base properties of the catalyst as a function of its products distribution: surface acid sites yield propene or diisopropyl ether while basic or redox properties lead to acetone [49,50].

The reaction was carried out in gas-phase in a stainless steel reactor (1/8 inch OD). The reactions were performed by loading the reactor with 100 mg of catalyst and 1 g of inert SiO_2. The catalyst was reduced under an H_2 flow (20 ml/min) while increasing the temperature until 200ºC (rate, 2ºC/min). The reaction was started by introducing propan-2-ol by passing a nitrogen flow of 10 ml/min through a saturator filled with propan-2-ol at room temperature. Analyses were carried out on-line by connecting the effluent to

a gas chromatograph (HP 5890 series II) equipped with a capillary column Supelcowax-10 (60 m long, 0.25 mm ID, 0.25 μm film thickness).

The above-described experiments were completed with diffuse reflectance infrared (DRIFT) spectroscopy of pyridine-saturated solids intended to identify the specific type of surface acid sites. Measurements were made with an ABB Bomen MB Series IR spectrophotometer equipped with a SpectraTech environmental chamber including a diffuse reflectance device capable of performing 258 scans at 8 cm^{-1} resolution at an adjustable temperature. Prior to analysis, the catalyst was cleaned by heating at 300ºC for 30 min. The catalyst was then saturated under pyridine atmosphere and heated to 100, 200 and 300ºC, recording the DRIFT spectra during the last few minutes of heating at each temperature.

V.2.3. Reactivity

The catalysts were tested for the catalytic hydrogenolysis of glycerol in a high pressure reactor (Berghof, operation limit conditions 250ºC, 100 bar and 80ml of volume). The reactor was filled with 10 mL of a water solution 1.36 M of Glycerol (99%, Sigma-Aldrich®, ref. G7757) and 100 mg of freshly reduced catalyst. Then, the reactor was closed, purged with H_2 for 1 min and filled with 6 bar of H_2. At this moment, the reaction temperature is set (160, 180 or 200ºC) and allow for stabilization for 1 hour. The reaction was started by switching on the stirring at 1000 rpm and stopped at selected times by introducing the reaction on an ice bath. Some reactions were carried with acetol (90%, Sigma-Aldrich®, ref. 138185) or 1,2-PDO (Sigma-Aldrich®, ref. 82280) 0.5 and 1 M, respectively, as starting substrates. Blank experiments were carried out in absence of catalyst and with bare supports. The gas-phase

was analyzed on line by coupling the reactor outlet to a GC-FID (Agilent® 6890) while the reactor was depressurized. The liquid phase mixture was homogenized, filtered through a syringe filter (0.45 μm) and analyzed off-line by GC-FID.

V.3. RESULTS AND DISCUSSION

V.3.1. Characterization of the solids

Supports and supported Pt catalysts were thoroughly characterized from textural, structural and chemical point of view by a number of techniques, Table 1 presenting the main features concerning catalysts characterization. Bare ZrO_2 presented a BET surface area of 126 $m^2 \cdot g^{-1}$ while its modification induced a decrease in surface area. Thus, incorporation of boric acid and phosphomolibdic acid led to a loss of surface area of 10-20% while sulphuric or silicotungstic acid led to BET area reduction down to 92 $m^2 \cdot g^{-1}$. The subsequent impregnation with Pt resulted in an additional reduction in surface area indicating again pore blocking or structural degradation of ZrO_2. Chemical analysis of Pt catalysts by ICP-MS and XPS is also presented in Table 1. According to ICP-MS, Pt incorporation to supports was close to the nominal value, ranging from 4.2 % for Pt//S/ZrO_2 to 4.7 % for Pt/ZrO_2. XPS gives slightly higher values probably due to a surface concentration of Pt species. Hydrogen chemisorption and XRD were used to obtain an estimated value for Pt particle size. According to XRD the average particle size, obtained from Scherrer equation, for all the catalysts is 8 nm except for Pt//PMo/ZrO_2 that presents a Pt particle size of 10 nm. Hydrogen chemisorption confirms the above commented values.

As for the dopant incorporation, the Dopant/Zr atomic ratio was determined by ICP-MS and XPS in calcined catalysts (Table 1). ICP-MS data

for Pt catalysts showed different trends regarding dopant incorporation. Thus, Pt//B/ZrO_2 catalyst presents a B/Zr ratio close to the theoretical (0.105) while for ZrO_2 modified with POM the dopant-to-Zr ratio is lower than expected, 0.078 and 0.070 for Pt//PMo/ZrO_2 and Pt//SiW/ZrO_2 catalysts, respectively. This poor incorporation of dopant could be due to partial lixiviation during Pt impregnation process. Sulphur content could not be analysed properly by ICP-MS. On the other hand, XPS provides somehow higher values for this ratio indicating a surface concentration of the dopant. Chemical analysis of Pt/S/ZrO_2 seems to indicate an accumulation of sulphate groups on the catalyst surface.

Furthermore, metal particle size data as determined via H_2 chemisorption are given in Table 1, assuming the presence of hemispherical Pt particles and a total incorporation of the metal. In all solids, values of particle size between 4 (Pt/ZrO_2) and 13 nm were obtained except for Pt//S/ZrO_2, for which the estimated particle size was around 200 nm. Nevertheless, it is important to note that these results are probably distorted by the observed H_2 consumption by the S/ZrO_2 support. This is the reason why it has not been included in the table. XRD particle sizes were estimated using Scherrer equation for the reduced catalysts. Bare doped support XRD signal was employed as baseline to avoid ZrO_2 interference.

Catalyst	SBET (m2/g)		Dporo (nm)		Dop:Zr Theoretical	Dop:Zr (ICP)	Dop:Zr (XPS)	%Pt ICP	% Pt XPS	Pt(nm) XRD	Pt(nm) Chemi	%Pt red 200 (XPS)
	Support	Pt	Support	Pt								
Pt/ZrO_2-Unred	126	109	4.5	4.7	--	--	--	4.77	6.56	8	4.3	4.56
$Pt//B/ZrO_2$-Unred	117	92	4.7	4.6	0.1	0.1047	0.1873	4.57	5.75	8	7.2	4.58
$Pt//S/ZrO_2$-Unred	92	71	5.1	5.5	0.1	n.d.	0.5204	4.24	4.46	8	n.d.	3.47
$Pt//PMo/ZrO_2$-Unred	109	86	4.4	4.7	0.1	0.0784	0.0708	4.65	4.13	10	12.9	2.87
$Pt//SiW/ZrO_2$-Unred	93	86	4.5	4.3	0.1	0.0703	0.1078	4.62	5.08	8	8.3	4.14

Table 1. Some features concerning characterization of the different support-metal systems.

V.3.1.A. X-ray diffraction analysis

XRD patterns corresponding to supports and catalysts used in this work are presented in Figure 1. As can be seen, all supports present a tetragonal ZrO_2 crystalline phase (PDF 14-0534) and a main monoclinic ZrO_2 phase (baddeleyite, PDF 37-1484), while dopants were not detected by this technique indicating that are uniformly dispersed on the ZrO_2 surface.

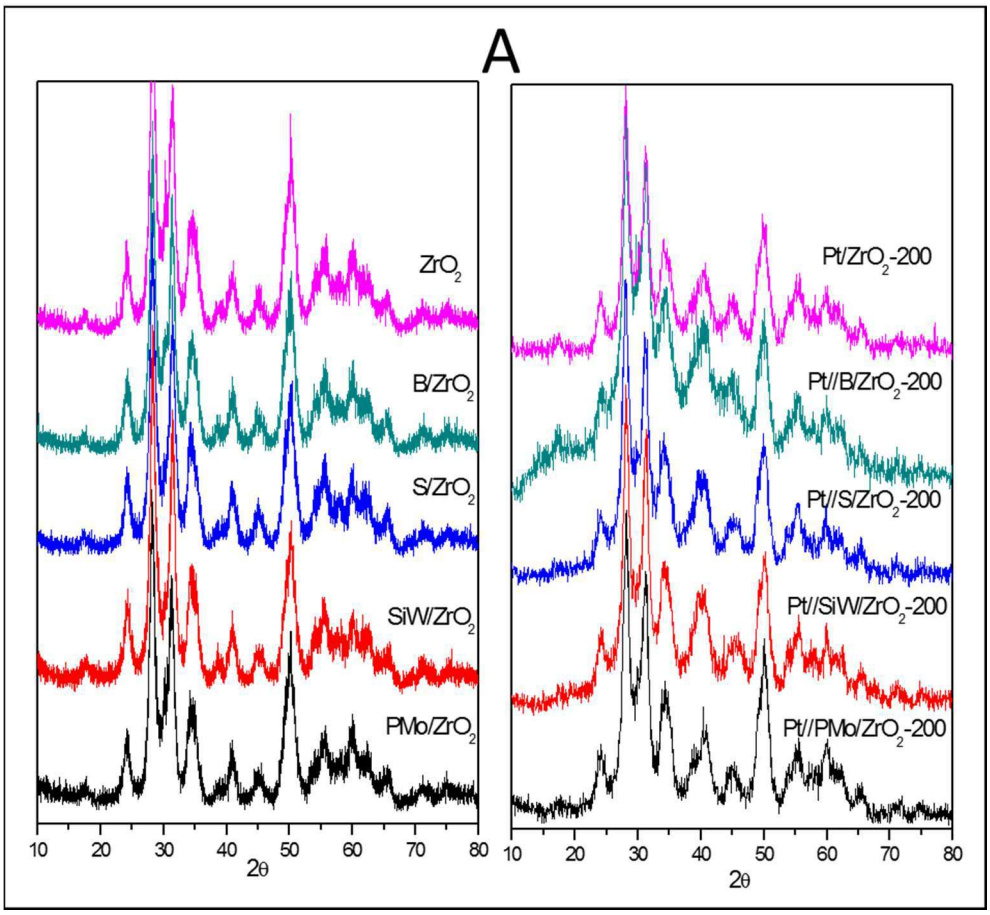

Figure 1A.- XRD patterns corresponding to supports and catalysts used in this work: Pt incorporation comparison full pattern.

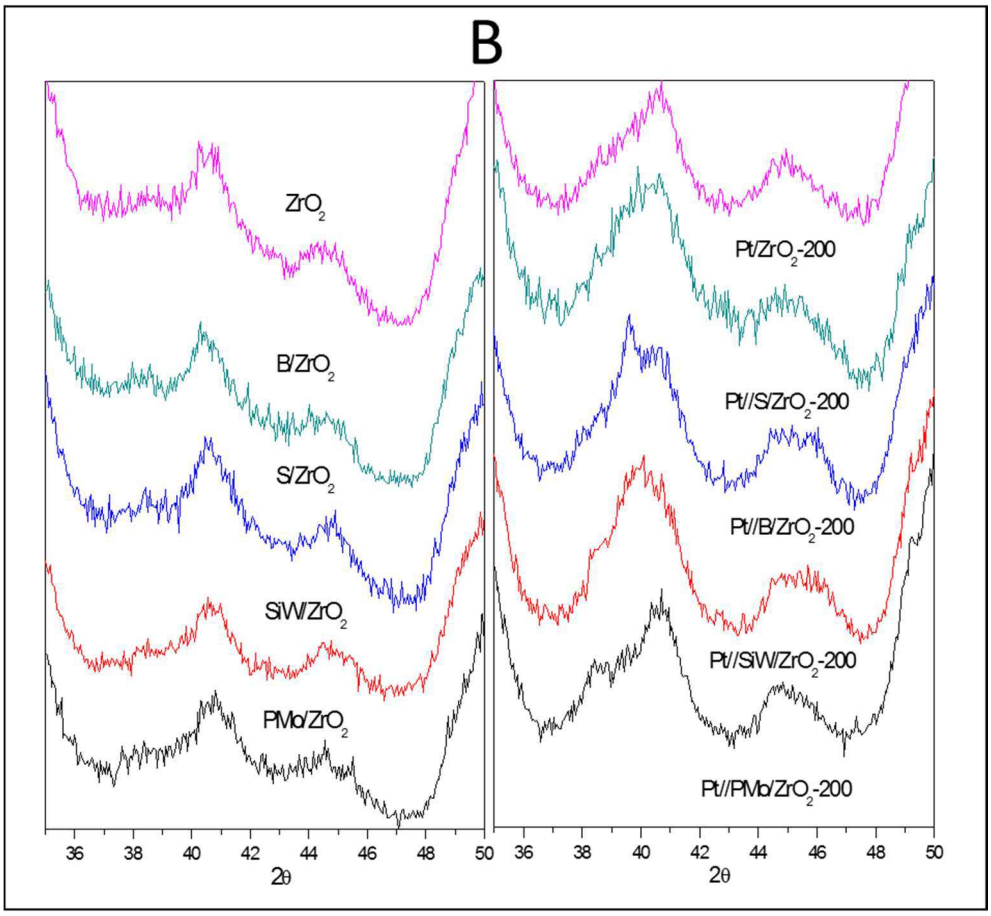

Figure 1.B.- XRD patterns corresponding to supports and catalysts used in this work: Pt zone in detail.

Moreover, Pt signal partially overlapped with a ZrO_2 band and therefore it is somehow complicated to estimate the Pt particle size by applying the Scherrer equation (Figure 1.B). In our case, an estimation was made by taking the support pattern as baseline for the supported Pt catalyst and the results are presented in Table 1.

V.3.1.B. Surface characterization by XPS

As far as XPS characterization is concerned, the obtained profiles for Zr, Pt and dopant are presented in Supplementary Figures 2 to 4. Zirconium appears as a two component signal associated to Zr in ZrO_2 (both $3d_{3/2}$ and $3d_{5/2}$ signals at 184.5 and 182.1 eV, respectively [52,53]) and a minor one at higher binding energy that could be associated to $Zr(OH)_x$ species [52], this one having different intensity depending on the dopant and the treatment. Except for B doping, in modified catalysts Zr 3d signals suffer a shift to higher binding energies that could be related to a dopant-support interaction as evidenced by Reddy *et al.* [53]. (Figure 2).

The incorporation of Pt ant its reduction is able to modify the dopant-ZrO_2 interaction, making it negligible for SiW and PMo doped catalysts, or creating new interactions as for B doped solids. Nevertheless, sulphated catalyst presents the most intense shift in Zr $3d_{5/2}$ signal from 182.1 e.V. to 182.7 e.V., indicative of a quite strong interaction between dopant and support. Platinum XPS signals ($4f_{5/2}$ and $4f_{7/2}$) are presented in Figure 3 for both calcined and reduced supported Pt catalysts. For calcined catalysts the main signal is associated to Pt^{+2} at 72.5 eV. Moreover, most of the catalysts exhibit a small component associated to Pt^{+4} (74.9 eV) while Pt//SiW/ZrO_2, and to a lesser extent Pt//S/ZrO_2, also presented a signal at 70.9 eV associated to Pt^0. For reduced catalysts, the main signal corresponds to Pt^0 although a Pt^{+2} component is clearly present in all solids indicating that platinum is easily re-oxidized when exposed to ambient.

In all cases the maximum observed for Pt^0 signal is slightly shifted to higher BE (0.2-0.4 eV), that can be related to the presence of Cl from metal precursor or to an interaction with additives or support [55].

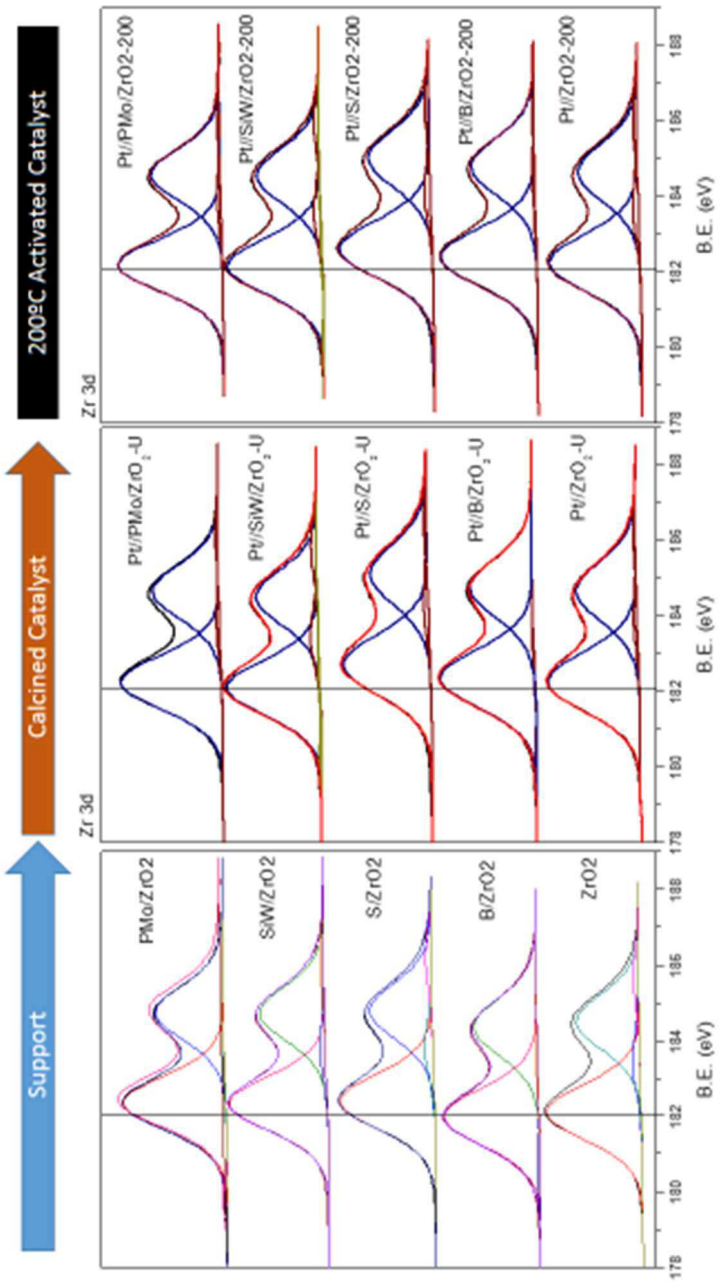

Figure 2. XPS of Zr 3d in support, calcined and activated catalyst.

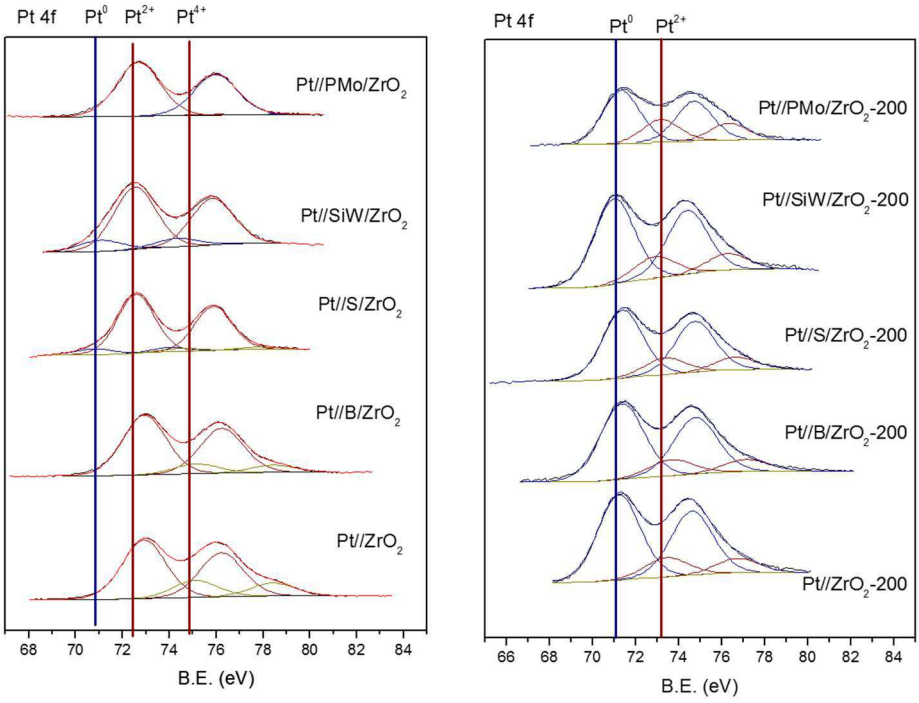

Figure 3. XPS of Pt 4f in calcined and activated catalyst.

Finally, the dopant regions were analysed and compared in Figure 4, observing some differences in solids doped with POM. In the case of SiW, W $4f_{7/2}$ region presents 2 types of environments whose relative proportion changes with the incorporation of Pt. This has been related in the bibliography to a metal-dopant interaction [54]. On the other hand, Mo $3d_{5/2}$ signal observed for PMo/ZrO_2 does not change after Pt incorporation although catalyst reduction induces the reduction of Mo^{6+} to Mo^{5+} probably favoured by Pt^0 in close contact with Mo species [56,57]. Cl 2p region presents intense signals associated to chlorine coming from the metal precursor. B 1s signal partially overlaps with the Cl 2p region being difficult to extract any chemical information. Finally, as far as the S 2p region is concerned, there are no significant changes between S/ZrO_2, $Pt//S/ZrO_2$ and $Pt//S/ZrO_2$-200 solids.

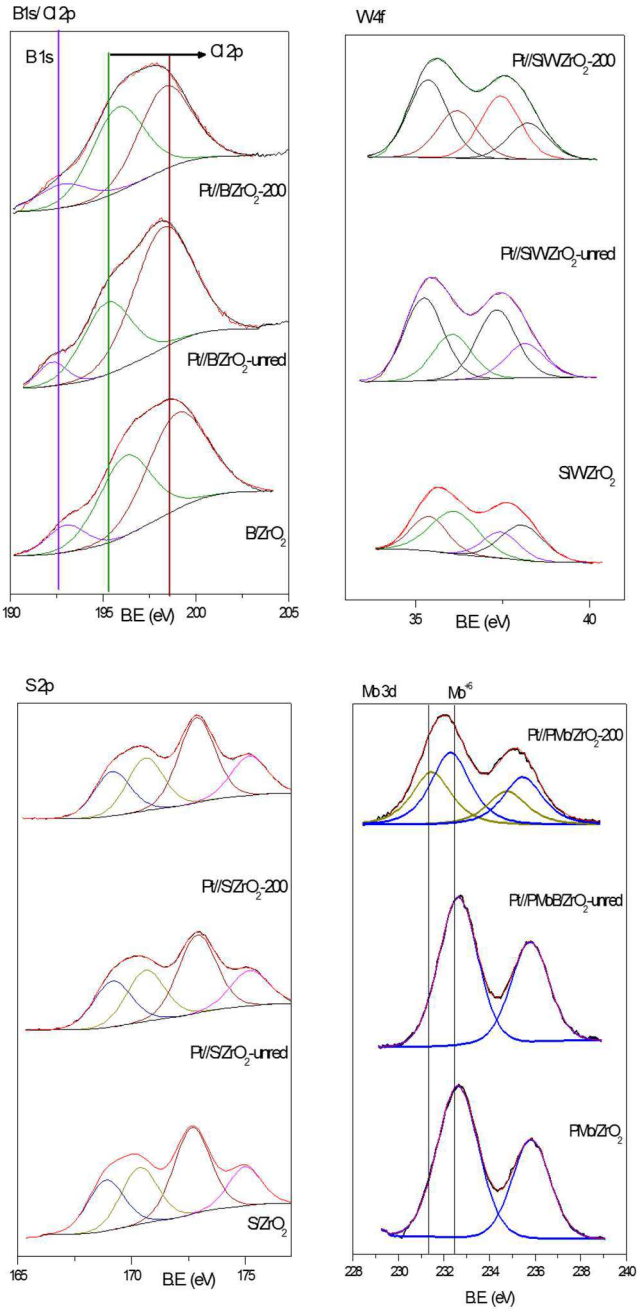

Figure 4. XPS Comparison of dopants in support, calcined and activated catalyst.

Catalyst		Zr (%)	Cl (%)	B (%)	P (%)	Mo (%)	Si (%)	W (%)	S (%)	Pt (%)	C (%)	Dop:Zr	Pt:Zr
Pt/ZrO_2	Support	24,44	15,26								16,5		
	Unred	23,38	16,61							1,3	15,48		0,0556
	200	21,9	11,74							0,87	14,23		0,0397
$Pt//B/ZrO_2$	Support	23,09	13,2	6,58							10,37	0,2850	
	Unred	19,96	12,15	3,74						1,01	15,09	0,1874	0,0506
	200	23,25	11,74	7,77						0,85	8,14	0,3342	0,0365
$Pt//S/ZrO_2$	Support	21,32	10,56						11,44		8,52	0,5366	
	Unred	18,62	10,08						9,68	0,78	16,23	0,5199	0,0419
	200	21,28	9,61						10,68	0,64	9,68	0,5019	0,0301
$Pt//SiW/ZrO_2$	Support	20,94	13,13				0,42	0,52			6,34	0,0248	
	Unred	16,83	10,07				3,69	1,24		0,87	24,39	0,0737	0,0517
	200	19,18	9,91				3,23	1,35		0,75	20,38	0,0704	0,0391
$Pt//PMo/ZrO_2$	Support	26,77	11,47		0,34	2,96					13,41	0,1106	
	Unred	19,38	11,44		0,51	2,09				0,78	14,29	0,1078	0,0402
	200	20,48	11,37		0,36	1,89				0,52	15,9	0,0923	0,0253

Table 2. XPS atomic concentration of the species in the support, calcined and activated

Surface chemical composition of the catalysts determined by XPS is shown in Table 2. These results indicate that all catalysts presented surface chlorine coming from platinum precursor at 10-17% atomic. Moreover, values observed for Pt//S/ZrO_2 indicate an excess of sulphate groups on the catalyst surface.

V.3.1.C. Temperature-programmed reduction (TPR)

TPR profiles of modified supports and supported Pt catalysts are presented in Figure 5. Under reducing atmosphere, only PMo/ZrO_2 support presents a reduction peak at temperature above 300ºC while SiW/ZrO_2 also shows a small peak at temperatures higher than 400ºC. Finally, S/ZrO_2 exhibits at temperatures above 400ºC an intense drift in the base line. These high temperature bands can be attributed to the reduction of POM structure and high temperature decomposition of sulphate groups, respectively [58,59]. All supported Pt catalysts exhibited a low temperature reduction peak (below 200ºC) that can be assigned to Pt^{2+} or Pt^{4+} reduction to Pt^0 [55,60]. Therefore, a complete reduction of the platinum incorporated to the catalyst can be assumed during the catalysts activation process (at 200ºC) previous to the glycerol hydrogenolysis reaction. Finally, the catalysts activation procedure keeps the structure of the dopants unaltered.

In the case of Pt//B/ZrO_2, the reduction profile is quite similar to Pt/ZrO_2 with a maximum over 175ºC, so the incorporation of B_2O_3 probably does not affect the reducibility of the metal particle. The rest of the catalysts present differences in the shape and temperature of the Pt reduction peak. Thus, Pt//PMo/ZrO_2 presents a very narrow reduction peak at about 110ºC together with a wide band at a temperature above 300ºC associated to the PMo reduction as commented for the PMo/ZrO_2 support. As for Pt//SiW/ZrO_2, the

Pt reduction peak is wider and with a maximum at about 150ºC. Again, a drift in the baseline at high temperatures indicates some reduction of SiW species.

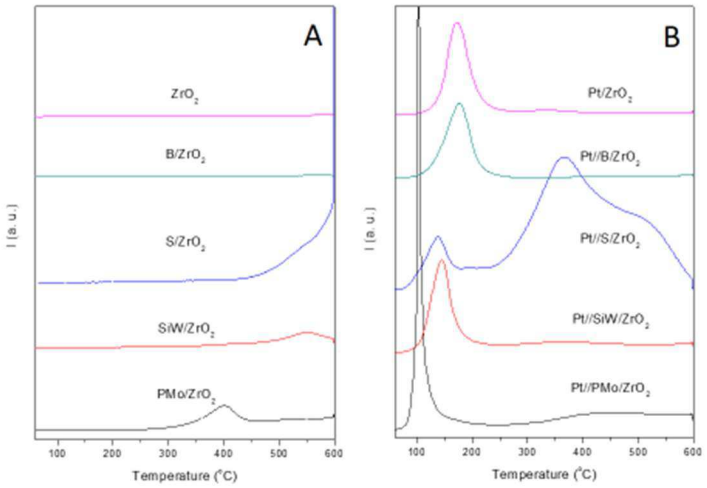

Figure 5. TPR profile of supports (A) and catalysts (B).

As regards to Pt//S/ZrO_2 solid, it is the only catalyst that clearly exhibits two reduction zones, a single peak at 100-120ºC associated to the reduction of Pt oxidized species and a second wider peak with a shoulder at higher temperatures (325-600ºC) associated to the decomposition of sulphated species that, in the presence of Pt, takes place at lower temperature than in the bare support [58,59].

V.3.1.D. Acid properties of the catalyst

The type of acid sites in calcined catalyst was analyzed by Py-DRIFT and data collected at 200ºC are shown in Figure 6. Pt//PMo/ZrO_2 and Pt//SiW/ZrO_2 present similar patterns as Pt/ZrO_2. On these catalysts both Lewis and Brönsted acid sites are present, being Lewis the major component.

At temperatures above 200ºC both components decrease. Pt//S/ZrO_2 acidity is composed by similar concentration of both type of sites although Lewis acidity disappear at 300ºC. Borated solids could not be analysed due to matrix interferences. Except for B, the incorporation of dopants modify the acidity of the original zirconia, supposing the appearance of a Brönsted acidity band (at 1542 cm^{-1}) absent for untreated ZrO_2 [61]. In all cases, metal incorporation modifies all Py-drift patterns, and the Lewis-Brönsted proportion changes in favor of the first ones.

Acid-base surface properties of both supports and Pt catalysts were determined by isopropanol decomposition test reaction [51], the obtained results being presented in Figure 7. This study allows to differentiate acid and basic properties of the catalysts by analyzing the products distribution for isopropanol transformation. When the reaction takes place over acid sites, propene and/or diisopropyl ether are produced [51]. On the contrary, if basic or redox sites are involved, acetone and/or diacetone alcohol are obtained [51]. As for the supports, SiW/ZrO_2 and S/ZrO_2 presented very high propan-2-ol conversion (100 and 95 % respectively) while B/ZrO_2 and ZrO_2 were nearly inactive (>5 and 0 % respectively) and PMo/ZrO_2 exhibited an intermediate conversion level (around 60 %). Isopropanol dehydration to propene is only appreciated in those supports showing the Brönsted acid sites (Py-DRIFT band at 1542 cm^{-1}, Figure 6).

On the other hand, although PMo and SiW doped zirconia presented similar Py-DRIFT profile, PMo/ZrO_2 presented some selectivity to acetone (17.7%) that is not present in SiW/ZrO_2. Impregnation of Pt over the solid had two different effects on propan-2-ol conversion: the new metal active sites induced an increase in conversion to values higher than 98 % in all cases, the selectivity depending on the catalyst tested.

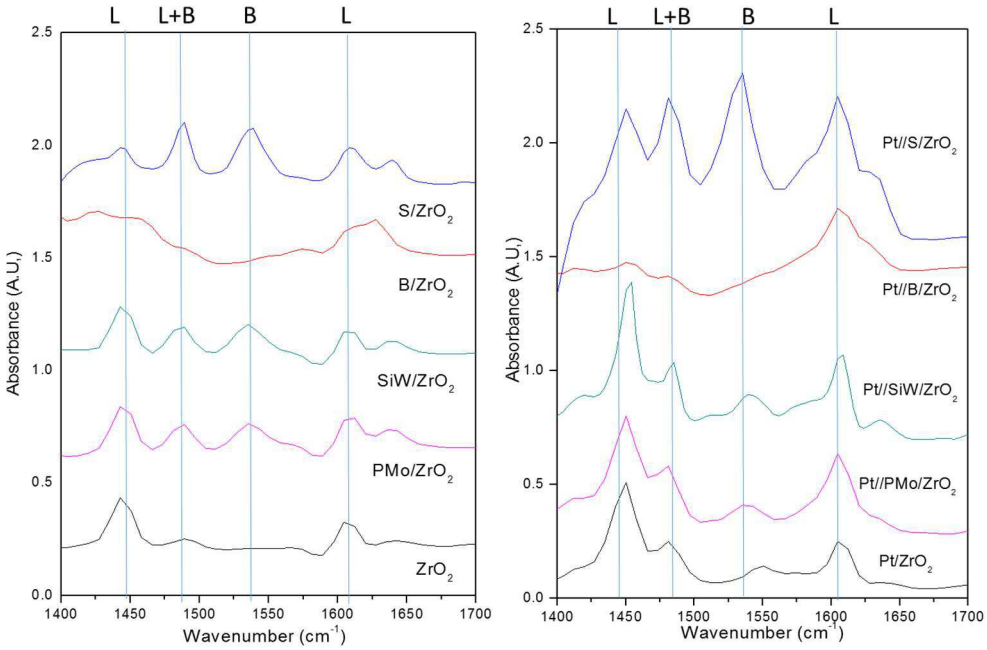

Figure 6. Py-Drift patterns for supports and calcined catalyst at 200ºC.

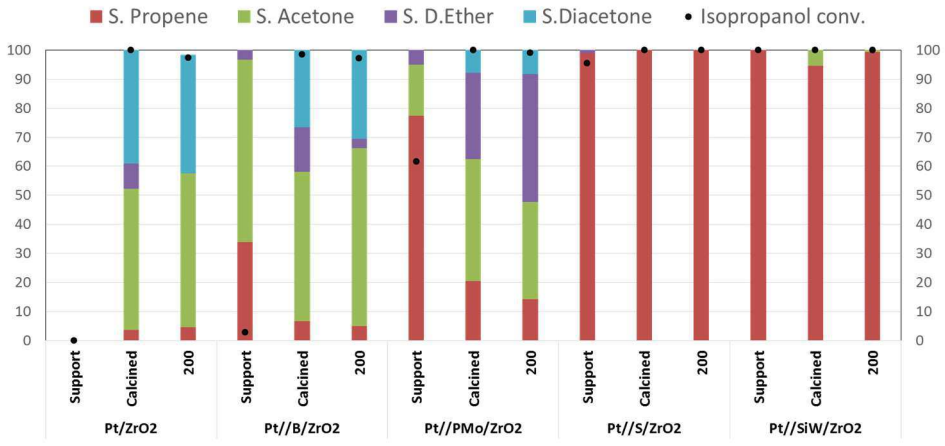

Figure 7. Conversion and selectivity observed in isopropanol test after 2h at 200ºC.

The incorporation of Pt over the least active supports (bare ZrO_2 and B/ZrO_2) provided some new metallic-redox sites that yielded acetone and diacetone alcohol (resulting from acetone self-condensation). Selectivity to propene or diisopropyl ether on theses catalysts is always under 10%. An intermediate behavior was observed for $Pt//PMo/ZrO_2$, yielding both products formed on acid and on basic/redox sites, diethyl ether and acetone being the main reaction products. Finally, $Pt//S/ZrO_2$ and $Pt//SiW/ZrO_2$ catalysts exhibited a 100% conversion with 100% selectivity to propene, indicating an acidic character also already present on the corresponding supports.

A comparison between data exposed in Figures 6 and 7 indicates that those catalysts whose supports presented enhanced Brönsted acidity produced isopropanol dehydration to propene (or diisopropyl ether) while for those supports with less marked Brönsted acidity the incorporation of Pt metal created some redox sites increasing the selectivity to acetone (or diacetone alcohol).

V.3.2. Glycerol hydrogenolysis

Glycerol hydrogenolysis reaction provides a wide range of products depending on conditions such as reaction time, pressure or temperature. For example, compounds detected in liquid phase can be classified in: diols (as 1,2-propanediol (1,2-PDO), 1,3-propanediol (1,3-PDO) or ethylene glycol (EG)), carbonyl compounds as 1-hydroxyacetone (ACETOL) and mono-alcohols (as 2-Propanol or n-Propanol) (Scheme 1).

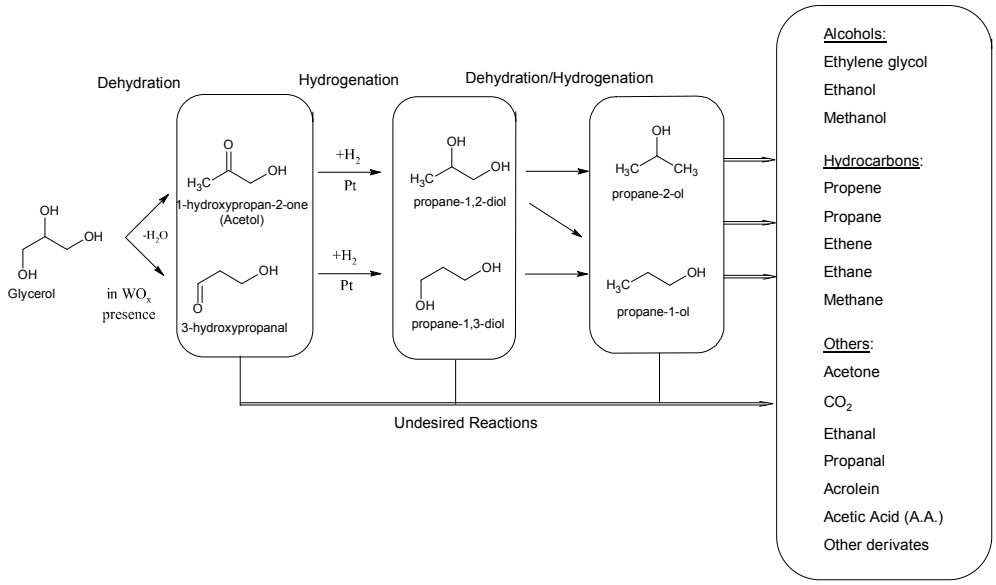

Scheme 1. Glycerol hydrogenolysis pathways

V.3.2.A. Reaction profile in glycerol hydrogenolysis

A time-dependent reaction profile was obtained for each catalyst, by carrying out individual reactions at different reaction times (3, 6, 12 and 24h). The obtained results are quite similar for all solids, Figure 8 presenting the profile obtained for Pt//SiW/ZrO_2. Typically, glycerol conversion increases with reaction time up to 12 h of reaction and then the reaction rate slowed down, so 12 h was selected as standard reaction time. In terms of product distribution, as shown in Figure 8, only n-propanol (n-PrOH) yield increases with reaction time, while the other reaction products remain constant with reaction time. Thus, longer reaction times would provide high yield to mono-alcohols while short reaction time would increase the selectivity to diols.

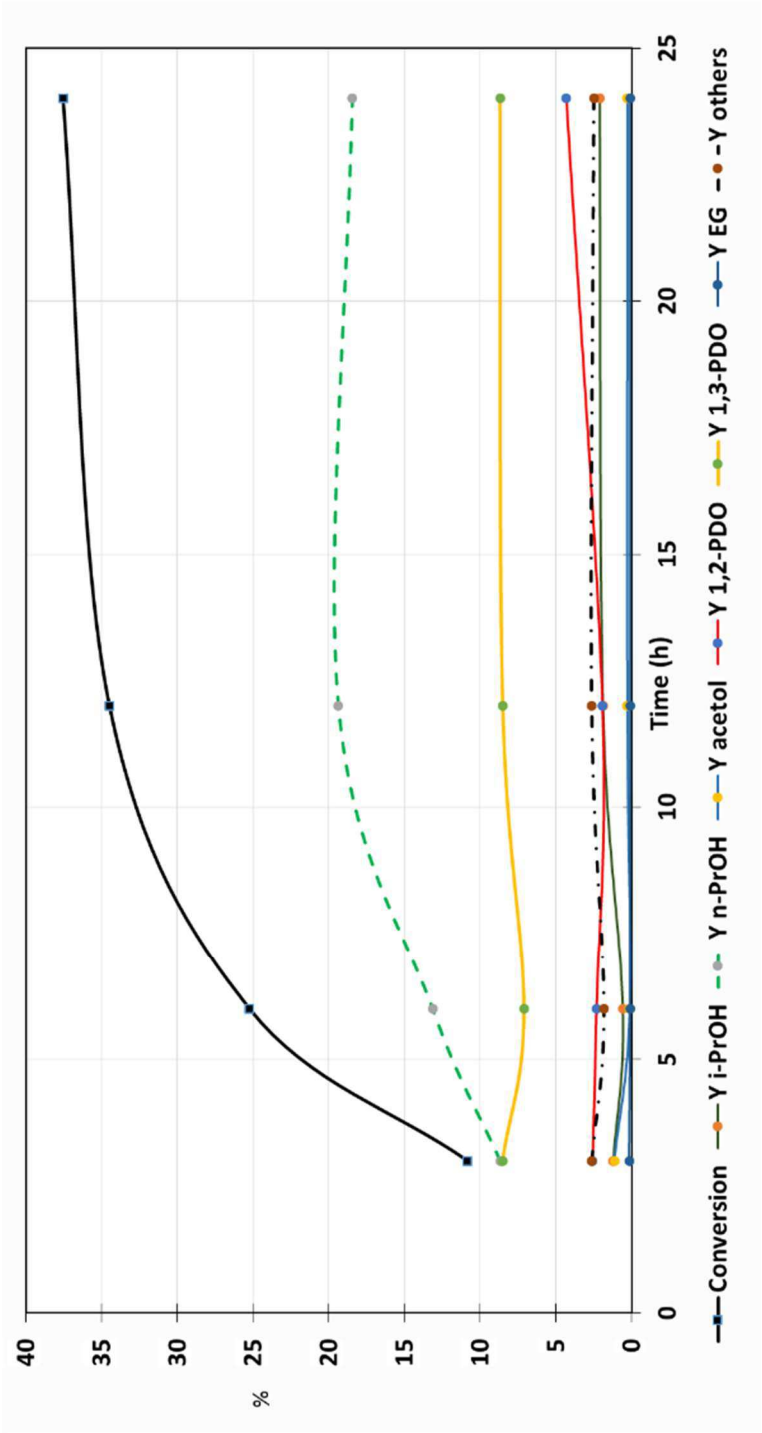

Figure 8. Kinetics study of glycerol hydrogenolysis with Pt//SiW/ZrO_2-200 at 180ºC, 6 bar of H_2 initial pressure, 100 mg of catalyst and 10 ml of glycerol 1.36 M.

V.3.2.A. Glycerol hydrogenolysis: first screening of catalytic systems

In order to evaluate the influence of the support on the catalytic activity, a first screening of the supported Pt catalysts was carried out. As stated above, catalysts were previously reduced at 200°C and the reaction conditions used were an initial hydrogen pressure of 6 bar (reaction maximum pressure 15 bar), a glycerol concentration of 1.36 M and a reaction temperature of 180°C. Blank experiments corresponding to glycerol hydrogenolysis without catalyst and with bare supports were also carried out and, in all cases, the conversion obtained was less than 1% after 24 h of reaction. This means that, in spite of the acid nature of bare supports, metal sites are necessary to promote glycerol dehydration to acetol, as already reported in the literature [25]. Figure 9 shows the results obtained after 12 h of reaction for the supported Pt catalysts synthesized in this work.

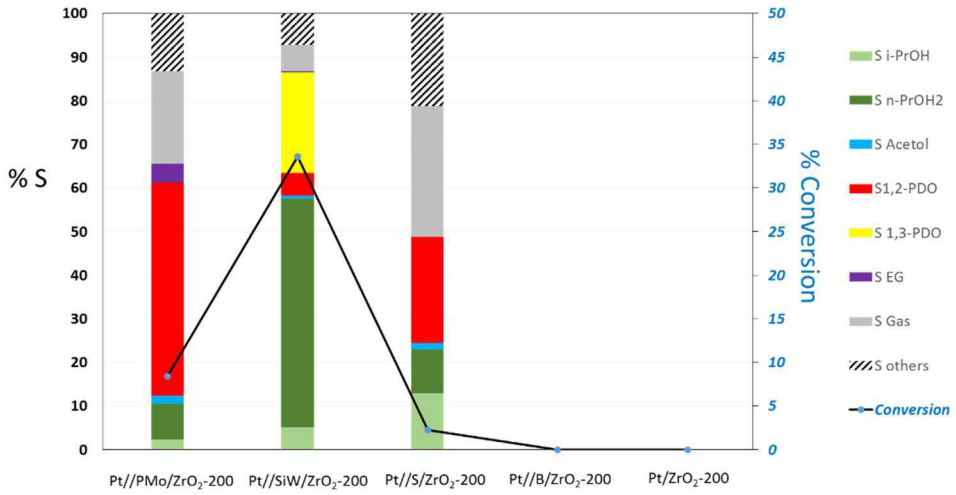

Figure 9. Result for the first screening of the catalyst expressed in terms of conversion and selectivity for t=12h.

Regarding catalytic conversion in glycerol hydrogenolysis, the most active solid was Pt//SiW/ZrO_2-200 (34% conv.) followed by Pt//PMo/ZrO_2-

200 (7% conv) and Pt//S/ZrO_2-200 (4% conv). These results are in agreement with those obtained in propan-2-ol transformation test reaction and commented above. Thus the three catalysts gave high selectivities to propene and diethyl ether (propan-2-ol dehydration processes) that were formed on the surface acid sites of the catalysts. The reactivity order observed could then be related with the surface acidity but Pt//S/ZrO_2-200 conversion is too low in respect to its activity in the propan-2-ol dehydration. The reason could be that the test reaction was carried out in the gas phase while glycerol hydrogenolysis was performed under hydrothermal conditions. Therefore, partial lixiviation of sulphate groups during the reaction could occur and, therefore, the catalyst losses its activity quickly. An alternative explanation is that sulphate groups are not in close contact with Pt metal particles but isolated on the ZrO_2 support. Thus, although this situation allows to dehydrate propan-2-ol it is not favorable for glycerol dehydration. A third explanation could be that the acidity of the catalyst is high enough to carbonize organic compounds into coke, resulting in a fast deactivation of the catalyst.

Finally, Pt//B/ZrO_2-200 and Pt/ZrO_2-200 catalysts were inactive in glycerol hydrogenolysis under the described reaction conditions. It is worth mentioning that these solids exhibited only basic/redox character yielding acetone and diacetone alcohol. It is hardly surprising that both catalysts were inactive in glycerol dehydration to acetol, since no dehydration to propene was reported. These results indicate that propan-2-ol transformation test reaction is able to provide some relevant information for the more complex glycerol hydrogenolysis.

According to the literature [25], in acid media acetol is obtained by dehydration of the primary hydroxyl group of glycerol whereas its subsequent hydrogenation leads to 1,2-PDO [62]. On the other hand, 1,3-PDO is usually

obtained in the presence of specific metallic compounds, among them W is the most common, and the reaction thus takes place via dehydration of the secondary hydroxyl group of glycerol and subsequent hydrogenation of the aldehyde obtained or alternatively by a direct hydrogenolysis mechanism [25].

As for the selectivity, Pt//SiW/ZrO_2-200 was the only catalyst leading to 1,3-PDO (23% sel. to 1,3-PDO) although the main product for this catalysts was *n*-propanol (52% sel. to n-PrOH). For Pt//PMo/ZrO_2-200 and Pt//S/ZrO_2-200 the main reaction product obtained in the liquid-phase was 1,2-PDO with selectivities of 49 and 24%, respectively. It is worth noting that, for all the active catalysts, the selectivity to acetol was less than 2% and *i*-PrOH was also obtained with selectivities ranging 2-13%. Different products such as methanol, ethanol or acetic acid are included in the other products selectivity. Finally, there are other reaction products that were detected in the gas-phase analysis. This analysis identified CO_2 and C_1-C_3 hydrocarbons (propane and propene mainly), as the main compounds, probably produced via glycerol aqueous phase reforming (APR) under hydrothermal reaction conditions [63]. Selectivity to gas-phase products was high in Pt//S/ZrO_2-200 and Pt//PMo/ZrO_2-200 but much lower for Pt//SiW/ZrO_2-200 (30, 21 and 6 % sel. respectively)

V.3.2.B. Influence of the reaction temperature

Additional experiments were carried out to analyze the influence of reaction temperature on catalytic activity and products distribution of liquid-phase glycerol hydrogenolysis over supported Pt catalysts. Tests were carried out at 6 bar of H_2 (reaction maximum pressure 12 bar), using 100 mg of activated catalyst and 10 mL of 1.36 M aqueous glycerol solution and a

reaction time of 12 h. Reaction temperatures essayed were 160, 180 and 200ºC, the results being presented in Table 3.

Results indicate that Pt//SiW/ZrO_2-200 is the most active catalyst at any temperature, being the only active catalyst at the lower reaction temperature (160ºC, 20% conversion). For this catalysts, the major reaction product obtained at 160 ºC is 1,3-PDO (42% sel). According to the results reported in the literature, 1,3-PDO production is the consequence of an interaction between the noble metal and W and a direct hydrogenolysis reaction mechanism [13,25]. For the Pt//SiW/ZrO_2-200 these interactions are evidenced by the shift to lower reduction temperature of the SiW reduction observed in TPR profile.

In experiments carried out at 180ºC, supported Pt over B/ZrO_2 and bare ZrO_2 are inactive as commented above. Moreover, Pt//SiW/ZrO_2-200 is the most active in terms of conversion (35%), while Pt//PMo/ZrO_2-200 and Pt//S/ZrO_2-200 exhibits 7% and 3% conversion values, respectively.

In terms of diols selectivity, at 180 ºC Pt//SiW/ZrO_2-200 still gives 1,3-PDO but at this temperature the major reaction product is *n*-PrOH indicative of a deeper hydrogenolysis process [64]. Pt//PMo/ZrO_2-200 is the best option for 1,2-PDO production at 180ºC. When the reaction temperature increases up to 200ºC, the catalytic activity obtained, at 12 h, for the catalysts follows the order:

Pt//SiW/ZrO_2-200 (54% conv) > Pt//S/ZrO_2-200 (16%) > Pt//PMo/ZrO_2-200 (8%) = Pt//B/ZrO_2-200 (8%) > Pt/ZrO_2-200 (5%)

.

			Selectivity Observed								Gas Phase Composition					
Catalyst	Temp	Conv.	S i-PrOH	S n-PrOH2	S Acetol	S1,2-PDO	S 1,3-PDO	S EG	S others	S Gas	%CH_4	% CO_2	% C_2	% C_3	% acetona	% I-PrOH
Pt//PMo/ZrO_2-200	200	8,4	0,0	5,1	7,6	6,6	0,0	0,9	60,5	19,3	0,1	8,3	9,0	78,9	2,9	0,8
	180	6,7	2,3	8,1	2,0	48,9	0,0	4,3	13,3	21,2	0,0	12,6	5,3	80,5	1,6	0,0
	160	0,0	0,0	0,0	0,0	0,0	0,0	0,0	0,0	0,0	0,0	0,0	0,0	0,0	0,0	0,0
Pt//SiW/ZrO_2-200	200	53,8	8,0	40,5	1,2	7,2	12,3	0,3	14,7	15,8	2,4	15,3	27,3	53,8	1,3	0,0
	180	34,5	5,1	52,4	0,8	5,2	23,0	0,3	7,1	6,1	0,6	10,5	10,6	63,2	7,9	7,2
	160	19,7	2,9	34,5	0,3	4,2	42,1	0,1	6,4	9,5	0,6	9,3	9,3	67,3	5,9	7,6
Pt//S/ZrO_2-200	200	15,7	5,1	18,3	0,9	13,4	0,0	0,6	27,0	34,6	0,0	8,6	9,3	81,7	0,4	0,0
	180	2,8	12,9	9,9	1,6	24,4	0,0	0,0	21,3	29,9	1,8	19,2	19,6	47,7	8,0	3,7
	160	0,0	0,0	0,0	0,0	0,0	0,0	0,0	0,0	0,0	0,0	0,0	0,0	0,0	0,0	0,0
Pt//B/ZrO_2-200	200	8,3	3,8	12,2	5,9	14,0	0,0	11,5	23,3	29,2	4,8	31,0	55,0	8,2	0,3	0,7
	180	0,0	0,0	0,0	0,0	0,0	0,0	0,0	0,0	0,0	0,0	0,0	0,0	0,0	0,0	0,0
	160	0,0	0,0	0,0	0,0	0,0	0,0	0,0	0,0	0,0	0,0	0,0	0,0	0,0	0,0	0,0
Pt/ZrO_2-200	200	5,4	3,8	10,7	8,9	18,9	0,0	18,0	39,8	0,0	1,2	10,3	28,9	59,2	0,3	0,1
	180	0,0	0,0	0,0	0,0	0,0	0,0	0,0	0,0	0,0	0,0	0,0	0,0	0,0	0,0	0,0
	160	0,0	0,0	0,0	0,0	0,0	0,0	0,0	0,0	0,0	0,0	0,0	0,0	0,0	0,0	0,0

Table 3: Glycerol conversion, product distribution and gas phase composition obtained under different temperatures. 100 mg Catalyst, 6 bar H_2 initial pressure, 12h and 10 ml of Glycerol 1.36 M.

As for products distribution, at 200 ºC there is an increase in the selectivity to the so-called other products fraction or even to gas phase products, appointing to a diols consumption at higher temperatures as a consequence of the undesired APR processes [63,64,65]. Again, Pt//SiW/ZrO_2-200 is the only catalyst yielding 1,3-PDO although with lower selectivity than that obtained at lower temperatures. From the point of view of the gas-phase selectivity, the observed selectivity increases with the reaction temperature [63,66]. In this line, Pt//S/ZrO_2-200 is the most interesting catalyst when reaction temperature is above 200ºC, due to the high selectivity to gaseous product observed, ranging from 16% for Pt//SiW/ZrO_2-200 to 35% for Pt//S/ZrO_2-200. As mentioned above, C-3 hydrocarbons (propane and propene) are the main components in the gas-phase fraction.

V.3.2.C. Stability of intermediates

In addition to glycerol hydrogenolysis, reactions with acetol or 1,2-PDO were carried out in order to gather some additional information on the origin of the observed products selectivity. Figure 10 shows the obtained results for the reaction carried out with acetol as starting substrate after 4 h of reaction at 180ºC.

High acetol conversions were obtained for the supports, from the 35% conversion obtained for bare ZrO_2 to the 65% conversion obtained for PMo/ZrO_2. However, 1,2-PDO selectivity was less than 2% at the best. For all supports, the main reaction product was acetic acid (30-54 %), although there was also a rehydration to glycerol with 20% selectivity.

Moreover, incorporation of Pt metal improved the conversion obtained and changed the products distribution profile, being 1,2-PDO the main product formed at the essayed reaction conditions. It is followed that the metal-support

interaction plays an important role on the products distribution profile (selectivity) for the process [67,68]. Again, there were some other products formed, including methanol, ethanol or condensation products like the furan derivate obtained by retro-aldol dimerization of acetol [68].

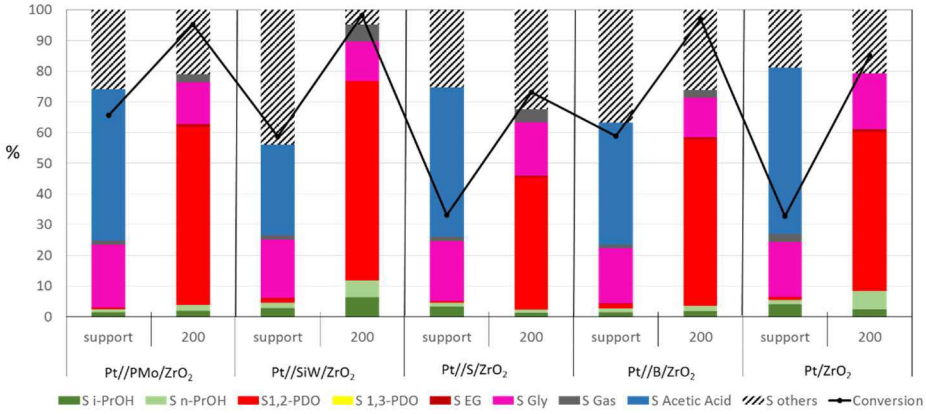

Figure 10. Results observed in acetol conversion with bare supports and the catalysts reduced at 200ºC. 100mg solid, 6 bar H_2 initial pressure, 180ºC reaction temperature, 4h and 10 ml of Acetol 0.5 M.

In addition to the above commented reaction, additional experiments with 1,2-PDO as the substrate were carried out in the same conditions than acetol hydrogenation. These experiments did not show any catalytic activity, so further experiments were performed using higher 1,2-PDO concentration and longer reaction time (1 M solution and 12 h). It was observed that, even with the presence of Pt metal, 1,2-PDO is a stable product except for Pt//SiW/ZrO_2-200 that is able to convert approximately a 33% of the diol into n-propanol (liquid phase) and gaseous products (mainly C-3 hydrocarbons). It is quite surprising that mono-alcohols (*n*-PrOH and *i*-PrOH) were present for all catalysts in glycerol or acetol reactions but, on the contrary, they were not

observed for reactions with 1,2-PDO as starting compound, except for Pt//SiW/ZrO_2.

V.3.2.D. Effect of the reaction on Pt//SiW/ZrO_2 activity and product distribution

For reusability tests, the Pt//SiW/ZrO_2 used catalyst was recovered by filtration, washed with 25 mL of water (3 times) and dried overnight at 110ºC before reuse. The recovered solid was reduced in the same conditions as the fresh catalyst. As can be observed in Figure 11, hydrothermal reaction conditions have a negative effect on catalytic activity obtained in the first reuse of the catalyst but, in the second reuse, the glycerol conversion remains stable. Catalyst reuse has also an important effect on products selectivity. The fresh catalyst yielded *n*-PrOH as main product (49 % sel.) followed by 1,3-PDO (23 % sel.) and 1,2-PDO (11% sel). During the first reuse 1,2-PDO was the main reaction product while 1,3-PDO and *n*-PrOH selectivities dropped (33, 23 and 22 % sel. respectively). Finally, during the second reuse, although the glycerol conversion kept constant, the selectivity to 1,2-PDO increased (34 % sel.) at the expense of 1,3-PDO (18 % sel.) and *n*-PrOH (12 % sel.). Moreover, selectivity to other products also increased from the first use to first and second reuses.

The observed activity decay after the first use could be due to two factors: deactivation via carbonaceous species deposited over active sites or the lixiviation process of the supported modifier and/or Pt. The XRD patterns obtained for the catalyst did not show any important difference, except after the second reuse, with an attenuation of the bands that could be associated to coke fouling or crystalline phase degradation (Figure 12).

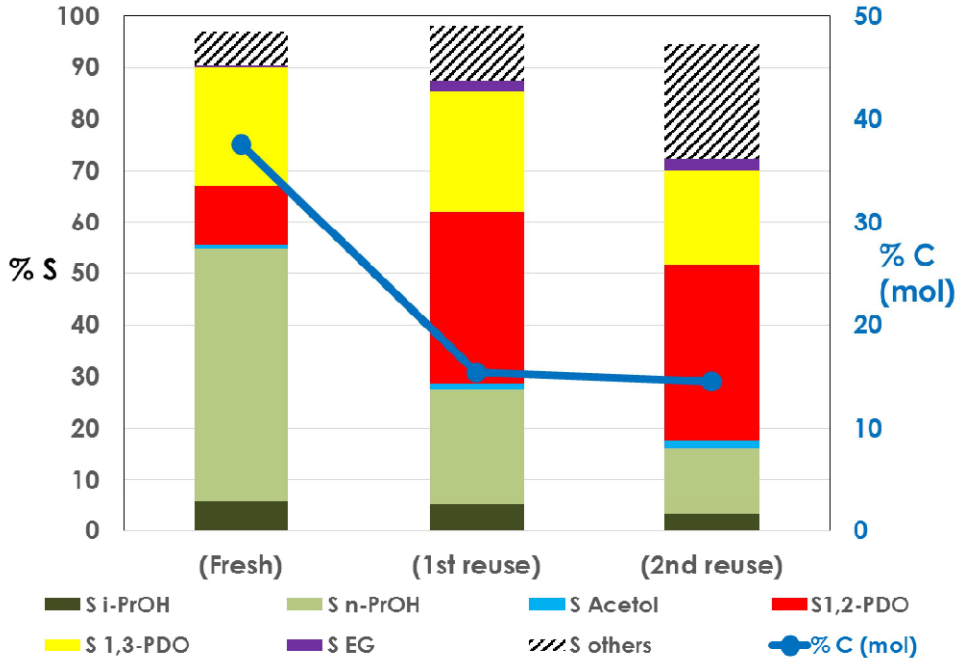

Figure 11. Activity observed during Reusability test of Pt//SiW/ZrO$_2$-200 in glycerol hydrogenolysis at 180ºC, 6 bar of H$_2$ initial pressure, 24h, 100 mg of catalyst and 10 mL of glycerol 1.36 M.

	%Pt	%W	%Zr	Pt/Zr (Atomic)
Pt/SiWZrO2	5.37	8.32	44.29	0.06
Pt/SiWZrO-Used	5.35	7.46	42.69	0.06
Aqueus Phase Detected	0.01	6.55	0.04	

Table 4. ICP-MS data obtained during Reusability test of Pt//SiW/ZrO$_2$-200 in glycerol hydrogenolysis. Comparison between Fresh, Used catalyst and filtered Reaction mixture.

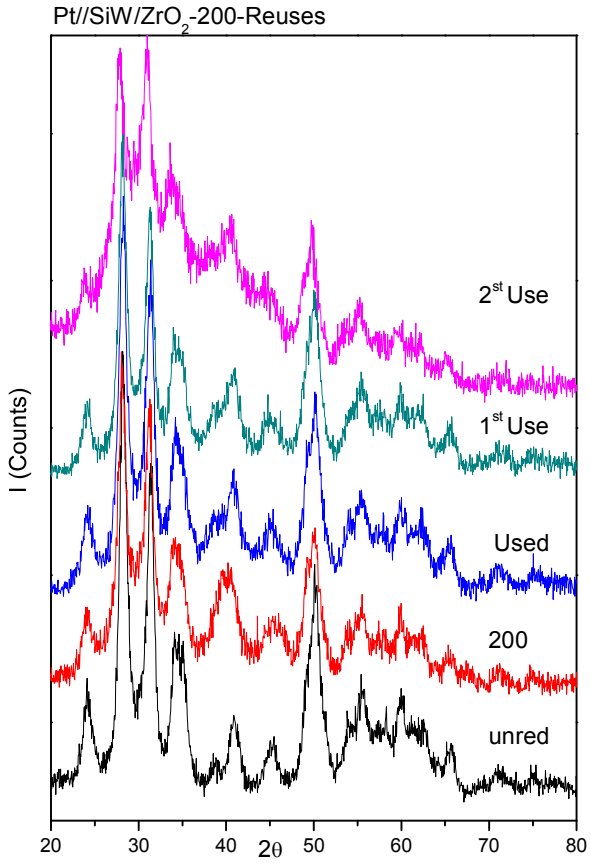

Figure 12. XRD patterns of Pt//SiW/ZrO_2 utilized in reusability test. Comparison between calcined (unred), reduced (200), and recovered catalyst.

ICP-MS analysis of the reaction liquid-phase and the spent catalyst after the first use were carried out (Table 4). Results indicate the presence of 6.5% of the incorporated W in the aqueous phase, revealing that some lixiviation of the W species occurs during the first reaction. On the contrary, less than 0.01% of the Pt incorporated was observed in the liquid phase. Therefore, it has to be assumed that W lixiviation could be the responsible of the activity lost after the first use. In order to rule out homogeneous catalysis by W species, an additional test was carried out with the equivalent amount of

W precursor dissolved in the reaction mixture, obtaining a negligible glycerol conversion, indicative of the absence of homogeneous catalysis.

V.4. CONCLUSIONS

Sol-gel synthesised ZrO_2 was modified by the incorporation of different dopants in order to obtain acidic supports for subsequent Pt impregnation (5% w/w, nominal). By this way, Pt/ZrO_2, $Pt//S/ZrO_2$, $Pt//B/ZrO_2$, $Pt//SiW/ZrO_2$ and $Pt//PMo/ZrO_2$ catalysts were synthesized, characterized and tested for glycerol hydrogenolysis.

Dopants incorporation increased Brönsted acidity of ZrO_2 (except for B/ZrO_2) while further incorporation of Pt improved Lewis acidity. Glycerol hydrogenolysis showed a correlation between glycerol conversion and catalysts acidity, as obtained from propan-2-ol test reaction, $Pt//S/ZrO_2$-200 being the exception. One of the reasons accounting for those results is sulphur lixiviation (occuring in the liquid phase transformation of glycerol but not in the gas-phase transformation of propan-2-ol) or, probably, due to some deactivation process involving acid sites deactivation by fouling. $Pt/SiW/ZrO_2$-200 was the most active catalyst followed by $Pt/PMo/ZrO_2$-200 while Pt/ZrO_2-200 and $Pt//B/ZrO_2$-200 were nearly inactive in glycerol hydrogenolysis, in agreement with their low acidity.

As for the selectivity, the major reaction product obtained depends on the modifier. Thus, $Pt//SiW/ZrO_2$-200 is the only catalyst able to produce 1,3-PDO although *n*-Propanol is the main reaction product. On the other hand, $Pt//PMo/ZrO_2$-200 led to 1,2-PDO mainly, while $Pt//S/ZrO_2$-200 and $Pt//B/ZrO_2$-200 gave high selectivity to gas-phase compounds, mainly C-3 hydrocarbons.

Reactions with acetol or 1,2-PDO as starting substrates provided some additional information on the reaction mechanism. Thus, both supports and supported Pt catalysts were found to be active in acetol hydrogenation with opposite behaviour. Supports mainly yielded acetic acid and oligomerization products while supported Pt catalysts led to 1,2-PDO as result of acetol hydrogenation. Finally, 1,2-PDO was found to be stable under reductive reaction conditions, Pt//SiW/ZrO_2 being the only catalyst able to induce 1,2-PDO hydrogenolysis yielding n-propanol and gas-phase products (C-3 hydrocarbons).

As regards the reusability study carried out with Pt//SiW/ZrO_2, glycerol conversion for the fresh catalyst significantly dropped in the first reuse, staying constant for the second one. Furthermore, as for the selectivity, successive reuses led to a lower 1,3-PDO selectivity associated to an increase in 1,2-PDO selectivity. Changes in activity and especially in 1,3-PDO selectivity could be explained by some lixiviation of W species as detected by ICP-MS analysis of the resulting liquid-phase.

V.5. ACKNOWLEDGMENTS

M.Checa acknowledges the Spanish Ministry of Education for a FPU grant. Staff of the Central Service for Research Support (SCAI) at the University of Córdoba is also acknowledged for its assistance in ICP-MS, TEM and XPS measurements. Supported by Spanish MICINN and MEC (CTQ2008-01330, CTQ2010-18126) and Junta de Andalucía (P08-FQM-3931 and P09-FQM-4781 projects), co-financed by FEDER funds.

V.6. REFERENCES

1. B.M.E. Russbueldt, W.F. Hoelderich, Journal of Catalysis, 271 (2010) 290-304.
2. M. Besson, P. Gallezot, C. Pinel, Chemical Reviews, 114 (2014) 1827-1870.
3. A. Talebian-Kiakalaieh, N.A.S. Amin, H. Hezaveh, Renewable Sustainable Energy Reviews, 40 (2014) 28-59.
4. J. Chaminand, L.A. Djakovitch, P. Gallezot, P. Marion, C. Pinel, C. Rosier, Green Chemistry, 6 (2004) 359-361.
5. F. Vila, M. López Granados, M. Ojeda, J.L.G. Fierro, R. Mariscal, Catalysis Today, 187 (2012) 122-128.
6. C.A.G. Quispe, C.J.R. Coronado, J. Carvalho, Renewable Sustainable Energy Reviews, 27 (2013) 475-493.
7. Z. Gholami, A.Z. Abdullah, K.T. Lee, Renewable Sustainable Energy Reviews, 39 (2014) 327-341.
8. T. Werpy, G. Petersen, Top Value Added Chemicals from Biomass VolumeI—Results of Screening for Potential Candidates from Sugars and SynthesisGas, US Department of Energy, Oak Ridge, 1 (2004) 1-76.
9. Mario Pagliaro, Michele Rossi, The Future of Glycerol: Edition 2, RSC, Cambridge, UK, 2010.
10. D.T. Johnson, K.A. Taconi, Environmental Progress, 26 (2007) 338-348.
11. M. Pagliaro, R. Ciriminna, H. Kimura, M. Rossi, C.D. Pina, European Journal of Lipid Science Technology, 111 (2009) 788-799.
12. J. Feng, B. Xu, Progress in Reaction Kinetics and Mechanism, 39 (2014) 1-15.
13. E.S. Vasiliadou, A.A. Lemonidou, Wiley Interdisciplinary Reviews: Energy and Environment, 4 (2014) 4864-520.

14. Z. Yuan, P. Wu, J. Gao, X. Lu, Z. Hou, X. Zheng, Catalysis Letters, 130 (2009) 261-265.
15. A. Marinas, P. Bruijnincx, J. Ftouni, F.J. Urbano, C. Pinel, Catalysis Today, 239 (2015) 31-37.
16. V. Montes, M. Checa, A. Marinas, M. Boutonnet, J.M. Marinas, F.J. Urbano, S. Järas, C. Pinel, Catalysis Today, 223 (2014) 129-137.
17. S. Zhu, Y. Zhu, S. Hao, L. Chen, B. Zhang, Y. Li, Catalysis Letters, 142 (2012) 267-274.
18. S. Priya, V. Kumar, M. Kantam, S. Bhargava, K. Chary, Catalysis Letters, (2014) 1-15.
19. G. Centi, R.A. van Santen, Catalysis for Renewables: From Feedstock to Energy Production, John Wiley and Sons, Messina (Italy), 2007.
20. Y. Nakagawa, K. Tomishige, Catalysis Surveys From Asia, 15 (2011) 111-116.
21. V. Montes, M. Boutonnet, S. Järas[a], M. Lualdi, A. Marinas, J.M. Marinas, F.J. Urbano, M. Mora, Catalysis Today, 223 (2014) 66-75.
22. M. Checa, F. Auneau, J. Hidalgo-Carrillo, A. Marinas, J.M. Marinas, C. Pinel, F.J. Urbano, Catalysis Today, 196 (2012) 91-100.
23. J. ten Dam, K. Djanashvili, F. Kapteijn, U. Hanefeld, ChemCatChem, 5 (2013) 497-505.
24. L. Liu, Y. Zhang, A. Wang, T. Zhang, Chinese Journal of Catalysis, 33 (2012) 1257-1261.
25. Nakagawa,Y., Tamura, M., Tomishige, K., Journal of Materials Chemistry A, 2 (2014) 6688-6702.
26. J. Hu, X. Liu, B. Wang, Y. Pei, M. Qiao, K. Fan, Cuihua Xuebao/Chinese Journal of Catalysis, 33 (2012) 1266-1275.
27. Y. Li, H. Liu, L. Ma, D. He, RSC Advances, 4 (2014) 5503-5512.

28. J. Tendam, U. Hanefeld, ChemSusChem, 4 (2011) 1017-1034.
29. C.I.C.B. Zanin, E. Jordao, D. Mandelli, F.C.A. Figueiredo, W.A. Carvalho, E.V. Oliveira, Reaction Kinetics, Mechanisms and Catalysis, 115 (2015) 293-311
30. S. García-Fernández, I. Gandarias, J. Requies, M.B. Güemez, S. Bennici, A. Auroux, P.L. Arias, Journal of Catalysis, 323 (2015) 65-75.
31. E.P. Maris, R.J. Davis, Journal of Catalysis, 249 (2007) 328-337.
32. P. Kittisakmontree, H. Yoshida, S.i. Fujita, M. Arai, J. Panpranot, Catalysis Communications, 58 (2015) 70-75.
33. A. Ciftci, B. Peng, A. Jentys, J.A. Lercher, E.J.M. Hensen, Applied Catalysis A: General, 431-432 (2012) 113-119.
34. Y. Choi, H. Park, Y.S. Yun, J. Yi, ChemSusChem, 8 (2015) 974-979.
35. J. Ten Dam, F. Kapteijn, K. Djanashvili, U. Hanefeld, Catalysis Communications, 13 (2011) 1-5.
36. F. Auneau, L.S. Arani, M. Besson, L. Djakovitch, C. Michel, F. Delbecq, P. Sautet, C. Pinel, Topics in Catalysis, 55 (2012) 474-479.
37. C. García-Sancho, R. Moreno-Tost, J. Mérida-Robles, J. Santamaría-González, A. Jiménez-López, P. Maireles-Torres, Applied Catalysis A: General, 433-434 (2012) 179-187.
38. Z. Helwani, M.R. Othman, N. Aziz, J. Kim, W.J.N. Fernando, Applied Catalysis A: General, 363 (2009) 1-10.
39. A. Osatiashtiani, A.F. Lee, D.R. Brown, J.A. Melero, G. Morales, K. Wilson, Catalysis Science and Technology, 4 (2014) 333-342.
40. A. Sinhamahapatra, P. Pal, A. Tarafdar, H.C. Bajaj, A.B. Panda, ChemCatChem, 5 (2013) 331-338.
41. G.S. Armatas, *Heterogeneous Polyoxometalate-Containing Mesoporous Catalysts*, in Steven Suib*, New and Future Developments in Catalysis:*

Hybrid Materials, Composites, and Organocatalysts Elsevier B.V., Heraklion (Greece), 2013, p.311-342.

42. L. Gong, Y. Lu, Y. Ding, R. Lin, J. Li, W. Dong, T. Wang, W. Chen, Applied Catalysis A: General, 390 (2010) 119-126.
43. L. Huang, Y. Zhu, H. Zheng, G. Ding, Y. Li, Catalysis Letters, 131 (2009) 312-320.
44. L. Pizzio, P. Vázquez, C. Cáceres, M. Blanco, Catalysis Letters, 77 (2001) 233-239.
45. S.H. Chai, H.P. Wang, Y. Liang, B.Q. Xu, Green Chemistry, 10 (2008) 1087-1093.
46. L. Shen, H. Yin, A. Wang, Y. Feng, Y. Shen, Z. Wu, T. Jiang, Chemical Engineering Journal, 180 (2012) 277-283.
47. P.Y. Hoo, A.Z. Abdullah, Chemical Engineering Journal, 250 (2014) 274-287.
48. D. Haffad, A. Chambellan, J.C. Lavalley, Journal of Molecular Catalysis A: Chemical, 168 (2001) 153-164.
49. M.A. Alves-Rosa, L. Martins, P. Hammer, S.H. Pulcinelli, C.V. Santilli, Journal of Sol-Gel Science and Technology, 72 (2014) 252-259
50. J. Bedia, J.M. Rosas, D. Vera, J. Rodríguez-Mirasol, T. Cordero, Catalysis Today, 158 (2010) 89-96.
51. A.Marinas, J.M.Marinas, M.A.Aramendía, J.F.Urbano, Heterogeneous catalysis on basic sites in organic synthesis, Nova Science, New York, 2005, p. 85.
52. B.M. Reddy, P.M. Sreekanth, Y. Yamada, Q. Xu, T. Kobayashi, Applied Catalysis A: General, 228 (2002) 269-278.

53. L.I. Kuznetsova, N.I. Kuznetsova, S.V. Koshcheev, V.A. Rogov, V.I. Zaikovskii, B.N. Novgorodov, L.G. Detusheva, V.A. Likholobov, D.I. Kochubey, Kinetics and Catalysis, 47 (2006) 704-714.
54. M. Consonni, D. Jokic, D. Yu Murzin, R. Touroude, Journal of Catalysis, 188 (1999) 165-175.
55. G. Li, R. Mu, Z. Fan, Y. Li, Y. Liu, Reaction Kinetics, Mechanisms and Catalysis, 110 (2013) 163-175.
56. E. Grinenval, J.M. Basset, F. Lefebvre, Inorganica Chimica Acta, 370 (2011) 297-303.
57. C.J. Dillon, J.H. Holles, R.J. Davis, J.A. Labinger, M.E. Davis, Journal of Catalysis, 218 (2003) 54-66.
58. I.J. Bear, Australian Journal of Chemistry, 20 (1967) 415-428.
59. A.F. Lee, K. Wilson, A. Goldoni, R. Larciprete, S. Lizzit, Surface Science, 513 (2002) 140-148.
60. N. Iwasa, T. Mayanagi, N. Ogawa, K. Sakata, N. Takezawa, Catalysis Letters, 54 (1998) 119-123.
61. M. Miranda, A. Ramírez S., S.G. Jurado, C.R. Vera, Journal of Molecular Catalysis A: Chemical, 398 (2015) 325-335.
62. X. Lin, Y. Qu, Y. Xi, C. Liu, Journal of Theoretical and Computational Chemistry, 13 (2014) 1450016.
63. A. Seretis, P. Tsiakaras, Renewable Energy, 85 (2016) 1116-1126.
64. S.S. Priya, V.P. Kumar, M.L. Kantam, S.K. Bhargava, S. Periasamy, K.V.R. Chary, Applied Catalysis A: General, 498 (2015) 88-98.
65. A. Martin, U. Armbruster, I. Gandarias, P.L. Arias, European Journal of Lipid Science Technology, 115 (2013) 9-27.
66. S.D. Blass, R.J. Hermann, N.E. Persson, A. Bhan, L.D. Schmidt, Applied Catalysis A: General, 475 (2014) 10-15.

67. I. Gandarias, P.L. Arias, J. Requies, M.B. Güemez, J.L.G. Fierro, Applied Catalysis B: Environmental, 97 (2010) 248-256.
68. W. Suprun, M. Lutecki, T. Haber, H. Papp, Journal of Molecular Catalysis A: Chemical, 309 (2009) 71-78.

Capítulo VI

Conclusiones

Chapter VI

Conclusions

Conclusiones

El objetivo general de la Tesis era evaluar las diferentes posibilidades de transformación del glicerol en productos de alto valor añadido, sintetizar y caracterizar diversos sólidos mediante diferentes métodos y estudiar su comportamiento catalítico.

Para ello se sintetizaron diversos catalizadores heterogéneos consistentes en nanopartículas metálicas soportadas buscando establecer relaciones estructura-actividad. Los catalizadores fueron sintetizados principalmente empleando los métodos de impregnación y deposición-precipitación. El precursor metálico escogido, el soporte, la temperatura de reducción o el método sintético fueron determinantes en aspectos tales como el tamaño final de partícula o la existencia de interacción metal-soporte y, en definitiva, en el comportamiento catalítico. La preparación de cada set de catalizadores respondía a una serie de requisitos dados por los parámetros estudiados en cada capítulo, lo que implicó la necesidad de llevar a cabo una síntesis del catalizador "a medida" para cada uno de los estudios, con el fin de optimizar los resultados.

Seguidamente se detallan los resultados encontrados en cada uno de los capítulos (a excepción del primero y segundo dedicados a la introducción e hipótesis y objetivos respectivamente) organizados en función de cada artículo publicado o en proceso de publicación.

Capítulo III. Transformación catalítica de glicerol sobre diferentes sistemas metálicos soportados sobre ZnO

Se seleccionaron diferentes óxidos reducibles (TiO_2, ZnO, SnO_2 y ZrO_2) para soportar platino y los sistemas de platino soportado se probaron

como catalizadores en la hidrogenolisis del glicerol. Los sólidos que exhibieron una interacción metal-soporte más fuerte, a través de la aleación con Pt (ZnO y SnO_2) fueron los sólidos más activos. Por otra parte, la mayor selectividad hacia 1,2-PDO se obtuvo con el sistema de Pt / ZnO, lo que nos llevó a elegir el óxido de zinc como soporte para nuevos estudios.

Se soportaron diversos metales nobles (Pt, Rh, Pd y Au) sobre ZnO a través de la técnica de deposición-precipitación (5% en peso) y se ensayaron para la transformación catalítica del glicerol bajo atmósfera de hidrógeno o helio. A igualdad de condiciones de reacción, la conversión de glicerol sigue la secuencia Pt> Rh >> Pd >> Au. Además, se observó que los sólidos reducidos a 473K eran más activos que los activados a 673 K. Este hecho podría deberse al aumento de tamaño de las partículas de metal y/o la formación de una aleación total (como se aprecia en TEM y XRD, respectivamente). Los resultados sugieren que la interacción metal soporte lograda a 473K podría ser beneficiosa para el proceso, evitando la formación eventual de la aleación total a temperaturas más altas (673K). Los sistemas más activos fueron el Pt/ZnO-473 y el Rh/ZnO-473, los cuales presentaban un tamaño de partícula similar (alrededor de 3-4 nm). Los estudios realizados en condiciones de iso-conversión y en medio neutro, evidenciaron selectividades similares para los sistemas de Pt y Rh soportado, mientras que los sistemas de Pd produjeron más acetol a expensas del 1,2-PDO. En cuanto al rendimiento a ácido láctico, los mejores resultados se lograron en medio básico (68% de Rh/ZnO-473 bajo H_2 en medio básico), mientras que, bajo condiciones de reacción similares, el rendimiento al 1,2-PDO fue más modesto (26% de Rh / ZnO-673).

Capítulo IV. Estudio de la desactivación de catalizadores de Pt soportado en la hidrogenolisis de glicerol

Se sintetizó una batería de catalizadores de Pt soportados mediante el método de impregnación sobre diferentes óxidos metálicos (Al_2O_3, CeO_2, La_2O_3 y ZnO). Todos los catalizadores se caracterizaron y se ensayaron en la hidrogenolisis del glicerol en fase líquida. De los resultados obtenidos, se extrajeron las siguientes conclusiones.

Los soportes puros calcinados exhibieron una amplia gama de acidez, siendo el ZnO el que presentó la acidez más baja de todos. Por otra parte, la acidez del sólido mejoraba tras la incorporación Pt, especialmente para el catalizador de Pt/ZnO, debido a la creación de nuevos centros ácidos asociados a las partículas metálicas de Pt.

Los catalizadores Pt / La_2O_3, Pt / CeO_2 y Pt / ZnO, fueron mejores que los basados en Pt / Al_2O_3 en términos de rendimiento a 1,2-PDO. Por otro lado, se observó que conforme la conversión del glicerol aumentaba había una pérdida progresiva en el rendimiento del 1,2-PDO debido a la formación de algunas especies poliméricas, responsables de los balances de masa negativos observados con algunos catalizadores.

Los experimentos llevados a cabo con acetol como sustrato de partida indican que los centros ácidos del soporte no asociados a los centros metálicos de Pt son perjudiciales para este proceso debido a que favorecen la oligomerización de acetol, siendo esta la principal causa de la pérdida de rendimiento de 1,2-PDO a tiempos de reacción largos.

La caracterización de los catalizadores utilizados reveló que bajo las condiciones hidrotermales de reacción, los sistemas de Pt soportado sobre CeO_2 y La_2O_3 sufren procesos de lixiviación, mostrando la pérdida de parte

de su superficie específica y presentando, además, señales de combustión intensas en ATG asociadas a depósitos orgánicos, hecho que concuerda con el pobre balance de masa observado para estos sólidos.

Como conclusión general, decir que entre todos los catalizadores estudiados, el Pt / ZnO presentó el mejor comportamiento en la reacción de hidrogenolisis en fase líquida tanto de glicerol como acetol, desde el punto de vista del rendimiento a 1,2-PDO. Estos buenos resultados se basan en varios factores tales como poseer una acidez superficial apropiada y asociada a las partículas de Pt, tener una baja tendencia a producir reacciones de oligomerización como consecuencia de la baja acidez del soporte de ZnO y una razonablemente alta estabilidad del catalizador frente a las condiciones hidrotermales de reacción.

Capítulo V. Estudio de la influencia de dopantes en catalizadores de Pt soportado sobre óxido de zirconio para la valorización de glicerol

Se preparó ZrO_2 mediante el método sol-gel y se modificó su acidez con diferentes dopantes. Posteriormente, se incorporó platino (5% en peso nominal) mediante el método de impregnación, obteniendo los sistemas Pt/ZrO_2, $Pt//B/ZrO_2$, $Pt//S/ZrO_2$, $Pt//SiW/ZrO_2$ y $Pt//PMo/ZrO_2$, que fueron caracterizados y ensayados en la reacción de hidrogenolisis glicerol.

La incorporación de los dopantes mejoró la acidez Brönsted superficial del ZrO_2 (excepto para el B/ZrO_2), mientras que la incorporación de Pt incrementó la acidez Lewis. Se observó una correlación entre la conversión del glicerol y la acidez del catalizador, al igual que con la actividad obtenida en la reacción modelo del isopropanol, excepto para $Pt//S/ZrO_2$. Entre las posibles causas de este hecho podrían estar el que la reacción test del propan-2-ol se realice en fase gas mientras que la hidrogenolisis del glicerol se lleva

a cabo en fase líquida, lo que podría dar lugar a fenómenos de lixiviación de grupos sulfato o la desactivación de los centros ácidos por coque durante la reacción. El Pt//SiWZrO$_2$-200 fue el catalizador más activo, seguido del Pt//PMo/ZrO$_2$-200, mientras que el Pt//B/ZrO$_2$ y el Pt/ZrO$_2$ fueron prácticamente inactivos en la hidrogenolisis de glicerol, hecho relacionado con su baja acidez.

En cuanto a la distribución de productos observada, las proporciones de estos y, en especial, el producto mayoritario en cada caso, dependerán fuertemente del dopante empleado. De este modo, el sistema Pt//SiW/ZrO$_2$-200 es el único de los catalizadores empleados capaz de producir 1,3-PDO, aunque el producto principal de este catalizador es el n-propanol. Por otro lado, el Pt//PMo/ZrO$_2$-200 presenta 1,2-PDO como el producto principal mientras que Pt//S/ZrO$_2$-200 y Pt//B/ZrO$_2$-200 dieron como resultado selectividades altas hacia compuestos en fase gaseosa, siendo los hidrocarburos C-3 los compuestos más importantes.

Las reacciones con acetol y 1,2-PDO como sustratos de partida suministraron información adicional acerca del mecanismo de reacción. De este modo, se observó que tanto el soporte como el catalizador con Pt eran activos en la transformación del acetol, pero con comportamiento distinto. Los sólidos sin platino orientaban la reacción hacia la producción de ácido acético y compuestos poliméricos mientras que los catalizadores de Pt soportado obtenían mayoritariamente 1,2-PDO como producto de hidrogenación. Finalmente, se comprobó que el 1,2-PDO era estable bajo condiciones reductoras de reacción, excepto con Pt//SiW/ZrO$_2$, el cual es capaz de producir la hidrogenolisis del 1,2-PDO para obtener n-PrOH y productos en fase gaseosa (hidrocarburos C-3).

Los estudios de reutilización del catalizador Pt//SiW/ZrO_2, mostraron que éste pierde fuertemente la actividad después del primer uso, manteniéndose constante tras el segundo. Además, en cuanto a la selectividad observada, los reusos conducen a una disminución en la selectividad a 1,3-PDO mientras que la selectividad a 1,2-PDO aumenta. Los cambios en la actividad, en especial en la selectividad a 1,3-PDO, puede ser explicada por la lixiviación de algunas especies de W que fueron detectadas mediante ICP-MS en la fase líquida resultante de la reacción.

Conclusions

The main objective of the thesis was to evaluate the different possibilities of glycerol transformation into products with high added value, synthesizing and characterizing various solids by different methods and testing their catalytic behaviour in glycerol valorisation.

Therefore, different heterogeneous catalysts consisting in supported metal nanoparticles were synthesized looking for some structure-activity relationships. The catalysts were synthesized by impregnation and deposition-precipitation methods, mainly. The metallic precursor, the support, the reduction temperature or the synthetic method of choice were found to be play a crucial role in some features such as the final particle size or the existence of metal-support interaction and thus in the catalytic behaviour. The preparation of each set of catalysts was designed following the requirements marked by the parameters studied in each chapter, which implied the necessity of a tailored-made synthesis, in order to optimize results.

The results found in each chapter (except for the first and second dedicated to the introduction and objectives respectively) are going to be commented now, organized according to the articles already published or in preparation.

Chapter III. Catalytic transformation of glycerol on several metal systems supported on ZnO

Different reducible oxides (TiO_2, ZnO, SnO_2 and ZrO_2) were screened as support for platinum and tested for glycerol hydrogenolysis. The solids exhibiting the greatest metal-support interaction, eventually forming an alloy

(ZnO and SnO_2) were the most active solids. Moreover, selectivity to 1,2-PDO was higher for ZnO what prompted us to select this solid as support for further studies.

Diverse ZnO-supported metals (Pt, Rh, Pd and Au) were then synthesized through the deposition-precipitation technique (5% by weight) and tested for catalytic transformation of glycerol under hydrogen and helium atmosphere. Under similar reaction conditions, glycerol conversion followed the sequence Pt>Rh>>Pd>>Au. Furthermore, the solids reduced at 473K were more active than those activated at 673K. The increase in metal particle size and/or the formation of an alloy (as evidenced by TEM and XRD, respectively) could account for that. Results suggest that the strong metal-support interaction achieved at 473K could be beneficial to the process though the eventual formation of the alloy at higher temperatures (673K) should be avoided. The most active systems were Pt/ZnO-473 and Rh/ZnO-473 which exhibited a similar particle size (ca. 3-4 nm). Studies at iso-conversion conditions in neutral medium evidenced similar selectivities for Pt and Rh-containing solids whereas Pd systems yielded more acetol at the expense of 1,2-PDO. All in all, quite high yields to lactic acid were achieved in basic medium (68% for Rh/ZnO-473 under H_2 in basic medium) whereas yield to 1,2-PDO was more modest (26% for Rh/ZnO-673 under similar reaction conditions).

Chapter IV. Deactivation study of supported Pt catalyst on glycerol hydrogenolysis

Several supported Pt catalysts were prepared by wet impregnation over different oxide supports such as Al_2O_3, CeO_2, La_2O_3 and ZnO. All those catalysts were characterized and tested in the liquid-phase glycerol

hydrogenolysis. From the obtained results, the following conclusions can be extracted.

The bare supports exhibited a wide range of acidity, ZnO presenting the lower acidity among all supports tested. Moreover, acidity was in general enhanced upon Pt incorporation, especially for the Pt/ZnO catalyst for which new acid sites associated to Pt metal particles were created.

Pt/La_2O_3, Pt/CeO_2 and Pt/ZnO behaved better than Pt/Al_2O_3 in terms of 1,2-PDO yield. Moreover, as glycerol conversion increases there is a progressive loss in 1,2-PDO yield due to the formation of some polymeric species, responsible for the poor mass balance observed for some catalysts.

Experiments carried out with acetol as starting substrate indicated that support acidity not associated to the Pt metal sites is detrimental to this process due to the oligomerization of acetol, being this the main cause of the loss of 1,2-PDO yield at long reaction times.

The characterization of used catalysts revealed that under hydrothermal reaction conditions CeO2 and La2O3 supported Pt catalysts suffer from leaching, lost some of their surface area and presented intense combustion signals associated to organic deposits in agreement with the poor mass balance observed for these solids.

All in all, among all studied catalysts, Pt/ZnO presented the best behavior in the liquid-phase hydrogenolysis in terms of yield to 1,2-PDO both from glycerol and acetol. These good results are based on several factor such as the appropriate surface acidity associated to Pt particles, a low oligomerization capability as consequence of the low acidity of the ZnO support and a reasonable high stability of the catalyst under hydrothermal reaction conditions.

Chapter V. Dopants influence on zirconia based Pt catalyst for glycerol valorisation

Sol-gel ZrO_2 was modified by the incorporation of different dopants in order to obtain acidic supports for subsequent Pt impregnation (5% w/w, nominal). By this way, Pt/ZrO_2, $Pt//S/ZrO_2$, $Pt//B/ZrO_2$, $Pt//SiW/ZrO_2$ and $Pt//PMo/ZrO_2$ catalysts were synthesized, characterized and tested for glycerol hydrogenolysis.

Dopants incorporation improved Brönsted acidity of ZrO_2 (except for B/ZrO_2) while further incorporation of Pt increased Lewis acidity. Glycerol hydrogenolysis showed a correlation between glycerol conversion and catalysts acidity, as obtained from propan-2-ol test reaction, $Pt//S/ZrO_2$-200 being the exception. One of the reasons accounting for those results is sulphur lixiviation (occuring in the liquid phase transformation of glycerol but not in the gas-phase transformation ofpropan-2-ol) or, probably, due to some deactivation process involving acid sites deactivation by fouling. $Pt/SiW/ZrO_2$-200 was the most active catalyst followed by $Pt/PMo/ZrO_2$-200 whereas Pt/ZrO_2-200 and $Pt//B/ZrO_2$-200 were nearly inactive in glycerol hydrogenolysis, in agreement with their low acidity.

As for the selectivity, the major reaction product obtained depends on the modifier. Thus, $Pt//SiW/ZrO_2$-200 is the only catalyst able to produce 1,3-PDO although *n*-Propanol is the main reaction product. On the other hand, $Pt//PMo/ZrO_2$-200 led to 1,2-PDO mainly, while $Pt//S/ZrO_2$-200 and $Pt//B/ZrO_2$-200 gave high selectivity to gas-phase compounds, mainly C-3 hydrocarbons.

Reactions with acetol or 1,2-PDO as starting substrates provided some additional information on the reaction mechanism. Thus, both supports and

supported Pt catalysts were found to be active in acetol trasnsformation with opposite behaviour. Supports mainly yielded acetic acid and oligomerization products while supported Pt catalysts led to 1,2-PDO as a result of acetol hydrogenation. Finally, 1,2-PDO was found to be stable under reductive reaction conditions, Pt//SiW/ZrO_2 being the only catalyst able to induce 1,2-PDO hydrogenolysis yielding n-propanol and gas-phase products (C-3 hydrocarbons).

As regards the reusability study carried out with Pt//SiW/ZrO_2, glycerol conversion for the fresh catalyst significantly dropped in the first reuse, staying constant for the second one. In addition, as for the selectivity, successive reuses led to a lower 1,3-PDO selectivity associated to an increase in 1,2-PDO selectivity. Changes in activity and especially in 1,3-PDO selectivity could be explained by some lixiviation of W species as detected by ICP-MS analysis of the resulting liquid-phase.

Resumen

Summary

RESUMEN DE LA TESIS DOCTORAL DE D. Manuel Checa Gómez

1. Introducción o motivación de la tesis

Durante las últimas décadas, los investigadores han dirigido sus esfuerzos hacia la protección del medio ambiente y al desarrollo de procesos sostenibles con el entorno [1,2]. Uno de los procesos en los que se han producido avances importantes es la síntesis de biocombustibles (biogás, biodiesel,…). En este sentido, el uso de la biomasa como fuente de energía no sólo satisface la necesidad energética sino que también proporciona una serie de compuestos químicos funcionalizados, que pueden ser empleados como punto de partida para multitud de procesos [1,3-6]. Con esta premisa, investigadores del *Pacific Northwest National Laboratory* (USA) y del *National Renewable Energy Laboratory* (USA) publicaron un informe en el que se analizaban posibles compuestos de partida (*building blocks* o *platform molecules*) para el desarrollo de una química basada en la biomasa, que emplearía estos compuestos fácilmente transformables en otros productos de alto valor añadido [5,6]. El glicerol (1,2,3-propanotriol) ha sido identificado como una de las 12 moléculas de partida derivadas de la biomasa que pueden ser convertidas en productos químicos o materiales de alto valor añadido [1,4-7].

El glicerol se encuentra en la biomasa utilizada como materia prima para la obtención de biodiesel en forma de ésteres de ácidos grasos o triglicéridos, provenientes principalmente de aceites vegetales [8]. La obtención del biodiesel se realiza vía hidrólisis o metanolisis de los

triglicéridos [9], alcanzando una proporción de 10 kg de glicerol por cada 100 kg de biodiesel en la biorefinería. Los diferentes procesos químicos que se han empleado en la valorización del glicerol pasan por su reformado en fase acuosa, polimerización, fermentación, deshidratación, eterificación, esterificación, oxidación selectiva e hidrogenolisis, para los que la catálisis heterogénea se posiciona como una herramienta fundamental [5].

En cuanto al proceso de hidrogenolisis, hasta ahora se han venido utilizando catalizadores basados en metales soportados, entre los que destacan metales de transición como el Cu [10] o el Ni [11] y metales nobles como Rh [12] y Pt [12,13], siendo este último el único descrito que es capaz de respetar el enlace C-C [14]. Por otro lado, existe una amplia gama de soportes para dichos catalizadores, que van desde óxidos de metales de transición, carbonatos, carbón activo hasta materiales mesoporosos, entre otros [15,16]. La hidrogenolisis de glicerol conduce a diferentes productos de interés como son el 1,2-Propanodiol (1,2-PDO), el 1,3-Propanodiol (1,3-PDO) y el Etilénglicol (EG), aunque las rutas de obtención de los mismos transcurren a través de otros intermedios de reacción de interés industrial como el Acetol.

Nuestro trabajo se ha centrado en la síntesis, caracterización y aplicación de catalizadores metálicos soportados al proceso de hidrogenolisis selectiva de glicerol.

2. Contenido de la investigación

La presente memoria de tesis doctoral puede dividirse en tres bloques que estudian: *i)* la influencia de las interacciones metal-soporte en la reacción de hidrogenolisis, *ii)* el estudio de la desactivación de los catalizadores durante

el proceso de reacción y, finalmente, *iii)* la influencia de la incorporación de dopantes (modificadores) en la actividad y selectividad del proceso de hidrogenolisis del glicerol.

El primer bloque se inició con el estudio de la influencia en la reacción del soporte empleado para la incorporación del metal. Para ello, se sintetizó una serie de catalizadores de Pt, seleccionando como soportes diversos óxidos metálicos parcialmente reducibles como son el TiO_2, ZrO_2, SnO_2 y ZnO. Los parámetros a estudiar fueron la temperatura de reacción, la temperatura de reducción del catalizador, el pH del medio de reacción, la concentración de glicerol y la influencia de la atmósfera de reacción en cuanto a la presión inicial y a la presencia de hidrógeno o de un gas inerte en la misma.

El segundo bloque se centró principalmente en el estudio de las propiedades ácido-básicas superficiales de los soportes y de la desactivación de los catalizadores durante el proceso químico. Para ello, se procedió inicialmente a sintetizar una serie de catalizadores metálicos depositados sobre soportes con propiedades acido-básicas superficiales bien definidas. Se seleccionaron Al_2O_3 activada (acida y básica), CeO_2, La_2O_3 y ZnO, y como metal se eligió Pt, debido a que fue el que presentaba mejores resultados hasta el momento. Las variables de estudio fueron, de nuevo, la temperatura de reducción del catalizador, la presión inicial de hidrógeno, la estabilidad de los productos intermedios de reacción y el proceso de desactivación de los catalizadores.

Finalmente, el tercer bloque se centró en el efecto de la incorporación de modificadores a los catalizadores metálicos soportados. Para ello, se preparó una nueva batería de catalizadores a base de Pt soportado sobre ZrO_2 modificado mediante la incorporación por impregnación de diferentes agentes

dopantes para modificar la acidez de los sólidos obtenidos. Los modificadores seleccionados fueron B_2O_3, H_2SO_4, ácido fosfomolíbdico ($H_3PMo_{12}O_{40}$) y ácido silicotúngstico ($H_3SiW_{12}O_{40}$). Los catalizadores se caracterizaron durante cada etapa de la síntesis, y fueron evaluados en la reacción de hidrogenolisis, prestando especial atención al efecto del modificador incorporado y a la influencia de la temperatura de reacción en la distribución de los productos de reacción.

3. Conclusiones

Se observó la aparición de interacciones fuertes metal-soporte (SMSI) en los catalizadores de Pt soportado sobre SnO_2 y ZnO en forma de aleaciones Sn:Pt y Zn:Pt. En cuanto a su aplicación en la reacción, las mayores conversiones las proporcionaron los catalizadores con los soportes más fácilmente reducibles, en especial el basado en ZnO, el cual presentó los mejores resultados en términos de producción de 1,2-PDO. A la vista de los resultados obtenidos, se decidió profundizar en el estudio realizando ensayos con catalizadores basados en otros metales (Au, Rh y Pd) soportados sobre ZnO. Paralelamente, se estudió la influencia de las condiciones de reacción, incluyendo el comportamiento del catalizador en atmósfera inerte o reductora, la influencia del pH del medio de reacción en el mecanismo de la misma y la evolución de los productos formados durante el proceso. De esta forma, pudo establecerse el orden de actividad para metales y soportes en la reacción de hidrogenolisis de glicerol:

- Orden de actividad para los soportes: $ZnO>SnO_2>ZrO_2>TiO_2$.
- Orden de actividad para los metales: Pt>Rh>>Pd>>Au.

Se comprobó que, en especial con Al_2O_3 (activada ácida y básica), CeO_2, La_2O_3 y ZnO como soportes, un aumento en la conversión no conducía necesariamente a un incremento de 1,2-propanodiol, ya que se generaban productos de oligomerización que desajustaban el balance de masa. Las reacciones llevadas a cabo empleando Acetol y 1,2-Propanodiol como reactivos de partida demostraron que el acetol era susceptible de reaccionar para generar parte de estos polímeros, mientras que el 1,2-Propanodiol es un compuesto estable que no conduce a oligómeros. La caracterización de los catalizadores usados mostró que la pérdida de actividad era debida, en gran medida, a la grafitización de estos oligómeros sobre los centros ácidos superficiales de los catalizadores, unido a los procesos de lixiviación de los soportes durante la reacción.

Finalmente, se confirmó que el empleo de soportes dopados puede ser una herramienta útil no solo a la hora de mejorar los rendimientos obtenidos, sino que además puede orientar la selectividad obtenida hacia un producto o un grupo de productos de interés. En este último punto cabe destacar al ácido silicotúngstico ($H_3SiW_{12}O_{40}$) como el único modificador capaz de orientar la reacción hacia el 1,3-propanodiol (1,3-PDO), un producto que no había sido observado en ninguno de los estudios anteriores de la presente memoria. Por otro lado, se obtuvieron una gran cantidad de monoalcoholes en la fase acuosa, en especial n-propanol, y una fase gas compuesta mayoritariamente por la mezcla propeno/propano, siendo ambos productos de interés industrial. Se confirmó que la distribución de productos depende tanto del dopante, como del tiempo y de la temperatura de reacción empleados.

4. Bibliografía

1. *J.H. Clark, F.E.I. Deswarte, and T.J. Farmer, The integration of green chemistry into future biorefineries, Biofuels, Bioproducts and Biorefining, 3 (2009) 72-90.*
2. *G. Centi and R.A. van Santen, Catalysis for Renewables: From Feedstock to Energy Production, John Wiley and Sons, 2007.*
3. *T.E. Amidon and S. Liu, Water-based woody biorefinery, Biotechnology Advances, 27 (2009) 542-550.*
4. *P. Gallezot, Catalytic routes from renewables to fine chemicals, Catalysis Today, 121 (2007) 76-91.*
5. *T. Werpy and G. Petersen, Top Value Added Chemicals from Biomass: Volume I -- Results of Screening for Potential Candidates from Sugars and Synthesis Gas. 1, 1-76. 2004. United States, National Renewable Energy Lab., Golden, CO (US).*
6. *N. Dimitratos, J.A. Lopez-Sanchez, and G.J. Hutchings, Green catalysis with alternative feedstocks, Topics in Catalysis, 52 (2009) 258-268.*
7. *K. Pathak, K.M. Reddy, N.N. Bakhshi, and A.K. Dalai, Catalytic conversion of glycerol to value added liquid products, Applied Catalysis A: General, 372 (2009) 224-238.*
8. *Brandner, K. Lehnert, A. Bienholz, M. Lucas, and P. Claus, Production of biomass-derived chemicals and energy: Chemocatalytic conversions of glycerol, Topics in Catalysis, 52 (2009) 278-287.*
9. *C.H. Zhou, J.N. Beltramini, Y.X. Fan, and G.Q. Lu, Chemoselective catalytic conversion of glycerol as a biorenewable source to valuable commodity chemicals, Chemical Society Reviews, 37 (2007) 527-549.*

10. *D. Sun, Y. Yamada, and S. Sato, Effect of Ag loading on Cu/Al2O3 catalyst in the production of 1,2-propanediol from glycerol, Applied Catalysis A: General, 475 (2014) 63-68.*
11. *J. Zhao, W. Yu, C. Chen, H. Miao, H. Ma, and J. Xu, Ni/NaX: A bifunctional efficient catalyst for selective hydrogenolysis of glycerol, Catalysis Letters, 134 (2010) 184-189.*
12. *Y. Shinmi, S. Koso, T. Kubota, Y. Nakagawa, and K. Tomishige, Modification of Rh/SiO2 catalyst for the hydrogenolysis of glycerol in water, Applied Catalysis B: Environmental, 94 (2010) 318-326.*
13. *E.S. Vasiliadou, E. Heracleous, I.A. Vasalos, and A.A. Lemonidou, Ru-based catalysts for glycerol hydrogenolysis-Effect of support and metal precursor, Applied Catalysis B: Environmental, 92 (2009) 90-99.*
14. *E.P. Maris and R.J. Davis, Hydrogenolysis of glycerol over carbon-supported Ru and Pt catalysts, Journal of Catalysis, 249 (2007) 328-337.*
15. *Z. Yuan, P. Wu, J. Gao, X. Lu, Z. Hou, and X. Zheng, Pt/solid-base: A predominant catalyst for glycerol hydrogenolysis in a base-free aqueous solution, Catalysis Letters, 130 (2009) 261-265.*
16. *C.H. Zhou, H. Zhao, D.S. Tong, L.M. Wu, and W.H. Yu, Recent advances in catalytic conversion of glycerol, Catalysis Reviews - Science and Engineering, 55 (2013) 369-453.*

SUMMARY OF THE DOCTORAL THESIS OF Mr. Manuel Checa Gomez

1. Introduction and motivation of the thesis

Over the last few decades, researchers have directed their efforts toward environmental protection and the development of sustainable processes [1,2]. This approach has led to major advances in some processes such as biofuels synthesis (biogas, biodiesel, ...). The use of biomass as an energy source not only supply an energetic demand but also provides a wide range of functionalized chemical compounds that can be used as a starting point for many processes [1,3-6]. Considering all these possibilities, researchers from both the *Pacific Northwest National Laboratory* (USA) and the *National Renewable Energy Laboratory* (USA) published a report including the most promising starting compounds (building blocks or platform molecules) for the development of a biomass based chemistry, with biomass as a renewable source of these building blocks that can be easily transformed into other products with high added value [5.6]. Glycerol has been identified as one of the 12 proposed starting molecules derived from biomass that can be converted into other added-value chemicals [1,4-7].

Glycerol can be found in the vegetable oils used as raw material for biodiesel, mainly as fatty acid esters or triglycerides [8]. Biodiesel production is carried out via hydrolysis or methanolysis of triglycerides [9], reaching a ratio of 10 kg of glycerol as by-product per 100 kg of biodiesel in biorefinery. Many different chemical processes have been described for the valorisation of glycerol, such as aqueous phase reforming, polymerization, fermentation,

dehydration, etherification, esterification, oxidation and selective hydrogenolysis , heterogeneous catalysis being a fundamental tool [5].

Regarding glycerol hydrogenolysis, supported metal catalysts have been frequently used, mainly transition metals such as Cu [10] or Ni [11] and noble metals such as Rh [12] and Pt [12, 13], specially Pt because is the only metal that avoids C-C cleavage in the glycerol molecule during the process [14]. Moreover, a wide range of catalytic supports have been used, including transition metal oxides, carbonates, activated carbon or mesoporous materials, among others [15, 16]. Glycerol hydrogenolysis leads to different interesting products, such as 1,2-propanediol (1,2-PDO), 1,3-propanediol (1,3-PDO) and ethylene glycol (EG), although during the reaction some other reaction intermediates of industrial interest such as Acetol are formed.

Our work has been focused on the synthesis, characterization of supported metal solids and their catalytic application to glycerol selective hydrogenolysis.

2. Research content

This dissertation can be divided into three blocks, concerning *i)* the identification of strong metal-support strong interactions (SMSI) in our catalytic systems and their influence on glycerol hydrogenolysis process, *ii)* the study of the deactivation process of the catalysts during the reaction and, finally, *iii)* the influence of the incorporation of dopants (modifiers) in the catalysts activity and selectivity of glycerol hydrogenolysis process.

The first block began with the study of the influence of the catalytic support in the reaction, synthetizing a set of supported Pt catalyst over different partially reducible metal oxides such as TiO_2, ZrO_2, SnO_2 and ZnO. The parameters studied were the reaction temperature, catalyst reduction temperature, pH and the initial pressure of either hydrogen or an inert gas.

The second part was focused on the study of the surface acid-base properties of the supports and the catalyst deactivation process during the reaction. To this end, a series of supported metal catalysts was synthesized over supports with well-defined acid-base properties. Activated Al_2O_3 (acidic and basic), CeO_2, La_2O_3 and ZnO were used as support while Pt was elected as active metal since it was found to give the best results in former experiments. The catalyst reduction temperature, initial hydrogen pressure, stability of reaction intermediates and catalyst deactivation were the variables under investigation.

Finally, the third block focused on the incorporation of modifiers, via impregnation, to a commercial ZrO_2 that was used as support for Pt in order to prepare new catalytic systems. This new set of Pt catalysts supported on modified ZrO_2 were characterized in terms of surface acidity. The modifiers selected were: boron trioxide (B_2O_3), sulphuric acid (H_2SO_4), phosphomolybdic acid ($H_3PMo_{12}O_{40}$) and silicotungstic acid ($H_3SiW_{12}O_{40}$). The solids were characterized for each stage of the synthesis, and were tested in the glycerol hydrogenolysis reaction, paying special attention to the temperature dependence on the distribution of the reaction products

3. Conclusions

The appearance of strong metal-support interactions (SMSI) was observed for the catalysts based on SnO_2 and ZnO as Sn:Pt and Zn: Pt alloys, respectively. As far as the SMSI is concerned, higher glycerol conversions were obtained when catalysts with easily reducible support were present, especially those based on ZnO, which exhibited the best results in terms of 1,2-PDO production. After the obtained results, ZnO was selected as support for a further study concerning the effect of the noble metal incorporated to the catalyst (Pt, Au, Rh or Pd). Moreover, a study of the reaction conditions was carried out, thus gathering some additional information on several aspects such as the behavior of the catalyst under inert or reductive atmosphere, the influence of the pH of the reaction mixture on the reaction mechanism and the dependence of the reaction products with the reaction time. In this way, two important relationships dealing with the catalytic supports and the noble metal incorporated to the catalyst and its influence on glycerol hydrogenolysis were established:

- Activity order for supports: ZnO> SnO_2> ZrO_2> TiO_2.
- Activity order for supported metals: Pt> Rh> >Pd >> Au.

For Pt supported over Al_2O_3 (acid and basic), CeO_2, ZnO and La_2O_3, it was found that an increase in conversion does not necessarily lead to an increase in 1,2-propanediol yield due to oligomerization processes that lead to by-products that disturbed the mass balance. Studies using acetol and 1,2-propanediol as reagents showed that the acetol was able to generate some of these polymers, especially on bare supports, while the 1,2-propanediol was stable in the presence of the catalyst. Characterization of the spent catalysts

indicated that the deactivation process could be explained by the graphitization of formed by-products on the acid centres of the catalyst, along with some leaching of the catalytic supports during the reaction.

Finally, it was confirmed that doped catalyst can be a useful tool not only for yields improvement, but also to modify the products selectivity in favour of an interesting product or a group of products. In this line, it is noteworthy to highlight the role of W polyoxomethalates as the only dopant able to produce 1,3-propanediol (1,3-PDO), a hydrogenolysis product that has not been observed in any of the previous studies of this work. Furthermore, a large amount of monoalcohols was observed, particularly n-propanol, obtained in the aqueous phase and a gas phase composed mainly of the propene / propane mixture, both products of industrial interest. In any case, for the same metal, products distribution would depend on the dopant employed, the reaction temperature and the reaction time.

4. References

1. *J.H. Clark, F.E.I. Deswarte, and T.J. Farmer, The integration of green chemistry into future biorefineries, Biofuels, Bioproducts and Biorefining, 3 (2009) 72-90.*
2. *G. Centi and R.A. van Santen, Catalysis for Renewables: From Feedstock to Energy Production, John Wiley and Sons, 2007.*
3. *T.E. Amidon and S. Liu, Water-based woody biorefinery, Biotechnology Advances, 27 (2009) 542-550.*
4. *P. Gallezot, Catalytic routes from renewables to fine chemicals, Catalysis Today, 121 (2007) 76-91.*

5. *T. Werpy and G. Petersen, Top Value Added Chemicals from Biomass: Volume I -- Results of Screening for Potential Candidates from Sugars and Synthesis Gas. 1, 1-76. 2004. United States, National Renewable Energy Lab., Golden, CO (US).*
6. *N. Dimitratos, J.A. Lopez-Sanchez, and G.J. Hutchings, Green catalysis with alternative feedstocks, Topics in Catalysis, 52 (2009) 258-268.*
7. *K. Pathak, K.M. Reddy, N.N. Bakhshi, and A.K. Dalai, Catalytic conversion of glycerol to value added liquid products, Applied Catalysis A: General, 372 (2009) 224-238.*
A. *Brandner, K. Lehnert, A. Bienholz, M. Lucas, and P. Claus, Production of biomass-derived chemicals and energy: Chemocatalytic conversions of glycerol, Topics in Catalysis, 52 (2009) 278-287.*
8. *C.H. Zhou, J.N. Beltramini, Y.X. Fan, and G.Q. Lu, Chemoselective catalytic conversion of glycerol as a biorenewable source to valuable commodity chemicals, Chemical Society Reviews, 37 (2007) 527-549.*
9. *D. Sun, Y. Yamada, and S. Sato, Effect of Ag loading on Cu/Al2O3 catalyst in the production of 1,2-propanediol from glycerol, Applied Catalysis A: General, 475 (2014) 63-68.*
10. *J. Zhao, W. Yu, C. Chen, H. Miao, H. Ma, and J. Xu, Ni/NaX: A bifunctional efficient catalyst for selective hydrogenolysis of glycerol, Catalysis Letters, 134 (2010) 184-189.*
11. *Y. Shinmi, S. Koso, T. Kubota, Y. Nakagawa, and K. Tomishige, Modification of Rh/SiO2 catalyst for the hydrogenolysis of glycerol in water, Applied Catalysis B: Environmental, 94 (2010) 318-326.*
12. *E.S. Vasiliadou, E. Heracleous, I.A. Vasalos, and A.A. Lemonidou, Ru-based catalysts for glycerol hydrogenolysis-Effect of support and metal precursor, Applied Catalysis B: Environmental, 92 (2009) 90-99.*

13. *E.P. Maris and R.J. Davis, Hydrogenolysis of glycerol over carbon-supported Ru and Pt catalysts, Journal of Catalysis, 249 (2007) 328-337.*
14. *Z. Yuan, P. Wu, J. Gao, X. Lu, Z. Hou, and X. Zheng, Pt/solid-base: A predominant catalyst for glycerol hydrogenolysis in a base-free aqueous solution, Catalysis Letters, 130 (2009) 261-265.*
15. *C.H. Zhou, H. Zhao, D.S. Tong, L.M. Wu, and W.H. Yu, Recent advances in catalytic conversion of glycerol, Catalysis Reviews - Science and Engineering, 55 (2013) 369-453.*

Otras Aportaciones Científicas

Articles

Authors*:* Checa-Gómez, Manuel; Marinas-Aramendía, Alberto; Marinas-Rubio, José María; Urbano-Navarro, Francisco José

Title: Deactivation study of supported Pt catalyst on glycerol Hydrogenolysis

Journal: Applied Catalysis A: General 507 (2015) 34-43

Authors: V. Montes, M. Checa, A. Marinas, J.M. Marinas, F. J. Urbano, M. Boutonnet, S. Järas, C. Pinel

Títle: Synthesis of different ZnO-supported metal systems through microemulsion technique and application to catalytic transformation of glycerol to acetol an 1,2-propanediol

Journal: Catalysis Today, Catalysis Today 223 (2014) 129 – 137

Authors*:* Checa-Gómez, Manuel; Auneau, Florian; Hidalgo-Carrillo, Jesus; Marinas-Aramendía, Alberto; Marinas-Rubio, José María; Pinel, Catherine; Urbano-Navarro, Francisco José

Title: Catalytic transformation of glycerol on several metal systems supported on ZnO

Journal: Catalysis Today 196 (2012) 91– 100

Communications to Congresses

Authors: Checa-Gómez, Manuel; Urbano-Navarro, Francisco José; Marinas-Aramendía, Alberto; Marinas-Rubio, José María

Title: Desactivación de Catalizadores de Platino soportado en la reacción de hidrogenolisis de glicerol.

Name: NANOUCO V. Encuentro sobre Nanociencia y Nanotecnología de Investigadores y Tecnólogos Andaluces.

Type of presentation: Poster communication **Date:** 06-02-2015

Authors: Checa-Gómez, Manuel; Urbano-Navarro, Francisco José; Marinas-Aramendía, Alberto; Marinas-Rubio, José María

Title: Sistemas de Platino soportado sobre tierras raras en la transformación catalizada de glicerol.

Name: I Encuentro de Jóvenes Investigadores de la SECAT

Type of presentation: Oral communication **Date:** 18-6-2014

Authors: Checa-Gómez, Manuel; Marinas-Aramendía, Alberto; Marinas-Rubio, José María; Urbano-Navarro, Francisco José

Title: Estudio de la influencia del soporte en la hidrogenolisis del glicerol sobre catalizadores de Platino.

Name: Secat 2013: Catalizadores y reactores estructurados

Type of presentation: Poster communication **Date:** 26-06-2013

Authors: Checa-Gómez, Manuel; Marinas-Aramendía, Alberto; Marinas-Rubio, José María; Urbano-Navarro, Francisco José

Title: Estudio del soporte en catalizadores de Platino para la hidrogenolisis de glicerol

Name: NANOUCO IV: Encuentro sobre Nanociencia y Nanotecnología de Investigadores Andaluces Type of presentation: Oral communication

Type of presentation: Oral communication **Date**: 08-02-2013

Authors: Checa-Gómez, Manuel; Marinas-Aramendía, Alberto; Marinas-Rubio, José María; Urbano-Navarro, Francisco José

Title: Screening of supported Pt metal catalyst for glycerol hydrogenolysis: role of catalytic support

Name: UBIOCHEM III Sustainable production of fuels/energy, materials and chemicals from biomass

Type of presentation: Poster communication **Date:** 01-11-2012

Authors: V. Montes, M. Checa, A. Marinas, J.M. Marinas, F. J. Urbano, M. Boutonnet, S. Järas, C. Pinel.

Title: Synthesis of different ZnO-supported metal systems through microemulsion technique and application to selective hydrogenation processes

Name: UBIOCHEM III Sustainable production of fuels/energy, materials and chemicals from Biomass (3rd joint meeting COST Action CM0903, UBIOCHEM)

Type of presentation: Oral communication. **Date:** 01-11-2012

Authors: Checa-Gómez, Manuel; Aramendia-Lopidana, Maria Angeles; Marinas-Aramendía, Alberto; Marinas-Rubio, José María; Urbano-Navarro, Francisco José

Title: HIDROGENOLISIS DE GLICEROL CON PLATINO SOPORTADO SOBRE DIFERENTES OXIDOS METALICOS

Name: SECAT 2011 (Zaragoza, Spain)

Type of presentation: Oral communication **Date:** 29-06-2011

Authors: Checa-Gómez, Manuel; Aramendía-Lopidana, María Ángeles; Marinas-Aramendía, Alberto; Marinas-Rubio, José María; Urbano-Navarro, Francisco José

Title: HIDROGENOLISIS DE GLICEROL CON CATALIZADORES DE PLATINO SOPORTADO SOBRE DIFERENTES OXIDOS METALICOS

Name: NANOUCO (III) CÓRDOBA (ESPAÑA)

Type of presentation: Oral communication **Date:** 08-01-2011

Anexo I

Copia del artículo 1

Catalysis Today 196 (2012) 91–100

Contents lists available at SciVerse ScienceDirect

Catalysis Today

journal homepage: www.elsevier.com/locate/cattod

Catalytic transformation of glycerol on several metal systems supported on ZnO

Manuel Checa[a], Florian Auneau[b], Jesús Hidalgo-Carrillo[a], Alberto Marinas[a], José M. Marinas[a], Catherine Pinel[b], Francisco J. Urbano[a,*]

[a] Faculty of Sciences, University of Córdoba, Campus de Rabanales, Marie Curie Building, E-14014 Córdoba, Spain
[b] IRCELYON, UMR 5256 CNRS/UCBL, 2 avenue Albert Einstein, 69626 Villeurbanne Cedex, France

ARTICLE INFO

Article history:
Received 14 November 2011
Received in revised form 8 February 2012
Accepted 8 February 2012
Available online 15 March 2012

Keywords:
Glycerol hydrogenolysis
Strong metal–support interaction (SMSI)
Platinum
Rhodium
Palladium
Gold
1,2-Propanediol (1,2-PDO)
Lactic acid
Acetol

ABSTRACT

Different metal systems consisting in platinum supported on several reducible supports (5% by weight) were synthesized through the deposition–precipitation technique and tested for glycerol hydrogenolysis. Interestingly, supports exhibiting the highest conversions were those with the greatest strong metal–support interaction (SMSI) effect, ZnO and SnO_2, eventually forming alloys (Pt–Zn and Pt–Sn, respectively). ZnO was subsequently selected for further studies as support for Rh, Pt, Pd and Au and the resulting solids were tested again for glycerol catalytic transformation under reductive or inert atmosphere at 453 K. Under similar reaction conditions, glycerol conversion order followed the sequence Pt > Rh ≫ Pd ≫ Au. Moreover, the solids reduced at 473 K were more active than those activated at 673 K, which evidences the detrimental effect of the increase in metal particle size and/or alloy formation on the catalytic performance. Quite high yields to lactic acid were achieved in a basic medium (e.g. 68% for Rh/ZnO-473 under H_2) whereas yield to 1,2-PDO was more modest (26% for Rh/ZnO-673 under similar reaction conditions).

1. Introduction

Glycerol, obtained as a by-product in biodiesel manufacture, is a versatile feedstock for the production of a full range of chemicals, polymers and fuels. Some of the processes described in the literature for glycerol valorization include polymerization [1], etherification to produce fuel additives as octane boosters [2], dehydration to acrolein, an important intermediate in the manufacture of polymers [3], or selective oxidation to dihydroxyacetone [4] a versatile compound extensively used as a cosmetic ingredient, among others. Moreover, glycerol catalytic transformation on different metals under hydrogen or inert atmosphere can lead to a wide range of chemicals [5–9], some of the routes being indicated in Fig. 1. Hydrogen generated through aqueous phase reforming allows the formation of reduction products under inert atmosphere. Two of the most interesting chemicals produced through glycerol catalytic transformation are 1,2-propanediol (1,2-PDO) and lactic acid (LA). The former can be used in the food industry, as a less toxic alternative to 1,2-ethanediol in antifreeze and as a deicer or as a feedstock in the preparation of polyester resins for film and fiber manufacture [9]. As for the latter, it is well-known as a moisturizer (cosmetics) and a mordant (i.e. a chemical that help fabrics accept dyes in textiles). Moreover, it is used in the dairy industry as pH regulator or preservative. Ethyl lactate is also a common solvent. Finally, poly-lactic acid is a well-known biodegradable polymer (for food packaging, surgical implants, etc.) [10].

Ruthenium is probably the most-widely used noble catalysts in glycerol hydrogenolysis [8,11] though some others such as Pt [6], Rh [12,13] Pd [12,13], Ir [14] or even first row transition metals (Cu [13], Ni [15], Co [16]), just to cite some examples, have also been reported. As can be inferred from Fig. 1, not only activity but also selectivity to the target molecule should be considered when choosing a metal. In this sense, Ru is probably the most active metal though it normally leads to large amounts of liquid (ethylene glycol and 1-propanol) and gaseous (methane, ethane and propane) by-products. There also have been several attempts at tuning the selectivity of metals through the addition of acid or bases [6,12] or the modification of the noble-metal with low-valent metal oxides (e.g. ReO_x) [17]. Finally, some other factors affecting the process are metal particle size or support [18–20].

In several previous papers we showed that reducible supports can lead to interesting catalytic performance in several oxidations and reductions [21,22] through the promotion of strong metal–support interactions (SMSI), eventually resulting, in some cases, in the formation of alloys.

* Corresponding author. Fax: +34 957212066.
E-mail address: FJ.urbano@uco.es (F.J. Urbano).

0920-5861/$ – see front matter © 2012 Elsevier B.V. All rights reserved.
doi:10.1016/j.cattod.2012.02.036

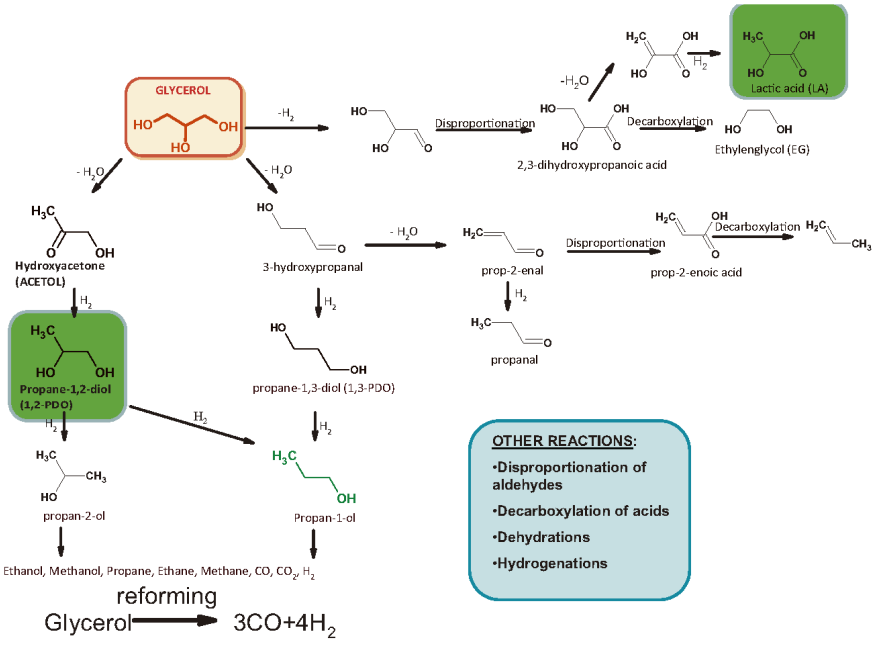

Fig. 1. Some catalytic transformation routes from glycerol described in the literature under hydrogen or inert atmosphere.

The present piece of research is aimed at exploring the effect of several reducible supports on the catalytic performance of diverse metal systems in glycerol transformation, paying special attention to the selectivity to 1,2-PDO or lactic acid.

2. Experimental

2.1. Synthesis of different platinum-supported systems

A first screening was carried out using different platinum-containing systems synthesized through the deposition–precipitation method. The synthesis and characterization of the solids are described elsewhere [22]. Therefore, an aqueous solution containing 8% (w/w) chloroplatinic acid (Sigma–Aldrich Ref. 262587) was used as the metal precursor and the following metal oxides as supports: tin (IV) oxide (Sigma–Aldrich Ref. 549657), zirconium (IV) oxide (Sigma–Aldrich Ref. 544760), zinc (II) oxide (Sigma–Aldrich Ref. 544906), and titanium (IV) oxide (Degussa, P-25).

The synthetic procedure was as follows: a volume of 6.57 mL of chloroplatinic acid solution was diluted to 200 mL with Milli-Q water and adjusted to pH 7 by adding 0.1 M NaOH (FLUKA Ref. 43617). Then, an amount of 4.75 g of support was added and the mixture readjusted to pH 7 with NaOH for acid supports or HCl for basic supports. The solution containing the support was refluxed at 353 K under vigorous stirring for 2 h. Then, a volume of 10 mL of isopropanol was added, the temperature raised to 383 K and refluxing continued for 30 min, after which the mixture was vacuum filtered and the filtrate washed with three portions of 25 mL of water each.

The resulting solid was dried in a muffle furnace at 383 K for 12 h, ground and calcined at 673 K for 4 h. After calcination, the solid was ground again, sieved through a mesh of 0.149 mm pore size and stored in a topaz flask. The nominal proportion of Pt in the catalyst thus obtained was 5 wt%. Finally, the catalyst was reduced under a hydrogen stream flowing at 30 mL min^{-1} at selected temperatures for 2 h. Reduction temperature was chosen according to significant features observed in the temperature-programmed reduction profiles. The solid names include the metal, its support and the reduction temperature used, in Kelvin (e.g. Pt/ZnO-473).

2.2. Synthesis of ZnO-supported metal systems

The first screening of supports resulted in the choice of ZnO for subsequent incorporation of metals (Pt, Rh, Au or Pd) in a 5 wt% nominal content. The synthetic procedure (see Supplementary information Fig. S1) was the same as described for Pt-containing solids but using the following precursors: H_2PtCl_6, $RhCl_3$, $HAuCl_4$ and $Pd(NO_3)_2$. In the case of palladium no chloride precursor was used since its solubility in water is very low, requiring the use of HCl to dissolve it which results in a pH 3 which could attack the support. Catalyst nomenclature follows the same criteria as described in Section 2.1. Therefore, for instance, Rh/ZnO or Pd/ZnO-673 describes the as-synthesized Rh-system or the palladium solid reduced at 673 K, respectively.

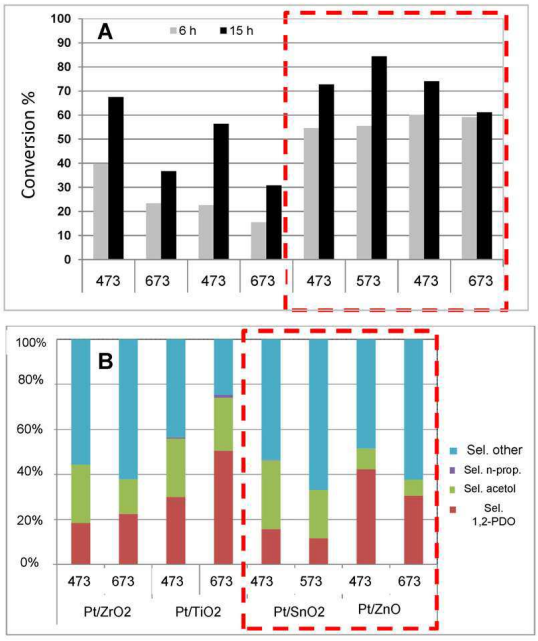

Fig. 2. Results obtained for hydrogenolysis of glycerol expressed in terms of conversion for t = 6 h or 15 h (A) or selectivity for t = 15 h (B). Reaction conditions: 20 mL of 1.36 M glycerol in water, 200 mg catalyst, 448 K, 6 bar H_2.

2.3. Characterization

Elemental analysis of metal containing samples was performed using inductively coupled plasma mass spectrometry (ICP-MS). Measurements were made on a Perkin-Elmer ELAN DRC-e instrument following dissolution of the sample in a 1:1:1 H_2SO_4/HF/H_2O mixture. Calibration was done by using PE Pure Plus atomic spectroscopy standards, also from Perkin-Elmer.

Surface areas of the solids were determined from nitrogen adsorption–desorption isotherms obtained at liquid nitrogen temperature on a Micromeritics ASAP-2010 instrument, using the Brunnauer–Emmett–Teller (BET) method. All samples were degassed to 0.1 Pa at 383 K prior to measurement.

Transmission electron microscopy (TEM) images were obtained using a Philips CM-10 microscope. All samples were mounted on 3 mm holey carbon copper grids.

X-ray patterns for the samples of the first screening for supports were obtained with a Siemens D-5000 diffractometer equipped with a DACO-MP automatic control and data acquisition system. The instrument was used with CoK_α radiation and a graphite monochromator. In the case of the ZnO-supported metal systems, the X-ray diffractograms were performed with a Bruker D8A25 Advance diffractometer (λ = 1.54184 Å) using a one dimensional multistrip fast detector (LynxEye) with 191 channels on 2.94° at 50 kV and 35 mA.

Temperature-programmed reduction (TPR) measurements were made with a Micromeritics TPD-TPR 2900 analyser. An amount of 200 mg of catalyst was placed in the sample holder and reduced in a 5:95 H_2/Ar stream flowing at 40 mL min^{-1}. The temperature was ramped from 313 to 758 K at 10 K min^{-1} (213 K and 673 K in the case of Pd/ZnO solid).

X-ray photoelectron spectroscopy (XPS) data were recorded on 4 mm × 4 mm pellets 0.5 mm thick that were obtained by gently pressing the powdered materials following outgassing to a pressure below about 2×10^{-8} Torr at 423 K in the instrument pre-chamber to remove chemisorbed volatile species. The main chamber of the Leibold–Heraeus LHS10 spectrometer used, capable of operating down to less than 2×10^{-9} Torr, was equipped with an EA-200MCD hemispherical electron analyser with a dual X-ray source using AlKα ($h\nu$ = 1486.6 eV) at 120 W, at 30 mA, with C(1s) as energy reference (284.6 eV).

2.4. Catalytic reaction and analytical method

Initial screening of the supports was conducted in a Berghof HR-100 stainless steel high-pressure autoclave equipped with a 75 mL PTFE vessel and a magnetic stirrer. Under standard conditions, 20 mL of a 1.36 M solution of glycerol in water and 200 mg catalysts were introduced in the vessel. Reactor was then purged with hydrogen and temperature (448 K) and hydrogen pressure (6 bar) adjusted. The stirring rate was 1000 rpm. After 6 h or 15 h of reaction, stirring was stopped and the vessel cooled with an ice bath. Reaction mixture was homogenized and analyzed by GC-FID (Agilent Technologies 7890, with a Supelco 25357 Nukol™ capillary column). Quantification was carried out through the corresponding calibration curves for glycerol, acetol, 1,2-PDO and n-propanol.

In the case of reactions on diverse ZnO-supported metal systems, two different reactors were used, utilising the same

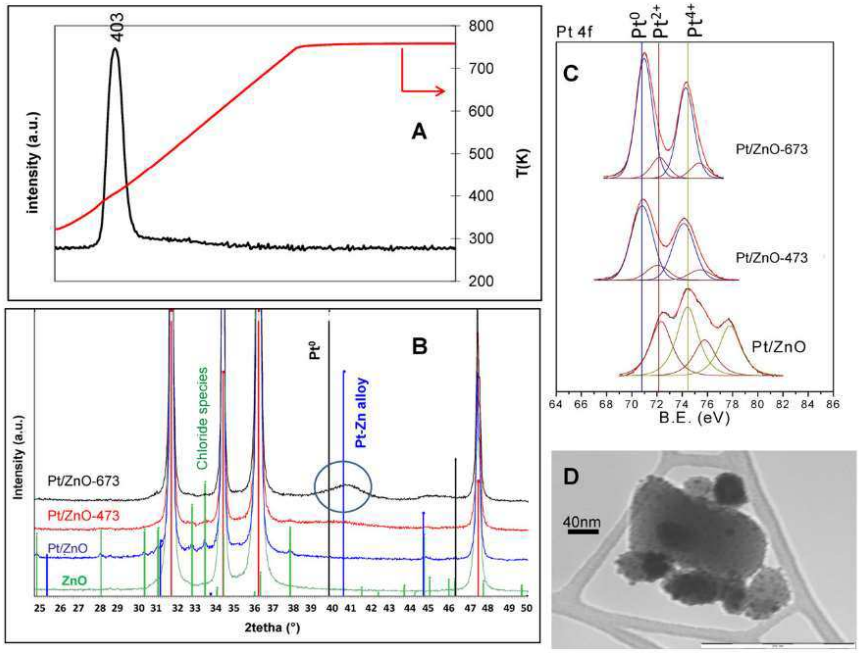

Fig. 3. Characterization of Pt/ZnO systems: TPR (A), XRD (B), XPS (C) and TEM micrograph of Pt/ZnO-673 (D).

temperature (453 K), pressure (20 bar of He or H_2) glycerol concentration (0.68 M, i.e. 5% glycerol in water), stirring rate (1000 rpm) and glycerol/catalyst ratio. The first reactor was a stainless still autoclave with a 200 mL Teflon vessel which allowed sampling at different time intervals. Reaction volume was 100 mL and catalyst weight 500 mg. The second reactor was a Slurry Phase Reactor 16 (AMTEC), using 6 mL of the 0.68 M glycerol aqueous solution and 30 mg of catalyst. Reaction time was 12 h. For reactions at pH 13, pH value was adjusted with NaOH 1 M. In both cases, quantification was carried out by HPLC on a CarboSep 107H column (0.5 mL min^{-1} 0.005 N H_2SO_4, 313 K). 1,3-PDO, 1,2-PDO, ethylene glycol, 1-propanol, 2-propanol, ethanol, methanol, acetol, lactic acid, formic acid and acetic acid were analyzed. GC–MS analysis confirmed the identification of lactic acid and 1,2-propanediol.

Conversion (Conv(%)) of glycerol was defined as the number of mol of glycerol consumed reported to the initial number of mol of glycerol. Selectivity to a given product i was calculated according to the following equation:

$$Sel_i^t\ (\%) = \frac{X_i^t \times nC_i}{X_{gly}^t \times 3} \times 100$$

Yields were similarly expressed as:

$$Y_i^t\ (\%) = Conv(\%) \times \frac{Sel_i^t(\%)}{100}, \quad \text{or} \quad Y_i^t\ (\%) = \frac{X_i^t \times nC_i}{X_{gly}^0 \times 3} \times 100$$

where X_i^t and X_{gly}^t mol of product i and mol of reacted glycerol at reaction time t, respectively; X_{gly}^0 initial amount of glycerol; nC_i standing for the number of carbon atoms of the product i.

3. Results and discussion

3.1. First screening of supports

Initially, different systems based on platinum supported on SnO_2, ZrO_2, ZnO and TiO_2 were synthesized through the deposition–precipitation method as described in Section 2.2. Platinum nominal content was 5% by weight. The systems were then tested for glycerol hydrogenolysis. Two different temperatures were used for reduction of the solids: 473 K and 673 K. In the case of using SnO_2 as the support, the higher temperature was 573 K in order to avoid tin sublimation. Results found in terms of conversion for t = 6 h and 15 h are represented in Fig. 2A. As can be seen, the most active systems were those supported on SnO_2 and ZnO. Results found for characterization of the above-mentioned systems (see Supplementary information, Figs. S2 and S3) showed that the most active systems Pt/SnO_2 and Pt/ZnO were those exhibiting a strongest metal–support interaction, eventually resulting, at the highest reduction temperature (573 K or 673 K), in the formation of an alloy. Considering both Pt/ZnO and Pt/SnO_2 solids, Pt/ZnO is the most selective solid to 1,2-PDO after 15 h of reaction (Fig. 2B) which prompted us to select Pt/ZnO for further studies.

3.2. Study of different metals supported on ZnO

Given the above reported results, ZnO was selected as a support for other metals. The synthesis was again carried out through the deposition–precipitation technique, in order to obtain a metal

Table 1
Some features concerning characterization of the different ZnO-supported metal systems.

Catalyst	BET ($m^2 g^{-1}$)[a]	Metal atomic %					BET ($m^2 g^{-1}$) of M/ZnO-673
		Nominal	ICP-MS	XPS			
				M/ZnO	M/ZnO-473	M/ZnO-673	
Pt/ZnO	19	5.00	5.17	5.26	5.26	4.42	17
Pd/ZnO	17	5.00	4.10	1.16	0.89	0.39	12
Rh/ZnO	25	5.00	2.37	3.21	2.90	2.76	20
Au/ZnO	14	5.00	5.05	2.13	1.87	1.39	11

Surface composition from XPS data[b]

	%Pt^0	%Pt^{+2}	%Pt^{+4}		%Rh^0	%Rh^{+1}	%Rh^{+3}
Pt/ZnO	0.0	43.9	56.1	Rh/ZnO	0	0	100
Pt/ZnO-473	82.2	17.8	0.0	Rh/ZnO-473	0.0	76.3	23.7
Pt/ZnO-673	90.4	9.6	0.0	Rh/ZnO-673	68.9	19.7	11.3

	%Pd^0	%Pd^{+2}		%Au^0
Pd/ZnO	0	100	Au/ZnO	100
Pd/ZnO-473	73.6	26.3	Au/ZnO-473	100
Pd/ZnO-673	75.6	24.3	Au/ZnO-673	100

[a] The support (ZnO) has a BET area of 15 $m^2 g^{-1}$.
[b] The possibility of certain re-oxidation of the samples during preparation for XPS analyses (especially in the case of Pd) cannot be ruled out.

nominal content of 5% by weight. Some features concerning the characterization of the as-synthesized solids as well as those resulting from the reduction at 473 K and 673 K are given in Table 1 and Figs. 3–6.

A first conclusion from Table 1 is that BET surface areas of all as synthesized solids are in the 14–25 $m^2 g^{-1}$ range. Moreover, reduction at 673 K results in a decrease in surface area which suggests that metal particle size could have increased, thus leading to a

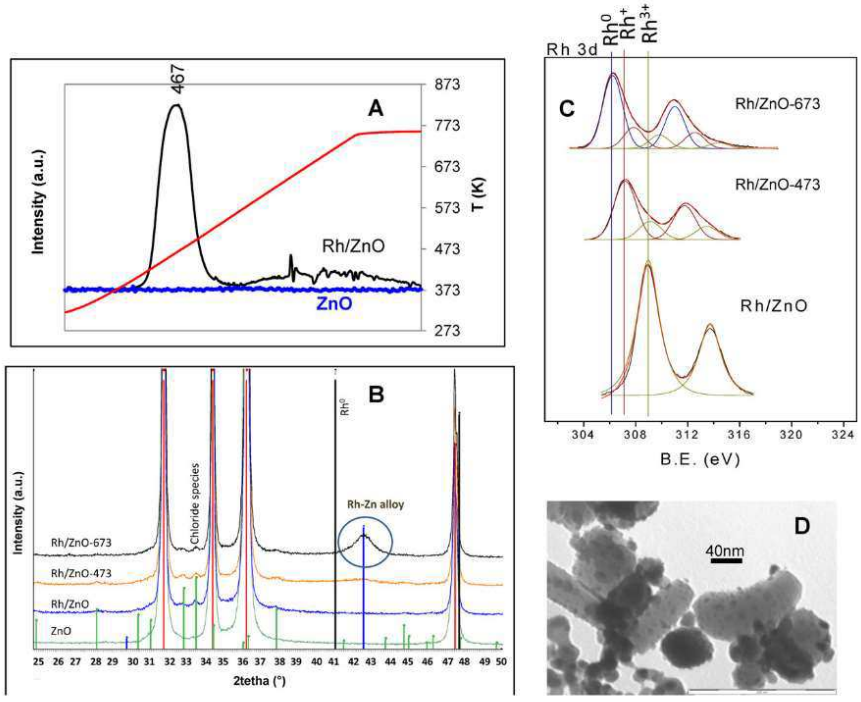

Fig. 4. Characterization of Rh/ZnO systems: TPR (A), XRD (B), XPS (C) and TEM micrograph of Rh/ZnO-673 (D).

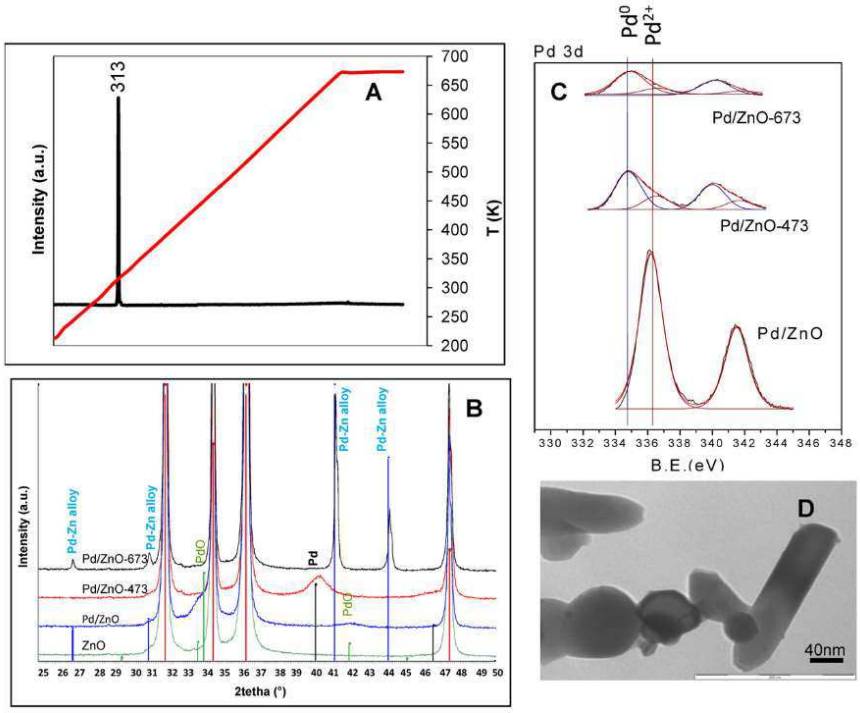

Fig. 5. Characterization of Pd/ZnO systems: TPR (A), XRD (B), XPS (C) and TEM micrograph of Pd/ZnO-673 (D).

partial blocking of pores. If metal content is considered, there has been a good incorporation of the metal, the exception being Rh/ZnO for which ca. only 50% of the metal was incorporated as evidenced by ICP-MS (Rh content of 2.37% instead of 5.0%, nominal value). Furthermore, XPS data reveal that in all cases the metal/Zn ratio decreases with the reduction temperature, thus suggesting the progressive decoration of metal particles by the support, a typical phenomenon in reducible supports such as TiO_2 or ZnO [21–23].

We are going to study now each metal system individually, having a look at Figs. 3–6. The TPR profile of Pt/ZnO (Fig. 3A) exhibited a strong reduction peak at 403 K in addition to another much weaker tail. The synthetic procedure could account for the appearance of our TPR peak ca. 423 K below the value described in the literature [24,25]. Therefore, the addition of 2-propanol to the reaction mixture may have caused the partial reduction of chloroplatinic acid. In fact, XPS spectrum of Pt/ZnO (Fig. 3C) exhibits not only Pt 4f 7/2 peaks of Pt^{4+} species but also of Pt^{2+} at binding energies of 74.4 and 72.3 eV, respectively [26]. Moreover, XRD of Pt/ZnO system (Fig. 3B) shows some peaks at 2θ values of 32.8°, 33.6° and 37.8° which can be ascribed to oxychloride species of the type $Zn_5(OH)_8Cl_2{\cdot}H_2O$ which suggests that during calcination of the system at 673 K, chloride species passed to the support. In line with TPR profile, reduction at 473 K (Pt/ZnO-473 solid) results in the appearance of Pt^0, as evidenced by the XPS peak at 70.9 eV [27]. Finally, Pt/ZnO-673 solid exhibits Pt^{2+} and Pt^0 peaks at 72.2 eV and 71.0 eV, respectively. XRD evidences the formation of a Pt–Zn alloy with a peak at $2\theta = 40.6$ eV. Interestingly, no Pt^0 peaks are observed in XRD of Pt/ZnO-473 or Pt/ZnO-673 solids which given the high metal content (ca. 5% by weight, as confirmed by ICP-MS) indicates that platinum particle size is low. In fact, TEM micrographs showed mean particle diameters of 3.1 nm and 5.2 nm (Fig. 3D), respectively.

As regards Rh/ZnO solid, TPR profile (Fig. 4A) shows two peaks, the major one exhibiting a maximum at ca. 467 K. This peak, which corresponds to a reduction between 373 K and 513 K could be ascribed to the reduction of Rh^{3+} to Rh^0, whereas the peak at higher temperatures could indicate the reduction of some rhodium species interacting with the support, since TPR profile of ZnO does not exhibit any peak. Hwang et al. [28] found that the reduction of RhO_x to Rh(0) occurs at 373 K whereas higher temperatures values (ca. 443 K) are required when a chloride precursor (as it is our case) have been used. XPS spectrum of Rh/ZnO (Fig. 4C) shows the presence of Rh^{3+} with Rh 3d 5/2 values of 308.8 eV. Reduction at 473 K results in the formation of Rh^+ (307.2 eV) whereas all three oxidation states (Rh^0, Rh^+ and Rh^{3+}), coexist at 673 K, with binding energies of 306.2, 307.6 and 306.8 eV r respectively [29]. In a similar way as for Pt/ZnO, no rhodium peaks are observed in X-ray diffractograms (Fig. 4B) but only Rh–Zn alloy, at $2\theta = 42.6°$ in Rh/ZnO-673 system. Again, this suggest a small rhodium particle size, TEM micrographs showing average particle sizes of 3.7 nm and 6.2 nm for Rh/ZnO-473 and Rh/ZnO-673, respectively (see TEM micrograph of Rh/ZnO-673 in Fig. 4D).

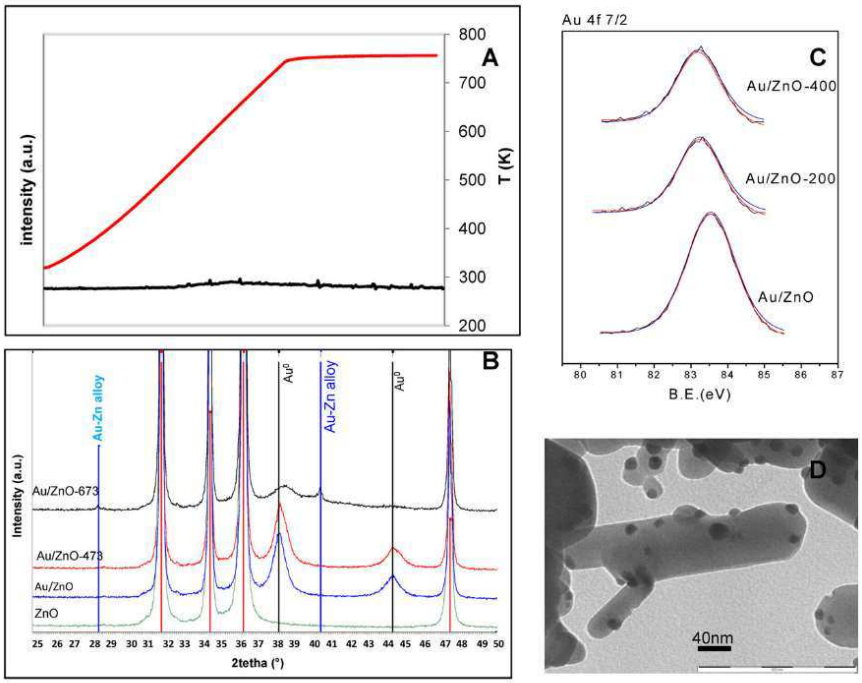

Fig. 6. Characterization of Au/ZnO systems: TPR (A), XRD (B), XPS (C) and TEM micrograph of Au/ZnO (D).

In the case of palladium, TPR profile (Fig. 5A) evidences that Pd^0 is easily reduced, the reduction peak appearing at 313 K. XPS spectra of Pd/ZnO solid (Fig. 5C) have Pd 3d 5/2 peaks at 336.2 eV which can be ascribed to PdO species which exhibit XRD peaks at $2\theta = 33.9°$ (1 0 1 reflection) [30] (Fig. 5B). Subsequent reduction at 473 K results in the formation of Pd^0 (XPS peak at 335.0 eV and XRD peak of 1 1 1 reflection at $2\theta = 40.4°$) [30,31]. Finally, at 673 K a Pd–Zn alloy is observed by XRD, with peaks at $2\theta = 41.2°$ and 44.2°. These results suggest that palladium particle size is bigger as compared to Pt and Rh (15 nm for Pd/ZnO-473 as estimated from XRD using Scherrer equation). Unfortunately, TEM micrographs are not clear enough as to estimate Pd particle size (see micrograph for Pd/ZnO-673, Fig. 5D as an example).

Finally, regarding gold systems, Au^0 is already formed during the synthetic procedure thus not exhibiting peaks in the TPR profile (Fig. 6A). This is also clear from XPS spectra (Fig. 6C) which show for all gold-containing solids a typical Au^0 4f7/2 signal at ca. 83.5 eV [32]. Moreover, X-ray diffractograms present a peak of Au^0 at $2\theta = 38.2°$ (1 1 1 reflection) [33] in Au/ZnO, the signal shifting to higher values with reduction temperature (just as the Au^0 XPS signal shifts to lower binding energies) which together with the appearance of a new peak at $2\theta = 40.5°$ in Au/ZnO-673 system suggests the formation of an Au–Zn alloy. Finally, TEM micrographs show that gold particle size is 12 nm and 14 nm for Au/ZnO-473 and Au/ZnO-673, respectively.

All in all, these results evidence that, as desired, in all cases there is a SMSI effect, a metal–Zn alloy is formed at 673 K and that particle size increases from M/ZnO-473 to M/ZnO-673 solids. Moreover, the smallest particle sizes correspond to Rh and Pt solids whereas the biggest ones are those of palladium and gold-containing systems.

3.3. Catalytic performance of M/ZnO-200 and M/ZnO-400 solids

Results found for liquid-phase catalytic transformation of glycerol on the different ZnO-supported systems are represented in Figs. 7 and 8. Analyses were performed in the "Parallel Slurry Phase Reactor" (SPR16) for $t = 12$ h, under two different atmospheres (H_2 or He) and using neutral or basic (pH 13) medium. A first conclusion from Fig. 7 is that in terms of conversion, the reaction is faster in the basic medium as compared to the neutral one and in helium as compared to hydrogen, which is consistent with results reported in the literature for other metals, such as iridium [14]. Moreover, under similar reaction conditions conversion order follows the sequence Pt > Rh ≫ Pd ≫ Au. If selectivity is considered, 1,2-PDO is preferentially obtained in neutral medium whereas, in general, the main product in basic medium is lactic acid. Auneau [34] studied the reaction mechanism of glycerol hydrogenolysis on several supported Rh systems. Experimental results together with the theoretical studies (DFT) on a model Rh surface (1 1 1) prompted him to suggest the reaction mechanism presented in Fig. 9, where glycerol is firstly dehydrogenated. As shown in such a figure, there are different equilibria from pyruvaldehyde (PAL) to 1,2-PDO whereas formation of lactic acid from that chemical through intramolecular Cannizaro reaction is favoured in basic media and there is no equilibrium. In fact, if we start from lactic acid, it is not converted to any other product whereas 1,2-PDO results in certain production of lactic

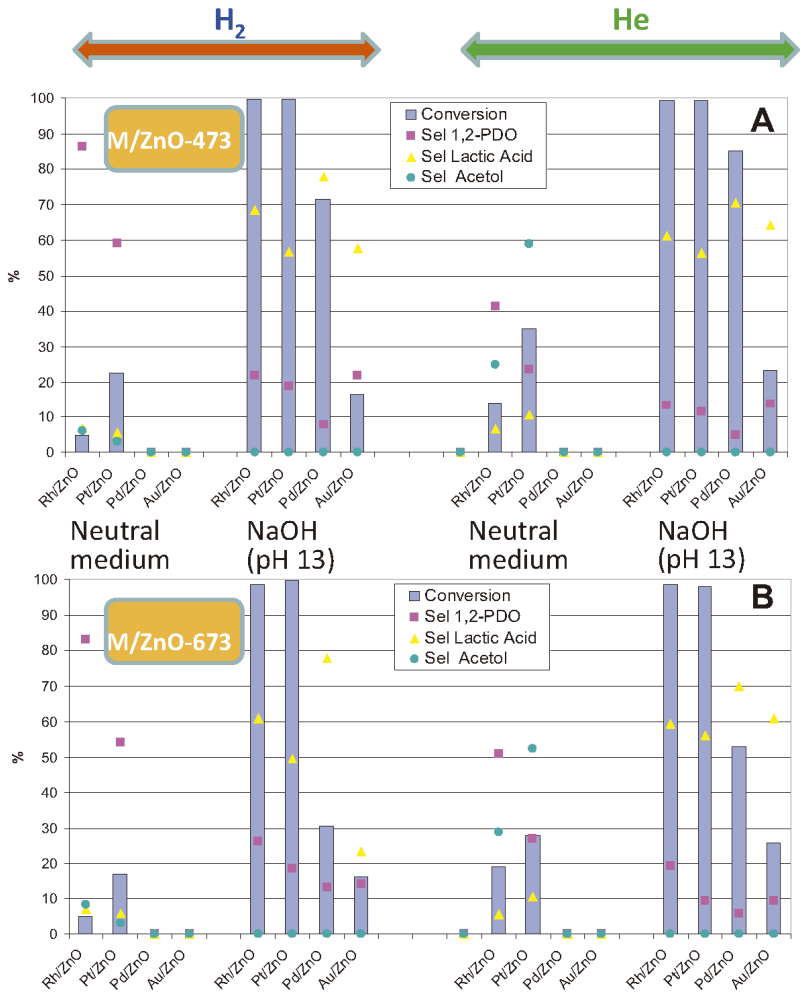

Fig. 7. Results found for glycerol catalytic transformation on the different ZnO-supported metal systems reduced at 473 K (A) or 673 K (B) expressed as conversion and selectivity for t = 12 h. Reaction conditions: 100 mL of a 0.68 M glycerol aqueous solution, 30 mg catalyst, 453 K, 20 bar of He or H_2.

acid under basic conditions. This mechanism also accounts for the production of acetol in helium whereas in the presence of a high hydrogen concentration equilibrium shifts up to 1,2-PDO.

When both M/ZnO-473 and M/ZnO-673 solids are compared (Fig. 7), the former is more active than the latter, which suggests that the strong metal–support interaction favors the reaction but the eventual formation of an alloy at 673 K and/or the increase in particle size (as evidenced by TEM) are detrimental to the activity. Finally, in terms of yield to 1,2-PDO or lactic acid (Fig. 8), Pt, Pd and Rh reduced at 473 K affords lactic acid in a 55–68% yield (basic medium), the highest value corresponding to Rh/ZnO-473, whereas production of 1,2-PDO is more modest (26% for Rh/ZnO-673).

All in all, Pt and Rh systems are the most active solids among the synthesized solids. One could think that, given the fact that both Pt/ZnO and Rh/ZnO solids exhibit quite similar metal particle sizes (3.3 nm and 3.7 nm for Pt/ZnO-473 and Rh/ZnO-473, respectively) the highest activity of the former is just a result of the highest metal content (ca. the double than for Rh/ZnO as evidenced by ICP-MS, see Table 1). However, conversion values achieved in neutral medium for Pt/ZnO are 22.6% and 35.0% under H_2 and He,

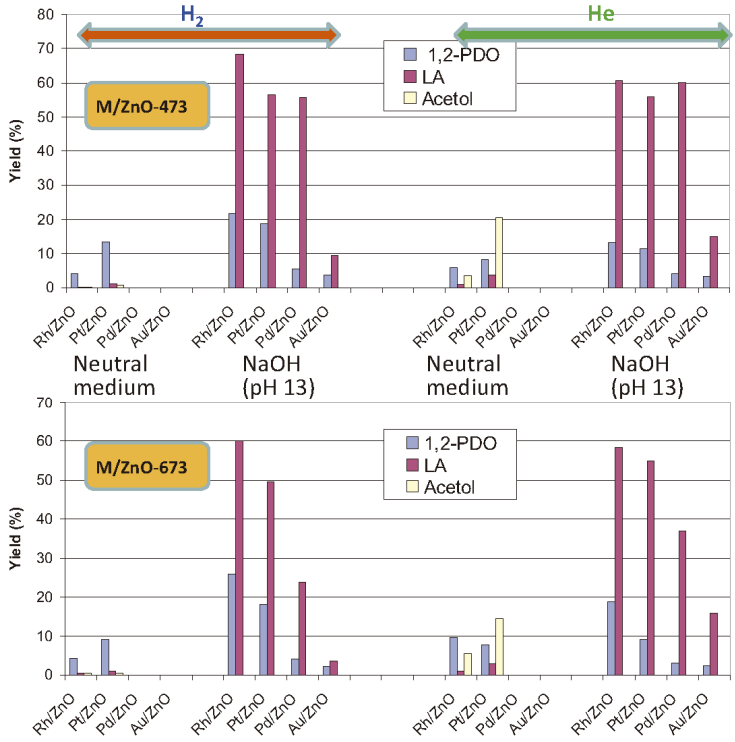

Fig. 8. Results found for glycerol catalytic transformation on the different ZnO-supported metal systems reduced at 473 K (A) or 673 K (B) expressed as yields for $t = 12$ h. Reaction conditions: 100 mL of a 0.68 M glycerol aqueous solution, 30 mg catalyst, 453 K, 20 bar of He or H_2.

respectively (Fig. 7), whereas under similar conditions, Rh/ZnO afforded 4.9% and 6.6%, respectively. This represents conversion values of ca. 4–5 times higher for Pt, which suggests that under our experimental conditions platinum systems are intrinsically more active than rhodium solid. Additional experiments in the 200-mL stainless steel autoclave, in neutral medium, showed that, for the same conversion value, selectivity to lactic acid or 1,2-PDO obtained with Pt/ZnO and Rh/ZnO solids are quite similar. Therefore, for instance, at 5% and 10% conversion, selectivity to 1,2-PDO is ca. 80–85% for both solids whereas the main product is acetol under helium (ca. 80%). In contrast, selectivity to acetol achieved with Pd-containing solids is higher at the expense of 1,2-PDO (18% acetol and 70% 1,2-PDO at 5% conversion, under H_2). Finally, this study was not possible with gold systems given their low activity.

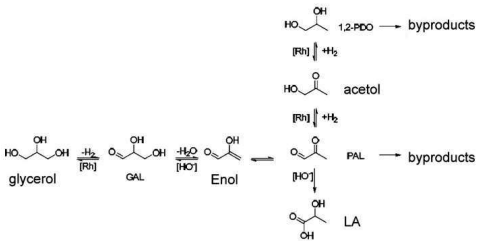

Fig. 9. Mechanism proposed by Auneau [34] for conversion of glycerol in lactic acid (LA) or 1,2-propanediol (1,2-PDO) considering dehydrogenation of glycerol as the initial step. GAL and PAL denote glyceraldehyde and pyruvaldehyde, respectively.

Some new synthetic procedures are currently being optimized in order to achieve a better control of the metal particle size with a view to perform a comparative study of metals with a range of particle sizes in glycerol hydrogenolysis.

4. Conclusions

Different reducible oxides (TiO_2, ZnO, SnO_2 and ZrO_2) were screened as support for platinum and tested for glycerol hydrogenolysis. The solids exhibiting the greatest metal–support interaction, eventually forming an alloy (ZnO and SnO_2) were the most active solids. Moreover, selectivity to 1,2-PDO was higher for ZnO what prompted us to select this solid as support for further studies.

Diverse ZnO-supported metals (Pt, Rh, Pd and Au) were then synthesized through the deposition–precipitation technique (5% by weight) and tested for catalytic transformation of glycerol under

hydrogen and helium atmosphere. Under similar reaction conditions, glycerol conversion followed the sequence Pt > Rh ≫ Pd ≫ Au. Furthermore, the solids reduced at 473 K were more active than those activated at 673 K. The increase in metal particle size and/or the formation of an alloy (as evidenced by TEM and XRD, respectively) could account for that. Results suggest that the strong metal–support interaction achieved at 473 K could be beneficial to the process though the eventual formation of the alloy at higher temperatures (673 K) should be avoided. The most active systems were Pt/ZnO-473 and Rh/ZnO-473 which exhibited a similar particle size (ca. 3–4 nm). Studies at iso-conversion conditions in neutral medium evidenced similar selectivities for Pt and Rh-containing solids whereas Pd systems yielded more acetol at the expense of 1,2-PDO. All in all, quite high yields to lactic acid were achieved in basic medium (68% for Rh/ZnO-473 under H_2 in basic medium) whereas yield to 1,2-PDO was more modest (26% for Rh/ZnO-673 under similar reaction conditions).

Acknowledgements

The authors are thankful to Spanish MICINN, MEC, Junta de Andalucia and FEDER funds (CTQ2008-01330, CTQ2010-18126, P08-FQM-3931 and P09-FQM-4781 projects) for financial support. F. Auneau is grateful to the French Government for a Doctorate grant. SCAI at the University of Cordoba is also acknowledged for ICP-MS measurements and the use of TEM and XPS. Finally, the authors are grateful to COST Action CM0903 for financial support, including a short-term scientific mission (STSM) of M. Checa. M. Checa also acknowledge the Spanish Ministery of Education for a FPU grant.

Appendix A. Supplementary data

Supplementary data associated with this article can be found, in the online version, at doi:10.1016/j.cattod.2012.02.036.

References

[1] A. Parvulescu, M. Rossi, C. Della Pina, R. Ciriminna, M. Pagliaro, Green Chem. 13 (2011) 143–148.
[2] J. Janaun, N. Ellis, J. Appl. Sci. 10 (2010) 2633–2637.
[3] M.H. Haider, N.F. Dummer, D. Zhang, P. Miedziak, T.E. Davies, S.H. Taylor, D.J. Willock, D.W. Knight, D. Chadwick, G.J. Hutchings, J. Catal. 286 (2012) 206–213.
[4] E.G. Rodrigues, M.F.R. Pereira, J.J. Delgado, X. Chen, J.J.M. Órfão, Catal. Commun. 16 (2011) 64–69.
[5] M. Balaraju, V. Rekha, P.S. Sai Prasad, B.L.A. Prabhavathi Devi, R.B.N. Prasad, N. Lingaiah, Appl. Catal. A 15 (2009) 82–87.
[6] J. Ten Dam, F. Kapteijn, K. Djanashvili, U. Hanefeld, Catal. Commun. 13 (2011) 1–5.
[7] Y. Nakagawa, Y. Shinmi, S. Koso, K. Tomishige, J. Catal. 272 (2010) 191–194.
[8] C. Montassier, J.C. Ménézo, L.C. Hoang, C. Renaud, J. Barbier, J. Mol. Catal. 70 (1991) 99–110.
[9] Z. Yuan, P. Wu, J. Gao, X. Lu, Z. Hou, X. Xheng, Catal. Lett. 130 (2009) 261–265.
[10] M.A. Abdel-Rahman, Y. Tashiro, K. Sonomoto, J. Biotechnol. 156 (2011) 286–301.
[11] K. Tomishige, Catal. Sci. Technol. 1 (2011) 179–190.
[12] T. Miyazawa, Y. Kusunoki, K. Kunimori, K. Tomishige, J. Catal. 240 (2006) 213–221.
[13] J. Chaminand, L. Djakovitch, P. Gallezot, P. Marion, C. Pinel, C. Rosier, Green Chem. 6 (2004) 359–361.
[14] F. Auneau, S. Noël, G. Aubert, M. Besson, L. Djakovitch, C. Pinel, Catal. Commun. 16 (2011) 144–149.
[15] M.C. Sanchez-Sanchez, R.M. Navarro, J.L.G. Fierro, Appl. Catal. B 106 (2011) 83–93.
[16] Q. Liu, X. Guo, Y. Li, W. Shen, Langmuir 25 (2009) 6425–6430.
[17] Y. Shinmi, S. Koso, T. Kubota, Y. Nakagawa, K. Tomishige, Appl. Catal. B 94 (2010) 318–326.
[18] A. Wawrzetz, B. Peng, A. Hrabar, A. Jentys, A.A. Lemonidou, J.A. Lercher, J. Catal. 269 (2010) 411–420.
[19] Y. Nakagawa, K. Tomishige, Catal. Sci. Technol. 1 (2011) 179–190.
[20] A. Iriondo, J.F. Cambra, V.L. Barrio, M.B. Guernez, P.L. Arias, M.C. Sanchez-Sanchez, R.M. Navarro, J.L.G. Fierro, Appl. Catal. B 106 (2011) 83–93.
[21] M.A. Aramendía, J.C. Colmenares, A. Marinas, J.M. Marinas, J.M. Moreno, J.A. Navío, F.J. Urbano, Catal. Today 128 (2007) 235–244.
[22] J. Hidalgo-Carrillo, M.A. Aramendía, A. Marinas, J.M. Marinas, F.J. Urbano, Appl. Catal. A 385 (2010) 190–200.
[23] S. Bernal, J.J. Calvino, M.A. Cauqui, J.M. Gatica, C. Lopez Cartes, J.A. Perez Omil, J.M. Pintado, Catal. Today 77 (2003) 385–406.
[24] M. Consonni, D. Jokic, D. Yu Murzin, R. Touroude, J. Catal. 188 (1999) 165–175.
[25] F. Ammari, J. Lamotte, R. Touroude, J. Catal. 221 (2004) 32–42.
[26] A. Katrib, C. Petit, P. Légaré, L. Hilaire, G. Maire, Surf. Sci. 189/190 (1987) 886–893.
[27] A.K Shukla, A.S Aricò, K.M El-Khatib, H. Kim, P.L. Antonucci, V. Antonucci, Appl. Surf. Sci. 137 (1999) 20–29.
[28] C.-P. Hwang, C.-T. Yeh, Q. Zhu, Catal. Today 51 (1999) 93–101.
[29] G. Munuera, A.R.González-Elipe, J.P. Espinos, A. Muñoz, J.C. Conesa, J. Soria, J. Sanz, Catal. Today 2 (1988) 663–673.
[30] G. Ketteler, D.F. Ogletree, H. Bluhm, H. Liu, E.L.D. Hebenstreit, M. Salmeron, J. Am. Chem. Soc. 127 (2005) 18269.
[31] O. Demoulin, M. Navez, P. Ruiz, Catal. Lett. 103 (2005) 149.
[32] K. Zakrzewska, Thin Solid Films 451–452 (2004) 93–97.
[33] J. Strunk, K. Kähler, X. Xia, M. Comotti, F. Schüth, T. Reinecke, M. Muhler, Appl. Catal. A 359 (2009) 121–128.
[34] F. Auneau, PhD, Université Claude Bernard Lyon I (France), 2011, p. 134.

Anexo II

Copia del artículo 2

.

Applied Catalysis A: General 507 (2015) 34–43

Contents lists available at ScienceDirect

Applied Catalysis A: General

journal homepage: www.elsevier.com/locate/apcata

Deactivation study of supported Pt catalyst on glycerol hydrogenolysis

Manuel Checa, Alberto Marinas, José M. Marinas, Francisco J. Urbano*

Department of Organic Chemistry, Campus de Excelencia Internacional CeiA3, University of Córdoba, Campus de Rabanales, Marie Curie Building (Annex), E-14014 Córdoba, Spain

ARTICLE INFO

Article history:
Received 4 June 2015
Received in revised form 7 September 2015
Accepted 21 September 2015
Available online 25 September 2015

Keywords:
Glycerol hydrogenolysis
Supported Pt catalysts
Support effect
1,2-Propanediol
Catalyst Deactivation
Catalysts fouling

ABSTRACT

Different Pt-based systems (5% by weight) were obtained through impregnation of chloroplatinic acid on Al_2O_3, CeO_2, La_2O_3 and ZnO. The solids were tested for glycerol hydrogenolysis. Results showed that metal sites are needed both for dehydration of glycerol and subsequent reduction to 1,2-propanediol (1,2-PDO). Moreover, as the reaction proceeds there is a progressive decrease in 1,2-PDO yield as a consequence of acetol oligomerization which already takes place at temperatures as low as 150 °C. Among all tested supports, ZnO was the one exhibiting better characteristics for glycerol selective transformation into 1,2-PDO as a result of the combination of the appropriate surface acidity, limited deactivation and stability under hydrothermal working conditions.

1. Introduction

Transportation fuels and chemicals have traditionally been produced from fossil sources. The increasing demand for these products together with the depletion of petroleum resources and environmental concern has led to the search for environmentally acceptable alternatives. Among them, only biomass can produce both energy and chemicals [1] and, therefore, the research on this field is continuously growing [2]. Some examples of the most relevant biomass-derived platform chemicals studied are furfural and its derivatives, succinic acid, sorbitol, lactic acid or glycerol [3–7]. The latter chemical has received much attention in recent years both from academia and industry due to its high functionalization, high reactivity, availability and low price [8]. In fact, glycerol is obtained as a by-product in biodiesel production by transesterification in large amount (10 kg of impure glycerol per 100 kg of produced biodiesel) [9,10]. Because of its high functionalization, glycerol can be transformed into a number of value-added products such as 1,2-propanediol (1,2-PDO), 1,3-propanediol (1,3-PDO), acrolein, olefins, etc., by a range of heterogeneously-catalyzed chemical processes that can compete with the classical petrochemical—route [11].

Regarding glycerol valorization, a great deal of reactions can be found in the literature, each one leading to different products as a function of the type of process or the proper reaction conditions [12]. One of the most interesting options is glycerol transformation under hydrogen pressure [2,7,13], consisting in glycerol reduction in such way that there is a dissociation of a C—OH chemical bond, the OH group being replaced by a H atom. The main products obtained in glycerol hydrogenolysis are 1-hydroxy-propan-2-one (ACETOL) [14], 1,2-PDO [15], 1,3-PDO [16] and ethylene glycol (EG), the latter involving a C–C cleavage [17]. However, depending on the used catalyst and reaction conditions, other products such as propan-1-ol and propan-2-ol can be obtained in high yields [18]. Selectivity of products can be tuned by using different metals [14], supports [19] or additives [16]. In particular, 1,2-PDO is the target of various investigations due to its interesting applications in pharmaceutical industry, costumer care products, antifreeze and tobacco industry, where it is used as humectant [13]. In the case of ACETOL, it is easy to find it as starting point in routes to produce polyols or acrolein [14]. Several transition metals have been described as catalysts in glycerol hydrogenolysis, the most common being Cu [20], Co [21] and Ni [22] and some noble metals such as Ru [23], Ir [24], Pd [14], Rh [25] or Pt [16,23]. Among them, Pt has been found to produce propylene glycol through glycerol hydrogenolysis, avoiding the C–C cleavage [26].

Platinum-catalyzed glycerol conversion into 1,2 or 1,3-propanediol on acid-base catalysts has been described to occur via glycerol dehydration followed by its hydrogenation to propanediols (Scheme 1). Depending on the hydroxyl group involved in glycerol dehydration (either primary or secondary), 1,2-PDO or 1,3-PDO can be obtained, respectively [14]. Platinum has been supported on a great variety of solids including both acid and basic ones and thus glycerol hydrogenolysis has been studied over Pt sup-

* Corresponding author. Fax: +34 957212066.
E-mail address: fj.urbano@uco.es (sc1 F.J. Urbano).

http://dx.doi.org/10.1016/j.apcata.2015.09.028
0926-860X/

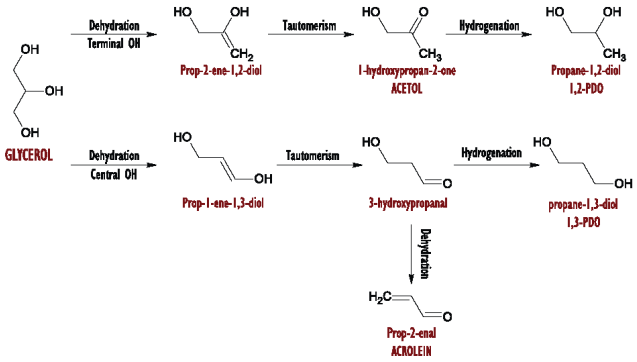

Scheme 1. Reaction network for the hydrogenolysis of glycerol aqueous solutions over supported metal catalysts.

ported on alumina [16], carbon [27], other transition metal oxides [15,28], zeolites [29], etc. In these studies, the role of both metal and surface acid sites in product selectivity has been pointed out as crucial for glycerol transformation into 1,2-PDO [30]. In a recent work, we reported that metal sites could participate not only in hydrogenation of ACETOL to 1,2-PDO but also in the previous dehydration step of glycerol to ACETOL [14]. Additional work on this subject is needed to clarify the synergies between metal and acid sites.

An additional point to take into account is catalyst deactivation which has been reported in both gas- and liquid-phase catalyzed glycerol transformation processes. There are some studies dealing with catalysts deactivation in the gas-phase glycerol dehydration to acrolein [31–33] or in the gas-phase glycerol reforming process [33,34]. Regarding the liquid-phase glycerol hydrogenolysis, there are some reports on the deactivation of supported copper or ruthenium [35–41]. In these cases, deactivation is associated to carbon deposition and metal particle aggregation. However, to the best of our knowledge, there are no in depth studies dealing with catalysts deactivation in the liquid-phase glycerol hydrogenolysis over supported Pt catalysts.

This work is aimed at studying the support effects in Pt-based catalysts used in the liquid-phase glycerol hydrogenolysis, looking for synergies between metal and acid sites. Moreover, a detailed study of the spent catalysts could give some valuable information on the role of such acid sites in the catalytic process and in deactivation of supported Pt catalysts.

2. Experimental

2.1. Synthesis of the catalysts

Aluminium oxide activated acid (Al_2O_3–AC Sigma–Aldrich ref. 199966), aluminium oxide activated basic (Al_2O_3–BA Sigma–Aldrich ref. 199443), cerium oxide (CeO_2, Sigma–Aldrich ref. 544841), lanthanum oxide (La_2O_3, Sigma–Aldrich ref. 634271) and zinc oxide (ZnO, Sigma–Aldrich ref. 544906) were selected as supports for the synthesis of supported Pt catalysts. All supports were calcined at 400 °C for 6 h in air flow (30 mL min^{-1}) before use.

Platinum was incorporated onto the support by incipient wetness impregnation with chloroplatinic acid (8% w/w, Sigma–Aldrich ref. 262587). The synthesis was designed to achieve a Pt loading of 5% (w/w). The procedure consisted in introducing 4.75 g of support in a 50 mL round bottom flask and 6.4 mL of chloroplatinic acid were subsequently added. In some cases, 2–3 mL of water were added in order to completely fill the porous system of the support. Then the mixture was rotated (150 rpm) at room temperature for 1 h and then evacuated under controlled temperature until dryness (1 h at 30 °C, 1 h at 50 °C and 80 °C until dryness). The flask was removed and placed in an oven at 110 °C overnight. After that, the catalyst was calcined at 400 °C for 6 h, in synthetic air flow (30 mL min^{-1}). Finally, the calcined material was crushed and sieved (0.149 mm) in order to prevent diffusional problems. The catalysts were reduced in H_2 flow (30 mL min^{-1}) at 200 or 400 °C for 2 h (heating rate 10 °C min^{-1}) in order to activate them for the reaction. Once reduced, the solid was cooled down in H_2 to room temperature and then purged for 15 min with N_2 (30 mL min^{-1}).

Solid nomenclature includes a suffix indicating the reduction temperature. Therefore, for instance, CeO_2 denotes the ceria support whereas Pt/CeO_2-400 refers to the ceria supported platinum system reduced at 400 °C.

2.2. Characterization of the catalysts

2.2.1. ICP-MS analysis

Elemental analysis of Pt-containing samples was carried out by the staff at the Central Service for Research Support (SCAI) of the University of Córdoba. It was performed by inductively coupled plasma mass spectrometry (ICP-MS). Measurements were made on a Perkin–Elmer ELAN DRC-e instrument following dissolution of the sample. Due to the different chemical properties of the supports, different recipes were needed.

Alumina-based catalysts were dissolved in a two-step process: 100 mg were treated with 25 mL of HF for 10 min at mild temperature and then 15 mL of HCl were added in order to complete the digestion of Pt particles. In the case of ZnO and La_2O_3 based catalyst, the treatment with 20 mL of the HCl:HNO_3 (3:1) mixture was enough to obtain a homogeneous solution. In order to dissolve CeO_2 supported Pt catalysts, (i) 25 mL of the H_2O_2:HNO_3 (4:1) oxidant mixture were carefully added and then (ii) 15 mL of HCl were incorporated at 50 °C and the mixture stirred until complete dissolution of the sample.

All solutions were diluted to 100 mL with 3% HNO_3 before analysis. Calibration plots were performed using Perkin Elmer Pure Plus atomic spectroscopy standards.

2.2.2. XRD analysis

XRD of all catalyst were performed on a Siemens D-5000 X-Ray diffractometer, using a cobalt source, CoKα, and a graphite monochromator. The voltage and current intensity used were 20 kV and 25 mA, respectively. Scans were performed at 0.05° 2θ intervals over the 2θ range from 5 to 75°.

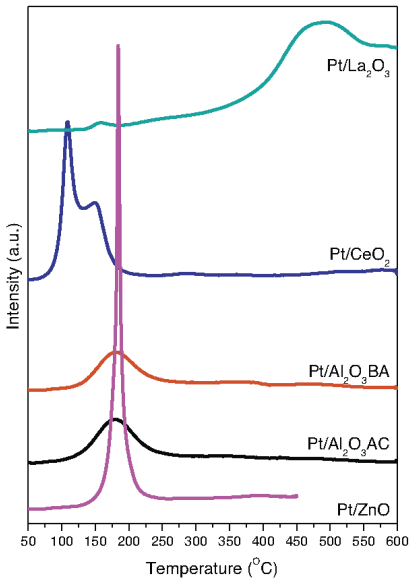

Fig. 1. Temperature-programmed reduction (TPR) profiles obtained for the supported Pt catalysts synthesized in this work.

2.2.3. TEM and SEM–EDX analysis

Transmission electron microscopy (TEM) images were obtained using a JEOL JEM 1400 microscope at the Central Service for Research Support (SCAI) of the University of Córdoba. All samples were mounted on 3 mm holey carbon copper grids.

SEM–EDX measurements were performed on a JEOL JSM-6300 scanning electron microscope (SEM) equipped with an energy-dispersive X-ray (EDX) detector. It was operated at an acceleration voltage of 20 keV with a resolution of 65 eV.

2.2.4. XPS analysis

X-ray photoelectron spectroscopy (XPS) analysis was carried out at the Central Service for Research Support (SCAI) of the University of Córdoba. XPS data were recorded on 4 mm × 4 mm pellets 0.5 mm thick that were obtained by gently pressing the powdered materials following outgassing to a pressure below about 2×10^{-8} Torr at 150 °C in the instrument prechamber to remove chemisorbed volatile species. The main chamber of the Leibold–Heraeus LHS10 spectrometer used, capable of operating down to less than 2×10^{-9} Torr, was equipped with an EA-200MCD hemispherical electron analyser with a dual X-ray source using AlKα (hv = 1486.6 eV) at 120 W, at 30 mA, with C(1 s) as reference energy (284.6 eV).

2.2.5. BET surface area

Surface areas of the solids were determined from nitrogen adsorption–desorption isotherms obtained at liquid nitrogen temperature on a Micromeritics ASAP-2010 instrument, using the Brunnauer–Emmett–Teller (BET) method. All samples were degassed to 0.1 Pa at 120 °C prior to measurement.

2.2.6. Temperature-programmed reduction (TPR)

Temperature-programmed reduction (TPR) measurements were performed on a Micromeritics Autochem II chemisorption analyser. An amount of 200 mg of catalyst was placed in the sample holder and reduced in a 10% H_2/Ar stream flowing at 40 mL min^{-1}. The temperature was ramped from 50 to 600 °C at 10 °C min^{-1} (50–450 °C in the case of Pt/ZnO).

2.2.7. Surface acid properties of the catalysts

Surface acidity of the catalysts were determined by temperature-programmed desorption of pyridine in a PID Eng&Tech instrument furnished with a TCD detector. The sample (50 mg) was placed in a quartz U tube, connected to a He flow (10 mL min^{-1}), introduced in an oven, and ramped up to its calcination temperature (at a rate of 10 °C min^{-1}) in order to remove chemisorbed species. After a cooling down process, the clean sample was treated with a pyridine saturated helium stream at room temperature for 30 min. Physisorbed pyridine was removed by flowing the sample with pure helium at 50 °C for additional 30 min. The pyridine desorption step starts heating the sample, in He flow, from 50 °C up to 400 °C at 10 °C min^{-1}.

2.2.8. TG–DTA of spent catalysts

The catalysts were subjected to thermogravimetric and differential thermal analysis on a Setaram SetSys 12 instrument. An amount of 20 mg of sample was placed in an alumina crucible for TGA–DTA analysis and heated at temperatures from 30 to 600 °C at a rate of 10 °C/min under a stream of synthetic air at 40 mL/min in order to measure weight loss, heat flow and derivative weight loss.

2.3. Reactivity tests

Supported Pt catalysts were tested in the liquid-phase glycerol hydrogenolysis in a Berghof HR-100 high pressure reactor. The 75 mL PTFE lined reaction vessel was loaded with 20 mL of an aqueous solution 1.36 M in glycerol (99%, Sigma–Aldrich, ref. G7757) or Acetol (90%, Sigma–Aldrich, ref. 13185) and 200 mg of freshly activated catalyst. Then, the reactor was closed and purged with H_2 for 1 min and then pressurized with hydrogen to 6 or 10 bar. At this moment, the temperature was set at 180 °C and waited for 1 h for stabilization. The reaction started by switching on the stirring at 1000 rpm for 15 h. Blank experiments were carried out without Pt catalyst and with bare supports. The reaction was stopped by cooling down the reactor in an ice bath. Then, the reactor was depressurized, the reaction mixture homogenized by adding water (1:1 ratio), centrifuged and filtered through a PTFE syringe filter (0.45 μm). Finally, the liquid phase was analyzed by GC–TCD (Agilent 7890) equipped with a 30 m Nukol capillary column (Supelco, ref. 25357). Quantification was based on the corresponding calibration plots obtained for reagents and products.

3. Results and discussion

3.1. Characterization of the solids

Supports and supported Pt catalysts were thoroughly characterized by a number of techniques, Table 1 presenting the main features.

Solids used as supports in this work present different surface areas ranging from 174 and 163 m^2/g for alumina based supports (activated acid and basic, respectively) to 18 and 14 m^2/g for ZnO and La_2O_3, CeO_2 presenting an intermediate surface area (60 m^2/g). Platinum was incorporated to the supports in a nominal loading of 5%. Chemical analysis of Pt catalysts by ICP-MS, SEM and XPS is given in Table 1. According to ICP-MS, Pt incorporation to the support was close to nominal value, ranging from 3.9% for Pt/La_2O_3 and

Table 1
Some features concerning characterization of the different supported Pt systems. BET surface area, surface acidity, Pt metal loading and Pt particle size of the catalysts used in this work.

Catalyst	S_{BET} m²/g	Pore diameter (A)	Acidity μmol PY/g	Acidity μmol PY/m²	%Pt (w/w)			Pt particle size TEM (nm)
					ICP-MS	SEM	XPS	
Al_2O_3-AC	174	4.1	110	0.6	–	–	–	–
Pt/Al_2O_3AC-200	158	5.1	120	0.8	3.9	6.8	4.7	2.3
Pt/Al_2O_3AC-400	163	5.0	136	0.8	3.9	6.5	5.2	2.6
Al_2O_3BA	163	4.5	87	0.5	–	–	–	–
Pt/Al_2O_3BA-200	151	5.2	128	0.8	4.6	5.7	5.4	1.7
Pt/Al_2O_3BA-400	153	5.6	91	0.6	4.6	6.9	5.0	1.9
CeO_2	60	7.9	59	1	–	–	–	–
Pt/CeO_2-200	46	9.0	43	0.9	4.2	4.3	4.7	2.7
Pt/CeO_2-400	49	8.1	42	0.9	4.2	4.1	6.4	2.8
La_2O_3	14	21.0	10	0.7	–	–	–	–
Pt/La_2O_3-200	12	45.6	70	5.8	3.9	2.5	2.6	n.d.
Pt/La_2O_3-400	12	30.8	10	0.9	3.9	2.4	2.4	2.3
ZnO	18	28.2	3	0.1	–	–	–	–
Pt/ZnO-200	10	41.3	32	3.2	6.1	3.4	5.7	2.1
Pt/ZnO-400	10	41.7	20	2	6.1	3.6	6.6	4.5

Pt/Al_2O_3–AC to 6.1% for Pt/ZnO. SEM–EDX and XPS normally give higher values probably due to a surface concentration of Pt species and/or to heterogeneous distribution of Pt particles. Regarding Pt particle size, it has been determined by TEM microscopy, the exception being the Pt/La_2O_3-200 catalyst for which TEM images gave too low contrast to reliable measuring Pt particle size.

3.1.1. Surface acid properties of the catalysts

The surface acid properties of supports and Pt catalysts were determined by temperature-programmed desorption of pyridine and the results are collected in Table 1.

Results indicate that the most acidic support used is Al_2O_3–AC followed by Al_2O_3–BA, CeO_2 and finally La_2O_3 and ZnO which are the least acidic supports. Incorporation of Pt to the supports has a diverging effect on the final catalysts acidity, also depending on the reduction temperature. Thus the incorporation of Pt on both acidic and basic Al_2O_3 increased moderately the acidity of the final catalyst, especially for the acidic one. On the other hand, incorporation of Pt to the ZnO support (which is the least acidic one) induced in the final catalyst an increase in acidity by a factor of 10. There was also an increase in acidity for the La_2O_3 support upon incorporation of Pt but only after reduction at 200 °C. Finally, ceria-based catalysts did not increase their acidity on Pt incorporation. The increase in the acidity observed for the catalysts after the incorporation of Pt from H_2PtCl_6 precursor could be related to the presence of chlorine atoms at the surroundings of the Pt particles [14–15].

3.1.2. X-ray diffraction analysis

XRD patterns corresponding to supports and catalysts used in this work are given as supplementary material (Fig. S1).

As for the supports, both basic and acidic alumina were amorphous as evidenced by the absence of diffraction peaks in their patterns, while cerium and zinc oxides show diffraction profiles corresponding to cerianite (PDF 34-0394) and zincite (PDF 36-1451) structures, respectively. As far as lanthanum oxide is concerned, the support calcined at 400 °C presented a diffraction profile corresponding mainly to both monoclinic and hexagonal lanthanum oxide carbonate (PDF 23-0320 and 37-0804) [42]. After the incorporation of Pt from H_2PtCl_6, in addition to lanthanum oxide carbonate, lanthanum oxychloride was formed and detected in the Pt/La_2O_3 XRD pattern (LaOCl, PDF 08-0477). Since thermal treatment can affect the carbonated phases [43], a sample of the Pt/La_2O_3 catalyst was calcined in air at 600 °C for 12 h and, as result, part of the carbonated phases decomposed into La_2O_3 although most of the $La_2O_2CO_3$ remained in the calcined solid. Therefore it is expected that Pt/La_2O_3 catalysts is stable under thermal treatment at reaction temperatures.

Furthermore, Pt is observed in the diffractograms as a wide and low intensity diffraction peak indicating high dispersion of small Pt metal particles [44]. Moreover, in the case of Pt/ZnO catalyst, the shape and position of the Pt diffraction peaks change depending on the reduction temperature as a consequence of sintering and alloying of Pt with Zn [45,46]. Thus, the Pt/ZnO-400 catalyst clearly presents a PtZn alloy band displaced to higher 2θ values as compared to Pt metal signal.

3.1.3. Temperature-programmed reduction (TPR)

The as-synthesized (calcined) supported Pt catalysts were analyzed by temperature-programmed reduction in order to collect some information on the reducibility of the catalytic systems. The obtained TPR profiles, presented in Fig. 1, indicate that all catalysts only show low temperature reduction peaks (below 225 °C), the exception being Pt/La_2O_3 that, in addition to a small reduction peak centered at 160 °C, exhibits a high-temperature peak (325–600 °C). However, the integrated area of this peak is too large to be associated to reduction of Pt species. As commented above, XRD profiles for the Pt/La_2O_3 indicate the presence of lanthanum oxycarbonate that partially decomposes at temperatures around 600 °C and therefore such a peak in the TPR profile of Pt/La_2O_3 could be assigned to the partial decomposition of lanthanum oxycarbonate (the TPR detection is based on TCD and thus it is not very selective).

The low temperature reduction peaks are usually associated to Pt^{2+} or Pt^{4+} reduction to metallic Pt [45,47]. Thus, in Pt/CeO_2, there are two different reduction peaks possibly indicating two Pt species interactions with the support. Pt/ZnO shows a narrow and intense reduction peak centered at 185 °C probably indicating a monomodal particle size distribution of Pt metal particles. Finally, both alumina supported Pt catalysts present a wide reduction peak centered at 180 °C.

Considering TPR profiles, the chosen catalyst reduction temperatures were 200 (low-temperature reduction, LTR) or 400 °C (high-temperature reduction, HTR), both ensuring the complete reduction of the Pt species on the catalysts.

3.2. Glycerol hydrogenolysis

3.2.1. First screening of catalysts

In order to evaluate the influence of the support on the catalytic activity, a first screening of the supported Pt catalysts was carried out. As stated above, catalysts were previously reduced at

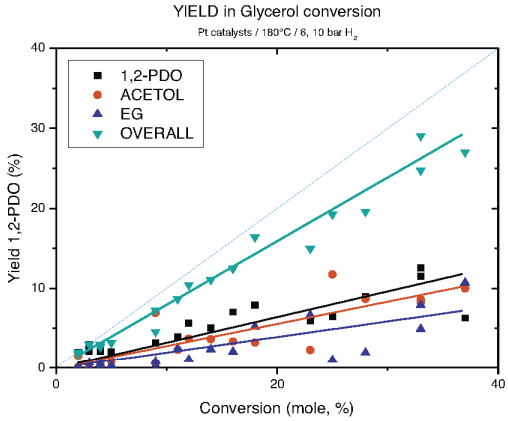

Fig. 2. Yield-conversion relationship obtained for the supported catalysts tested in glycerol hydrogenolysis. Reaction conditions: 1.36 M glycerol in water at a reaction temperature of 180 °C, an initial hydrogen pressure of 6 or 10 bars and 15 h of reaction. Overall refers to the sum of the yield to 1,2-PDO, acetol and ethyleneglycol.

200 °C (LTR) or 400 °C (HTR), and the reaction conditions used were an initial hydrogen pressure of either 6 or 10 bars, an initial glycerol concentration of 1.36 M and a reaction temperature of 180 °C. The main reaction products detected were 1,2-propanediol (1,2-PDO), 1-hydroxypropan-2-one (ACETOL) and ethylene glycol (EG) in addition to some traces of n-propanol and ethanol. According to the literature, acetol is obtained by dehydration of the primary hydroxyl group of glycerol whereas its subsequent hydrogenation leads to 1,2-PDO [14].

Blank reactions corresponding to glycerol hydrogenolysis without catalyst and with bare supports were carried out and, in all cases, no reaction products were detected after 15 h of reaction. Therefore, this seems to suggest that both acid and metal sites are needed to promote glycerol dehydration to acetol [14,30].

The results obtained for the supported Pt catalysts, in terms of glycerol conversion, products selectivity and yield to 1,2-PDO for t = 15 h, are presented in Table 2. As can be observed in this Table, high hydrogen pressure (10 bars) led to lower glycerol conversions but higher 1,2-PDO selectivities, the exception being Pt/CeO_2-400 and Pt/La_2O_3-400 that exhibited high selectivities to acetol to the detriment of 1,2-PDO. Briefly, at 6 bar the selectivity to 1,2-PDO is in the 17–44% range (11–37% conv.) in contrast to the reactions at 10 bar for which the 1,2-PDO selectivity is the 35–98% range (2–12% conv.). Overall, 1,2-PDO yield is better for the experiments carried out at 6 bars (Table 2).

Moreover, no clear pattern or trend is observed when analyzing the effect of the catalyst reduction temperature on catalytic activity. This effect, if any, could be due to many different factors such as a possible increase in metal particle size at HRT, the appearance of strong metal-support interactions or some kind of alloying between Pt and the reduced supports.

However, when 1,2-PDO yield is plotted against conversion (Fig. 2) it is observed that as the reaction proceeds there is a progressive loss in 1,2-PDO yield probably due to the formation of polymeric species that could not be detected by GC. Gas phase was analyzed by GC–FID, accounting for 1–2% of the reaction products. CO_2 was identified as the main gaseous product in all cases but for CeO_2 catalyst, in which case C_2 hydrocarbons were the main gaseous compounds. Therefore, the mass balance (considering liquid and gas phase) is not closed and the gap is increasing as the glycerol conversion does.

For the reactions at 6 bar (Table 2), the best performing catalysts in terms of 1,2-PDO yield are Pt/La_2O_3-400 and Pt/CeO_2-200 (13 and 12% yield, respectively). Moreover, Pt/CeO_2-400 presents the highest glycerol conversion (37%) but associated to a rather low selectivity to 1,2-PDO (17%), thus leading to a 1,2-PDO yield of 6%. On the other hand, Pt/ZnO catalyst presents an intermediate yield to 1,2-PDO (9% and 7% yield for the catalyst reduced at 200 and 400 °C, respectively). Finally, in general, Al_2O_3 based catalysts are the solids yielding less 1,2-propanediol (1,2-PDO yield in the 4–7% range). According to the above presented yields to 1,2-PDO, a general sequence of catalytic activity can be stated:

$$Pt/La_2O_3 > Pt/CeO_2 > Pt/ZnO > Pt/Al_2O_3\text{–}BA \approx Pt/Al_2O_3\text{–}AC$$

Therefore, Pt/La_2O_3-400, Pt/CeO_2-400 and Pt/ZnO-400 were selected in order to perform new experiments to gain some additional information on the reaction mechanism and the deactivation process.

3.2.2. Acetol hydrogenation

As commented above, production of 1,2-PDO is known to occur through hydrogenation of acetol which, in turn, is obtained via dehydration of a primary hydroxyl group of glycerol (Scheme 1) [14]. Our results indicate that calcined supports showed no activity in glycerol dehydration in spite of their acidic properties (Table 1) and, therefore, both acid and metal functions are needed to accomplish the dehydration of glycerol to acetol. Moreover, it has been reported that dehydration of glycerol to acetol is slower than hydrogenation of acetol to 1,2-PDO [48]. Therefore, in order to get some additional information on the role of both support and Pt metal particles, acetol hydrogenation experiments were carried out, the results being presented in Table 3.

Calcined supports easily transform acetol, at a reaction temperature of 180 °C, with conversion in the 67–80% range after 5 h of

Table 2
Glycerol conversion, selectivity to products and 1,2-PDO yield obtained in glycerol hydrogenolysis over supported Pt catalysts. Reaction conditions: 1.36 M glycerol in water at a reaction temperature of 180 °C, an initial hydrogen pressure of 6 or 10 bars and 15 h of reaction time.

Catalyst	Pressure (bar)	Conversion (mole, %)	Product selectivity (%)				Yield (1,2-PDO, %)
			1,2-PDO	ACETOL	EG	Others	
Pt/Al_2O_3-AC-200	6 bar	14	36	26	17	21	5
Pt/Al_2O_3-AC-400	6 bar	23	26	10	29	35	6
Pt/Al_2O_3-BA-200	6 bar	16	44	21	13	22	7
Pt/Al_2O_3-BA-400	6 bar	11	36	21	22	21	4
Pt/CeO_2-200	6 bar	33	35	25	15	25	12
Pt/CeO_2-400	6 bar	37	17	27	29	27	6
Pt/La_2O_3-200	6 bar	18	44	18	29	9	8
Pt/La_2O_3-400	6 bar	33	38	32	30	15	13
Pt/ZnO-200	6 bar	28	32	31	7	30	9
Pt/ZnO-400	6 bar	25	26	47	4	23	7
Pt/Al_2O_3-AC-200	10 bar	5	41	17	6	36	2
Pt/Al_2O_3-AC-400	10 bar	9	35	7	9	49	3
Pt/Al_2O_3-BA-200	10 bar	3	72	5	23	0	2
Pt/Al_2O_3-BA-400	10 bar	4	60	3	11	26	2
Pt/CeO_2-200	10 bar	12	47	31	9	13	6
Pt/CeO_2-400	10 bar	2	4	78	8	10	0
Pt/La_2O_3-200	10 bar	4	54	11	2	33	2
Pt/La_2O_3-400	10 bar	9	4	77	0	19	0
Pt/ZnO-200	10 bar	3	98	2	0	0	3
Pt/ZnO-400	10 bar	2	98	2	0	0	2

Table 3
Acetol conversion and selectivity to products in the liquid-phase acetol transformation on bare supports and supported Pt catalysts. Reaction conditions: 1.36 M acetol in water, reaction temperature of 150 or 180 °C, an initial hydrogen pressure of 6 bar and 5 or 15 h of reaction time.

Support Catalyst	Reaction time (h)	Reaction temperature (°C)	Acetol conversion (%)	S_{GLY}	$S_{1,2\text{-PDO}}$	S_{EG}	Mass balance(%)
CeO_2-400	5	180	67	15	1	0	16
La_2O_3-400	5	180	68	12	1	1	14
ZnO-400	5	180	80	11	1	0	13
CeO_2-400	15	180	95	10	2	0	12
La_2O_3-400	15	180	90	10	10	1	21
ZnO-400	15	180	83	11	2	0	13
Pt/CeO_2-400	5	180	58	16	84	0	100
Pt/La_2O_3-400	5	180	62	17	71	0	88
Pt/ZnO-400	5	180	75	8	64	0	72
Pt/CeO_2-400	15	180	96	11	4	0	15
Pt/La_2O_3-400	15	180	98	12	8	3	23
Pt/ZnO-400	15	180	92	18	59	2	79
Pt/CeO_2-400	15	150	87	8	13	1	22
Pt/La_2O_3-400	15	150	81	7	10	1	18
Pt/ZnO-400	15	150	70	9	66	0	75

reaction and 83–95% for 15 h reactions. As for the reactions products, glycerol is obtained with a ca. 10% selectivity, indicating that bare supports are capable of partly perform acetol re-hydration to glycerol. This is hardly surprising considering that both species are in equilibrium and in a water medium. On the other hand, 1,2-PDO and EG selectivities are normally under 2% and 1%, respectively. Therefore, acetol is converted into other products that were not identified in this work but that could be observed as many, small chromatographic peaks or as water insoluble polymeric species appearing deposited on the catalysts surface and reaction vessel. These sub-products account for 79–88% of converted acetol (Table 3). This is consistent with results found in the literature, where it is described that acidic solids deactivated in the gas-phase acetol transformation as a consequence of oligomerization processes leading to furan derivatives or even to phenolic compounds [31]. In our case, GC–MS studies evidenced the formation of several water insoluble C4–C9 liquid oxygenates, as ethers or esters, that could account for the low mass balance observed in these reactions.

As far as the Pt supported catalysts are concerned, acetol conversion at 5 h of reaction are in the 58–75% range, increasing up to 92–98% for $t = 15$ h. Among reaction products, glycerol is also obtained at similar levels than those obtained for bare supports. Thus glycerol selectivity obtained for supported Pt catalysts is in the 8–17% range at 5 h of reaction and maintaining this selectivity level after 15 h in the 11–18% range. However, the most interesting distinctive behavior between bare supports and supported Pt catalysts is in the 1,2-PDO selectivity. Thus, Pt catalysts exhibited 64–84% selectivity to 1,2-PDO for $t = 5$ h, in contrast to the ca. 1% selectivity obtained for calcined supports. It is reasonable to conclude that acetol hydrogenation needs a metal function to proceed [8]. After 15 h of reaction, Pt/ZnO-400 affords a 1,2-PDO selectivity level of about 59% while Pt/La_2O_3-400 and Pt/CeO_2-400 exhibit 1,2-PDO selectivities of 8 and 4%, respectively. Probably, the C4–C9 oligomeric compounds formed at longer reaction time from acetol condensations on the support acid sites finally deposited on the metallic active sites deactivating them for acetol hydrogenation to 1,2-PDO. Alternatively, it could be argued that, when close to 100% acetol conversion (92–98%), catalysts convert the formed 1,2-propanediol into additional reaction products, thus lowering the 1,2-PDO yield. However, experiments carried out with 1,2-propanediol as starting substrate revealed that neither bare supports nor supported Pt catalysts were able to convert it under the reaction conditions (180 °C, 6 bar, 15 h).

The role of the support on the oligomerization processes is also confirmed by the low mass balance obtained for the bare supports (13-16%, 5 h) in contrast to the mass balance for the supported Pt catalysts for the same reaction time: 100, 88 and 72% for Pt/CeO_2-400, Pt/La_2O_3-400 and Pt/ZnO-400 respectively.

For longer reaction time, the mass balance significantly decreases for Pt/La_2O_3-400 (23%, 15 h) and Pt/CeO_2-400 (15%, 15 h) catalysts whereas Pt/ZnO-400 maintains a higher mass balance level (79%, 15 h). These results point out that ZnO behaves better than La_2O_3 or CeO_2 as supports for supported Pt catalysts since it is able to keep the acetol oligomerization under control. It is interesting to note here that bare ZnO presented very low surface acidity and that Pt incorporation generated new acid sites probably located around Pt metallic particles. Therefore, this metal-acid bifunctional sites are responsible for glycerol dehydration to acetol and its subsequent hydrogenation to 1,2-PDO, thus enhancing 1,2-PDO selectivity versus other by products.

Finally, in an attempt to reduce the extent of acetol oligomerization reactions, some experiments consisting in acetol hydrogenation were carried out at 150 °C and 15 h of reaction for supported Pt catalysts (Table 3). As expected, lower conversion levels were obtained at 150 °C as compared to 180 °C. Moreover, a slight increment in selectivity to 1,2-PDO was observed for Pt/ZnO-400 (66%) a system which also kept low oligomerization activity (mass balance, 75%) while both Pt/La_2O_3-400 and Pt/CeO_2-400 solids presented low 1,2-PDO selectivities (10–13%) and poor mass balances (18–22%). Therefore, it has to be concluded that oligomerization also takes place significantly at low temperature and that the reaction time is essential to determine the extent of this process.

Taking the above presented discussion into account, it seems to be clear that, both metal and acidic functions are needed to dehydrate glycerol to acetol and further hydrogenate acetol to 1,2-propanediol, that behaves as stable secondary product in our reaction conditions (no further transformation was observed). Moreover, the support acidity that is not associated to Pt metal sites is detrimental to this process since acetol oligomerization takes place on these acid sites leading to catalysts deactivation. Some additional information could be obtained from characterization of the catalysts used in glycerol hydrogenolysis.

3.2.3. Characterization of spent catalysts

In order to collect some additional information on the reaction mechanism and to justify changes in 1,2-PDO selectivity with reaction time, Pt catalysts were recovered from the reaction mixture after 15 h of reaction by filtration, washed with 3 portions of water (25 mL each) and dried overnight at 110 °C in an oven, before characterization. Used Pt catalysts were analyzed by determining their BET surface area and performing XPS, TGA, TEM and XRD analysis. The results obtained are presented in Table 4, Figs. 3 and 4 and in Suplementary Figs. S2 and S3.

From Table 4, it is clear that Pt/CeO_2-400 and Pt/La_2O_3-400 used catalysts exhibit a small loss of surface area (around 25% loss) after 15 h of reaction, suggesting that there is some degradation of the porous structure of CeO_2 and La_2O_3 supports due to the hydrothermal reaction conditions. Alternatively, there could have been some pore blocking by adsorbed species. On the contrary, Pt/ZnO-400 used catalyst does not lose any surface area suggesting that ZnO support is rather stable at such reaction conditions. Additionally, ICP-MS analyses were carried out for the liquid-phase resulting after 15 h of reaction. The results obtained indicate that the amount of Pt in the liquid phase is below 0.01% pointing to a good stability of Pt metal particles in the reaction conditions. On the contrary, as far as the supports are concerned, the percentages of lixiviated support are 7.8% (ZnO), 28.4% (La2O3) and 29.5% (CeO2).

Pt particle size of the spent catalysts as determined by TEM (Supplementary material, Fig. S2) showed an increase as compared to fresh catalysts. This increase is larger for Pt/La_2O_3-400 (from 2.3 to 9.7 nm for fresh and used catalyst, respectively) and Pt/ZnO-400 (from 4.5 to 11.0 nm). For Pt/CeO_2-400, the change is somehow smaller, just increasing Pt particle size from 2.8 to 3.6 nm for fresh and used catalysts, respectively.

XRD pattern for the used Pt/CeO_2-400 catalyst presented in Fig. 3 shows, in addition to cerium oxide (ICDD PDF 34-0394), new diffraction peaks corresponding to cerium carbonate hydroxide (ICDD PDF 32-0189) as a consequence of the partial degradation of CeO_2 under hydrothermal reaction conditions. Moreover, in agreement with TEM results, an increase in the intensity of the Pt^0 diffraction peak is observed associated to an increase in Pt particle size. Similarly, the XRD pattern for the spent Pt/La_2O_3-400 catalyst also presents new diffraction peaks associated to lanthanum carbonate hydroxide (ICDD PDF 26-0815) and, with lower intensity, lanthanum hydroxide (ICDD PDF 36-1481) formed under hydrothermal reaction conditions (Fig. 3). As far as Pt diffraction signals are concerned, small diffraction peaks appear below $2\theta = 46°$ that could be associated to LaPt alloy (ICDD PDF 17-0364 or 19-0657) formed under reductive and hydrothermal reaction conditions. Finally, for the Pt/ZnO-400 used catalyst, no change in the ZnO support is observed by XRD under reaction conditions, indicating a stable support. However, as far as platinum is concerned, Pt^0 signal almost disappears and a very intense signal associated to PtZn alloy is clearly observed (ICDD PDF 04-0802) in the XRD profile. Recently, Oberhauser et al. described the effect of carbonaceous supports on Pt sintering on the structure-sensitive glycerol hydrogenolysis, so we assume that the structural changes observed, both in support as in Pt particle size, have an important role in catalyst deactivation [49]. To sum up, CeO_2 and specially La_2O_3 are unstable at the reaction conditions, while ZnO is quite stable and, in addition, metallic function also changes during reaction, since an increase in Pt metal particle and/or alloying is observed in the spent catalysts. This Pt:Zn alloy provide a new catalyst surface with different properties and, according to Penner et al., the formation of an intermetallic compound can stabilise the metal particle in terms of morphology and crystallography [50].

TGA–DTA experiments performed for the used Pt catalysts revealed different behaviors for the three systems (Fig. 4). Overall mass losses obtained for the spent catalysts were 12%, 22% and 30% for Pt/CeO_2-400, Pt/La_2O_3-400 and Pt/ZnO-400, respectively. However, most of the mass lost by Pt/ZnO-400 catalyst (Fig. 4c) takes place at temperatures below 110 °C indicating that it corresponds to water or volatile species weakly adsorbed on the catalyst surface (endothermic process). For this catalyst there is only a very small exothermic combustion peak centered at around 525 °C associated to some graphitized carbonaceous residues. On the contrary, used Pt/CeO_2-400 (Fig. 4a) presents three exothermic processes associated to combustion of poorly graphitized organic deposits (main mass loss, centered at 275 °C) and two additional small exothermic peaks appearing at 450–475 °C and associated to the combustion of more graphitized carbonaceous deposits. Finally, spent Pt/La_2O_3-400 (overall mass lost ca. 22%) exhibits a continuous mass loss in the 400–525 °C range that could be associated to combustion of carbonaceous deposits (exothermic signal) and probably to the partial decomposition of lanthanum oxide carbonate formed under reaction conditions (endothermic signal observed at temperatures above 500 °C).

These results clearly correlates with the reactivity results for the catalysts tested in glycerol and acetol transformations. Catalysts exhibiting a poor mass balance due to condensations and/or polymerization reactions leading to carbonaceous residues (Pt/CeO_2-400 and Pt/La_2O_3-400, Table 3, 15 h), present high-temperature combustion peaks in TGA–DTA experiments, associated to the accumulation of deposits on the catalysts surface. Interestingly, Pt/ZnO-400 catalyst, that exhibited a 30% selectivity to 1,2-PDO in acetol hydrogenation at long reaction time, only presents very small high-temperature combustion peaks, in agreement with its low polymerization capability and, also, in concordance with its better mass balance (Table 3, mass balance >79% at 15 h).

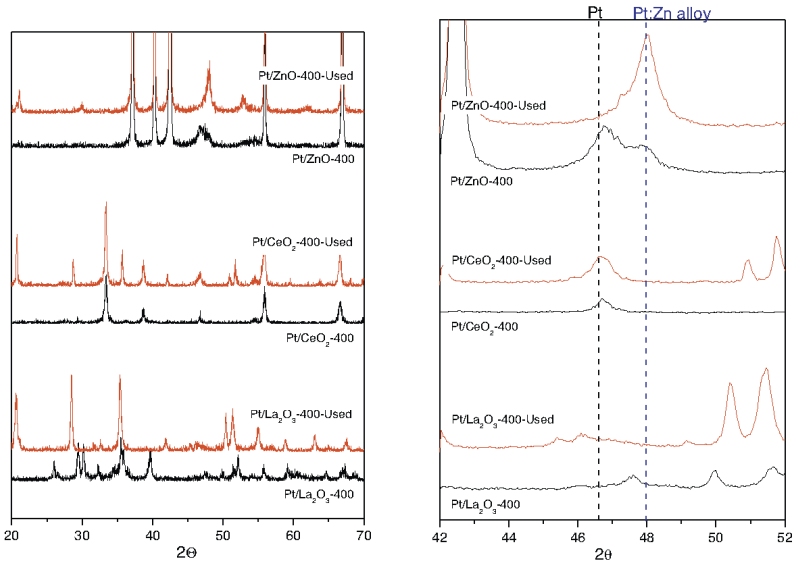

Fig. 3. XRD patterns corresponding to fresh (black line) and used (red line) Pt catalysts in glycerol hydrogenolysis (180 °C, 6 bar, 15 h).

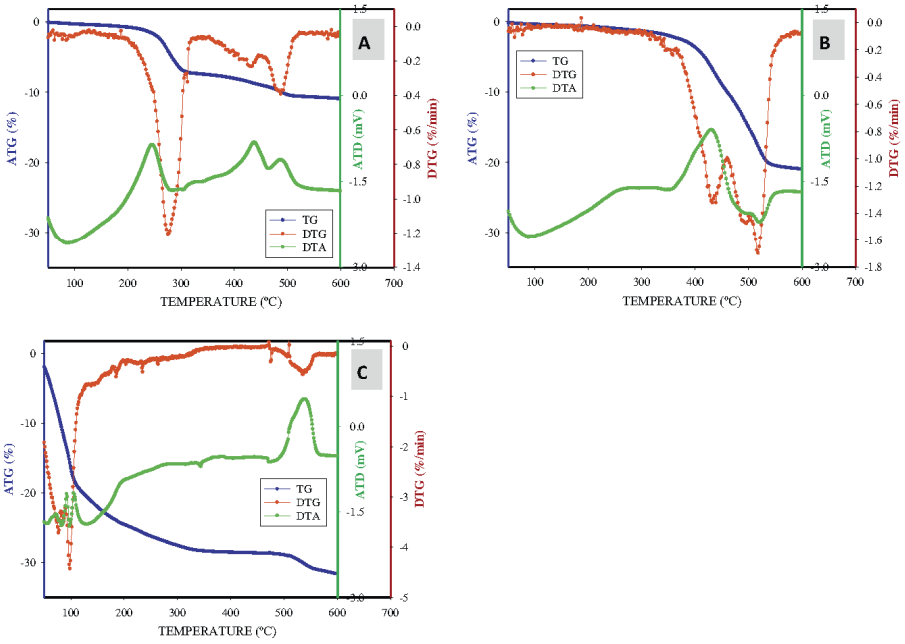

Fig. 4. TGA–DTG–DTA analysis of the supported Pt catalysts used in glycerol hydrogenolysis (180 °C, 6 bar, 15 h). (A) Pt/CeO2-400; (B) Pt/La2O3-400 and (C) Pt/ZnO-400.

Table 4
Comparison of textural and metallic properties corresponding to fresh and used catalysts.

		S_{BET} (m^2/g)	Pore diameter D_P (A)	Pt particle size TEM (nm)	Pt content (weight%) (XPS)	Pt content (weight%) (ICP-MS)
Pt/CeO_2-400	Fresh	49	8.1	2.8	6.4	4.2
	Used	40	7.2	3.6	8.2	6.0
Pt/La_2O_3-400	Fresh	12	30.8	2.3	2.4	3.9
	Used	9	20.8	9.7	2.5	4.4
Pt/ZnO-400	Fresh	10	41.7	4.5	6.6	6.1
	Used	10	42.7	11.0	7.4	2.5

XPS profiles obtained for all three used Pt supported catalysts (Supplementary material Fig. S3) do not give any valuable additional information. Only a slight re-oxidation of Pt is observed which, however, could be due to manipulation of the catalysts after reaction (filtration, washing and drying processes).

4. Conclusions

Several supported Pt catalysts were prepared by wet impregnation over different oxide supports such as Al_2O_3, CeO_2, La_2O_3 and ZnO. All those catalysts were characterized and tested in the liquid-phase glycerol hydrogenolysis. From the obtained results, the following conclusions can be extracted.

- The bare supports exhibited a wide range of acidity, ZnO presenting the lower acidity among all supports tested. Moreover, acidity was in general enhanced upon Pt incorporation, especially for the Pt/ZnO catalyst for which new acid sites associated to Pt metal particles were created.
- Pt/La_2O_3, Pt/CeO_2 and Pt/ZnO behaved better than Pt/Al_2O_3 in terms of 1,2-PDO yield. Moreover, as glycerol conversion increases there is a progressive loss in 1,2-PDO yield due to the formation of some polymeric species, responsible for the poor mass balance observed for some catalysts.
- Experiments carried out with acetol as starting substrate indicated that support acidity not associated to the Pt metal sites is detrimental to this process due to the oligomerization of acetol, being this the main cause of the loss of 1,2-PDO yield at long reaction times.
- The characterization of used catalysts revealed that under hydrothermal reaction conditions CeO2 and La2O3 supported Pt catalysts suffer from leaching, lost some of their surface area and presented intense combustion signals associated to organic deposits in agreement with the poor mass balance observed for these solids.
- All in all, among all studied catalysts, Pt/ZnO presented the best behavior in the liquid-phase hydrogenolysis in terms of yield to 1,2-PDO both from glycerol and acetol. These good results are based on several factor such as the appropriate surface acidity associated to Pt particles, a low oligomerization capability as consequence of the low acidity of the ZnO support and a reasonable high stability of the catalyst under hydrothermal reaction conditions.

Acknowledgments

The authors are thankful to Junta de Andalucía and FEDER funds for financial support (P07-FQM-02695, P08-FQM-3931 and P09-FQM-4781 projects). M. Checa acknowledges the Spanish Ministry of Education for a FPU grant (Ref AP2009-1221). Central Service for Research Support (SCAI) of the University of Córdoba is also acknowledged for the ICP-MS, TEM and XPS measurements.

Appendix A. Supplementary data

Supplementary data associated with this article can be found, in the online version, at http://dx.doi.org/10.1016/j.apcata.2015.09.028.

References

[1] M. Besson, P. Gallezot, C. Pinel, Chem. Rev. 114 (2014) 1827–1870.
[2] C.H. Zhou, H. Zhao, D.S. Tong, L.M. Wu, W.H. Yu, Cat. Rev. Sci. Eng. 55 (2013) 369–453.
[3] J.J. Bozell, G.R. Petersen, Green Chem. 12 (2010) 539–554.
[4] L. Chen, S. Ren, X.P. Ye, Fuel Process. Technol. 120 (2014) 40–47.
[5] S. Dutta, S. De, B. Saha, M. Alam, Catal. Sci. Technol. 2 (2012) 2025–2036.
[6] T. Werpy, G. Petersen, Top Value Added Chemicals from Biomass Volume I—Results of Screening for Potential Candidates from Sugars and Synthesis Gas, US Department of Energy, Oak Ridge, 2004, pp. 1–76.
[7] Y. Nakagawa, K. Tomishige, Catal. Surv. Asia 15 (2011) 111–116.
[8] Y. Nakagawa, K. Tomishige, Catal. Sci. Technolog. 1 (2011) 179–190.
[9] B.M.E. Russbueldt, W.F. Hoelderich, J. Catal. 271 (2010) 290–304.
[10] H.W. Tan, A.R. Abdul Aziz, M.K. Aroua, Renewable Sustainable Energy Rev. 27 (2013) 118–127.
[11] A. Marinas, P. Bruijnincx, J. Ftouni, F.J. Urbano, C. Pinel, Catal. Today 239 (2015) 31–37.
[12] D.T. Johnson, K.A. Taconi, Environ. Prog. 26 (2007) 338–348.
[13] A. Martin, U. Armbruster, I. Gandarias, P.L. Arias, Eur. J. Lipid Sci. Technol. 115 (2013) 9–27.
[14] V. Montes, M. Checa, A. Marinas, M. Boutonnet, J.M. Marinas, F.J. Urbano, S. Järas, C. Pinel, Catal. Today 223 (2014) 129–137.
[15] M. Checa, F. Auneau, J. Hidalgo-Carrillo, A. Marinas, J.M. Marinas, C. Pinel, F.J. Urbano, Catal. Today 196 (2012) 91–100.
[16] J. ten Dam, K. Djanashvili, F. Kapteijn, U. Hanefeld, ChemCatChem 5 (2013) 497–505.
[17] M. Pagliaro, R. Ciriminna, H. Kimura, M. Rossi, C.D. Pina, Eur. J. Lipid Sci. Technol. 111 (2009) 788–799.
[18] S. Zhu, Y. Zhu, S. Hao, H. Zheng, T. Mo, Y. Li, Green Chem. 14 (2012) 2607–2616.
[19] E.S. Vasiliadou, E. Heracleous, I.A. Vasalos, A.A. Lemonidou, Appl. Catal. B: Environ. 92 (2009) 90–99.
[20] D. Sun, Y. Yamada, S. Sato, Appl. Cata. A: Gen. 475 (2014) 63–68.
[21] X. Guo, Y. Li, W. Song, W. Shen, Catal. Lett. 141 (2011) 1458–1463.
[22] W. Yu, J. Zhao, H. Ma, H. Miao, Q. Song, J. Xu, Appl. Catal. A 383 (2010) 73–78.
[23] J. Feng, W. Xiong, B. Xu, W. Jiang, J. Wang, H. Chen, Catal. Commun. 46 (2014) 98–102.
[24] F. Auneau, C. Michel, F. Delbecq, C. Pinel, P. Sautet, Chem. Eur. J. 17 (2011) 14288–14299.
[25] Y. Shinmi, S. Koso, T. Kubota, Y. Nakagawa, K. Tomishige, Appl. Catal. B: Environ. 94 (2010) 318–326.
[26] E.P. Maris, R.J. Davis, J. Catal. 249 (2007) 328–337.
[27] O.M. Daniel, A. DeLaRiva, E.L. Kunkes, A.K. Datye, J.A. Dumesic, R.J. Davis, ChemCatChem 2 (2010) 1107–1114.
[28] Z. Yuan, P. Wu, J. Gao, X. Lu, Z. Hou, X. Zheng, Catal. Lett. 130 (2009) 261–265.
[29] J. Zhao, W. Yu, C. Chen, H. Miao, H. Ma, J. Xu, Catal. Lett. 134 (2010) 184–189.
[30] I. Gandarias, P.L. Arias, J. Requies, M.B. Güemez, J.L.G. Fierro, Appl. Catal. B: Environ. 97 (2010) 248–256.
[31] W. Suprun, M. Lutecki, T. Haber, H. Papp, J. Mol. Catal. A Chem. 309 (2009) 71–78.
[32] W. Suprun, M. Lutecki, R. Gläser, H. Papp, J. Mol. Catal. A Chem. 342–343 (2011) 91–100.
[33] M. Massa, A. Andersson, E. Finocchio, G. Busca, J. Catal. 307 (2013) 170–184.
[34] V. Nichele, M. Signoretto, F. Menegazzo, A. Gallo, V. Dal Santo, G. Cruciani, G. Cerrato, Appl. Catal. B 111–112 (2012) 225–232.
[35] S. Zhu, X. Gao, Y. Zhu, W. Fan, J. Wang, Y. Li, Catal. Sci. Technol. 5 (2015) 1169–1180.
[36] E.S. Vasiliadou, A.A. Lemonidou, Appl. Catal. A 396 (2011) 177–185.
[37] E.S. Vasiliadou, T.M. Eggenhuisen, P. Munnik, P.E. de Jongh, K.P. de Jong, A.A. Lemonidou, Appl. Catal. B: Environ. 145 (2014) 108–119.
[38] D. Durán-Martín, M. Ojeda, M.L. Granados, J.L.G. Fierro, R. Mariscal, Catal. Today 210 (2013) 98–105.
[39] S. Zhu, X. Gao, Y. Zhu, Y. Zhu, H. Zheng, Y. Li, J. Catal. 303 (2013) 70–79.
[40] S. Wang, Y. Li, H. Liu, Acta Chim. Sinica 70 (2012) 1897–1903.

[41] J. Feng, B. Xu, D.R. Liu, W. Xiong, J.B. Wang, Adv. Mater. Res. 791 (2013) 12–15.
[42] M.H. Lee, W.S. Jung, Bull. Korean Chem. Soc. 34 (2013) 3609–3614.
[43] B. Faroldi, M.L. Bosko, J. Múnera, E. Lombardo, L. Cornaglia, Catal. Today 213 (2013) 135–144.
[44] M.S. Avila, C.I. Vignatti, C.R. Apesteguía, T.F. Garetto, Chem. Eng. J. 241 (2014) 52–59.
[45] M. Consonni, D. Jokic, D.Y. Murzin, R. Touroude, J. Catal. 188 (1999) 165–175.
[46] N. Iwasa, T. Mayanagi, N. Ogawa, K. Sakata, N. Takezawa, Catal. Lett. 54 (1998) 119–123.
[47] F. Ammari, J. Lamotte, R. Touroude, J. Catal. 221 (2004) 32–42.
[48] J. Tendam, U. Hanefeld, ChemSusChem 4 (2011) 1017–1034.
[49] W. Oberhauser, C. Evangelisti, R.P. Jumde, R. Psaro, F. Vizza, M. Bevilacqua, J. Filippi, B.F. Machado, P. Serp, J. Catal. 325 (2015) 111–117.
[50] S. Penner, M. Armbrüster, ChemCatChem 7 (2015) 374–392.